

Tunable Electroacoustic Resonators through Active Impedance Control of Loudspeakers

THÈSE N° 5331 (2012)

PRÉSENTÉE LE 25 MAI 2012

À LA FACULTÉ DES SCIENCES ET TECHNIQUES DE L'INGÉNIEUR
LABORATOIRE D'ÉLECTROMAGNÉTISME ET ACOUSTIQUE
PROGRAMME DOCTORAL EN GÉNIE ÉLECTRIQUE

ÉCOLE POLYTECHNIQUE FÉDÉRALE DE LAUSANNE

POUR L'OBTENTION DU GRADE DE DOCTEUR ÈS SCIENCES

PAR

Romain BOULANDET

acceptée sur proposition du jury:

Prof. J.-Ph. Thiran, président du jury
Prof. J. R. Mosig, Dr H. Lissek, directeurs de thèse
Prof. A. Berry, rapporteur
Dr C. Faller, rapporteur
Dr Ph. Herzog, rapporteur



ÉCOLE POLYTECHNIQUE
FÉDÉRALE DE LAUSANNE

Suisse
2012

si seulement nous avons
le courage des oiseaux
qui chantent dans le vent glacé

— Dominique A. La Fossette —

Remerciements

En préambule à ce mémoire je souhaitais adresser mes remerciements les plus sincères aux personnes qui ont contribué à la réussite de cette thèse de doctorat.

En premier lieu, mes co-directeurs de thèse, le Prof. Juan Mosig et le Dr. Hervé Lissek, sans qui ce mémoire n'aurait jamais vu le jour. Merci Juan d'avoir accepté de co-diriger ce travail et merci aussi d'avoir soutenu le maintien du Groupe Acoustique au sein du LEMA. Merci à toi Hervé pour ta confiance et ton soutien sans faille tout au long de ma thèse, pour avoir su réorienté mon travail toujours à bon escient lorsque cela était nécessaire, et surtout merci d'avoir été l'instigateur d'un sujet si passionnant.

Je tiens aussi à adresser ma reconnaissance au Prof. Mario Rossi pour m'avoir ouvert les portes du LEMA à l'occasion de mon stage de Master, pour ses conseils avisés et généreusement partagés.

Merci également au Prof. Vincent Martin pour ses enseignements et ses encouragements.

J'adresse également toute ma gratitude aux membres du jury, le Dr. Philippe Herzog, le Pr. Alain Berry, le Dr. Christof Faller, et le Pr. Jean-Philippe Thiran pour leur vif intérêt porté à mon travail et pour la critique constructive apportée.

Merci aux étudiant(e)s dont j'ai eu le plaisir de superviser les projets et qui ont apportés leur contributions enthousiastes à mes recherches: Anne-Sophie Moreau, Iris Rigas, Romain Fleury, Nicolas Cherix, Luc Mosca, Martin Maugard, avec une mention spéciale à Etienne Rivet pour son aide très précieuse sur la partie de mon travail portant sur la synthèse de filtres, et pour la relecture attentive de ce manuscrit.

Je n'oublie pas non plus les acouticiens du LEMA, Patrick Marmaroli, Xavier Falourd, Pierre-Jean René, Philippe Martin, Cédric Montchâtre, avec une pensée particulière à mes collègues de bureau, François Aballéa, Lukas Rohr et Patrick Roe pour la bonne humeur qu'ils ont manifesté tout au long de cette aventure.

Mes pensées vont aussi à l'ensemble du groupe Hyper Fréquence du LEMA, et en particulier à Michael Mattes pour sa généreuse disponibilité et ses réponses à tous les problèmes que se posent un doctorant. Un grand merci à Eulalia Durussel pour son efficacité souriante à résoudre les difficultés administratives.

Mes remerciements vont également à l'équipe de l'atelier mécanique de la section STI de l'EPFL et tout particulièrement à Roland Dupuis pour ses conseils experts et ses nombreuses réalisations qui ont servies de support aux expériences effectuées.

Je voudrais aussi remercier le Fonds National Suisse (FNS) pour la recherche scientifique pour son soutien financier apporté à ce projet.

Acknowledgements

Et enfin mille mercis à ma famille qui a toujours été là, et surtout à mes deux chéries Eléna et Néva, pour leur compréhension, leur patience et leur amour, et pour me rendre le vie si belle chaque jour.

Lausanne, 21 mars 2012

Romain

Preface

The use of loudspeakers as absorbers of sound is not a novel concept in itself. It has been long studied, since the very early days of *active noise control* in the 1930's by Paul Lueg, where a loudspeaker was first turned into a noise control source, which was later found to be equivalent to *active sound absorption*. But the intrinsic duality of loudspeakers to act both as sound source and receiver has been surprisingly ignored during several decades, although it allows much possibilities to employ loudspeakers as sound absorbers. Apart from some lonesome attempts early in the 1970's, the concept of *shunt loudspeakers* has found a substantial interest in the literature only since a few years. The main contribution of this thesis is to bridge a conceptual gap between the two distinct concepts of *shunt loudspeakers* and *active sound absorption*, with a view to unifying the physical behaviors of both systems into a single formalism: the *electroacoustic resonator*.

This document, although it reports a research thesis, should be primarily read as a tutorial document, that can be easily followed by any newcomer to the field. Its objective is to describe the loudspeaker dynamics, through straightforward models that are commonly used in audio design, and the different manner to turn it into a sound absorber, from passive shunt techniques to more complex – but still simple to implement – active control systems. It covers several aspects of loudspeaker design, electrical engineering, control theory, and general linear acoustics, with the constant constraint of making the developments as reproducible as possible. But the work reported in this document has not always been a long quiet river, and when specific challenges have been encountered, the thesis reports such difficulties and the technical methodology required to have them overcome.

Romain Boulandet gathers, in his thesis, some key conceptual ideas into a straightforward, self-explanatory and tutorial document. It makes its thesis a very good piece of work, which I hope will be inspiring for any scientist that is willing to work on practical applications of active sound absorption, or even to go beyond the state of the art.

Lausanne, March 19th 2012

H. L.

Abstract

The current trend for multipurpose rooms requires enhanced acoustic treatments capable to meet ever more demanding specifications in terms of performance, compactness and versatility. The reason is the variety of activities to be hosted and the corresponding requirements in terms of acoustic quality which may be very different and even conflicting. In any process to improve listening comfort, the treatment of low-frequency sound is a major concern. The problem stems from the proven ineffectiveness of passive soundproofing solutions of the state of the art, or from their bulkiness that may be prohibitive. This thesis focuses on the analysis, design, realization and characterization of *tunable electroacoustic resonators* intended to specifically address this issue. This concept deals with loudspeakers, the acoustic impedance of which can be easily adjusted in a controlled fashion. Creating an electroacoustic resonator out of a loudspeaker is the result of an interdisciplinary effort. Such a challenging task combines conceptual tools, models, and applied solutions, drawing from the fields of audio engineering, control theory, and electrical engineering, both in the analog and digital domains.

A unifying theory is introduced, covering different strategies from passive electrical shunt to active control of acoustic impedance in a single formalism. This research shows that achieving a desired acoustic impedance at the transducer diaphragm is equivalent to the implementation of a specific functional relationship between the electrical current and voltage across the transducer terminals, and vice versa. From a design perspective, the specific electrical load is tailored by using an internal model of the transducer. The result is an innovative model-based synthesis methodology where the active control of acoustic impedance is reformulated as an electrical impedance synthesis, thus removing the use of sensor. This concept opens new opportunities to improve listening spaces by providing efficient acoustic absorption at low frequencies. Experiments clearly show the benefits of the proposed methodology in a field where there is currently no competitive solution. It is believed that the technological advances resulting from the coupling of a loudspeaker with a synthetic load should pave the way to innovative techniques in noise control and, hopefully, stimulate research in related areas.

Key Words: Active control of acoustic impedance, Tunable electroacoustic resonator, Shunt loudspeakers, Sensorless control, Electroacoustic absorber, Room modal equalization.

Zusammenfassung

Mit dem Aufkommen von immer mehr Mehrzwecksälen werden die Anforderungen an deren akustische Ausrüstungen in Sachen Leistung, Kompaktheit und Polyvalenz immer grösser. Die Verschiedenheit der darin stattfindenden Anlässe und deren sehr unterschiedliche, wenn nicht gar gegensätzliche akustische Bedürfnisse erklären diesen Trend. Bei jedem Verfahren, das den Hörkomfort erhöhen soll, muss dem Umgang mit tiefrequentigen Tönen Sorge getragen werden. Der Ursprung des Problems liegt bei der nachgewiesenen Ineffektivität von Materialien oder klassischen passiven Lösungen, deren Platzbedürfnis prohibitiv sein kann. Die vorliegende Dissertation konzentriert sich auf die Analyse, die Entwicklung, die Realisierung und die Charakterisierung von *stimmbaren elektroakustischen Resonatoren*, die speziell auf diese Problematik zugeschnitten sind. Das Konzept besteht aus Lautsprechern, deren akustische Impedanz mit einfachen Mitteln geregelt werden kann. Die Gestaltung von auf Lautsprecher basierenden elektroakustischen Resonatoren beruht auf einer interdisziplinären Vorgehensweise. Prinzipien, Werkzeuge, Modelle und Anwendungen von verschiedenen Fachrichtungen wie Audio Engineering, Regelungstechnik und Elektrotechnik im analogen sowie im digitalen Bereich wurden hinzugezogen.

Diese Arbeit stellt eine neue vereinende Theorie zwischen der passiven elektrischen Shunt-Technik und der aktiven akustischen Impedanzregelung vor. Es wird gezeigt, dass es durch die Implementierung eines spezifischen funktionalen Verhältnisses zwischen Strom und Spannung an den Anschlüssen des Lautsprechers möglich ist, eine gewünschte akustische Impedanz an dessen Membran zu erreichen und umgekehrt. In der Praxis wird die spezifische elektrische Last anhand eines internen Modelles des Lautsprechers berechnet. Daraus resultiert eine neuartige Methode, bei der die aktive Regelung der akustischen Impedanz zu einer sensorlosen elektrischen Impedanz-Synthesetechnik umformuliert wird. Dieses Konzept eröffnet neue Möglichkeiten bei der Verbesserungen von Räumen durch die effiziente Dämpfung von tieffrequentigem Schall. Die angestellten Messungen zeigen die Vorteile der vorgeschlagenen Methodologie in einem Bereich, wo bisher keine leistungsfähige Alternativlösung besteht. Der technologische Fortschritt, der aus der Koppelung zwischen einem Lautsprecher und einer synthetischen elektrischen Last resultiert, wird den Weg für innovative Lärmregelungstechniken ebnet und hoffentlich die Forschung in verwandten Bereichen stimulieren.

Preface

Schlüsselwörter: Akustische Impedanzregelung, stimmbarer elektroakustischer Resonator, Aktivregelung, Shunt-Lautsprecher, Impedanzpaarung, elektrodynamischer Lautsprecher, sensorlose Regelung, elektroakustische Dämpfung, modales Raum-Equalizing

Résumé

La tendance actuelle à construire des salles polyvalentes requiert de nouveaux types de traitements acoustiques capables de répondre à une demande toujours plus exigeante en termes de performance, compacité et polyvalence. Ces besoins s'expliquent par la variété des activités programmées dans ces espaces et leurs exigences acoustiques souvent très différentes, voire contradictoires. Dans tout processus visant à améliorer le confort d'écoute, le traitement des sons aux basses fréquences est une préoccupation majeure. Le problème provient principalement de l'inefficacité avérée des solutions passives classiques, ou de leur encombrement intrinsèque pouvant être rédhibitoire. Cette thèse porte sur l'analyse, la conception, la réalisation et la caractérisation de *résonateurs électroacoustiques accordables* destinés à répondre spécifiquement à cette problématique. Ce concept désigne des haut-parleurs dont l'impédance acoustique peut être facilement ajustée par contrôle. La création de résonateurs électroacoustiques sur la base d'un haut-parleur est le fruit d'une démarche interdisciplinaire, mettant en perspective différents outils conceptuels, modèles et techniques empruntés aux domaines de l'ingénierie audio, de la théorie du contrôle et du génie électrique.

Ce travail crée un lien conceptuel inédit entre deux techniques, les haut-parleurs "shuntés" passifs et le contrôle actif d'impédance acoustique. Cette recherche démontre que réaliser une impédance acoustique souhaitée au niveau de la membrane du haut-parleur revient à définir une relation fonctionnelle spécifique entre le courant électrique et la tension appliquée à ses bornes, et réciproquement. Il en résulte une méthodologie de synthèse originale dans laquelle le contrôle actif d'impédance acoustique est converti en une charge électrique spécifique, via un modèle interne du haut-parleur. Cette approche sans capteur ouvre une nouvelle voie pour l'amélioration des espaces d'écoute en permettant d'absorber efficacement l'énergie acoustique dans les basses fréquences. Les expériences montrent clairement les avantages de la méthodologie proposée dans un domaine où il n'existe actuellement aucune solution alternative performante. L'avancée technologique résultant du couplage d'un haut-parleur avec une charge synthétique devrait permettre le développement de techniques nouvelles en matière de contrôle du bruit et, peut-être même, stimuler de futures recherches dans des domaines connexes.

Mots clés : Contrôle actif d'impédance acoustique, Résonateur électroacoustique accordable, Haut-parleur shunté, Commande sans capteur, Absorbeur électroacoustique, Egalisation modale des salles.

Contents

Acknowledgements	v
Preface	vii
Abstract (English/Français/Deutsch)	ix
List of figures	xviii
List of tables	xxi
1 Introduction	1
1.1 Context and scope of the research	1
1.2 Thesis statement	2
1.3 Motivation	2
1.4 Objectives and technological challenges	3
1.5 Outlines and original contributions	4
2 Noise control engineering: fundamentals and key concepts	7
2.1 Introduction	7
2.2 Fundamentals of sound	8
2.3 Concept of impedance	10
2.4 Active noise cancellation	12
2.5 Impedance based control	14
2.6 Sensorless control	18
2.7 Conclusions	19
3 Electrodynamic loudspeaker: description and modeling	21
3.1 Introduction	21
3.2 Core assumptions	22
3.2.1 Linearity	22
3.2.2 Fundamental radiation hypothesis	23
3.2.3 Piston-like movement	23
3.2.4 Transducer reciprocity	23
3.3 Electrodynamic conversion	24

Contents

3.3.1	Electromagnetic force	25
3.3.2	Motional electromotive force	27
3.3.3	Induced electromotive force	28
3.3.4	Polarity and sign convention	28
3.4	Motional equations	29
3.4.1	Lumped parameter model	29
3.4.2	Newton's second law	30
3.4.3	Kirchhoff's circuit law	31
3.4.4	Characteristic equations	32
3.4.5	Electrical coupling	33
3.4.6	Motional impedance	34
3.4.7	State-space representation	36
3.5	Conclusions	38
4	Electroacoustic resonators: concept and formulation	39
4.1	Introduction	39
4.2	Damped harmonic oscillator	41
4.2.1	Governing equation	41
4.2.2	Quality factor and bandwidth	42
4.2.3	Frequency response function	42
4.2.4	Operating range	44
4.2.5	General solution	45
4.2.6	Sensitivity analysis	46
4.2.7	System poles and zeros	49
4.3	Electromechanical system	52
4.3.1	Coupling to an electrical source	52
4.3.2	Coupling to an electrical load	53
4.3.3	Dynamics of a third-order system	54
4.4	System performance	56
4.4.1	Specific acoustic admittance	56
4.4.2	Reflection coefficient	57
4.4.3	Absorption coefficient	58
4.4.4	Routh's stability criterion	59
4.5	Conclusions	60
5	Changing the acoustic impedance using feedback control	61
5.1	Introduction	61
5.2	Active control on a loudspeaker	62
5.2.1	Problem statement	62
5.2.2	Control law formulation	63
5.2.3	Loudspeaker as an active control element	65
5.3	Control system design	66
5.3.1	feedforward control	66

5.3.2	Motional feedback control	69
5.3.3	Combined feedback and feedforward control	70
5.4	Advanced control system design	72
5.4.1	Uncompensated control system analysis	72
5.4.2	PID controller	74
5.4.3	Lead-lag compensator	76
5.4.4	Advanced design procedure	79
5.4.5	Closed-loop transfer functions with lead-lag compensation	79
5.5	System performance using feedback control	82
5.5.1	System stability	82
5.5.2	System poles and zeros	82
5.5.3	Experimental setup	84
5.5.4	Sound absorption/reflection capability	86
5.5.5	Open-loop gain	90
5.6	Conclusions	94
6	Matching the acoustic impedance through electrical network	95
6.1	Introduction	95
6.2	Design of matching electrical network	96
6.2.1	Problem formulation	96
6.2.2	Electrical network topology	97
6.2.3	Model of the unplugged loudspeaker	98
6.2.4	Coupling to a resistor	99
6.2.5	Coupling to a negative impedance network	102
6.2.6	Coupling to a parallel RLC network	104
6.2.7	Coupling to a series RLC network	111
6.3	System performance using electrical matching networks	114
6.3.1	Experimental setup	114
6.3.2	Sound absorption/reflection capability	116
6.4	Conclusions	119
7	Synthesis of electrical loads for acoustic impedance matching	121
7.1	Introduction	121
7.2	Merging active sound absorption and shunt methods	122
7.2.1	Identifying the formal analogies	122
7.2.2	Combining the feedback control techniques and shunt methods	124
7.2.3	Expressing the equivalent electrical load	126
7.2.4	Extending the bandwidth by synthesizing an electrical load	127
7.3	Synthesis of electrical admittance using digital filters	131
7.3.1	Problem formulation	131
7.3.2	Methodology for acoustic impedance synthesis	131
7.3.3	Filter realization	133
7.3.4	Real time implementation	137

Contents

7.3.5	Reconfigurable I/O platform	139
7.3.6	Voltage to current conversion	139
7.4	System performance using synthetic electrical loads	140
7.4.1	Practical implementation	140
7.4.2	Sound absorption/reflection capability	143
7.5	Conclusions	145
8	Modal equalization of a room using electroacoustic resonators	147
8.1	Introduction	147
8.2	Semi-active modal equalization of a room	148
8.2.1	Objectives	148
8.2.2	Problem statement	149
8.2.3	Room description	149
8.2.4	Identifying the natural frequencies of the room	150
8.2.5	Defining the location of electroacoustic resonators in the room	153
8.3	Results and discussion	154
8.3.1	Experimental setup	154
8.3.2	Damping of low-frequency modes	157
8.3.3	Improved acoustic energy decay rate	161
8.4	Conclusions	163
9	Conclusions and perspectives	165
A	Solving a cubic equation using hyperbolic functions	169
B	Optimization of electroacoustic absorbers by means of designed experiments	171
	Bibliography	193
	Curriculum Vitae	195

List of Figures

2.1	Illustration of the process of silencing sound oscillation	12
2.2	Schematic representation of a transmission line	14
2.3	Basic principle of acoustic impedance control in a semi-infinite duct . . .	15
2.4	Illustration of the concept of electronic sound absorber	16
2.5	Illustration of passive piezoelectric structural damping	17
2.6	Illustration of the concept of active electroacoustic transducer	17
3.1	Sectional view of an electrodynamic loudspeaker	22
3.2	Schematics of a loudspeaker operating as sensor and actuator	24
3.3	Principle of electrodynamic conversion using a moving coil	26
3.4	Force balance on the loudspeaker diaphragm	31
3.5	Electrical circuit modeling of the voice coil	32
3.6	Circuit representation of an electrodynamic loudspeaker	34
3.7	Electrical impedance of a loudspeaker mounted on an infinite screen . . .	35
3.8	State-space representation of an electrodynamic loudspeaker	36
4.1	Schematics of systems of one degree of freedom	40
4.2	Control model in Simulink [®] environment	47
4.3	Velocity response of a damped harmonic oscillator	48
4.4	Pole-zero diagram of an underdamped second-order oscillator	50
4.5	Coupling of a loudspeaker to an electrical source and to an electrical load	52
4.6	Pole-zero diagram of a third-order system	55
4.7	Bode plot of the specific admittance of the loudspeaker when unplugged .	56
4.8	Real and imaginary part of the diaphragm specific impedance when unplugged	57
4.9	Absorption coefficient at the loudspeaker diaphragm	58
5.1	Basic block diagram of a feedback control system	62
5.2	Block diagram of a loudspeaker as an active control element	65
5.3	Diagram of a loudspeaker under feedforward control	67
5.4	Computed frequency response with feedforward and feedback control . . .	68
5.5	Computed absorption coefficient with feedforward and feedback control .	68
5.6	Diagram of a loudspeaker under motional feedback control	69
5.7	Diagram of a loudspeaker under combined feedback/feedforward control .	71
5.8	Computed frequency response with combined feedback/feedforward control	72

List of Figures

5.9	Computed absorption coefficient with combined feedback/feedforward control	73
5.10	Block diagram representation of a PID control architecture.	74
5.11	Magnitude and phase plots for typical lead and lag compensators	76
5.12	Block diagram of a loudspeaker under control with phase compensators	78
5.13	Computed frequency response with advanced controller	80
5.14	Computed absorption coefficient with advanced controller	81
5.15	Pole-zero diagram of the loudspeaker under control	83
5.16	Picture of the experimental setup.	84
5.17	Schematics of the setup used for the feedback control techniques	85
5.18	Measured acoustic performance with feedforward and feedback control	87
5.19	Measured acoustic performance with combined and PID control	88
5.20	Measured acoustic performance with phase compensation	89
5.21	Picture of the experimental setup for the measurement of open-loop gains	90
5.22	Measured open-loop gains with purely proportional gains	91
5.23	Measured open-loop gains with PID control and lead-lag compensation	93
6.1	Schematics of various topologies of matching networks	97
6.2	Plot of the real part and imaginary part of the mechanical impedance	98
6.3	Equivalent circuit of the loudspeaker shunted by a resistor	99
6.4	Plot of the real part and imaginary part of the mechanical impedance	100
6.5	Computed acoustic performance with positive and negative shunt impedances	102
6.6	Pole-zero diagram of the loudspeaker shunted by a positive and negative load	104
6.7	Equivalent circuit of the loudspeaker shunted by a parallel RC network	104
6.8	Real and imaginary parts of the mechanical impedance equivalent to a parallel RLC network	106
6.9	Equivalent circuit of the loudspeaker shunted by a parallel RL network	108
6.10	Computed acoustic performance in case of a parallel or series RLC network	109
6.11	Pole-zero diagram of the loudspeaker shunted by a parallel or series RLC network	110
6.12	Equivalent circuit of the loudspeaker shunted by a series RLC network	111
6.13	Plot of the real part and imaginary part of the mechanical impedance	112
6.14	Pole-zero diagram of the loudspeaker shunted by a series RLC network	113
6.15	Picture of the experimental setup.	114
6.16	Schematics of the experimental setup used with the shunt electrical method	114
6.17	Schematics of the practical realization of the electrical matching networks	116
6.18	Measured acoustic performance with a positive and negative impedance	117
6.19	Measured acoustic performances with a parallel or series RLC network	118
7.1	Diagram of a loudspeaker under hybrid control	124
7.2	Representation of a loudspeaker under combined feedforward and shunt control	125

7.3	Connecting an equivalent electrical impedance to the loudspeaker terminals	128
7.4	Computed results with equivalent and synthesized load	130
7.5	Methodology for acoustic impedance synthesis	132
7.6	Measured and computed electrical impedances in free field	133
7.7	Filter structure of direct form I and direct form II	136
7.8	Picture of the control system	137
7.9	Block diagram of the LabVIEW FPGA VI	138
7.10	Block diagram of the LabVIEW real-time host VI	138
7.11	Voltage to current conversion circuit	139
7.12	Frequency response of the power amplifier and conversion circuit	141
7.13	Measured frequency response of analog I/O modules	141
7.14	Measured frequency response after improving the synthesized electrical admittance	142
7.15	Measured absorption coefficient after improving the synthesized electrical admittance	142
7.16	Measured frequency response of the synthesized electrical loads	143
7.17	Measured acoustic performances using synthesized electrical loads	144
8.1	Sketch of the rectangular room	149
8.2	Sound pressure level computed in corner 8 of the room	151
8.3	Acoustic energy distribution of the lowest fifteen modes of the room	152
8.4	Location and orientation of the electroacoustic resonators in the room	154
8.5	Pictures of some configurations experienced in the room	155
8.6	Measured absorption coefficient of the loudspeakers when connected to synthetic loads	156
8.7	Measured electrical admittance of the synthetic loads connected to the loudspeakers	156
8.8	Sound pressure level measured with configuration C ₁ and C ₂	158
8.9	Sound pressure level measured with configuration C ₄	159
8.10	Sound pressure level measured with configuration C ₅ and C ₈	159
8.11	Sound pressure level measured with configuration C ₆ and C ₉	160
8.12	Illustration of the decay time of sound energy in the room after switching off the source	162
8.13	Illustration of the measured decay time of sound energy for the one-third octave band 80 Hz	162
A.1	Characteristic curve describing the loudspeaker as a cubic polynomial	169

List of Tables

4.1	Operating range of a damped oscillator according to the radial frequency.	45
4.2	Influence of varying mechanical parameters on the velocity response of a damped harmonic oscillator.	47
5.1	Small signal parameters of the loudspeaker considered for the simulations	85
5.2	Control settings for the simulations with proportional control	86
5.3	Control settings for the simulations with PID control	86
5.4	Control settings for the simulations with combined control and compensation	86
5.5	Phase and gain margins measured in impedance tube and in free field . .	92
6.1	Small signal parameters considered for the simulations	115
6.2	Parameter settings for the simulations and experiments with electrical matching networks	115
7.1	Parameter settings for the simulations with hybrid control	125
8.1	Natural frequencies of the room	151
8.2	Summary of the sound pressure level gains measured for each configuration	157
8.3	Summary of the measured decay time of acoustic energy per one-third octave bands for each configuration	161

1 Introduction

1.1 Context and scope of the research

The current trend for multipurpose rooms requires enhanced acoustic treatments capable to meet ever more demanding specifications in terms of performance, compactness and versatility. The challenge is usually to achieve a balanced distribution of sound energy in order to provide good listening conditions for the audience [1–3]. In practice, the task is to choose materials for the walls or wall coverings with acoustic properties appropriate for use of the room. The problem is that listening spaces must often accommodate variety of events for which they have not been designed. Needs for acoustic treatments may be very different, and sometimes conflicting. This is the case of an auditorium most often used as a concert hall but occasionally as a conference room [4, 5]. The ideal solution would be a way to change the sound environment to suit an activity. In architectural acoustics, key issues are basically the control of the reverberated sound field, the time and space distribution of the early reflections, and the removal of ringing and flutter echoes that may affect sound perception. To this end, various arrangements of sound absorbers, diffusers and reflectors are commonly used to meet acoustic requirements within the audio-frequency range [1, 2, 6, 7].

A major concern in closed spaces is the occurrence of standing waves and acoustic interferences at low frequencies. In this frequency range, the response of a room presents high sound pressure levels at certain frequencies which coincide with the natural frequencies of the room [1, 8–10]. This even leads to an uneven spatial distribution of acoustic energy depending on the nodes and antinodes of sound pressure. When the sound stops the natural resonances of the room may even sustain. In case of modulated sound signal diffusion (music), such room effect can be detrimental in terms of sound clarity and definition, or even harmful to intelligibility [11]. Low-frequency resonances may have prejudicial audible effects in the rendering of sound in listening spaces. Unfortunately, the state of the art solutions of passive soundproofing are not effective, or their embodiments are so bulky that they become almost impractical.

1.2 Thesis statement

This observation leads us to consider in this thesis the development of soundproofing means doted with adaptable functions to specifically address the low-frequency range. The underlying idea is to allow corrective actions in listening spaces such as concert halls, home-theaters, or even in workspaces, offices and open spaces. Potential applications could include the low-frequency room equalization, a controllable sound absorption according to the frequency or angle of incidence, the assisted reverberation control, etc.

The thesis will focus specifically on the analysis, design, realization and characterization of tunable electroacoustic resonators. By tunable electroacoustic resonators, we mean active loudspeakers the acoustic impedance of which can be significantly changed in a controlled fashion. The acoustic impedance is a useful parameter that characterizes the resistance of a medium (material or fluid) to sound waves propagation. If the apparent acoustic impedance of the material (here the transducer diaphragm) differs much from the characteristic impedance of the medium (here the air), then most of the incident sound energy will be reflected; otherwise part of sound energy is absorbed [1, 2, 12].

1.3 Motivation

The inadequacy of usual passive soundproofing treatments [1, 11, 13] and practical issues associated with the implementation of active noise cancellation (ANC) [14, 15] has motivated the development of active loudspeakers with variable acoustic impedance [16]. Passive means are basically robust, cheap, easily available, simple to implement, but their efficiency does not always fit with the frequency range of interest. Furthermore, they are mono-functional, i.e. they can only absorb, or reflect, sound energy. ANC methods are known to be effective in the low frequencies, more compact than passive means, and able to counteract the noise selectively [17–19]. Good performances can be observed in case of simple geometries or with stationary tones. Real situations facing a broadband noise or unsteady sound fields are quite difficult to treat. In addition, the number of needed secondary sources quickly becomes prohibitive and distributed control algorithms may be quite complicated to implement.

The approach taken in this thesis differs from the usual ANC techniques based on the principle of destructive interferences. The chosen strategy is to control the acoustic impedance of diaphragms acting as refracting surfaces instead of seeking to compensate for unwanted sound inside a given zone by using control sources. The idea is to control the boundaries of the sound field rather than targeting a global control that requires an input of acoustic energy. The proposed approach is intended to function without complex signal processing. Unlike active noise cancellation, complex sound fields can be addressed without thorough knowledge of the characteristics of acoustic disturbances. This should result in much straightforward practical implementations.

From this observation, it seems attractive to divert the primary use of a loudspeaker system to turn it into a sound control device [11]. The direct-radiating electrodynamic loudspeaker is an obvious candidate for several reasons: immediate availability, cost, and electromagnetic properties that can alter transducer dynamics in a controlled fashion. It is basically a damped harmonic oscillator that resonates usually between 20 Hz and 100 Hz in a frequency range where it is controlled by resistances. Another notable feature is its ability to act both as sensor and as actuator. Transducer reciprocity is of primary interest since it suggests a perspective even more interesting: the development of "smart" electroacoustic transducers able to provide information on the surrounding sound field while simultaneously altering it. To make the loudspeaker truly adaptable, a control element must be involved. With the concept of loudspeakers with a variable acoustic impedance [20], we mean to get over the complexities related to the practical implementation of ANC techniques while improving performance, compactness, and versatility of passive acoustical resonators.

1.4 Objectives and technological challenges

The objective of this thesis is the development of tunable electroacoustic resonator concept for noise control applications. Acoustic absorption via a loudspeaker can basically be achieved in two ways: either by feedback control of acoustic quantities involving sensors and a control system, or by coupling an electrical charge to the transducer terminals. Whilst the latter allows significant broadening of sound absorption performances at the loudspeaker diaphragm, the former has the advantage of being particularly simple to implement, and often does not require energy to operate. However, a lower performance is expected in terms of bandwidth. The role of electroacoustic resonators is therefore to achieve an acoustic impedance matching over a relatively large frequency range. Once incorporated into the walls or simply placed in the room, they allow corrective actions especially in the low frequencies. The benefits are expected in terms of sound level reduction, improved listening comfort and speech intelligibility.

The main challenge of the thesis is to bypass the use of sensors so as to reduce both cost and stability issues but while targeting a broadband control. The challenging problem of sensorless control facing resonant sound fields reflects on the difficulties of synthesizing electrical loads both stable and efficient. The thesis will therefore examine the implementation of a specific functional relationship between electric variables, both in the analogue and digital domains.

To summarize, this research expects to contribute to the dissemination of knowledge in all sectors where the control of acoustic impedance via electroacoustic transducers can meet requirements for acoustic treatments.

1.5 Outlines and original contributions

This section summarizes the contents and the original contributions of the chapters of the thesis.

Chapter 2: Noise control engineering – fundamentals and key concepts

Description: the fundamentals of sound and the key concepts involved in noise control engineering are presented. The general goal is to justify the choice of strategy to meet acoustical requirements for large rooms. The focus is put on controlling the surface impedance using electroacoustic transducers.

Original contribution: the points raised in this introductory chapter are covered extensively in the literature but they provide a basis for future developments which are discussed in subsequent chapters. The state of the art techniques to control the acoustic impedance is presented to clearly identify the challenge of bypassing the use of sensors.

Chapter 3: Electrodynamic loudspeaker – description and modeling

Description: the physics necessary for a comprehensive understanding of electrodynamic loudspeakers is provided. This chapter provides a very simple model which covers the core assumptions, the principle of electromechanical transduction, and gives the linearized, lumped motional equations of a direct-radiating loudspeaker system.

Original contribution: this chapter aims to remove any ambiguity when using a loudspeaker, not as a sound transmitter, but for control of acoustic impedance. A thorough analysis of electromagnetic phenomena related to a vibrating surface (the transducer diaphragm) is provided. It helps to determine what current in – or motion of – an electric conductor is capable of producing an electromechanical effect. This key aspect in a control perspective will be widely used in the following chapters.

Chapter 4: Electroacoustic resonators – concept and formulation

Description: the comprehensive knowledge required for the design of electroacoustic resonators is introduced from analogies with the damped harmonic oscillator. The theoretical aspects related to altering the parameters of a loudspeaker and their consequences on the sound absorption capability are discussed. Various relevant analysis tools such as frequency response, system poles and zeros, or the Routh criterion of stability are introduced. The acoustic metrics that govern the performance of the controlled loudspeaker system under normal plane wave incidence are also defined.

Original contribution: the conceptual tools and theoretical results discussed in this chapter are not new. They help to define the objective in terms of performance and stability. The two ways to turn the loudspeaker into electroacoustic resonator are first introduced by considering the open circuit, then by coupling with an electrical load or a voltage source. Ways to tune it optimally in view of maximal sound absorption are described analytically.

Chapter 5: Changing the acoustic impedance using feedback control

Description: the development of electroacoustic resonators is investigated from the control theory perspective. The strategy is to change the acoustic impedance at the transducer diaphragm by means of sensors and controllers. Analytical and numerical implementations are described to illustrate the effect of applying feedback control of acoustic variables.

Original contribution: this chapter presents a thorough analysis of classical active control techniques applied to a loudspeaker system. The condition for acoustic impedance matching is reformulated as a control law. Experimental results show that the specific acoustic impedance at the transducer diaphragm can be matched to the characteristic impedance of air over a rather large bandwidth by choosing the control settings correctly. To further improve performances, or to overcome practical issues, more elaborate controllers including PID algorithm and phase compensation techniques are studied. This work gives insights into the ability of loudspeakers to achieve optimal sound absorption. Therefore, it provides valuable information for the design of dedicated controllers.

Chapter 6: Matching the acoustic impedance through electrical network

Description: in this chapter the development of electroacoustic resonators is discussed from the viewpoint of electrical engineering. The control of acoustic impedance is investigated via the coupling of an electrical load to the transducer terminals. With the help of dipoles interconnected in series or in parallel, some basic functional relationships between current and voltage can be readily implemented. It results that the dynamics of electroacoustic resonant systems can be properly altered so as to achieve optimal sound absorption. This strategy removes the need of sensors and is thus extremely relevant in view of a cost-effective implementation. The major drawback is a limited bandwidth around the resonance of the transducer.

Original contribution: this chapter provides workable guidelines for the design and the practical realization of optimized matching networks such as pure resistor, negative impedance networks, and series or parallel RLC circuits. The effect of the electrical coupling on the mechanical behavior of the loudspeaker is solved analytically using circuit theory.

Chapter 7: Synthesis of electrical loads for acoustic impedance matching

Description: Based on the acquired knowledge, an original strategy for the control of acoustic impedance is proposed. This chapter combines and unifies the formalism used in Chapter 5 and Chapter 6. This research shows that achieving a desired acoustic impedance at the transducer diaphragm is equivalent to the implementation of a functional relationship between the electrical current and voltage across the transducer terminals, and vice versa. Duality between electric and acoustic admittances of both sides of the loudspeaker is at the heart of the synthesis process. The methodology used to develop an optimal electric load is presented in analog and digital domains.

Original contribution: This chapter concentrates the most of original contributions of the thesis. A joint approach merging the shunt based methods and the feedback control approach is discussed. This theoretical result brings together in a single formalism techniques of active sound absorption and the shunt loudspeakers. Based on the internal model of the transducer, a specific electrical load can be tailored in view of achieving a desired acoustic impedance at the diaphragm. The technological advance resulting from the coupling of a loudspeaker with a synthetic load paves the way to innovative techniques for sound control. The practical realization is proposed by means of digital filters which are processed on a real-time FPGA platform. This research work has resulted in the design of a novel electronic circuit allowing to achieve a prototype electroacoustic absorber which is the subject of a patent application.

Chapter 8: Modal equalization of a room using electroacoustic resonators

Description: this chapter gives insights into the qualitative and quantitative aspects of the performance of electroacoustic resonator in a real situation. For illustrative purposes, the equalization of the low-frequency resonances of a room is discussed. This experimental work emphasizes the relevance of the concept of electroacoustic resonators with respect to the usual soundproofing treatments.

Original contribution: experimental results demonstrate the feasibility of damping the low-frequency resonances of a room by using electroacoustic resonators. This experimental work focuses on the benefits of the proposed methodology in an area where there is currently no competitive passive solution.

Chapter 9: Conclusions and perspectives

Description: a summary of the key findings of the work achieved in this thesis is presented while suggesting some lines of research to pursue.

2 Noise control engineering: fundamentals and key concepts

2.1 Introduction

Acoustic absorption is the phenomenon of sound power reduction by passage of sound waves in material media, under given conditions and for a specific frequency. Acoustic absorbers are materials or objects with ability to absorbing sound energy. They are commonly used as soundproofing means in listening rooms in view of improving acoustics. They can take the form of porous layers such as mineral wool, glass or polyester fibers, felt or foam. Porous materials generally provide high sound absorption in the middle- and high-frequency range, typically above a few of hundred of Hertz. Absorbing properties result from the conversion of acoustical energy into heat; the oscillating air molecules inside pores lose their energy due to friction [13,21]. A noticeable disadvantage concerning particle detachment makes them inappropriate in situations where sustainability of health requests are a priority [22]. The use of micro-perforated materials (MPP) the operating principle of which is also based on viscous losses is an alternative [23]. When a sound wave penetrates the MPP, friction between the moving air and the holes in the MPP dissipates acoustical energy. The coupling of MPP and porous materials is a widespread assembly in the aircraft and automotive applications. Acoustic absorption capability of materials is frequency-dependent and is affected by size, shape, location and the mounting method used. Alternatively, active control techniques can be considered to provide acoustic absorption and vibration damping. Interest is recognized in terms of performance and compactness in the low-frequency range, and ability to selectively counteract the noise. A major disadvantage is the need of sensors and complex processing algorithms, particularly to address sound fields in rooms [15,18,19,24–28]. Active control systems are commercially applied in rather simple situations: small volume, one-dimensional sound propagation, quasi-periodic noise, isolated modes [18,24,29]. Passive and active solutions can be advantageously combined so as to improve overall performance. Such strategy is often referred to as hybrid passive/active absorption [12,22,25,27,30–32]. In this chapter, the fundamentals of sound and the key concepts involved in noise control engineering are presented.

2.2 Fundamentals of sound

Sound generation and propagation result from a movement of particles around an equilibrium position in an elastic medium. The sound field is the medium in which a sound wave and all the deformations of the fluid propagate. It is characterized by physical quantities which vary as functions of space and time. When the medium is a compressible fluid, each particle is subjected to successive compressions and expansions during its motion. This section summarizes some results extensively described in [3].

A particle is a portion of fluid which dimensions are small compared to the spatial variations of acoustic quantities. The motion of the particles is usually characterized by the particle velocity vector $\mathbf{v} = v(\mathbf{r}, t)$, expressed in m s^{-1} , where \mathbf{r} is the vector of spatial coordinates of the particle and t the time. The deformations or the transformation of the particles can be characterized by a scalar quantity called acoustic pressure $p(\mathbf{r}, t)$, expressed in Pa. The propagation of sound waves in a lossless fluid (such as air) can be modeled by an equation of motion (also called the local form of Newton's law) and an equation of continuity

$$\begin{aligned}\nabla p &= -\rho \frac{\partial \mathbf{v}}{\partial t} \\ \frac{\partial p}{\partial t} &= -\kappa \nabla \cdot \mathbf{v}\end{aligned}\tag{2.1}$$

where ∇ is the nabla operator, κ is the bulk modulus of the fluid, expressed in Pa, and ρ is the mass density of the fluid, expressed in kg m^{-3} . Newton's equation governs the motion of particles when subjected to a pressure force and the continuity equation states that the mass of particles remains constant. Combining these two equations yields the acoustic wave propagation equation. For the sound pressure, it can be expressed as

$$\nabla^2 p(\mathbf{r}, t) - \frac{\rho}{\kappa} \frac{\partial^2}{\partial t^2} p(\mathbf{r}, t) = 0\tag{2.2}$$

The dimensional analysis of Eq. (2.2) shows that the ratio κ/ρ has the dimension of the squared celerity. The celerity of sound waves is thus defined as

$$c = \sqrt{\frac{\kappa}{\rho}}\tag{2.3}$$

and expressed in m s^{-1} . Substituting c as in Eq. (2.3) in Eq. (2.1) yields

$$\nabla^2 p(\mathbf{r}, t) - \frac{1}{c^2} \frac{\partial^2}{\partial t^2} p(\mathbf{r}, t) = 0\tag{2.4}$$

An equation of this type, linking second derivatives with respect to space and time, is called d'Alembert equation. It is to be found in many other scientific fields such as in electromagnetics when it comes to describe the phenomena of lossless linear propagation.

Assuming now that the acoustical quantities depend only on the time and on one single direction, the x -axis of a cartesian coordinate system for instance, the d'Alembert equation (2.4) reads

$$\frac{\partial^2 p}{\partial x^2} - \frac{1}{c^2} \frac{\partial^2 p}{\partial t^2} = 0 \quad (2.5)$$

The general solution of Eq. (2.5) depends on x and t only, and can be written

$$p(x, t) = p_+(ct - x) + p_-(ct + x) \quad (2.6)$$

where p_+ and p_- are arbitrary functions whose second derivative exists. The first term $p_+(ct - x)$ represents a plane traveling wave with a celerity c in the direction of increasing x , while the other one $p_-(ct + x)$ describes a plane wave traveling with a celerity c in the opposite direction.

Solutions of particular importance are obtained by specifying p_+ and p_- as exponential functions with imaginary arguments. The wave propagating in the positive x -axis can then be expressed in complex representation as

$$p(x, t) = A e^{jk(ct-x)+\phi} = \hat{A} e^{j(\omega t - kx)} \quad (2.7)$$

where ω denotes the radial frequency and $k = \omega/c$ is the wavenumber. The use of complex representation allows combining the peak amplitude A of the oscillation and phase shift ϕ of the wave function into a single complex valued amplitude $\hat{A} = A e^{j\phi}$. This results in a useful compact notation for manipulating vibrations and waves algebraically. Equation (2.7) describes a temporal and spatial harmonic vibration whose time period T and the wavelength λ (spatial period) are related to the radial frequency and wavenumber by

$$k = \frac{\omega}{c} = \frac{2\pi}{cT} = \frac{2\pi f}{c} = \frac{2\pi}{\lambda} \quad (2.8)$$

where $f = \omega/2\pi$ is the frequency of the wave, expressed in Hz.

Since any observable physical quantity is always real, only the real part of Eq. (2.7) has a physical meaning. Therefore, we consider Eq. (2.7) as a shorthand of the real-valued equation representing an actual plane wave traveling along a single line, given by

$$p(x, t) = A \sin(\omega t - kx + \phi) \quad (2.9)$$

which could, for example, be considered in the case of plane wave traveling along a duct.

2.3 Concept of impedance

The concept of impedance was first defined in the field of electrical engineering by Heaviside in the 1880's, and the analogy of the acoustic impedance was introduced by Webster in 1919 [33–35].

Generally speaking, when an ac¹ electric circuit is driven by an electromotive force (emf) ε , the complex electrical impedance is

$$Z_e = \frac{\varepsilon}{i} \quad (2.10)$$

where i is the alternating current.

In a device without resistance, if an electric charge q passes through it, and gains an energy W , the emf is defined in terms of the difference of electromagnetic potential that holds between the terminals of the device. The emf is the amount of work done in moving the unit charge q from low to high potential, i.e. $\varepsilon = W/q$. The electromagnetic potential is defined as the potential energy per unit charge in order for the quantity to be independent of an arbitrary charge magnitude [35].

In the footsteps of this formulation, Webster adopted an electrical analogy for describing a plane sound wave traveling in a duct [33]. Identifying the particle displacement ξ to charge q , he defined the acoustic impedance as

$$Z_a = \frac{p}{Sv} \quad (2.11)$$

where $p(x, t)$ is the sound pressure, S is the inner cross-sectional area, and $Sv(x, t)$ is the volume velocity, expressed in m s^{-3} .

The acoustic impedance has since become one of the most important quantities in acoustics. Basically, it characterizes the resistance of a medium (material or fluid) facing incident sound waves. This quantity can be useful for determining, for instance, the properties of acoustic components. The impedance concept in acoustical systems is, however, ambiguous compared to electrical systems. Unlike with electrical quantities, there does not exist neither "acoustical emf", nor impedance stated in terms of "unit charge". This approach does not invoke the concept of electromagnetic potential, which would lead to an acoustical analogy in the potential energy per unit displacement ξ of fluid, while p^2 is proportional to the potential energy per unit volume $dV = d\xi$ of fluid [35].

Nevertheless, the comparison of sound pressure to electrical emf has led to various definitions of impedance in the context of acoustical engineering. According to the American Standard Association (ASA), should be considered [34]:

¹ac: alternating current

2.3. Concept of impedance

$Z_a = p/(Sv)$ the acoustic impedance of a medium on a given surface S lying in a wave front, which is the complex quotient of the sound pressure p on that surface divided by the volume velocity Sv through the surface; its unit is the acoustic ohm of dimension Pa s m^{-3} ,

$Z_m = Sp/v$ the mechanical impedance which is equal to the ratio of the forced exerted over a given area to the resulting linear velocity produced; its unit is the mechanical ohm of dimension N s m^{-1} ,

$Z_c = \rho c$ the characteristic impedance of a medium in which sound waves are traveling; it corresponds to the specific acoustic impedance at a point in a progressive plane wave propagated in a free field; it is expressed in Pa s m^{-1} ,

$Z_s = p/v$ the specific acoustic impedance of a medium on a given surface lying in a wave front, which is the complex quotient of the sound pressure on that surface divided by the linear velocity v ; it is expressed in Pa s m^{-1} ,

$z = Z_s/\rho c$ the specific acoustic impedance ratio, which is the ratio of specific acoustic impedance to the characteristic impedance of the medium; it is a dimensionless parameter.

The use of these definitions depends on the benefits that each provides to address a specific problem. For instance, the specific acoustic impedance Z_s is useful for computing the solution to boundary-value type problems. A typical example is the computation of the magnitude of standing waves along a duct to determine the acoustic properties of materials [36].

Mechanical impedance and mobility (or admittance) concepts became popular when the analysis of electroacoustic transducers were addressed by drawing an analogous electric circuit. The major interest was to take advantage of the powerful and well-developed techniques of circuit theory [11, 37]. In ac circuits, admittance parameter is used to describe the current response of a linear electrical network composed of resistances and reactances to a driving voltage, taking into account the phase difference between them. By analogy, the admittance parameter of an electromechanical system (eg. a transducer) defines the diaphragm velocity response when subjected to a driving force. In general, mechanical admittance would seem more appropriate for analytical purposes since the reaction to a driving force is to be determined, and not the contrary. From a physical point of view, mobility describes the response of the system upon the application of a force, whereas impedance describes the effect on the resultant force of the application of a velocity [38]. Notwithstanding this, impedance has become the most popular of the two concepts.

2.4 Active noise cancellation

Pioneering idea

The pioneering idea of reducing noise by antinoise through active technologies was first proposed by Lueg in the 1930's [14]. This early formulation of active noise cancellation (ANC) described how to cancel sinusoidal tones in a duct according to the principle of destructive interferences, as shown in Fig. 2.1.

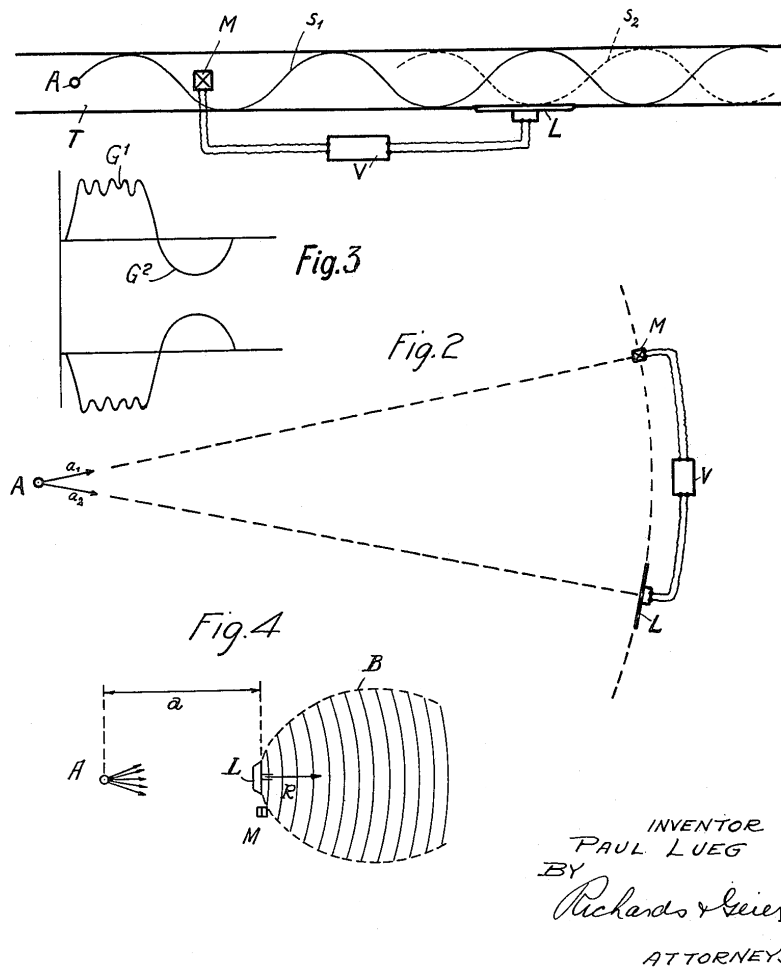


Figure 2.1: Process of silencing sound oscillation, as illustrated by Lueg (1936).

The first laboratory experiments on active noise cancellation were documented by Olson and May in the 1950's [15]. Unlike the disposal described in [14] a microphone is employed to send back a control signal to a loudspeaker used as a secondary source, resulting in a reduction of sound pressure near the microphone. By closing the loop, Olson introduced the principle of feedback control in the field of noise control engineering.

Adaptive noise cancellation

Modern ANC architectures are commonly based on feedback or feedforward control algorithms. Basically, feedforward techniques need a reference signal which is filtered before being applied downstream in order to cancel the acoustic disturbance. As in open-loop control systems, the performance of a feedforward system is extremely sensitive to the "plant" environment and filter variation [18, 19]. Commercial applications of such coherent active control systems include the noise reduction in aircraft, vehicle, or helicopter cabins, but in these situations protection is mainly restricted to periodic noise such as engine-, propeller- or rotor-induced noise [19, 24, 29].

Unwanted sound characteristics are generally time-varying and the environment in which sound waves propagate can fluctuate, thus requiring a constant update of the control signal intended to the secondary sources. In the 1990's, the joint development of microcontrollers and digital signal processing made possible the realization of adaptive noise cancellation. Although the concept of adaptive filtering is simple, its implementation requires significant resources to provide good performance in real time. The benefit provided relies on an accurate control of secondary sources at any moment and without any external action [18]. Since this technological breakthrough, the most common techniques of ANC generally use some kind of adaptive feedback or feedforward algorithms to tackle real-world noise problems [18, 19, 27, 39], which can be combined with passive materials [12, 22, 25, 30, 40].

Practical issues for room applications

Some practical issues limit the application of ANC techniques in the context of architectural acoustics. The sound field in a large enclosure can be complex, the result of multiple reflections of sound waves on the walls and of possible variations in the medium (temperature, hygrometry). It results practical issues to both observe and globally control the sound field. The number of sensors and actuators required to provide spatially extended efficiency become rapidly prohibitive. Active noise control is still currently the subject of much research because many practical issues are far from being solved. The pending issues mainly relate to optimizing the number and location of control sources, the management of multichannel systems, or the development of control algorithms efficient and robust enough to deal with all kinds of noise [18, 19].

Another key issue is related to the transducers used to sense and counteract the unwanted sound. Generally speaking, the physics of enclosed sound fields and processing algorithms are often favored over the coupling of actuators with the medium in which they are supposed to interact. A loudspeakers used as secondary source cannot be considered as an ideal source of volume velocity over the entire frequency range of interest. The frequency response of the bandpass type of most electroacoustic transducers can cause a phase shift which may affect the stability of the closed loop control system [41]. Even

more than for audio reproduction systems the choice of electroacoustic transducers is of primary interest. Another important aspect is the coupling between the actuators and the sound field. The strong interaction between the dynamics of control sources and the sound field usually results in complications that occur when the wavelength of the sound waves coincide with the geometrical dimensions of the room [8, 9, 41–43]. The mechanical impedance of the loudspeaker diaphragm is much higher than the acoustic load in which it radiates. As a consequence, the sound pressure resulting from the diaphragm oscillation will vary depending on the acoustic load. To overcome some of these practical issues, an alternative strategy has emerged. By placing the loudspeaker in the heart of the noise control process, the goal is then to control the acoustic impedance at its diaphragm. The following will review the main ways to achieve acoustic impedance control.

2.5 Impedance based control

Drawing on the concept of "electronic sound absorber" introduced by Olson and May in the 1950's [15], and then on that of "active electroacoustic transducer" proposed by Bobber in the 1970's [44], an alternative to ANC techniques has emerged. Instead of canceling some unwanted tones in a sound field according to the principle of destructive interferences, the idea is to act on the boundaries of the acoustical domain. The main objective is to absorb part of the incident acoustic energy through a simple control of transducers dynamics [25, 45–49].

Transmission lines

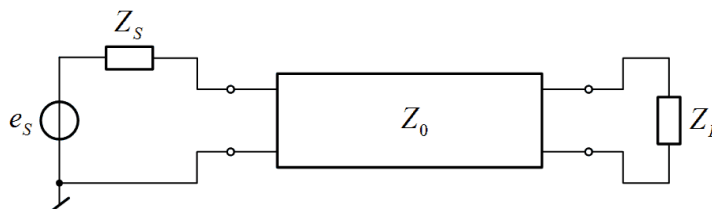


Figure 2.2: Schematic representation of a transmission line. The source is represented as a Thévenin source e_s and Z_s , Z_0 is the characteristic impedance of the medium where waves propagate, and Z_L is the load impedance.

The easiest way to introduce the concept of impedance control is to consider the transmission lines theory. An electrical transmission line is commonly modeled as a two-port network, as depicted in Fig. 2.2. When the transmission line is uniform, its behavior may be described by a single parameter called the characteristic impedance of the medium and denoted Z_0 . In electrical engineering, impedance matching is the practice of designing the input impedance of an electrical load in order to maximize the power transfer and minimize reflection from the load.

Acoustic impedance matching

Similar to transmission lines in electrical engineering, impedance matching can be applied when transferring sound power from air to an acoustic load. By "acoustic load", we mean a material the surface of which is subjected to incident sound waves. When the apparent acoustic impedance of this interface differs much from the characteristic impedance of the medium, most of the sound energy will be reflected; otherwise part of sound energy is absorbed [26].

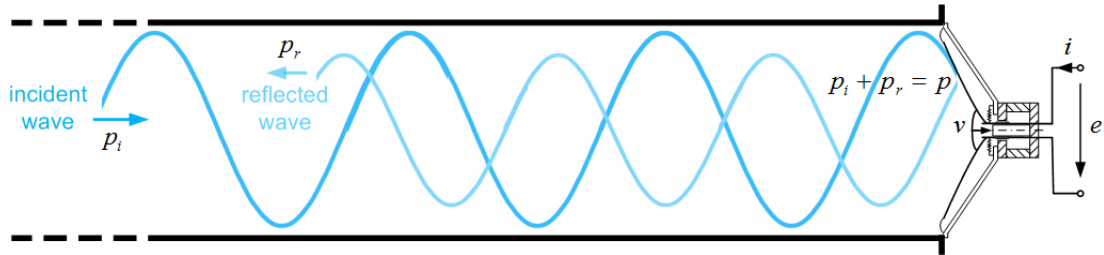


Figure 2.3: Basic principle of acoustic impedance control in a semi-infinite duct. An incident sound wave p_i propagates from a source located at infinity and is reflected on the diaphragm of an electroacoustic transducer with an amplitude p_r .

Basically, a smooth rigid-walled duct whose lateral dimensions are small enough compared to the wavelength can be considered as a non-dissipative acoustic transmission line [3]. The resulting sound field from the source to the load is made of two plane waves traveling in opposite directions. In Fig. 2.3, the acoustic load is a direct-radiator loudspeaker. When no reflection is desired, the specific acoustic impedance presented by the material interface with the medium should equal the characteristic impedance of the medium [44], i.e. $Z_s = Z_0$. Obviously, the diaphragm is reflective when the value of load impedance moves away from the characteristic impedance Z_0 . To prevent all reflection of incident sound waves the load must be matched exactly to the impedance of the acoustical transmission line, implying that both should be totally resistive. Real-world problems in acoustical engineering usually involve complex impedances for both the load and the acoustic radiation conditions. In the case of a material with a complex surface impedance (eg. a loudspeaker diaphragm), the reactive part of the load may lead to a mismatch with the characteristic impedance. The purpose of the strategies discussed below is to investigate ways to address this problem.

Active control approach

Active techniques based on the feedback control of acoustic variables are commonly applied in view of reduction of unwanted sound, systems stabilization, attainment of some desired transfer function, or improvement of a system's robustness to changes in its open-loop dynamics [15, 27, 46, 48, 50–53].

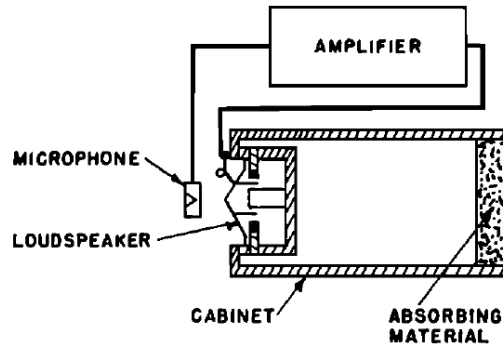


Figure 2.4: Concept of electronic sound absorber, as illustrated by Olson & May (1953).

In [15], the pressure-release condition is achieved by feedback control, thus leading to active noise reduction near a microphone collocated with the controlled loudspeaker, as depicted in Fig. 2.4. In [46], the active control of acoustic impedance is implemented at the end of a duct by using a velocity-controlled loudspeaker and a microphone. The common feature of all these strategies is to absorb (or reinforce) incident sound energy by controlling the dynamics of the actuator. For assigning a desired acoustic impedance, one technique is to drive the transducer with a command voltage that is proportional to a linear combination of the sound pressure and velocity in its vicinity [20, 25, 49, 54]. Another possibility results in getting a feedback controller that minimizes in the least squares sense an error signal based on these acoustic quantities. This is achieved through the development of an optimal quadratic regulator [55]. A common feature to these methods is the need to sense acoustic pressure and/or velocity in the vicinity of the electroacoustic device which is intended to noise control. Notice that the collocation of the actuator and the sensor plays an important role in the stability and the performances of the controlled device, especially when active elements are distributed within arrays [56].

Passive control approach

Passive control approach is often referred as "shunt-based" technique since it consists of connecting an electrical matching network to a transducer. This strategy has been first investigated in the context of damping of structural resonances with piezoelectric transducers.

As detailed in [57], shunting with a resistor and inductor introduces an electrical resonance, which can be optimally tuned to structural resonances in a manner analogous to a mechanical vibration absorber (see Fig. 2.5). Subsequently, shunt-based methods have been adapted to electrodynamic loudspeakers in view of damping a resonant sound field [43].

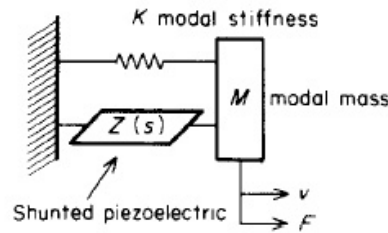


Figure 2.5: Passive piezoelectric structural damping, as illustrated by Hagood (1991).

"Semi-active" control approach

The technique known as "semi-active" follows directly from the passive shunt approach. By semi-active control, we mean electrical shunt networks that require energy to work. First introduced by Bobber [44] in the context of underwater electroacoustic measurements, and recently reconsidered by Fleming *et al.* [43], it is another way to turn an electroacoustic transducer into a sound absorber. Instead of feeding back a command voltage proportional to relevant acoustic variables, an electrical matching network is connected across the terminals with a view to altering the transducer dynamics.

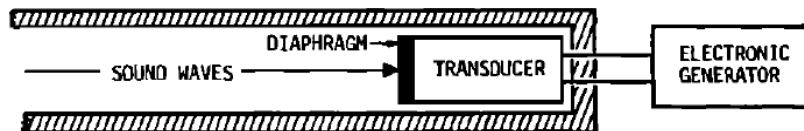


Figure 2.6: Concept of active electroacoustic transducer, as illustrated by Bobber (1970).

In [44], an electroacoustic actuator is driven such that it behaves as the characteristic impedance of an acoustical transmission line. In short, an electronic generator consisting of an oscillator and circuitry for the control of phase and amplitude is connected to the transducer terminals in view of enhancing the particle velocity through the transducer. The primary function of the electronic generator is to impose a voltage across the transducer terminals that will have the effect of canceling the voltage drop across the reactance. Once the reactance has been compensated, it remains to adjust the apparent acoustic resistance of the transducer so as to match the characteristic impedance of the medium. This ascertainment is the reason for using active circuitry (such as negative impedance converters) in view of obtaining a broadband control [43, 44]. With a pure resistive load (eg. a basic resistor), acoustic impedance matching can be achieved around natural mechanical resonance of the transducer only. [43, 58].

2.6 Sensorless control

Control systems that achieve the desired performance without sensors are increasingly attractive. Reasons for this include cost reduction, an increased reliability and noise immunity, and less maintenance [59]. In order to remove the sensor, information on the relevant mechanical variable is usually extracted from electrical quantities measured at the transducer terminals [60–62]. Some open-loop estimators or closed-loop observers are commonly used to that purpose. They differ in terms of accuracy, robustness, and sensitivity with regard to model parameter variations. In induction motors for instance, ongoing research has concentrated on the elimination of the speed sensor at the machine shaft without deteriorating the dynamic performance of the drive control system [63].

In [62], the vibrations of a mechanical structure are damped by measuring the voltage at the coil terminals and applying a related current to an electromagnetic actuator, or vice versa. It is shown that sensorless control is feasible through synthesis of active shunt impedances. The "synthetic" impedances are designed with the help of optimal control theory and require some precise knowledge to the transducers dynamics. By revealing the underlying feedback structure of electromagnetically actuated systems, the problem is addressed as a standard multi-input, multi-output (MIMO) control problem. The regulation of electrical quantities across the actuator terminals is obtained by applying synthesis techniques such as linear quadratic regulator (LQR) and \mathcal{H}_2 [55, 64]. By involving \mathcal{H}_2 or LQR, the problem of controlling the transducer comes down to a classic optimization problem, i.e. find a causal controller which stabilizes the system while minimizing a cost function. More details can be found in [62].

Few references concerning sensorless control of electroacoustic transducers have been published. In [65], sensorless control means using a self-sensing velocity observer as input of the controller. Through control theory also, the feedback \mathcal{H}_∞ robust control and feedforward \mathcal{H}_2 model matching control are implemented to achieve robust stabilization and tracking performance. Here, robust control is used to deal with uncertainty in the approach to controller design. In \mathcal{H}_∞ methods, the control problem is expressed as a mathematical optimization problem. The goal is to synthesize a controller that achieves robust performance and stabilization, especially for multivariable systems. Drawbacks of \mathcal{H}_∞ techniques include the level of mathematical understanding required to apply them successfully and the need for a reasonably good model of the system to be controlled.

Discussing the interest of methods for sensorless control requires a thorough understanding of the dynamic properties of the transducer to be controlled. Current and potential applications of sensorless control include: vehicle suspension systems, vibration isolation platforms, or control of enclosed sound fields, i.e. dynamic control applications for which the reciprocity of transducers can be used advantageously.

2.7 Conclusions

In this chapter, a short review of the key concepts involved in noise control have been discussed with an emphasis to surface impedance control using electroacoustic transducer. It clearly appears that an impedance based control is the most appropriate strategy with a view to room applications. Practically speaking the technical implementation can be active or passive, and sometimes the result of advantageous combinations with porous layers. Active methods generally involve sensors and control systems, and require algorithms in order to process the sensed acoustic signals. It is often referred to as "direct acoustic impedance control" in the literature. Passive methods are basically implemented by connecting some electrical matching networks, made of dipoles arranged in series or parallel, to the transducer terminals. The technique is often referred to as "shunt loudspeaker". These control strategies are different ways to turn a loudspeaker into a noise control device. Chapter 5 will address the feedback control techniques by relying on control theory. Chapter 6 will investigate the intake of the shunt-based approach from the electrical engineering perspective. The idea of unifying these two approaches, or even merging them so as to further alter the acoustic impedance at the transducer diaphragm, is one of the motivations for this thesis. This topic will be specifically discussed in Chapter 7.

3 Electrodynamic loudspeaker: description and modeling

3.1 Introduction

Electroacoustics is an engineering science combining acoustics and electrical engineering. Its object is the study, design and realization of audio devices generally intended to the production, transmission, reproduction, measurement or recording of sound. All areas of applied acoustics involve electroacoustic devices, be it musical, industrial or architectural acoustics, biomedical, nondestructive testing, active noise control, etc. The design of transducers is usually based on specifications according to desired performances (directivity, efficiency, sensitivity, bandwidth, etc.), as well as technological and practical constraints.

The electroacoustic transducer is the device involved within the transformation from acoustical to electrical energy and vice versa [11, 66]. Generally speaking, the term transducer is used to describe actuating (transmitting) and sensing (receiving) functions. Principles of coupling can be broadly classified according to whether the mechanical forces are produced by the action of electric fields on electric charges, or by the interaction of magnetic fields and electric current [66]. When used as an actuator, electrical energy is converted into acoustical energy, while used as a sensor the conversion is in the opposite direction. Transducers are passive if all the energy delivered to the electric (or acoustic) load is obtained from the energy accepted by the transducer from the acoustic (or electric) source. Conversely, when part of the energy comes from an auxiliary source, the transducer is active [11].

The vast majority of transducers combines a mechanical structure (the diaphragm) and an electrical system that senses the motion or provides a force for actuation. In the thesis, we will limit the discussion to a direct-radiating electrodynamic loudspeaker [67]. This type of transducer is essentially designed to radiate sound power in air in the audio-frequency range [11].

Chapter 3. Electrodynamic loudspeaker: description and modeling

This chapter aims to provide the basis for the analysis of electrodynamic loudspeakers while dissipating certain ambiguities sometimes encountered in the literature. The purpose is to properly formulate the interactions between electrical current and magnetic field that define the coupling equations of the transducer. The idea is to have a better insight into electromagnetic phenomena related to a vibrating structure (the diaphragm), and to determine what current in – or motion of – an electric conductor is capable of producing an electromechanical effect.

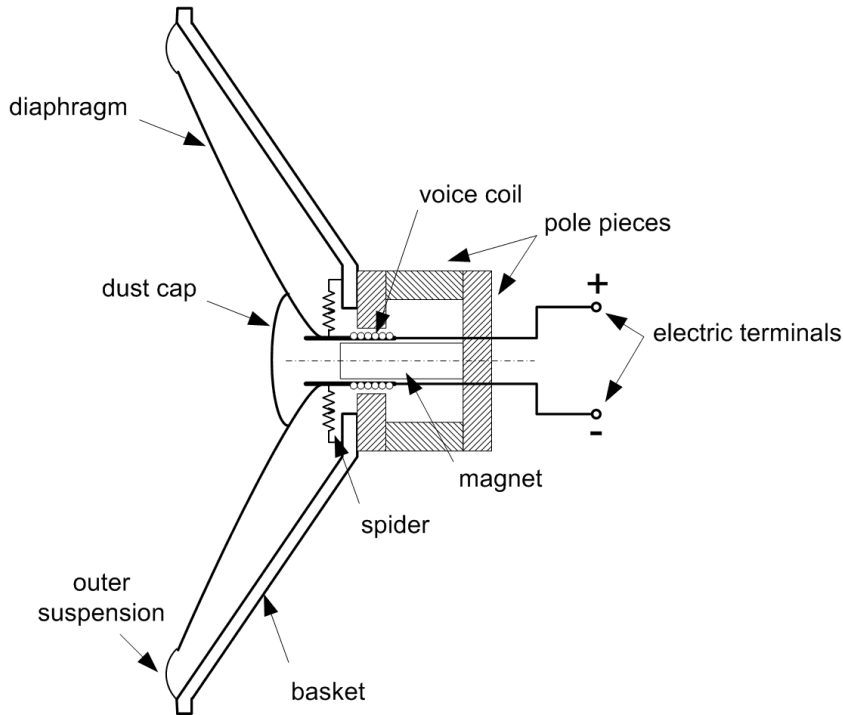


Figure 3.1: Sectional view of an electrodynamic loudspeaker.

3.2 Core assumptions

3.2.1 Linearity

Modeling an electrodynamic loudspeaker requires some assumptions. The first hypothesis concerns the operating conditions of the system and especially the linearity. From an acoustic or mechanical point of view, all forces acting on the system are small enough so that the displacements remain proportional to applied forces. Transducers are linear if the variables describing their output, such as sound pressure and normal velocity (or voltage and current), are linear functions of the related quantities describing the transducer input. It is then assumed that the loudspeaker driver is operated in the "small-signal" range [11]. Otherwise, some of the loudspeaker's parameters may become time-varying nonlinear functions which depend on the diaphragm displacement amplitude [68–71].

3.2.2 Fundamental radiation hypothesis

The sound field produced by an electrodynamic loudspeaker results from the vibration of its diaphragm, and the communication of the vibratory movement to the surrounding fluid. Airborne or structure-borne sound is at the origin of the medium's disturbance being propagated in the form of a wave. When the source is an electroacoustic transducer the primary function is to drive the immediately neighboring particles of the medium. Sound radiation is conditioned by the transducer diaphragm, i.e. the surface of the moving part in contact with the medium [72]. Experiments show that when diaphragm and medium are in motion they remain in contact: there are neither detachment nor fluid rotations at the interface [11]. Therefore, the normal velocity is the representative quantity of the diaphragm and fluid's movement. On any element dS of the interface between a loudspeaker diaphragm and air, the continuity of fluid and structure velocities leads to

$$v_s \mathbf{n} = v \mathbf{n} \tag{3.1}$$

where \mathbf{n} is the unit-normal in dS , v_s is the velocity of the diaphragm (structure), and v is the particles velocity (fluid). The friction force of the fluid on the diaphragm are usually negligible and the applied forces are normal to the axis of motion. The fundamental radiation hypothesis is only valid if the velocity magnitude is not too high, i.e. in the limit of nonlinearity in the medium [11].

3.2.3 Piston-like movement

When a loudspeaker is intended to serve as an acoustic absorber or reflector, the diaphragm must be viewed as a complex refracting surface. One hypothesis assumes that the force of reaction in each point of the surface is proportional to the velocity communicated by the sound field [3]. In accordance to the principle of equality of the action and reaction, and taking the continuity condition given by Eq. (3.1) into account, the relationship is linear for small displacements and the velocity normal to the surface is proportional to the pressure. In other words, we consider a piston-like movement which is not affected by fluid motion tangential to the diaphragm.

3.2.4 Transducer reciprocity

In the context of electroacoustic transducers, the reciprocity principle describes their ability to operate in both direction. Roughly speaking, it states that the ratio of the "microphone function" of the transducer to its "loudspeaker function" is a quantity which is independent of the nature and construction of the transducer [73, 74]. Electroacoustic transducers are referred to as reciprocal when the electromechanical coupling coefficients are equal in absolute value. When this is so, the diaphragm velocity at one side of

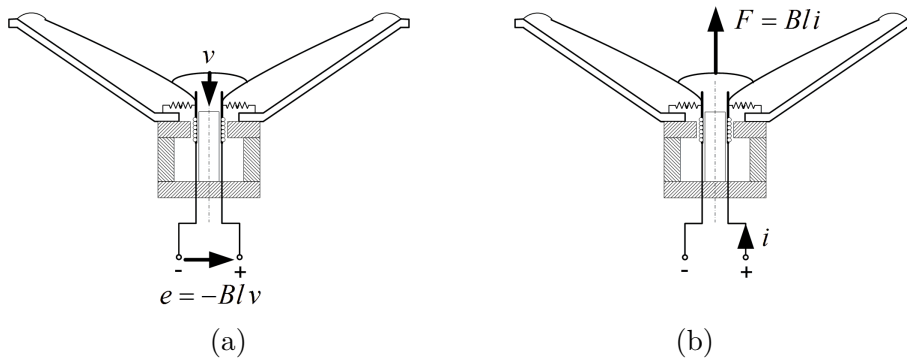


Figure 3.2: Schematics of a loudspeaker operating as sensor (a) and actuator (b).

the transducer, resulting from a driving pressure force on the other side, has the same direct proportionality to the applied force as when the locations of driving force and velocity are interchanged. Such feature is similar to that found in many systems involving electromagnetic or mecano-acoustical conversion [66]. For transducers of the electrostatic or piezoelectric type, the transduction coefficients are bilateral, i.e. symmetrical. For transducers of the electrodynamic or moving conductor type, the transduction coefficients are identical in magnitude but reversed in algebraic sign, as it will be seen in the next section. The validity of the reciprocity conditions for a transducer that is linear and passive will depend upon the nature of the materials employed in its construction and the type of electromechanical conversion [73].

3.3 Electrodynamic conversion

Electrodynamic conversion is a principle of transduction where motor and generator action are produced by the current in, or the motion of, an electric conductor located in a fixed transverse magnetic field [75]. In audio, the most common realization of the electrodynamic conversion involves a moving coil conductor in the form of a cylindrical coil, the axis of which determines the axis of motion.

As shown in Fig. 3.1, the moving coil is a solenoid that has partially iron and partially air core. For the magnetic force to be along this axis, the magnetic flux density has to be radial. To meet this requirement, the coil of a loudspeaker, which is commonly referred to as "voice coil", is thus placed in a ring-shaped gap in a magnetic circuit, made up of a permanent magnet and pole pieces, as depicted in Fig. 3.1. By involving electrodynamic conversion, the laws of induction have to be considered so as to take into account the motion of the voice coil when immersed in a magnetic field [76]. When operating in sensing mode, the coil is driven by the mechanical system subjected to exogenous forces. In actuating mode, conversely, an input voltage applied to the coil terminals will drive the mechanical system [11, 77].

3.3.1 Electromagnetic force

The principle of the electrodynamic conversion using a moving coil is illustrated in Fig. 3.3. It is assumed here that an electrical current i is running through the wire in the counterclockwise direction and that the magnetic flux density at the location of the wire is constant over time and position and radially oriented, i.e. $\mathbf{B} = -B_0 \mathbf{e}_r$. Since there is no electric field, the Lorentz force, which is defined as the force on a point charge due to electromagnetic fields, is given by

$$\begin{aligned}
 d\mathbf{F} &= dq \mathbf{v}_c \times \mathbf{B} \\
 &= dq \frac{d\mathbf{l}}{dt} \times \mathbf{B} \\
 &= \frac{dq}{dt} d\mathbf{l} \times \mathbf{B} \\
 &= i d\mathbf{l} \times \mathbf{B}
 \end{aligned} \tag{3.2}$$

where \mathbf{F} is the force expressed in N, q is the electric charge expressed in C, \mathbf{B} is the magnetic flux density expressed in T, \mathbf{v}_c is the instantaneous velocity of the particle expressed in ms^{-1} , and the current is given by the amount of charge dq carried per time interval dt , $i = dq/dt$. The infinitesimal vector element of the contour $d\mathbf{l}$ can be expressed as

$$d\mathbf{l} = R d\theta \mathbf{e}_\theta \tag{3.3}$$

where R is the radius of the wire loop. From the notation of Fig. 3.3, Eq. (3.2) can be rewritten

$$\begin{aligned}
 d\mathbf{F} &= i R d\theta \mathbf{e}_\theta \times (-B_0) \mathbf{e}_r \\
 &= -i B_0 R d\theta (\mathbf{e}_\theta \times \mathbf{e}_r) \\
 &= +i B_0 R d\theta \mathbf{e}_z
 \end{aligned} \tag{3.4}$$

Equation (3.4) represents the force per angular element $d\phi$. The total force is then

$$\begin{aligned}
 \mathbf{F} &= \int_{\theta=0}^{2\pi N} i B_0 R d\theta \mathbf{e}_z \\
 &= i B_0 R \int_{\theta=0}^{2\pi N} d\theta \mathbf{e}_z \\
 &= i(2\pi R) N B_0 \mathbf{e}_z \\
 &= B_0 l i \mathbf{e}_z
 \end{aligned} \tag{3.5}$$

$l = 2\pi RN$ is the total length of the conductor. After projection along the axis of motion, Eq. (3.5) yields the general form the electrodynamic coupling equation on the

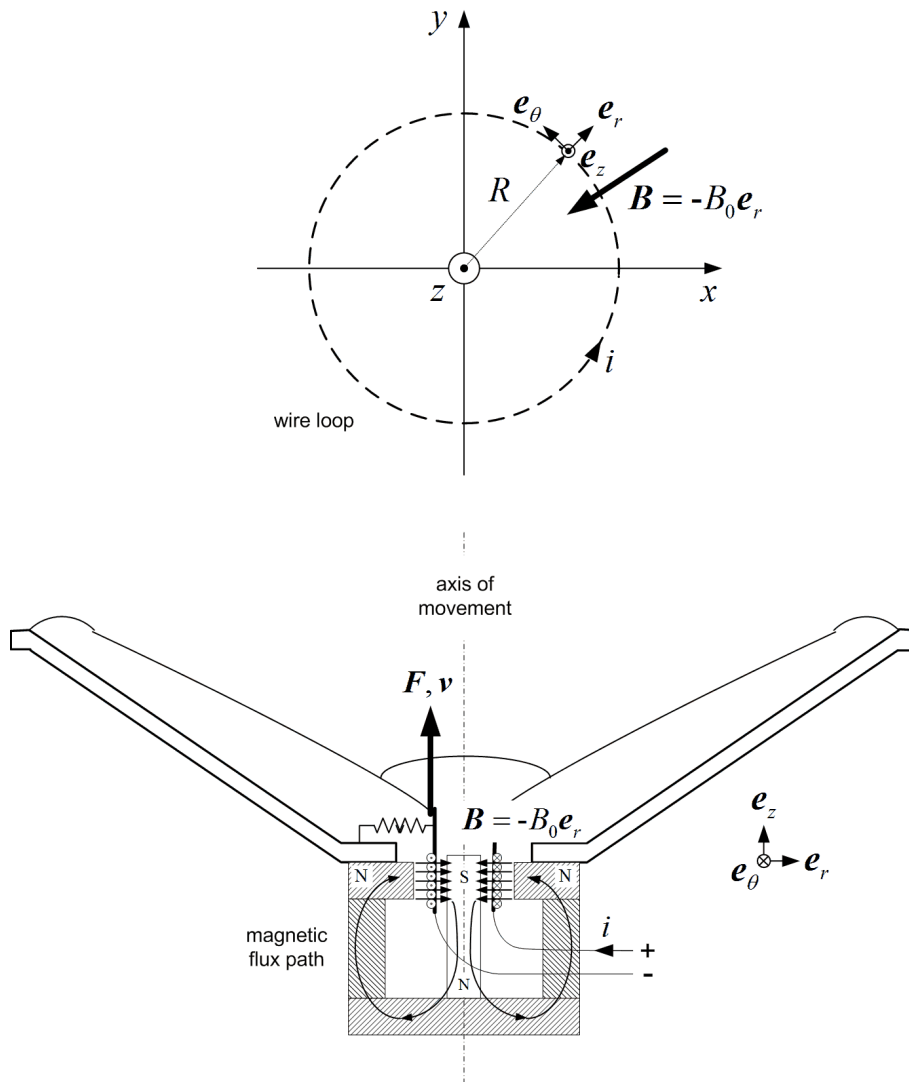


Figure 3.3: Principle of electrodynamic conversion using a moving coil.

mechanical side

$$F = Bl i, \quad B = |\mathbf{B}| = B_0 \quad (3.6)$$

where Bl is the electrodynamic coupling coefficient, or force factor, expressed in N A^{-1} or in Tm . As a result, the interaction of the current flowing in the coil and the magnetic flux density generates a mechanical force that causes the coil, and thus the attached diaphragm, to move back and forth. In the context of an "ensemble" of particles, the sum of Lorentz forces on the individual particles is called Laplace force, which is the typical case in a current-carrying wire.

3.3.2 Motional electromotive force

Basically, the electromotive force (emf) in a voice coil is equal to the rate of change of the magnetic flux through the coil. It applies when the magnetic flux is altered, either because the strength of magnetic force changes¹ or because the coil is moving (or both) [75]. As soon as the coil begins to move, in response to the generated force for instance, a voltage is induced in it, caused by its motion in the magnetic field. For a current i and a magnetic flux as in Fig. 3.3, the force is oriented in z -direction resulting in the velocity $\mathbf{v} = v_0 \mathbf{e}_z$. Here, \mathbf{v} is the velocity of the coil and must be distinguished from \mathbf{v}_c which is the speed of the charges yielding the current i .

According to the Lorentz force, when a coil is moving with a velocity \mathbf{v} in a uniform magnetic field, the charge distribution will change and the electromotive force (emf) is given by

$$\varepsilon = \oint (\mathbf{v} \times \mathbf{B}) \cdot d\mathbf{l} \quad (3.7)$$

After some further manipulations, the induced emf can be expressed as

$$\begin{aligned} \varepsilon &= - \int_{\theta=0}^{2\pi N} v_0 B_0 R \, d\theta (\mathbf{e}_z \times \mathbf{e}_r) \cdot \mathbf{e}_\theta \\ &= -v_0 B_0 R \int_{\theta=0}^{2\pi N} d\theta \\ &= -v_0 B_0 (2\pi R) N \\ &= -v_0 B_0 l \end{aligned} \quad (3.8)$$

With the normal velocity $v = |\mathbf{v}| = v_0$, the electrodynamic coupling equation from the electrical side can be written

$$\varepsilon = -Blv, \quad B = |\mathbf{B}| = B_0 \quad (3.9)$$

Since the emf is associated with the motion of the coil through the magnetic field, it is called motional emf. The motional emf induced in the circuit is thus directly proportional to the velocity of the voice coil. If the terminals of the coil are connected with a circuit providing a return path for the accumulated charges, the coil becomes a voltage source. The minus sign indicates that ε always strives to oppose the action that caused it, in accordance to the Lenz law. Consequently, ε has such polarity that it tends to reduce voice coil's current. As it will be seen in the next chapter, this mechanism can provide electrical damping to the loudspeaker.

¹Note that in our hypothesis, the linearity assumption prevents from considering the case where the magnetic field varies along the coil displacement; but this can also be taken into account considering [70].

3.3.3 Induced electromotive force

A change in the magnetic flux passing through a loop of conductive wire will also cause an induced emf, and therefore an electric current [76]. After Faraday's law of induction, which states that the induced electromotive force (emf) in any closed circuit is equal to the time rate of change of the magnetic flux through the circuit, the inductive emf in the moving coil is given by

$$\varepsilon = -N \frac{d\phi}{dt} \quad (3.10)$$

where N is the total number of turns, and ϕ is the magnetic flux, expressed in Wb. The magnetic field inside an ideal solenoid is

$$B = \frac{\mu N}{h} i \quad (3.11)$$

where μ is the permeability of the core of the coil, h is the height of the coil, and i is the current flowing in the coil. If the coil has a radius R , then the magnetic flux in it is

$$\begin{aligned} \phi &= \iint \mathbf{B} \, d\mathbf{S} \\ &= -B \mathbf{e}_r \iint d\mathbf{S} \\ &= \pi R^2 \frac{\mu N}{h} i \end{aligned} \quad (3.12)$$

and the induced emf becomes

$$\begin{aligned} \varepsilon &= -\pi R^2 \frac{\mu N^2}{h} \frac{di}{dt} \\ &= -L_e \frac{di}{dt} \end{aligned} \quad (3.13)$$

where $L_e = \pi R^2 \mu N^2 / h$ is the inductance of the coil considered as an ideal solenoid. It depends on the square of the number of turns and how easy the flux of the voice coil is able to flow. Since the emf is due to a change in the current through the coil it is called self-induced emf.

3.3.4 Polarity and sign convention

Maintaining a correct phase relationship between electrical variables, and between acoustical ones is an essential condition to the proper implementation of a loudspeaker. This is especially true when it is subjected to dynamic control. In audio engineering, absolute phase or polarity refers to the preservation of initial acoustic waveform all the way through the recording and reproducing system. In this way, a compression that reaches the recording microphone will be reproduced by the audio diffusion system as a

compression reaching the ears of a listener. In the context of active control of acoustic impedance, the absolute polarity of input voltage must also be properly applied across the transducer terminals. By the term "absolute polarity" we mean here the correct arrival of the command signal with respect to the control objective. A leading edge in the control signal must generate a positive pressure wave (or compression), and not vice versa. Applying a signal with wrong polarity may cause unexpected or unstable behavior of the loudspeaker.

Using the sign convention $d\mathbf{l} = R d\theta \mathbf{e}_\theta$ as in Fig. 3.3, the electrodynamic coupling equations are given by Eq. (3.6) and Eq. (3.9). In other words, if the positive direction of ε and i , and of F and v , coincide, these scalar relations are $F = Bl i$, and $\varepsilon = -Bl v$. This underlines the antisymmetry of moving coil transducers. Therefore, a proper analytical formulation of the electrodynamic transduction principle must always include rules for determining the direction of the mechanical and electromotive forces arising from the interaction between magnetic field and electrical current.

As a practical matter, the transducer may possibly be in inverted polarity with respect to the command signal coming from the controller. Such situation would mean to force the driver to "pull" when it is supposed to "push" so as to counteract acoustic disturbances. Correct polarity with active loudspeakers under voltage-drive is simply the one that produces the right polarity at the diaphragm. It is then essential to determine unequivocally whether the whole system (sensors, controller, and transducer) inverts polarity or not, from component to component. By the way, depending on the windings of the voice coil, there is an even chance that a reversal polarity occurs. A trial and error approach may help in determining proper orientation. If a phase reversal switch is not available on the controller one must invert polarity at the loudspeaker's electrical terminals.

3.4 Motional equations

3.4.1 Lumped parameter model

A lumped parameter model is a type of representation in which the electrical and mechanical parameter values are considered to be represented by a quantity concentrated at a location in space [11]. In this thesis, it is assumed that the voice coil and all parts of the diaphragm move in phase with the same amplitude. Furthermore, the mass of the system, the effective stiffness and the mechanical resistance to the movement are regarded as lumped constants. This approximation is valid as long as system dimensions are well below the wavelength of interest (corresponding to a one-dimensional plane wave propagation). It is quite coarse and the results obtained using lumped parameter models are to be considered as indicative of the direction of evolution of the phenomenon, rather than a rigorous numerical evaluation.

3.4.2 Newton's second law

An electrodynamic loudspeaker is made up of a moving body comprising a diaphragm, a dust cap, and a coil, the whole being brought back to the equilibrium position through suspensions, as depicted in Fig. 3.4. The coil is interdependent of the mechanical system and is immersed in a magnetic field from a permanent magnet fixed to the loudspeaker's frame.

Applying Newton's second law to the moving mass of the loudspeaker yields

$$-M_{ms} \frac{d\mathbf{v}}{dt} = \frac{1}{C_{ms}} \xi(t) \mathbf{e}_z + R_{ms} \mathbf{v}(t) - Bl i(t) \mathbf{e}_z + \mathbf{F}_+(t) + \mathbf{F}_-(t) \quad (3.14)$$

where

\mathbf{v} is the normal velocity of the diaphragm, in m s^{-1}

ξ is the displacement of the diaphragm, in m

i is the electrical current, in A

\mathbf{F}_+ is the total exogenous force acting on the diaphragm, in N

\mathbf{F}_- is the total force acting on the rear face of the diaphragm, in N

M_{ms} is the combined mass of the diaphragm, suspensions, and voice coil, in kg

C_{ms} is the equivalent compliance of both the outer suspension and spider, in N m^{-1}

R_{ms} is the mechanical resistance due to loss in the suspensions, in N s m^{-1}

Bl is the force factor, in N A^{-1} or Tm

When the diaphragm is subjected to surrounding sound field, the driving force is

$$|\mathbf{F}_+| = Sp \quad (3.15)$$

where p is the sum of the incident and reflected sound pressure at the surface of the diaphragm.

When the loudspeaker is loaded by a rear volume V_b , \mathbf{F}_- is the reaction of the fluid that acts on the rear face. It is commonly assumed that the rear acoustic load is mainly due to the acoustic compliance $C_{ab} = V_b/(\rho c^2)$ of the enclosure [11]. The effective mechanical compliance of the closed-box loudspeaker is then given by

$$C_{mc} = \frac{C_{ms} C_{ab}}{C_{ab} + S^2 C_{ms}} \quad (3.16)$$

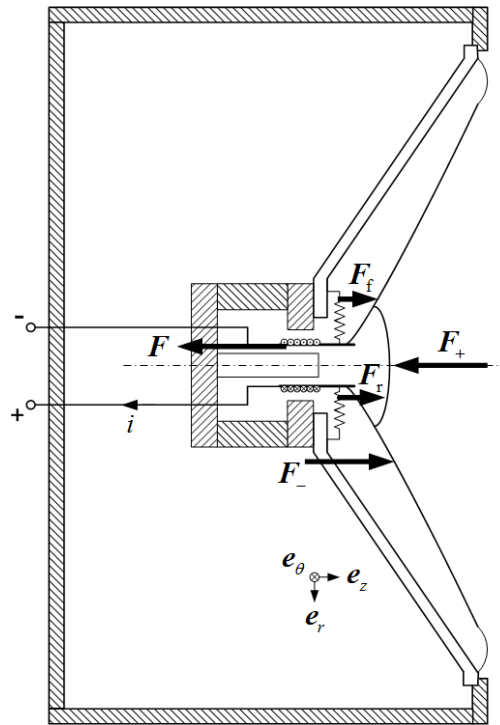


Figure 3.4: Force balance on the loudspeaker diaphragm where $|\mathbf{F}_+|$ is the exogenous pressure force acting on the diaphragm, $|\mathbf{F}| = Bl i$ is due to Lorentz force, $|\mathbf{F}_f| = R_{ms} v$ is the frictional force, $|\mathbf{F}_r| = C_{ms}^{-1} \xi$ is the restoring force, and $|\mathbf{F}_-|$ is the contribution of the enclosure in terms of pressure force.

3.4.3 Kirchhoff's circuit law

Applying Kirchhoff's law to the voice coil of the loudspeaker, the electric dynamics can be modeled with a first-order differential equation

$$e(t) = R_e i(t) + L_e \frac{di}{dt} + Bl v(t) \quad (3.17)$$

where

e is the voltage applied to the electrical terminals, in V

i is the electrical current flowing in the coil, in A

v is the normal velocity of the diaphragm, in m s^{-1}

R_e is the dc resistance of the coil, in Ω

L_e is the voice coil electrical inductance, in mH

Bl is the force factor, in N A^{-1} or Tm

Figure 3.5 illustrates the electrical circuit that is equivalent to the voice coil.

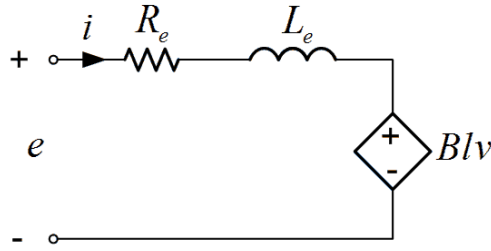


Figure 3.5: Electrical circuit modeling of the voice coil. The variable e is the voltage at the electrical terminals, i is the current flowing in the voice coil, Blv is the motional emf, and the parameters R_e and L_e are the dc resistance and inductance of the coil, respectively.

This model can be further improved by taking into account eddy currents. Eddy currents are created when a conductor (here the voice coil) experiences changes in the magnetic field, in accordance with Faraday's law of induction. As a practical matter, they are responsible, often substantially, for changes in the magnitude and the phase relationship between voltage and current in L_e [68–71].

3.4.4 Characteristic equations

For small displacements and below the first modal frequency of the diaphragm, the generalized governing equations of an electrodynamic loudspeaker subjected to a surrounding sound field can be expressed as

$$\begin{aligned} Sp(t) &= M_{ms} \frac{dv}{dt} + R_{ms}v(t) + \frac{1}{C_{mc}}\xi(t) - Bl i(t) \\ e(t) &= R_e i(t) + L_e \frac{di}{dt} + Bl v(t) \end{aligned} \quad (3.18)$$

A consistent sign convention must be used in order to obtain appropriate transfer functions. Here, outward currents are shown as positive, and inward velocities are considered as positive.

Expressing Eq. (3.18) with the use of Laplace transform yields the characteristic equations of the electrodynamic loudspeaker

$$\begin{aligned} SP(s) &= \left(sM_{ms} + R_{ms} + \frac{1}{sC_{mc}} \right) V(s) - Bl I(s) \\ E(s) &= (R_e + sL_e)I(s) + Bl V(s) \end{aligned} \quad (3.19)$$

where $s = j\omega$ is the Laplace variable.

Introducing the blocked electrical impedance Z_e and the mechanical impedance Z_m , Eq. (3.18) may be rewritten more compactly as

$$\begin{aligned} SP(s) &= Z_m(s)V(s) - BlI(s) \\ E(s) &= Z_e(s)I(s) + BlV(s) \end{aligned} \tag{3.20}$$

where $Z_e = R_e + sL_e$ and $Z_m = sM_{ms} + R_{ms} + 1/sC_{mc}$. The blocked electrical impedance Z_e is shown here comprising the voice coil's dc² resistance R_e plus an ideal inductance L_e .

The characteristic equations allow the basic analysis of an electrodynamic loudspeaker, whatever its use [11]. When operating in "driving" mode, there are no external forces applied to the mechanical system and $SP(s)=0$. When operating in "generator" mode, there is no external electrical source connected to the terminals and $E(s)=0$. Obviously, the two processes have to be considered when the loudspeaker is subjected to a surrounding sound field and simultaneously actuated by an auxiliary electrical source or coupled to an electrical load.

3.4.5 Electrical coupling

In normal operation the voice coil is coupled to other electrical components, passive or active. Two types of electrical coupling are possible: by connecting an impedance load, or by involving an auxiliary electrical source at the transducer terminals. The nature of input voltage should be specified to provide a complete description of the loudspeaker system [73].

By connecting an electrical load impedance Z_L at the terminals, the relationship between e and i is

$$e = -Z_L i \tag{3.21}$$

By involving a source of internal impedance Z_L , the amplifier from which the drive unit is actuated is commonly described as a Thévenin equivalent source [11]

$$e = e_g - Z_L i \tag{3.22}$$

including an auxiliary source voltage e_g . Similarly, the transducer diaphragm is coupled to an acoustic domain which may or may not contain source. When subjected to a surrounding sound field, e_g and Z_L may be tailored so as to alter the behavior of the

²dc: direct current

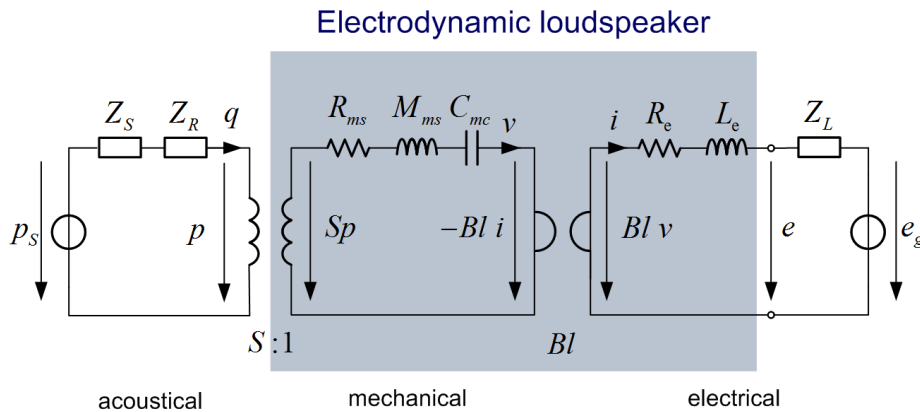


Figure 3.6: Circuit representation of an electrodynamic loudspeaker. This representation in an electric form allows to show what reaction the mechanical system will have upon the electrical system (shown here coupled to a voltage source), and conversely the effect of the electrical circuit upon the motion of the mechanical system when a mechanical force is acting. Z_s is the acoustic impedance of a pressure source p_s while Z_r accounts for the radiation conditions at the transducer diaphragm.

loudspeaker. Under the reciprocity principle mentioned above, it will be seen in the next chapters how each quantity may contribute to transform a loudspeaker into a tunable electroacoustic resonator.

3.4.6 Motional impedance

Along with sensitivity or directivity the electrical impedance is a common and standard parameter in the calibration of electroacoustic transducer [11, 78]:

1. it provides information for impedance matching between the transducer and the electrical load or auxiliary electrical source,
2. it is used in the computation of transducer efficiency and driving voltage from current responses (or vice versa),
3. it is an analytical tool for studying the performance of a transducer.

Although it is measured electrically, the impedance is also a function of the mechanical and acoustical (or radiation) characteristics of a transducer. The mechanical mass, compliance, and resistance appear as electrical impedance through the electromechanical coupling of the transducer. That is, it depends on whether the transducer has electrical coupling (piezoelectric) or electromagnetic coupling (moving coil). Consequently, the electrical impedance of a loudspeaker can be divided into several parts. The "pure" electrical part, depicted in dashed curve in Fig. 3.7), is the part that would be measured

if the transducer could be prevented from vibrating. It is called the blocked electrical impedance. When the transducer is free to vibrate, the difference between the resulting impedance and the blocked one is called the "motional" impedance. As shown in Fig. 3.7, the motional impedance acts especially at low frequencies. When the frequency increases, the electrical impedance is dominated by the inductance of the circuit.

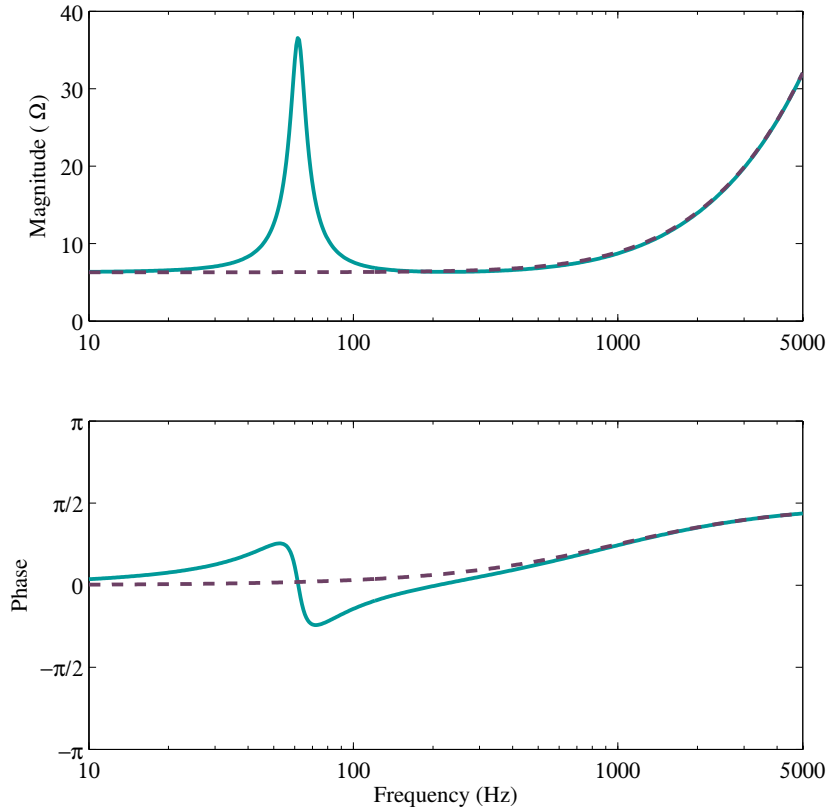


Figure 3.7: Computed electrical impedance of a loudspeaker when mounted on an infinite screen. The dashed curve represents the electrical impedance of the voice coil when blocked and the plain line is the electrical impedance when the transducer is free to oscillate.

According to Eq. (3.9), a motional emf always appears when the voice coil is moving, regardless the cause of motion. When used in driving mode, i.e. $SP(s) = 0$, the motion is due to the generated force, that in turn, is directly proportional to the current. Combining the characteristic equations (3.20) when the loudspeaker is connected to an auxiliary electrical source yields

$$e = \left(Z_e + \frac{(Bl)^2}{Z_m} \right) i \tag{3.23}$$

where the motional impedance² caused by the emf induced in the circuit is

$$Z_{em} = \frac{(Bl)^2}{Z_m} \quad (3.24)$$

When the system is linear, all effects on the motional emf are incorporated in Z_{em} .

3.4.7 State-space representation

An electrodynamic loudspeaker is single-input and single-output (SISO) system that can be described alternatively in state-space [79]. From the perspective of control theory, the input voltage $e(t)$ can be viewed as a command variable and the diaphragm velocity is the process variable to be controlled. Being not directly controllable, the sound pressure $p(t)$ may be regarded as a disturbance that may affect the process output, as shown in Fig. 3.8.

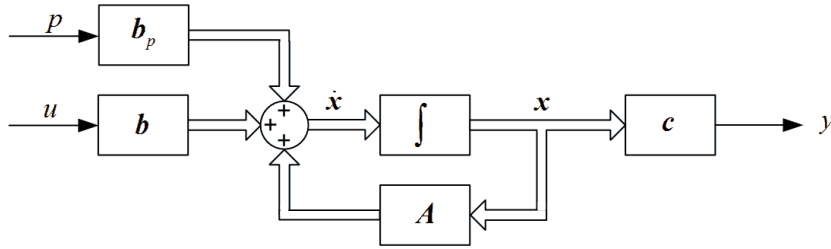


Figure 3.8: State-space representation of an electrodynamic loudspeaker. The variable u is the command input, the output variable y is here the diaphragm velocity, the disturbance p is the sound pressure acting on the diaphragm, and \mathbf{x} is the state vector that accounts for the internal variables of the transducer.

The physical quantities $v(t)$, $\xi(t)$ and $i(t)$ previously introduced are the internal state variables of the plant (here the transducer) since they are involved in the circulation of energy [80]. Introducing the state vector and scalar command variable, respectively as

$$\mathbf{x}(t) = \left(\xi(t), v(t), i(t) \right)^T \quad \text{and} \quad u(t) = e(t) \quad (3.25)$$

the set of differential equations (3.18) can be reformulated in state-space as

$$\begin{aligned} \dot{\mathbf{x}}(t) &= \mathbf{A} \mathbf{x}(t) + \mathbf{b} u(t) + \mathbf{b}_p p(t) \\ y(t) &= \mathbf{c}^T \mathbf{x}(t) \end{aligned} \quad (3.26)$$

²Here we neglect the radiation impedance of the diaphragm for sake of simplicity.

where

$$\begin{aligned}
 \mathbf{A} &= \begin{bmatrix} 0 & 1 & 0 \\ -1/(C_{mc}M_{ms}) & -R_{ms}/M_{ms} & Bl/M_{ms} \\ 0 & -Bl/L_e & -R_e/L_e \end{bmatrix} \\
 \mathbf{b} &= \begin{bmatrix} 0 \\ 0 \\ 1/L_e \end{bmatrix} & \mathbf{b}_p &= \begin{bmatrix} 0 \\ S/M_{ms} \\ 0 \end{bmatrix} \\
 \mathbf{c}^T &= \begin{bmatrix} 0 & 1 & 0 \end{bmatrix}
 \end{aligned} \tag{3.27}$$

As stated in Eq. (3.27), matrices \mathbf{A} , \mathbf{b} and \mathbf{b}_p are made up of the loudspeaker small signal parameters, whereas the output matrix \mathbf{c}^T depends on which output quantity of $\mathbf{x}(t)$ is used as controlled variable. Note that a command variable $u(t)$ can be constructed to transfer the system from any initial output $y(t_0)$ to any final output $y(t_1)$ in a finite time interval $t_0 \leq t \leq t_1$ since the observability matrix $[\mathbf{c}^T \quad \mathbf{c}^T \mathbf{A} \quad \mathbf{c}^T \mathbf{A}^2]^T$ is of rank 3, and the controllability matrix $[\mathbf{c}^T \mathbf{b} \quad \mathbf{c}^T \mathbf{A} \mathbf{b} \quad \mathbf{c}^T \mathbf{A}^2 \mathbf{b}]$ is of rank 1, meaning that the system is both observable and controllable [79].

The model given by Eq. (3.26-3.27) is equivalent to Eq. (3.19). State space representation is sometimes preferred in order to implement advanced control laws, like a linear quadratic regulator (LQR) [55, 81]. This approach is often referred to as output feedback control. In [82–84], it is used for modeling the dynamics of an acoustic duct with various boundary conditions at its ends, in view of achieving global active noise control of the duct resonances. The state space method that is described is however difficult to implement. A straightforward approach via separation of variables of the wave equation will not succeed for this problem since it is not self-adjoint. As a result the eigenvalues are not real, and the eigenfunctions neither span nor are mutually orthogonal. To overcome this, a new inner product is introduced in [85] under which the resolvent of the implied differential operator becomes normal and the now mutually orthogonal eigenfunctions span the space of all initial acoustic modal shapes.

3.5 Conclusions

In this chapter, the electrodynamic loudspeaker has been formalized by deriving the coupling equations of the transducer. This helps to explain, in particular, what current in – or motion of – an electrical conductor (the moving coil) in a magnetic field is capable of producing an electromechanical effect. Core assumptions including linearity, continuity of velocity at the transducer diaphragm, and transducer reciprocity have been discussed in view of providing a comprehensive understanding of the transduction principle. The linearized characteristic equations have then been established from a simple lumped parameter model. The model discussed so far is basically an approximation of the loudspeaker. The following will show, however, how helpful it is in view of analysing the loudspeaker behavior for small displacements and below the first modal frequency of the diaphragm. An equivalent representation of the loudspeaker in the state space has also been discussed. In order not to burden the rest of the thesis, the control problem will be considered by classical control approach only, i.e. using a model based on transfer functions. Notice, however, that a state space model could be used as well. We shall now see how an electrodynamic loudspeaker can be turned into an electroacoustic resonator.

4 Electroacoustic resonators: concept and formulation

4.1 Introduction

Principles of sound energy dissipation

Acoustic absorption relates to the ability of materials, structures or walls to dissipate a part of an incident sound energy. Through dissipative mechanisms, the amplitude of the reflected waves can be reduced compared to the incident waves. For instance, acoustic absorption allows reducing amplitude and duration of the noise levels resulting from a source placed in a closed space. Without energy dissipation, the sound environment of a classroom, an auditorium, a workshop or a conference room would result from an accumulation of all the energy emitted from their creation. Noise levels would be intolerable and loss of intelligibility would alter any transmission of information.

The mechanisms responsible for the dissipation of acoustic energy can be divided into three categories [21]:

1. viscous dissipation when there is a relative motion between particles in a porous material,
2. dissipation by internal damping of a solid material when bending (elastic deformations),
3. dissipation by effect of resonance (fluid or solid).

Practically speaking, the problem is to choose the materials for the walls or wall coverings with the appropriate acoustic absorption, particularly in relation with the frequency range of the sound spectrum to reduce. Typically, an efficient treatment for the low-frequency range requires the embodiment of heavy enclosures, large barriers or bulky sound absorbers due to the large sound wavelength.

Sound absorption by passive resonant systems

To address low-mid frequencies sound absorption, actual soundproofing solutions are usually based on resonant panels (or membranes) and Helmholtz resonators [1,6,11,86–88]. A typical example of passive resonant system is the bass trap [6]. Such resonating type absorber is free to oscillate in sympathy with the incident sound waves acting on the diaphragm. In view of providing acoustic absorption, the real part of the resulting specific impedance must be fairly close to the characteristic impedance of air, so that there is impedance matching (see Section 2.5). The control bandwidth is usually restricted to a narrow frequency range around the resonance, typically a fraction of octave. This typical feature makes it suitable for single frequency excitation (room mode, engine noise, etc.). Acoustic absorption by resonant systems is often advantageously combined with porous materials [1], with piezoelectric composite diaphragm [89] or with MPP [90] for improving performances (especially bandwidth).

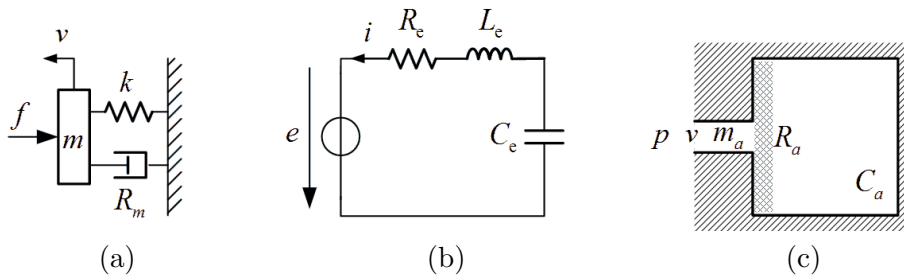


Figure 4.1: Schematics of a mechanical (a), electrical (b), and acoustical (c) systems of one degree of freedom.

Although different in nature, the systems shown in Fig. 4.1 are analog, i.e. they share the same equations and properties [11,15,86]. In the mechanical system (a), which could be a piston resiliently suspended or tensed membrane, a driving force f acts upon a mass m tied to a spring of stiffness k with a frictional force proportional to the velocity and the mechanical resistance R_m . In the electrical system (b) an input voltage e acts upon an inductance L_e , an electrical resistance R_e , and a capacitance C_e , thus forming a series resonant circuit. In the acoustical system (c), typically a Helmholtz absorber, incident sound waves of pressure p acts upon an acoustical mass m_a and an acoustical resistance R_a comprising the air in the opening which is connected to the volume or acoustical compliance C_a acting as a stiffness. These oscillating systems are mainly characterized by a resonance associated with some damping and bandwidth. Unlike porous materials, broadband sound absorption is difficult to achieve in one device, and so one of the challenges in the design of resonant structures is to extend the bandwidth [6].

This chapter provides some conceptual tools for the analysis of a system known as "resonant". Based on the extensive description of the damped harmonic oscillator, it is shown how an electrodynamic loudspeaker is turned into electroacoustic resonator.

4.2 Damped harmonic oscillator

4.2.1 Governing equation

Let us assume an electrodynamic loudspeaker as introduced in Chapter 3. The behavior of the loudspeaker diaphragm (without driving voltage) exhibits the physical characteristics of a damped harmonic oscillator. When moved away from its equilibrium position and released, the diaphragm is experiencing a restoring force proportional to the displacement as well as a frictional force proportional to the velocity. Without accounting for the electro-mechanical coupling, the diaphragm displacement x is governed by a second order time-dependent ordinary differential equation, which can be expressed as

$$f(t) - kx - R_m \frac{dx}{dt} = m \frac{d^2x}{dt^2} \quad (4.1)$$

where m is the combined mass of the diaphragm and voice coil, expressed in kg, k is the stiffness constant of the suspension, expressed in N m^{-1} , R_m is the viscous damping coefficient (or resistance constant), expressed in N s m^{-1} , and $f(t)$ is an externally applied force, in N.

The motion equation (4.1) merely states that the acceleration of the mass is proportional to the sum of the forces acting, according to Newton's second law. The friction term R_m mainly consists of internal diaphragm friction, and to a lesser extend of acoustic radiation resistance. Note that the minus sign indicates that internal force opposes to the motion. For ease of understanding, Eq. (4.1) is frequently rewritten into the general form

$$\frac{d^2x}{dt^2} + 2\zeta\omega_0 \frac{dx}{dt} + \omega_0^2 x = \frac{f(t)}{m} \quad (4.2)$$

where the parameters

$$\omega_0 = \sqrt{\frac{k}{m}} \quad \text{and} \quad \zeta = \frac{R_m}{2m\omega_0} \quad (4.3)$$

are the natural radial frequency, expressed in rad s^{-1} , and the damping ratio, respectively. The value of the damping ratio ζ critically determines the behavior of the system:

- $0 < \zeta < 1$, the system is underdamped and the transient response is oscillatory,
- $\zeta = 1$, the system is critically damped, i.e. non-oscillatory and without overshoot,
- $\zeta > 1$, the system is overdamped and the transient response does not oscillate.

Note that if $\zeta = 0$ the transient response becomes undamped and oscillations continue indefinitely.

The resonance frequency of the underdamped case is

$$\omega_s = \omega_0 \sqrt{1 - \zeta^2} \quad (4.4)$$

Unlike the natural frequency ω_0 , the resonance frequency is affected by the damping of the system. The case where the frequency of the driving force equals the natural frequency of the oscillator is called resonance. At resonance, the system stores and easily transfer vibrational energy such as kinetic and potential energy. Then, even small periodic driving forces can produce large amplitude oscillations.

4.2.2 Quality factor and bandwidth

To reflect the performance of resonant systems it is useful to introduce the parameters

$$Q = \frac{1}{2\zeta} \quad \text{and} \quad \Delta\omega = \frac{\omega_0}{Q} \quad (4.5)$$

which are defined as the quality factor (Q -factor) and the bandwidth of the resonance, respectively. The Q -value describes the ratio of the total energy stored in the resonator to the energy lost, per cycle, and $\Delta\omega$ refers to the useful frequency range that bounds the system efficiency. These parameters can be applied to any oscillator whether it is mechanical, electrical or acoustical [11]. In mechanical systems, the stored energy is the sum of potential and kinetic energies whereas the dissipated energy is the work that is done by an external conservative force, per cycle, to maintain amplitude. In electrical systems, the stored energy is the sum of energies stored in lossless inductors and capacitors and the dissipated energies is due to Joule losses in resistors. Roughly speaking, the Q -factor describes the sharpness of the system's response. The higher the Q -value, the more frequency selective the resonator.

The bandwidth is defined by $\Delta\omega = \omega_2 - \omega_1$, where ω_2 and ω_1 are the quadrantal frequencies for which there is an amplitude decrease of $\sqrt{2}$ (-3 dB for the levels), compared to the value at ω_0 when the driving force is constant. At these frequencies, $R_m = -\omega_1 m + k/\omega_1 = \omega_2 m - k/\omega_2$. By subtracting one of these equations from the other, it can be shown that $\omega_1 \omega_2 = \omega_0^2$. Likewise, with some further manipulations it comes $R_m/2m = (\omega_2 - \omega_1)/2$.

4.2.3 Frequency response function

The frequency response approach is commonly used for investigating the behavior of resonant systems. It consists in solving the differential equation (4.2) by introducing the complex notation $x(t) = X e^{j\omega t}$ and $f(t) = F e^{j\omega t}$, where X and F are complex numbers and $j = \sqrt{-1}$.

Using the complex notation, Eq. (4.2) can be rewritten as

$$X = \frac{F/m}{\omega_0^2 - \omega^2 + j 2\zeta\omega_0\omega} = H(j\omega) F \quad (4.6)$$

where the quantity $H(j\omega)$ is called the (complex) frequency response function. Note that the function $e^{j\omega t}$ can be cancelled since it never equals zero.

Following the rules for manipulating complex numbers [79] yields

$$X = \frac{F/m}{\sqrt{(\omega_0^2 - \omega^2)^2 + (2\zeta\omega_0\omega)^2}} e^{-j\theta} \quad (4.7)$$

where the phase of the complex number is given by

$$\theta = \tan^{-1} \frac{2\zeta\omega_0\omega}{\omega_0^2 - \omega^2} \quad (4.8)$$

The complex solution of Eq. (4.7) can finally be expressed as

$$x(t) = \frac{F/m}{\sqrt{(\omega_0^2 - \omega^2)^2 + (2\zeta\omega_0\omega)^2}} e^{j(\omega t - \theta)} \quad (4.9)$$

Differentiating the complex solution with respect to time t yields the expression of the velocity response as:

$$v(t) = \frac{\omega F/m}{\sqrt{(\omega_0^2 - \omega^2)^2 + (2\zeta\omega_0\omega)^2}} e^{j(\omega t - \theta + \frac{\pi}{2})} \quad (4.10)$$

Note that for the representation of the physical quantity we use only the real part of the complex solution.

Equations (4.7) to (4.10) give instructive information about the steady-state behavior of the forced oscillator:

1. the phase delay between the driving force f and the system velocity response depends upon the radial frequency ω and the constants ω_0 and ζ of the oscillator,
2. the amplitude of the system velocity response to force f depends upon the constants ω_0 and ζ of the oscillator,
3. the steady-state velocity is completely independent of the initial conditions since both amplitude and phase only depend on the driving force and oscillator constants m , ω_0 , and ζ .

Equation (4.10) reveals that the velocity amplitude and phase vary with ω , the radial

frequency of the driving force. Obviously, zero velocity is expected when $\omega = 0$. As ω increases, the velocity increases up to a maximum value where the denominator of Eq. (4.10) is minimum at $\omega = \omega_0$, or in other words the velocity resonance. At this single frequency, velocity and force are in phase. Clearly, resonance is the most favorable circumstance for the transfer of energy from the driving force to the oscillator.

4.2.4 Operating range

When discussing the transfer of energy, it is instructive and physically meaningful to describe the steady state motion in terms of operating range [11]. By applying the Fourier transform to Eq. (4.1) and by differentiating with respect to time, the velocity of the moving body can be expressed as

$$V = \frac{F}{R_m + j\left(\omega m - \frac{k}{\omega}\right)} = \frac{F}{Z_m} \quad (4.11)$$

where Z_m is the mechanical impedance of the system shown in Fig. 4.1 (a).

Examining now Eqs. (4.6)-(4.11) leads to identify three control domains.

1. When $\omega \simeq \omega_0$, the amplitude of the steady-state velocity response is reduced to F/R_m ; the forced harmonic oscillator is controlled by the resistance.
2. When $\omega \ll \omega_0$, the amplitude of velocity follows $\omega F/k$; the response of the oscillator is controlled by the stiffness at very low frequency.
3. When $\omega \gg \omega_0$, the velocity magnitude tends to $F/\omega m$ for a weak damping, indicating that the magnitude of oscillations falls off as ω is increased. The oscillator is controlled by the mass.

The phase constant θ of the forced harmonic oscillator gives complementary information about the whole behavior of the system.

1. At the resonance, i.e. for $\omega \simeq \omega_0$, the velocity is in phase with the driving force.
2. When $\omega \ll \omega_0$, Eq. (4.8) gives $\tan \theta \simeq 2\zeta\omega/\omega_0$, so that $\tan \theta$ is a small positive quantity tending to zero in the limit $\omega \mapsto 0$. After Eq. (4.10), the velocity response is $\pi/2$ out of phase with the driving force when the frequency of the driving force is very small compared to the natural frequency of free oscillations.
3. When $\omega \gg \omega_0$, Eq. (4.8) gives $\tan \theta \simeq -2\zeta\omega_0/\omega$, which indicates that $\theta \simeq -\pi$. After Eq. (4.10), the velocity response will be $-\pi/2$ out of phase with the driving force when the frequency of excitation is very high compared to ω_0 .

4.2. Damped harmonic oscillator

Table 4.1 summarizes the dependence of the amplitude and phase of the damped oscillator upon the frequency of the driving force.

Table 4.1: Operating range of a damped oscillator according to the radial frequency.

Control domain	Mechanical impedance N s m^{-1}	Velocity response m s^{-1}	Frequency range rad s^{-1}
Stiffness-control	$Z_m \simeq k/(i\omega)$	$v(t) \simeq (\omega F/k)e^{i\omega t}$	$\omega < \omega_1$
Resistance-control	$Z_m \simeq R_m$	$v(t) \simeq (F/R_m)e^{i\omega t}$	$\omega_1 < \omega < \omega_2$
Mass-control	$Z_m \simeq i\omega m$	$v(t) \simeq (F/\omega m)e^{i\omega t}$	$\omega > \omega_2$

If the amplitude F of the driving force is constant with regard to the frequency, the system is characterized by a velocity proportional to the frequency in the stiffness-control domain, inversely proportional to the frequency in the mass-control domain, and practically independent of the frequency in the resistance-control domain. As discussed later, the desired operating range $\Delta\omega$ should be more or less constant, i.e. the amplitude-frequency response should be almost constant. When acting as an electroacoustic resonator, the loudspeaker is intended to operate in the resistance-control domain.

4.2.5 General solution

The time response of a harmonic oscillator consists of two parts: the transient and steady state response. The transient state characterizes the first moments of the dynamics response of a system when it is set into motion. The steady state determines the behavior of the system when time goes to infinity; it is completely independent of the way in which the system is set into motion [79].

The generalization of the theory of Kirchhoff networks, originally developed for electrical, to mechanical and acoustic systems allows studying their behavior by expressing their transfer function as an isomorphic response function linking the Laplace transform of the driving force and response [11].

For the underdamped case ($0 < \zeta < 1$), Eq. (4.2) can be rewritten

$$\frac{V(s)}{F(s)} = \frac{1}{k} \frac{\omega_0^2 s}{s^2 + 2\zeta\omega_0 s + \omega_0^2} \quad (4.12)$$

where $V(s)$ and $F(s)$ are the Laplace transforms of the velocity and driving force, respectively. For a unit-step input, i.e. $f(t) = 1, \forall t > 0$, and $f(t) = 0, \forall t \leq 0$, $V(s)$ can

be written

$$V(s) = \frac{1}{k} \frac{\omega_0^2}{s^2 + 2\zeta\omega_0 s + \omega_0^2} \quad (4.13)$$

Using a table of Laplace transforms [79] the velocity for a unit-step force is

$$v(t) = \frac{1}{k} \frac{\omega_0}{\sqrt{1-\zeta^2}} e^{-\zeta\omega_0 t} \sin \omega_0 \sqrt{1-\zeta^2} t \quad (4.14)$$

Similarly, for a unit-impulse input, i.e. $f(t) = \delta(t)$, $V(s)$ becomes

$$V(s) = \frac{1}{m} \frac{s}{s^2 + 2\zeta\omega_0 s + \omega_0^2} \quad (4.15)$$

and the velocity response is given by

$$v(t) = \frac{1}{m} \frac{1}{\sqrt{1-\zeta^2}} e^{-\zeta\omega_0 t} \sin(\omega_0 \sqrt{1-\zeta^2} t - \phi) \quad (4.16)$$

where $\phi = \tan^{-1} \sqrt{1-\zeta^2}/\zeta$.

From Eqs. (4.14) and (4.16), it can be seen that the radial frequency of transient oscillation is $\omega_s = \omega_0 \sqrt{1-\zeta^2}$. Whatever the input signal, the transient response will consist in damped harmonic oscillations around the rest position of the mass. If the system has relatively large damping, the term $e^{-\zeta\omega_0 t}$ causes the transient response to damp out very quickly. Therefore, the transient part of the general solution is often ignored while designing or analyzing devices. If, on the other hand, the system is lightly damped, ζ very small, the transient part of the solution may last long enough to be significant and should not be ignored [79].

4.2.6 Sensitivity analysis

From a design perspective, it is important to study how the amplitude of steady state motion is affected by changing constitutive parameters of the system under investigation. The following analysis aims at investigating the influence of damping or the effects of varying the effective mass and stiffness of the system. To that purpose, Bode plot and step response are useful to describe how the system will react when altering its parameters. Formally, knowing the step response of a dynamical system gives information on system stability, and on its ability to reach one stationary state when starting from a given initial state. Bode plot, on the other hand, allows to graph the frequency-dependent behavior of the system. This representation will be meaningful when discussing the gain margin, phase margin and control bandwidth in the next chapters.

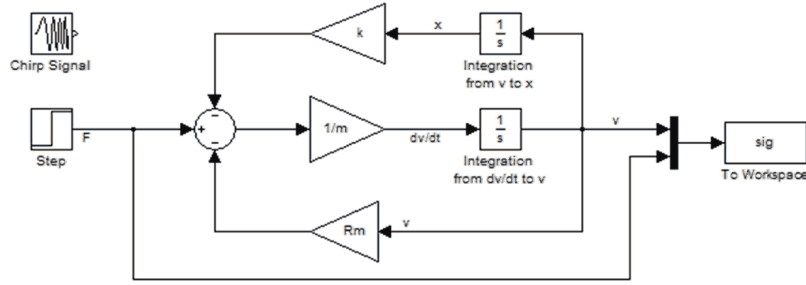

 Figure 4.2: Control model in Simulink[®] environment.

Figure 4.2 illustrates the model in Simulink[®] environment that is used for running the simulations. A driving force $F = 1 \text{ N}$ is applied to an underdamped harmonic oscillator that is made up of a mass $m = 0.01 \text{ kg}$ and a stiffness $k = 1430 \text{ N m}^{-1}$ yielding to $\omega_0 = 378 \text{ rad s}^{-1}$, and a mechanical resistance $R_m = 0.8 \text{ N m s}^{-1}$ such that $\zeta = 0.106$. The resulting velocity is computed and the results are shown as a function of the frequency ratio ω/ω_0 .

The values of constitutive parameters for the oscillator that is considered for the case study are summarized in Tab. 4.2.

Table 4.2: Influence of varying mechanical parameters on the velocity response of a damped harmonic oscillator ($m = 0.01 \text{ kg}$, $k = 1430 \text{ N m}$, $R_m = 0.8 \text{ N s m}^{-1}$, $\zeta = 0.106$, $\omega_0 = 378 \text{ rad s}^{-1}$, $Q = 4.7$, and $\Delta\omega = 80 \text{ rad s}^{-1}$).

Case	Mass kg	Stiffness N m	Resistance N s	Damping ratio	Q -factor	Bandwidth rad s^{-1}
A	m	k	R_m	ζ	Q	$\Delta\omega$
B	m	k	$R_m/2$	$\zeta/2$	$2Q$	$\Delta\omega/2$
C	m	k	$2R_m$	2ζ	$Q/2$	$2\Delta\omega$
D	m	k	$4R_m$	4ζ	$Q/4$	$4\Delta\omega$
E	$2m$	k	R_m	$\zeta/\sqrt{2}$	$\sqrt{2}Q$	$\Delta\omega/\sqrt{2}$
F	m	$2k$	R_m	$\zeta/\sqrt{2}$	$\sqrt{2}Q$	$\Delta\omega/\sqrt{2}$

Figure 4.3 (a) illustrates the influence of the resistance R_m on the amplitude and phase response versus frequency ratio ω/ω_0 . As expected, the velocity amplitude in the steady state is maximum when $\omega = \omega_0$. When R_m is increased, the peak of resonance gradually reduces until it disappears. The peak in the curve is sharp if the damping is small and becomes broader as R_m increases. Apart from the resonance, damping has no influence on the velocity response and the resulting velocity is never in phase with the applied force. As expected, the phase delay between velocity and applied force is $\pi/2$ when ω tends to 0, zero when $\omega = \omega_0$, and $-\pi/2$ when ω is very large. Figure 4.3 (a) also illustrates

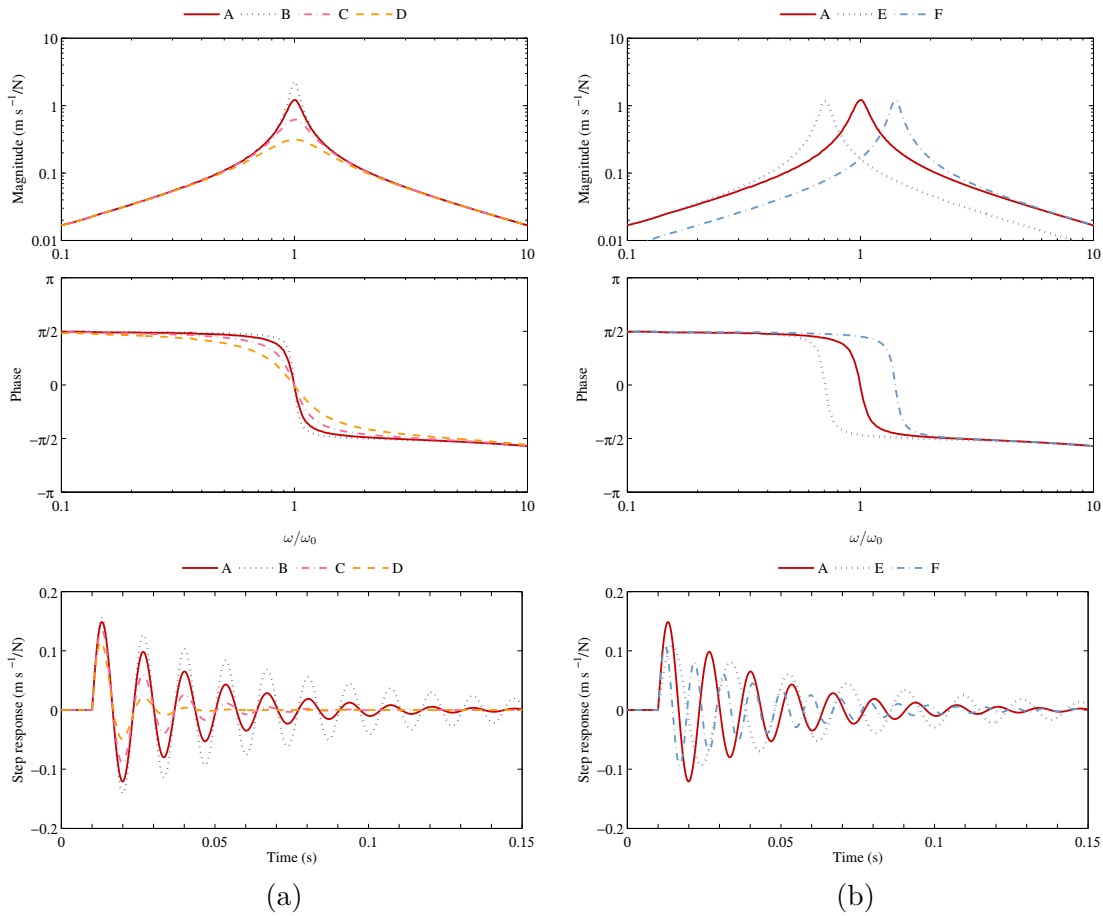


Figure 4.3: Frequency response (top) and step response (bottom) of a harmonic oscillator for various degrees of damping (a) and when varying mass or stiffness (b). The solid line denotes the reference oscillator. On the left, the dotted line is the oscillator with a damping two times lower, the dash-dot line is for a damping two times greater, and the dashed line is for a damping four times greater. On the right, the dotted line represents the oscillator when the mass is halved and the dashed line when the stiffness is halved.

the effect of varying the damping in the time domain. The step response shows that the increase in damping prevents the system from oscillating. Figure 4.3 (b) clearly shows that varying the mass or the stiffness significantly alters the system velocity response. A significant effect is to shift the resonance peak. Doubling the mass or stiffness leads to a slightly higher Q -factor with narrower bandwidth. The resonator becomes more frequency selective. By making the system more rigid (increase of stiffness k), it turns out that the transient response is faster, without overshoot. Conversely, adding mass in the system makes the transient response slower with more pronounced oscillations.

The following instructive remarks may be made about the damped harmonic oscillator:

1. Increasing the mechanical resistance value allows adding damping to the system; if the target resistance is higher, some damping must be added to the system whereas it should be subtracted when the natural resistance is initially greater.
2. Increasing the mass leads to decreasing the resonance frequency without substantially modifying the Q -value and bandwidth of the oscillator.
3. Increasing the stiffness leads to increasing the resonance frequency without substantially modifying the Q -value and bandwidth of the oscillator.

As discussed later, these remarks help to understand the control objective. These requirements can reasonably be met within a certain frequency range by making the damping large enough so that its effects outweigh those of the stiffness or mass. With a view of allowing sound absorption, the control objective is first to provide damping such that the acoustic resistance of the loudspeaker diaphragm is equal to the characteristic impedance of air, namely ρc . In addition, the mass or stiffness may be altered whether the natural frequency of the loudspeaker is far from the operating range where the device is supposed to work. Using "off-the-shelf" loudspeaker with given characteristics, it simply requires a proper choice of control settings that make possible to meet these specifications.

4.2.7 System poles and zeros

The poles and zeros are properties of the transfer function, and therefore of the differential equation describing the input-output system dynamics. Together with the gain constant, the location of the poles and the zeros in the s -plane provides qualitative insight into the response of any invariant linear system [79, 80]. In this section, we shall discuss how the concept of poles and zeros can help to designing an acoustic resonator in the low-frequency range where it may be approximated by lumped, linear parameters.

In general, the poles and zeros of a transfer function are complex, and the system dynamics may be graphed by plotting their locations on the complex s -plane, whose axes represent the real and imaginary parts of the complex variable s , as shown in Fig. 4.4.

For the underdamped case

$$\frac{V(s)}{F(s)} = \frac{1}{k} \frac{\omega_0^2 s}{s^2 + 2\zeta\omega_0 s + \omega_0^2} \quad (4.17)$$

the poles, which are the roots of the characteristic equation

$$s^2 + 2\zeta\omega_0 s + \omega_0^2 = 0 \quad (4.18)$$

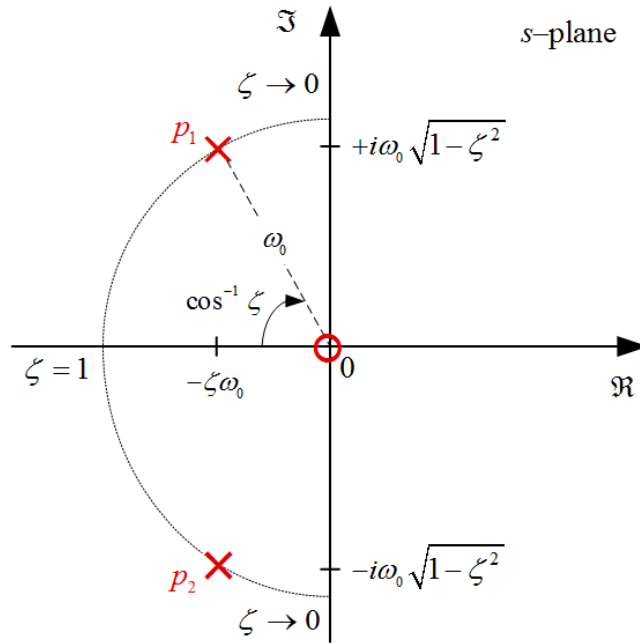


Figure 4.4: Pole-zero diagram of an underdamped, second-order oscillator as a function of the parameters ω_0 and ζ .

form a complex conjugate pair

$$p_{1,2} = -\zeta\omega_0 \pm j\omega_0\sqrt{1-\zeta^2} \quad (4.19)$$

that is located in the left-half plan. In Fig. 4.4, it can be seen that the poles for an underdamped second-order system lie at a distance ω_0 from the origin, and at an angle $\pm \cos^{-1} \zeta$ from the negative real axis.

In a general way, the location of the poles in the s -plane will influence the dynamic response of the system in such a way:

1. A real pole $p_k = -\sigma$ in the left-half of the s -plane denotes an exponentially decaying component $Ae^{-\sigma t}$ in the free response: poles far from the origin in the left-half plane correspond to components that decay rapidly, while poles near the origin correspond to slowly decaying components.
2. A pole at the origin $p_k = 0$ denotes a component that is constant in amplitude and defined by the initial conditions.
3. A real pole in the right-half plane leads to an exponentially increasing component $Ae^{\sigma t}$ in the free response, thus defining an unstable system.
4. A complex conjugate pole pair $\sigma \pm j\omega$ in the left-half of the s -plane combines to

generate a response that is a decaying sinusoid of the form $Ae^{-\sigma t} \sin(\omega t + \phi)$ where A and ϕ are determined from Eqs. (4.6) and (4.7). The rate of decay is specified by σ whereas the frequency of oscillation is determined by ω .

5. An imaginary pole pair $\pm j\omega$, i.e. a pole pair lying on the imaginary axis, generates an oscillatory component with a constant amplitude determined by the initial conditions.
6. A complex pole pair in the right half plane leads to an exponentially increasing component.

Similarly, the location of poles and zeros may also find significance in the frequency domain. Even though the gain constant cannot be determined from the pole-zero diagram, the following generalizations may be made about the frequency response of a linear system, based upon a geometric interpretation:

1. When the system has an excess of poles over the number of zeros the magnitude of the frequency response tends to zero as the frequency becomes large. Conversely, an excess of zeros will increase the gain without bound as the frequency of the input raises. This cannot happen in physical systems because it implies an infinite power gain through the system.
2. A pole at the origin of the s -plane (corresponding to a pure integral term in the transfer function) implies an infinite gain at zero frequency, whereas a zero at the origin of the s -plane (corresponding to a pure differentiation) implies a zero gain for the system at zero frequency.
3. When the system has a pair of complex conjugate poles close to the imaginary axis, the magnitude of the frequency response will show a resonance at frequencies in the proximity of the pole. If the pole pair lies directly upon the imaginary axis, the system exhibits an infinite gain at that frequency.
4. When the system has a pair of complex conjugate zeros close to the imaginary axis, the frequency response will exhibit a notch in its magnitude function at frequencies in the vicinity of the zero.

As the objective of any synthesis is to produce a system that is as good as possible under certain specifications or physical constraints, the pole-zero concept is useful for the design procedure. In order for the system to exhibit a strong resonance, complex conjugate poles should be near the imaginary axis; otherwise, they should be moved away. Through a simple graphical representation, it helps to convey certain properties of the system such as stability and causality. Note that these general remarks apply for all frequency response functions, whether they are impedances, admittances, or ratio of quantities at one point to quantities at other points.

4.3 Electromechanical system

The dynamics of systems with one degree of freedom, such as an unplugged loudspeaker, is completely described by a second-order differential equation. When the loudspeaker is coupled to an electrical source or load, the second-order model is no longer sufficient. To more thoroughly describe such a multifunctional device, the electrodynamic effects mentioned in Section 3.3 have to be considered. As stated in Section 3.4.5, the loudspeaker can be connected either to a source or to a load. In the following part we shall examine both aspects.

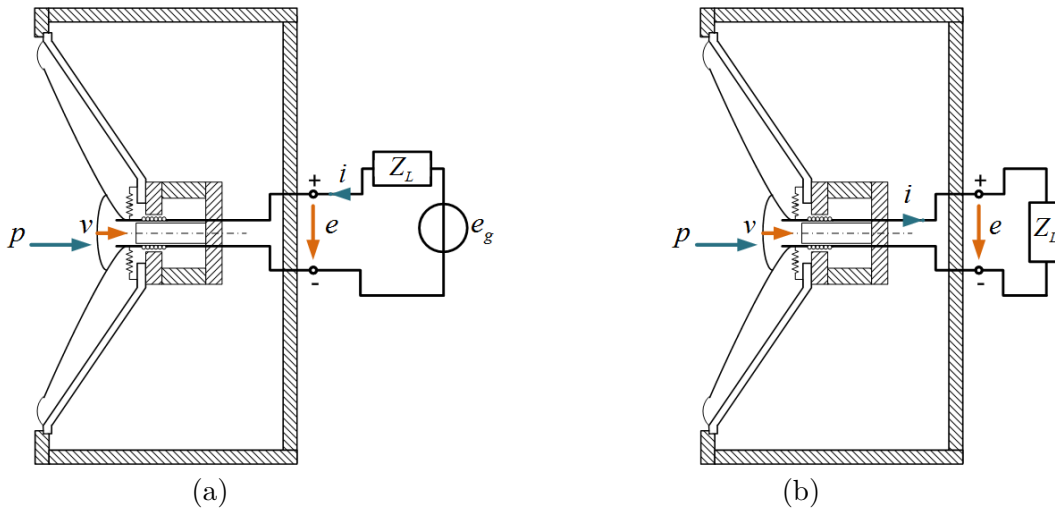


Figure 4.5: Schematics of the coupling of a loudspeaker to an electrical source (a) and to an electrical load (b).

4.3.1 Coupling to an electrical source

Basically, control strategies are characterized by electrical coupling. With a direct feedback control of acoustic variables, the control process is implemented by connecting the loudspeaker to an auxiliary electrical source which delivers the input signal. The control signal is an input voltage that can be proportional to pressure or velocity, or a combination of both [15, 16, 25, 49, 50, 54].

By combining the characteristic equations (3.20) with the electrical coupling (3.22), the electrical current flowing through the coil can be written as

$$I(s) = \frac{1}{Z_e(s) + Z_L(s)} E_g(s) - \frac{Bl}{Z_e(s) + Z_L(s)} V(s) \quad (4.20)$$

where E_g is an auxiliary source voltage and Z_L the source internal impedance.

The resulting diaphragm velocity can be expressed as a function of the driving pressure force and applied voltage as

$$V(s) = \frac{Z_e(s) + Z_L(s)}{Z_m(s)(Z_e(s) + Z_L(s)) + (Bl)^2} SP(s) - \frac{Bl}{Z_m(s)(Z_e(s) + Z_L(s)) + (Bl)^2} E_g(s) \quad (4.21)$$

where Z_e is the blocked electrical impedance of the voice coil and Z_m is the mechanical impedance.

According to the applied feedback control voltage E_g , the behavior of the electromechanical system can be altered within certain bounds. The sensed pressure or velocity signals can be processed by the control system separately or in combination. Chapter 5 is devoted to show how the performance of a conventional electrodynamic loudspeaker can be substantially improved through feedback control.

4.3.2 Coupling to an electrical load

Connecting an electrical network to the terminals as depicted in Fig. 4.5 is another way to alter the dynamics of a transducer. After Kirchhoff's circuit law, the total voltage drop across the voice coil impedance is equal to the difference of the voltage e applied to the loudspeaker and the motional electromotive force Blv . Physically speaking, the electromechanical coupling introduces a feedback voltage which is proportional to the velocity (see Chapter 3). When coupling an electrical load of impedance Z_L to the loudspeaker, the electrical current flowing through the coil can be written as

$$I(s) = -\frac{Bl}{Z_e(s) + Z_L(s)} V(s) \quad (4.22)$$

where Z_e is the blocked electrical impedance of the voice coil. By combining the characteristic equations (3.20) with (4.22), the resulting diaphragm velocity can be expressed as a function of the driving pressure

$$V(s) = \frac{Z_e(s) + Z_L(s)}{Z_m(s)(Z_e(s) + Z_L(s)) + (Bl)^2} SP(s) \quad (4.23)$$

Depending on the nature of the elements constituting the analog electrical network, the behavior of the electromechanical system can be altered within certain bounds. The shunt network can be made up of a combination of positive or negative, reactive or resistive components, in series or parallel. All associations are however not practically feasible for stability reasons. It will be seen in Chapter 6 how the performance of an electrodynamic loudspeaker can be substantially improved by the use of analog networks.

4.3.3 Dynamics of a third-order system

A common feature to both types of electroacoustical coupling is to transform the damped oscillator into a third-order dynamical system. By neglecting the inductance L_e , it can be readily shown that the lumped-parameter model of the loudspeaker is second-order [11, 16, 43, 91]. When the coil inductance cannot be neglected, the denominator in Eqs. (4.21) and (4.23), become a cubic polynomial

$$g(s) = a s^3 + b s^2 + c s + d \quad (4.24)$$

where $s = j\omega$ and the coefficients

$$\begin{aligned} a &= M_{ms}L_e \\ b &= M_{ms}R_e + R_{ms}L_e \\ c &= R_{ms}R_e + \frac{L_e}{C_{mc}} + (Bl)^2 \\ d &= \frac{R_e}{C_{mc}} \end{aligned} \quad (4.25)$$

are positive real numbers (see Section 3.4.2).

If the method for extracting one real root of any cubic polynomial is well-known, there exists different ways for getting the remaining roots [77, 92, 93]. In appendix A, a method is introduced for evaluating all the roots of Eq. (4.24) by deriving a set of compact algebraic formulae based on hyperbolic functions.

As detailed in Appendix A, the denominator of Eqs. (4.21) and (4.23) can be rewritten

$$g(s) = (s - p_1)(s - p_2)(s - p_3) \quad (4.26)$$

and after some further manipulation, Eq. (4.26) may also be expressed as

$$g(s) = (s + \sigma) \left(s + \zeta\omega_0 + j\omega_0\sqrt{1 - \zeta^2} \right) \left(s + \zeta\omega_0 - j\omega_0\sqrt{1 - \zeta^2} \right) \quad (4.27)$$

where

$$\begin{aligned} \sigma &= -p_1 \\ 2\zeta\omega_0 &= -p_2 - p_3 \\ \omega_0^2 &= p_2 p_3 \end{aligned} \quad (4.28)$$

Figure 4.6 shows the typical pole-zero diagram of an electrodynamic loudspeaker as a function of the parameters ω_0 , ζ and σ .

When coupled to an electrical source e_g of internal impedance Z_L , the closed form expression for the diaphragm velocity can be expressed as a function of the driving

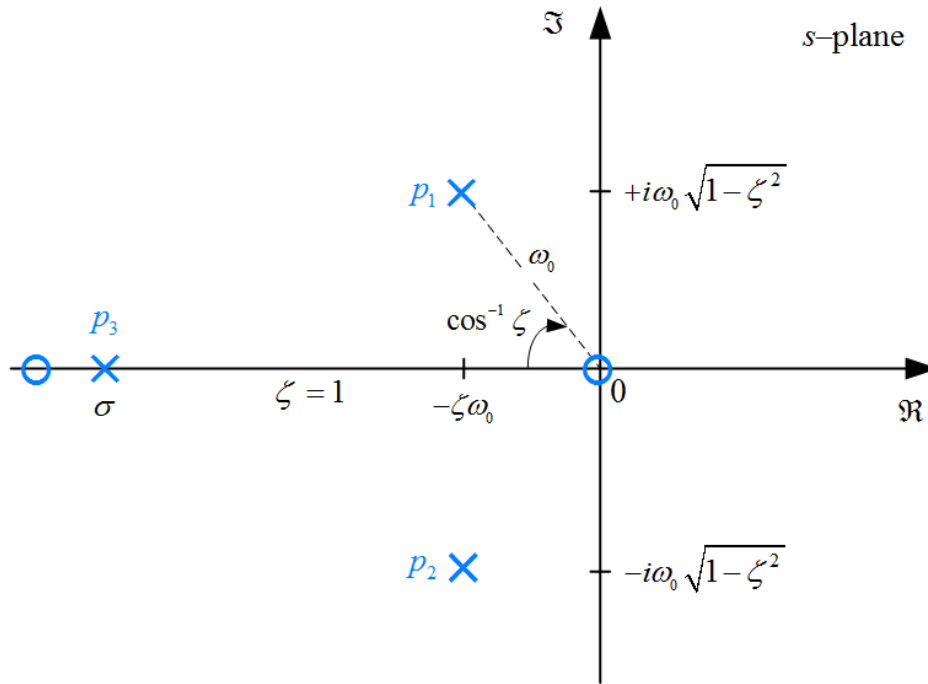


Figure 4.6: Pole-zero diagram of a third-order system as a function of the parameters ω_0 , ζ and σ .

pressure force and applied voltage as

$$V(s) = \frac{Z_e(s) + Z_L(s)}{(s + \sigma)(s^2 + 2\zeta\omega_0 s + \omega_0^2)} SP(s) - \frac{Bl}{(s + \sigma)(s^2 + 2\zeta\omega_0 s + \omega_0^2)} E_g(s) \quad (4.29)$$

where the real root corresponds to a linear factor and the complex conjugate roots correspond to a quadratic factor.

Similarly, by connecting to an electrical load of impedance Z_L , the resulting diaphragm velocity can be expressed as a function of the driving pressure as

$$V(s) = \frac{Z_e(s) + Z_L(s)}{(s + \sigma)(s^2 + 2\zeta\omega_0 s + \omega_0^2)} SP(s) \quad (4.30)$$

It is shown that a loudspeaker when connected to an electrical load or source is a third-order system. Given real coefficients, such system can always be rearranged into linear and quadratic factors such as $(s + \sigma)$ and $(s^2 + 2\zeta\omega_0 s + \omega_0^2)$, where σ , ζ , and ω_0 are real. We now have a simple analytical design procedure. It will be seen further that using control over the loudspeaker may alter, to some extent, the closed-loop poles so that the system satisfies certain specifications.

4.4 System performance

This section presents some of the quantities that will be used for assessing the acoustic performances of resonators and absorbers under plane wave assumption.

4.4.1 Specific acoustic admittance

Acoustic properties of materials are completely defined by specifying the specific acoustic impedance as a function of frequency [3]. However, the specific acoustic admittance, defined as the reciprocal of the specific acoustic impedance, is more suited to the analysis of the dynamical system under study [37]. As discussed in Section 2.3, the motion of the diaphragm is caused by acoustic pressure and not vice versa. The concept of admittance will be deliberately used to discuss the performances of the electroacoustic system in terms of frequency response (Bode plot). The concept of specific acoustic impedance will be used for discussing the analysis of the real and imaginary parts.

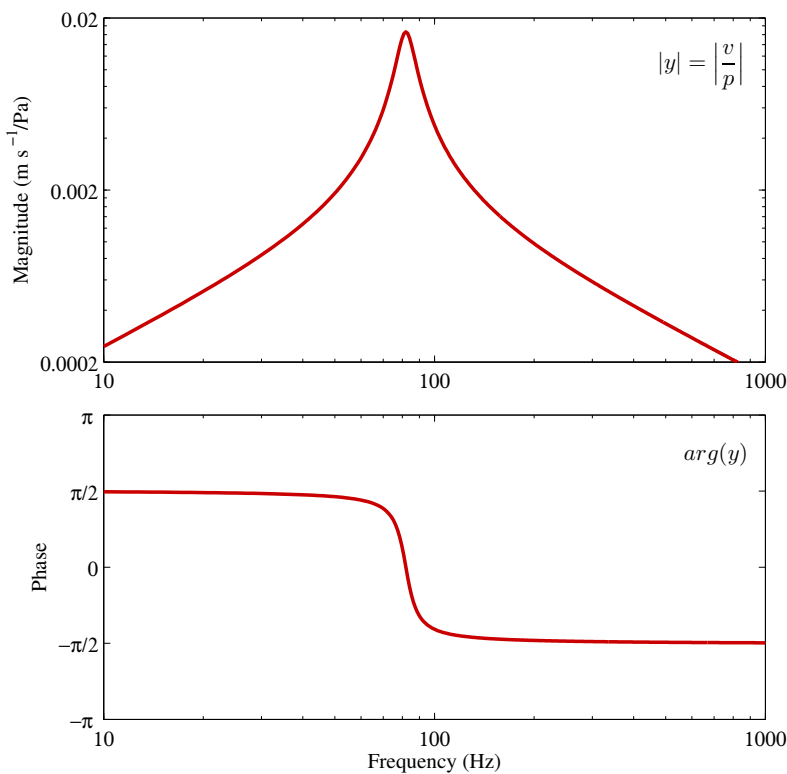


Figure 4.7: Bode plot of the specific acoustic admittance of the loudspeaker when unplugged.

The specific acoustic admittance ratio (see Section 2.3) is defined as the ratio between the normal velocity of the diaphragm and the acoustic pressure at a point near the surface,

relative to the characteristic impedance of air. This dimensionless parameter can be expressed as

$$y = \rho c \frac{v}{p} \tag{4.31}$$

where ρ is the density of air and c is the sound celerity in air. Note that it is always possible to derive the system of Eq. (3.18) in order to write the specific acoustic admittance of the loudspeaker diaphragm according to Eq. (4.31). Figure 4.7 shows a typical frequency response of the specific acoustic admittance at the diaphragm of a loudspeaker when unplugged. Note that the Bode magnitude plot exhibits a resonance and the phase varies from $\pi/2$ to $-\pi/2$ which is typical of a positive real system. Another convenient way to visualize the behavior of the loudspeaker is to consider the real part and imaginary part of the specific acoustic impedance. As shown in Fig. 4.8, the real part of the specific acoustic impedance remains constant at all frequencies while the imaginary part increases with frequency and crosses zero at resonance.

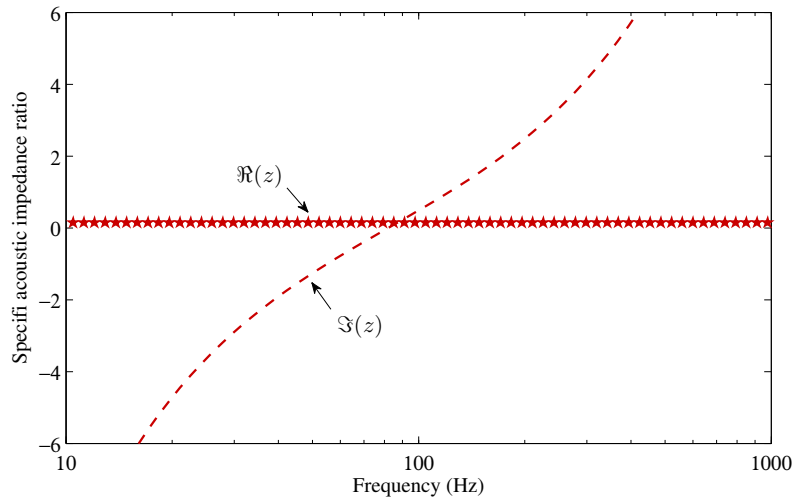


Figure 4.8: Real (\star) and imaginary part (---) of the specific acoustic impedance at the diaphragm of the loudspeaker when unplugged.

4.4.2 Reflection coefficient

The reflection coefficient at normal incidence is defined as the ratio of the complex pressure amplitude of the reflected waves with respect to plane waves under normal incidence. From the specific impedance ratio z the corresponding reflection coefficient can be derived after [3]

$$r = \frac{1 - y}{1 + y} \tag{4.32}$$

Notice that if y is purely imaginary (reactive), then the magnitude of r is unity; the reflected wave differs only in phase angle from the incident wave and no energy is absorbed by the surface.

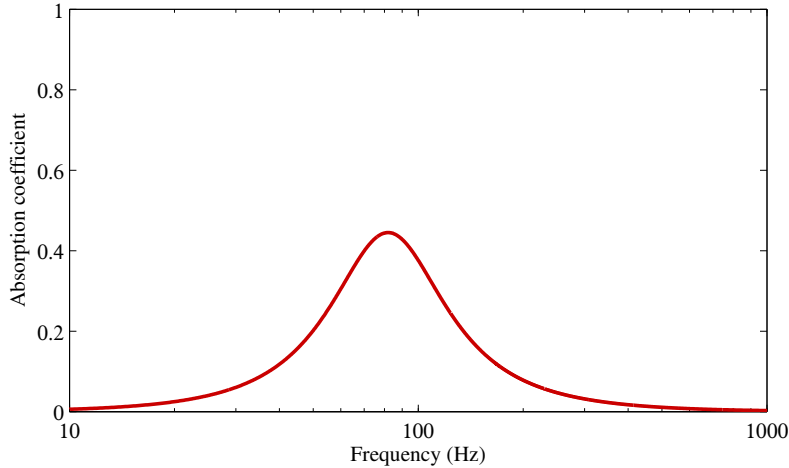


Figure 4.9: Plot of the absorption coefficient at the loudspeaker diaphragm under normal incidence.

4.4.3 Absorption coefficient

The sound absorption coefficient at normal incidence is defined as the ratio of the acoustic power absorbed by the surface of materials with respect to the incident sound power for normal incident plane waves. It is derived after extracting the magnitude $|r|$ of the reflection coefficient as

$$\alpha = 1 - |r|^2 \tag{4.33}$$

A full absorption is achieved when $\alpha = 1$ and zero absorption corresponds to $\alpha = 0$. The reflection coefficient r depends on field quantities while the absorption coefficient α is concerned by power quantities, which means that r is complex and α is a real parameter. Notice that the relationship between r and α is not linear, which leads to the noticeable consequences. An absorption coefficient $\alpha \simeq 0.9$ corresponds to a reflection coefficient $r \simeq 0.32$, indicating that the amplitude of the reflected sound wave equals one-third of that of the incident wave. It must also be pointed out that r and α are frequency-dependent since y is also frequency-dependent. Equations (4.31-4.33) indicate that the type of electrical coupling will impose certain absorption characteristics at the vicinity of the loudspeaker diaphragm. Chapters 5 and 6 will provide the general expressions of the specific acoustic admittance ratio for various cases of control.

4.4.4 Routh's stability criterion

The most important problem in linear control systems concerns stability. That is, under what conditions will a system become unstable? If it is unstable, how should we stabilize the system? The stability of a linear system may be determined directly from its transfer function. Generally speaking, an n th order linear system is asymptotically stable only if all of the components in the homogenous response from a finite set of initial conditions decay to zero as time increases [79, 80], which is equivalent to write

$$\lim_{t \rightarrow \infty} \sum_{k=1}^n A_k e^{p_k t} = 0 \quad (4.34)$$

where the p_k are the poles of the system. If any pole has a positive real part there is a component in the output that increases indefinitely, causing the system to be unstable, as mentioned in Section 4.2.7. In order for a linear system to be stable, all of its poles must have negative real parts, that is they must all lie within the left-half of the s -plane, as given in Fig. 4.4.

From the general form of a single-input, single-output, third-order LTI system

$$\frac{V(s)}{E(s)} = \frac{a_2 s^2 + a_1 s + a_0}{b_3 s^3 + b_2 s^2 + b_1 s + b_0} \quad (4.35)$$

information about absolute stability can be obtained directly from the coefficients of the characteristic equation using Routh's stability criterion. If any of these coefficients are zero or negative in the presence of at least one positive coefficient, there is a root that is imaginary or has positive real part. In such a case the system is not stable.

As stated earlier the characteristic equation of a loudspeaker can always be rearranged into linear and quadratic terms. The quadratic factor $(s^2 + 2\zeta\omega_0 s + \omega_s^2)$ yields roots having negative real parts only if $\zeta\omega_0$ and ω_s^2 are both positive. Given that the product of any number of linear and quadratic factors containing only positive coefficients always yields a polynomial with positive coefficients, then this condition ensures stability. Another way to express the necessary condition for stability for a third-order system is

$$b_3, b_2, b_1, b_0 > 0 \quad \text{and} \quad b_2 b_1 > b_3 b_0 \quad (4.36)$$

which guarantees that all roots have negative real parts.

Notice that the Routh's tables, as given in [79], can be used to anticipate stability issue for higher-order systems. It should also be noticed that this criterion does not account for various phenomena that may have a prejudicial impact on the whole stability of the system such as the variation of electric resistivity and self-inductance with frequency, non-linear behavior for the stiffness of suspensions, or even heat phenomena occurring in the coil.

4.5 Conclusions

In this chapter, the concept of electroacoustic resonator has been discussed by relying on the well-known model of a damped harmonic oscillator. By taking into account the electrodynamic coupling, the dynamics of the loudspeaker is shown as a third-order including one real and two complex conjugate poles. This coupling suggests two ways to control an electrodynamic loudspeaker. The first, via an active control system, is to apply a command voltage related to relevant acoustic variables. The second, passive, is to connect a specific load impedance across the transducer terminals.

The step response and Bode plot have been presented to describe the effect of varying the system parameters in both the time and frequency domain. The concept of pole-zero of transfer functions has also been introduced to assist in the design of electroacoustic resonators while keeping in mind practical issues related to system stability and causality. The Routh criterion has also been discussed as a way to anticipate stability issues that the transducer under control could experience in actual situations. These conceptual tools will be useful in the following chapters in order to meet the specifications given in terms of damping, control bandwidth and phase margin.

In view of noise control applications, it is shown that the electrodynamic loudspeaker is an obvious candidate. Reasons for this include the immediate availability, a relatively low cost, and electromagnetic properties that can advantageously alter the dynamics of the loudspeaker in a controlled fashion, especially around the resonance where it is controlled by resistance. In addition, this transduction principle does not require any power supply. In short, the electrodynamic loudspeaker is already well-designed for rudimentary acoustic treatments. The idea of the following chapters is to investigate how to provide additional resistance (damping) to the system, while minimizing reactance.

5 Changing the acoustic impedance using feedback control

5.1 Introduction

Forewords

Control engineering is a discipline that deals with the modeling of dynamical systems and the design of control systems. In practice, sensors are used to measure the states and outputs of the process. The information is transmitted to a controller which, in turn, delivers a command signal to an actuator so that it makes the necessary corrective actions. In control theory there are two major branches, namely the classical and modern control, and many classes of control techniques or methods such as robust, adaptive, optimal, nonlinear, fuzzy logic, state feedback, etc. Classical control theory refers to single-input, single-output (SISO) dynamical systems. The system analysis can be carried out in the time domain using differential equations, in the complex- s domain with Laplace transform, or in the frequency domain. Modern control theory is studied in the state space and may handle multi-input, multi-output (MIMO) systems. This feature overcomes some limitations of classical control theory in more sophisticated design problems. In modern design, a system is represented as a set of first order differential equations using state variables [79, 80].

There exist two basic types of control technique, namely feedforward and feedback. With feedforward control, the disturbances are measured and accounted for before they have actually affected the system. In feedback systems, the input of the controller is closely related to the process output to control. This is commonly called "closed-loop control". Both can be combined to optimize performance or stability of the control process.

In this chapter, the general structure of control systems is introduced by focusing the discussion on the intake of control theory for developing an active electroacoustic device. Design procedures appropriate for such linear time-invariant system are described on the basis of the frequency-response approach.

Feedback control system

One reason for implementing a control system is to force the output of a process to follow a desired set-point. This tracking problem must be as accurate as possible regardless of the trajectory of the manipulated variable while simultaneously minimizing the effects of external disturbance or changes in the system dynamics [79].

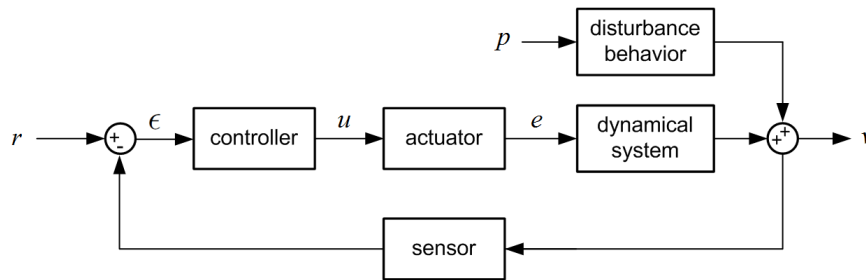


Figure 5.1: Basic block diagram of a feedback control system. The signals in the closed loop are denoted by v for the controlled variable (actual value), r for the command variable (set point), ϵ for the control error, u for the manipulated variable, e for the input voltage, and p for the disturbance.

A schematics of a generalized feedback system is shown in Fig. 5.1. There are many variations of this system; these may be either simpler or more complex depending upon the application. From the block diagram in Fig. 5.1, the task of the control system is to hold the process output $v(t)$ either on a constant set point (fixed command control, $r(t)$ is constant), or tracking a time-varying reference (variable command control, $r(t)$ being not constant). In the most ideal case, the feedback system should operate independently of any disturbance $p(t)$. The term disturbance means here any quantity other than the manipulated variable that may influence the process variable.

The controller shall process the control error $\epsilon(t) = r(t) - v(t)$, i.e. the difference between the set point $r(t)$ and the actual value $v(t)$. In return, it delivers a control signal $u(t)$ which contains the necessary corrective actions (proportional gain or other) to the actuator. The actuator is the chain element allowing for the system behavior to be altered. The role of the feedback loop is thus to cancel the control error $\epsilon(t)$, or at least to hold it as small as possible.

5.2 Active control on a loudspeaker

5.2.1 Problem statement

An electrodynamic loudspeaker can be viewed as a dynamical system with energy storage (or reactive) elements. As a result, it cannot respond immediately but exhibits a transient response whenever it is subjected to voltage input or acoustic disturbance. From a control

perspective, the most straightforward way should be to design a dedicated control systems by transient response approach. In audio or acoustical engineering, however, specifications are commonly drawn up in the frequency domain. By frequency response approach, actually, the transient response performance is indirectly accessible. For instance, the Q -factor gives a rough estimate of the system damping, the phase margin provides information on the system relative stability, and the resonant frequency and bandwidth indicate how fast the system will respond to a sudden change [79,80]. A straightforward way is based on pole placement, as introduced in Section 4.2.7. The purpose is to achieve a feedback control of acoustic variables such that the closed-loop poles take preassigned values that satisfy the specifications [94–96]. This requires developing an input-output or state-space model of the process, and then to express the desired behavior in terms of feedback gains or other. It will be shown later that control of the loudspeaker dynamics is possible over a relatively large bandwidth around the resonance frequency.

In view of implementing an efficient control of acoustic impedance, the main objectives are basically to

1. meet the desired control bandwidth over which the transducer diaphragm is supposed to have prescribed behavior,
2. ensure that the diaphragm velocity follows the time-varying reference as accurately and as fast as possible,
3. make the closed loop as insensitive as possible relative to change in the transducer parameters,
4. guarantee the stability of the closed-loop system.

Generally speaking, strict adherence to all requirements over the entire audio-frequency range is limited by the technological design of the transducer. In the following, the general structure of feedback control applied to a loudspeaker is introduced by focusing the discussion on the intake of control theory for developing an active electroacoustic resonator.

5.2.2 Control law formulation - case of ideal sound absorption

Let us consider an unplugged loudspeaker at one end of a semi-infinite duct where plane waves propagate, as depicted in Fig. 2.3. When subjected to a sound field, the diaphragm will oscillate in sympathy with incident sound waves. The total sound pressure in front of the diaphragm can be written as [97]

$$p = p_i + p_r = (1 + r)p_i \tag{5.1}$$

Chapter 5. Changing the acoustic impedance using feedback control

where p_i and p_r are the amplitude of incident and reflected sound waves, respectively, and r is the reflection coefficient.

As stated in Section 2.3 and from Eq. (4.32), the reflection coefficient can be defined by

$$r = \frac{Z_s - Z_c}{Z_s + Z_c} = \frac{1 - y}{1 + y} \quad (5.2)$$

where $Z_s = p/v$ is the specific acoustic impedance and $Z_c = \rho c$ is the characteristic impedance of the medium.

After simplification, Eq. (5.1) becomes

$$p = \frac{2Z_s}{Z_s + Z_c} p_i \quad (5.3)$$

After some further manipulations, the total pressure at the loudspeaker diaphragm can be expressed as

$$p + \rho c v = 2p_i \quad (5.4)$$

Equation (5.4) identifies a straightforward relationship between incident sound waves, total sound pressure, and resulting velocity at the diaphragm.

In order to provide perfect sound absorption, i.e. $r = 0$ at the diaphragm, the relationship between the total sound pressure and resulting velocity should be

$$v = \frac{p}{\rho c} \quad (5.5)$$

If the diaphragm velocity can be controlled to satisfy Eq. (5.5), then $p = p_i$ and incident sound waves do not see impedance mismatch (or discontinuity) at the interface with air. There is impedance matching, as introduced in Section 2.5.

From a control theory perspective, this matching condition can be reformulated as an error signal $\epsilon(t)$ to be minimized by a controller

$$\epsilon(t) = \frac{p(t)}{\rho c} - v(t) \quad (5.6)$$

where $p(t)/\rho c$ is the time-varying reference (set point), and $v(t)$ is the measured process variable.

5.2.3 Loudspeaker as an active control element

When the "plant" to control is an electrodynamic loudspeaker, the system and actuator are the same entity. This specific feature leads to some changes in the overall architecture of the feedback system depicted in Fig. 5.1. Here, the process output v is the normal velocity of the diaphragm and the sound pressure acting on it may be considered as a disturbance p , since being not directly controllable. The system dynamics will be fully described by the diaphragm velocity response over time resulting to changes in the input voltage u and effects on disturbance p , as proposed in Fig. 5.2. Note that the variables in capital letters in Fig. 5.2 are the Laplace transforms of the signals used in Fig. 5.1.

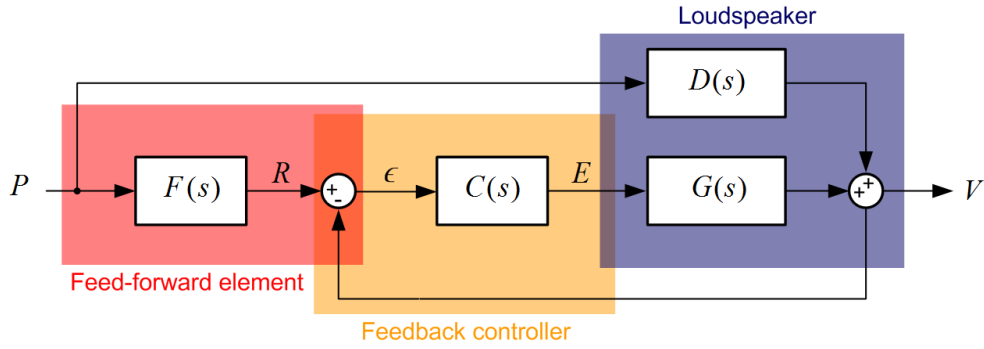


Figure 5.2: Block diagram of a loudspeaker as an active control element. The variables V is the diaphragm normal velocity (process variable), P is the sound pressure disturbance that may alter the process variable V , ϵ is the control error, E is the input voltage (manipulated variable), and R is the time-varying reference (set point).

For acoustic impedance control the objective is to impose a relationship between the variables v and p . The set-point for the velocity will be to track a time-varying reference that depends on the sound pressure acting on the diaphragm. The control error is given by Eq. (5.6). The command signal $u(t)$ generated by the controller is the input voltage $e(t)$ that will be applied directly to the electrical terminals of the loudspeaker.

Introducing the transfer functions $G(s)$, $D(s)$, $F(s)$ and $C(s)$ for the loudspeaker, disturbance, feedforward and feedback controller, respectively, the process output can be written as

$$V(s) = D(s)P(s) + (F(s)P(s) - V(s))C(s)G(s) \quad (5.7)$$

The transfer functions $G(s)$ and $D(s)$ can be easily derived after eliminating the electrical current I in Eq. (3.20) as

$$G(s) = \frac{Bl}{Z_m(s)Z_e(s) + (Bl)^2} \quad (5.8)$$

and,

$$D(s) = \frac{S Z_e(s)}{Z_m(s)Z_e(s) + (Bl)^2} \quad (5.9)$$

where Z_e is the blocked electrical impedance of the voice coil, Z_m the mechanical impedance, S the diaphragm surface, and Bl the force factor, as defined in Sec. 3.4. Rearranging Eq. (5.7) yields the general form of the loudspeaker under control as

$$\frac{V(s)}{P(s)} = \frac{D(s) + F(s)C(s)G(s)}{1 + C(s)G(s)} \quad (5.10)$$

In the following, we shall give the closed form expression of the specific acoustic admittance ratio when the loudspeaker is under feedforward $F(s)$ or feedback $C(s)$ control. The aim is to show various ways to control the diaphragm velocity response.

5.3 Control system design

This section discusses active control techniques for modifying the acoustic impedance at the loudspeaker diaphragm. The effect of applying feedforward control on pressure disturbance and motional feedback is first presented. Both control systems are then combined. The small signal parameters of the loudspeaker considered for the simulations can be found in Tab. 5.1. The control settings used for running the simulations are given in Tab. 5.2.

5.3.1 feedforward control

In feedforward control, the manipulated variable (here the input voltage) is only related to the time-varying reference. No information on the process variable (here the diaphragm velocity) is provided to the controller. As a consequence, feedforward control often requires the inclusion of a mathematical model of the system into the control algorithm. In this way, the controller determines the type of action to take according to the state of the system. The "electronic sound absorber" described in [15] can be considered of the feedforward type¹. As mentioned in Section 2.4, it is used to reduce the sound pressure at the vicinity of a microphone. The general idea is to detect noise components which are to be cancelled and drive the loudspeaker accordingly. The function of the electronic sound absorber is to impose an appropriate relationship in terms of amplitude and phase between the incident and reflected sound waves at the diaphragm. In [27] also, a two-microphone system is used to calculate the control signal with the same

¹even though this concept is commonly referred to as "feedback" in the context of active noise cancellation, the term "feedback" is used, in this thesis, when the control signal is based on the output variable (here the diaphragm velocity).

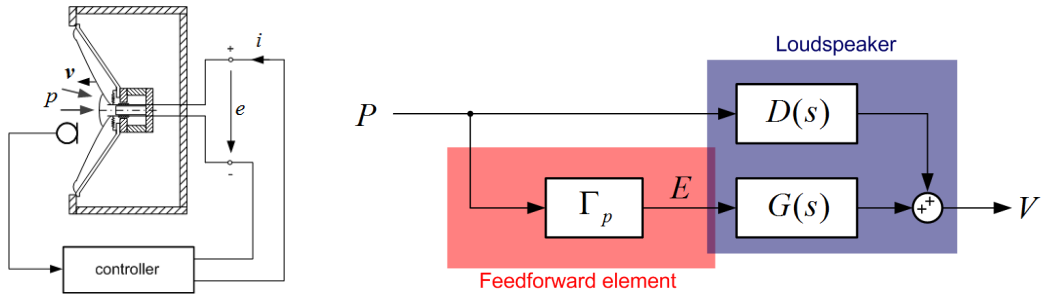


Figure 5.3: Diagram of a loudspeaker under feedforward control. On the left a schematic representation of the loudspeaker under control with the representative variables and on the right the corresponding block diagram.

functionality. These control systems are of feedforward type since only the pressure is involved in the command signal. Indeed, no velocity sensor is used to directly control the output variable. In view of controlling the acoustic impedance through a loudspeaker [49], the microphone must be located as close as possible to the diaphragm, as depicted in Fig. 5.3.

When expressing the control problem with the aforementioned formalism, one identifies the input voltage applied to the loudspeaker terminals as

$$e(t) = \Gamma_p p(t) \quad (5.11)$$

where Γ_p is the proportional gain and e the command voltage. Substituting the Laplace transform of Eq. (5.11) in the characteristic equations (3.19) of the loudspeaker gives the general expression of the specific acoustic admittance as

$$\frac{V(s)}{P(s)} = \frac{SL_e s + SR_e + Bl \Gamma_p}{M_{ms} L_e s^3 + (M_{ms} R_e + R_{ms} L_e) s^2 + \left(R_{ms} R_e + \frac{L_e}{C_{mc}} + (Bl)^2 \right) s + \frac{R_e}{C_{mc}}} \quad (5.12)$$

As stated in Eq. (5.12), the loudspeaker controlled by feedforward behaves as a third-order system. The feedforward gain Γ_p is only at the numerator. Consequently, it allows varying the system gain but will not have any effect upon the control bandwidth, as shown in Fig 5.4(a). Notice that both the real and imaginary part of the specific acoustic impedance are affected. Applying a gain $\Gamma_p > 0$ leads to decreasing the acoustic resistance while the opposite occurs for a negative gain (see Fig. 5.4(c)). Also note that both the increase and decrease of the acoustic resistance are frequency-dependent. The variation of the gain Γ_p on the absorption coefficient is shown in Fig. 5.5(a). From a control perspective, the transducer stability is theoretically always ensured when controlled by feedforward. The coefficients in the denominator are all positive real since they do not depend on control settings.

Chapter 5. Changing the acoustic impedance using feedback control

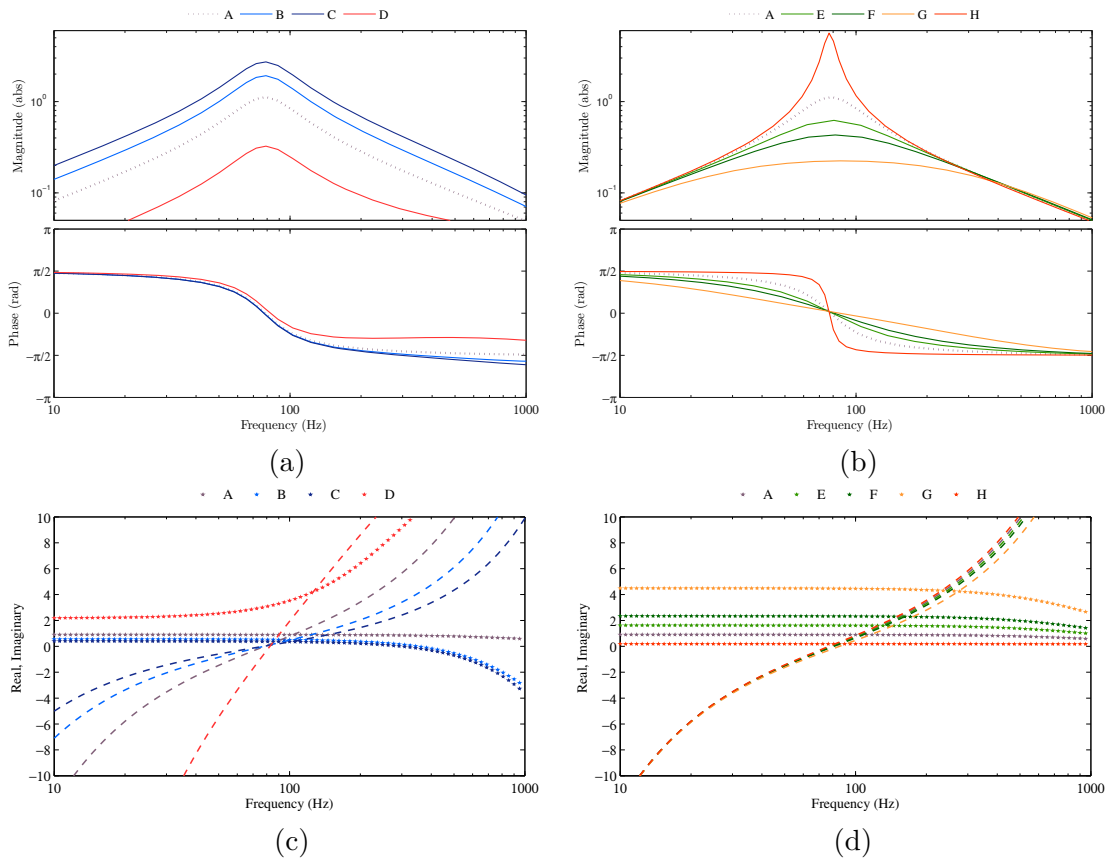


Figure 5.4: Computed frequency response of the loudspeaker under feedforward (a) and feedback (b) control. The Bode plot of the specific acoustic admittance ratio is shown at the top and the real (\star) and imaginary part (---) of the specific acoustic impedance ratio are shown at the bottom.

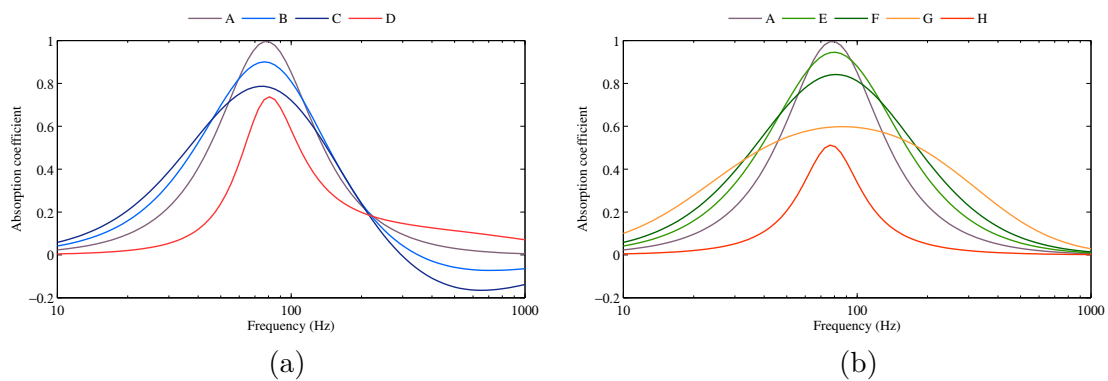


Figure 5.5: Computed absorption coefficient of the loudspeaker under feedforward (a) and feedback (b) control.

5.3.2 Motional feedback control

The technique of motional feedback has been known since the late of 1950's [50, 98–100]. In audio, this technique can be used to improve the transient response, to reduce non-linearity and distortion, or to extend the frequency range of a loudspeaker in the low frequencies [51, 53, 68, 99, 101].

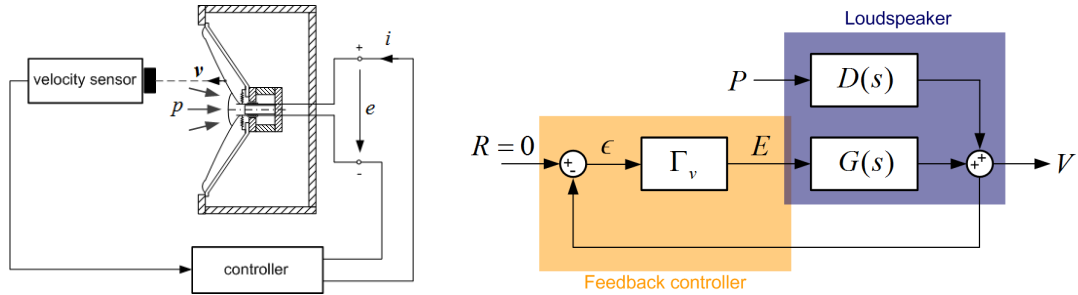


Figure 5.6: Diagram of a loudspeaker under motional feedback control. On the left a schematic representation of the loudspeaker under control with the representative variables and on the right the corresponding block diagram.

In motional feedback control, the manipulated variable, here the applied voltage, depends on the diaphragm velocity only. The idea is to drive the loudspeaker with a voltage proportional to the velocity of the diaphragm, allowing dynamic control. The sensing of diaphragm velocity can be performed indirectly by electrical means. For instance, the separation of induced emf (proportional to velocity) and driving voltage can be achieved with the help of an impedance bridge, as detailed in [50]. Obviously, any motion sensor (accelerometer, velocimeter) can be used to provide the command voltage directly [51]. It is also possible to derive a velocity signal using the same principle as described above, but with the help of control theory. In [65], the analog circuitry providing the velocity signal is referred to as an observer model that is used to generate a feedback signal for a digital feedforward controller to provide linear adaptive equalization.

From the aforementioned formalism, motional feedback can be formulated as the following command voltage

$$e(t) = -\Gamma_v v(t) \quad (5.13)$$

where Γ_v is the proportional gain and e is the voltage applied across the transducer terminals.

Substituting the Laplace transform of Eq. (5.13) in the characteristic equations (3.19) of the loudspeaker leads to a closed form expression of the specific acoustic admittance,

which can be written as

$$\frac{V(s)}{P(s)} = \frac{SL_e s + SR_e}{M_{ms}L_e s^3 + (M_{ms}R_e + R_{ms}L_e) s^2 + \left(R_{ms}R_e + \frac{L_e}{C_{mc}} + (Bl)^2 + Bl\Gamma_v\right) s + \frac{R_e}{C_{mc}}} \quad (5.14)$$

As stated in Eq. (5.14), the loudspeaker under motional feedback control is still a third-order system, but with some ability to change the coefficients in the denominator. From the perspective of control, the motional feedback technique is a way to move the closed-loop poles, and hence helps to improve the control bandwidth (Fig. 5.4(b)), as discussed later. Compared to the feedforward control, the gain Γ_v has no influence on the system zeros. Motional feedback also has the effect of increasing the acoustic resistance, but without changing the imaginary part of the acoustic impedance (see Fig. 5.4(d)). The effect of feedback gain Γ_v on the real part of the specific acoustic impedance is inversely related to that of feedforward gain Γ_p . The acoustic resistance of the diaphragm increases as the gain increases and tends to zero as Γ_v becomes negative. As shown in Fig. 5.5(b), the absorption coefficient with positive gain decreases as Γ_v increases, while the Q -factor diminishes. The application of the motional feedback to a loudspeaker may cause stability issues. When varying the gain Γ_v , some coefficients of the denominator may become negative, thus contradicting Routh's stability criterion (See Section 4.4.4). When applying a too high negative gain, the complex conjugate poles may cross the imaginary axis, thus yielding to exponentially increasing behavior (see Fig. 5.15(b)).

5.3.3 Combined feedback and feedforward control

Feedback control systems that include a feedforward element generally improves performances whenever there is a major disturbance that can be measured before it affects the plant output. Through feedback control actually, unknown disturbance is handled without having the exact knowledge on how the system will react to it. By including the feedforward control, the plant is now capable of responding to the disturbance before it can affect the system [79].

In the scope of acoustic impedance control, various arrangements combining feedback and feedforward have been discussed under different names [16, 25, 46, 49, 54, 55]. In [25], the feedforward control based on pressure sensing is combined with porous materials so as to improve performances in terms of target acoustic resistance. In [54], a microphone is used to monitor the pressure, a miniature accelerometer is attached to the diaphragm and connected to an integrator to provide the instantaneous velocity, and a mixer is required so as to establish a desired relationship between both acoustic quantities. In [49], the use of accelerometer and integrator to get the diaphragm velocity is replaced by an impedance bridge with the same functionality. This strategy is often referred to as direct

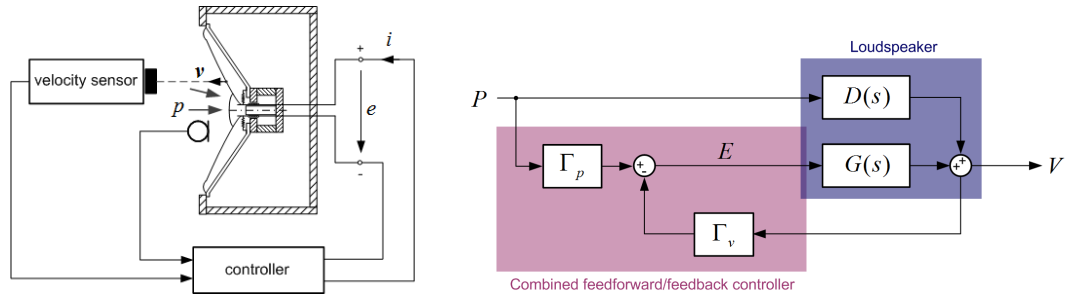


Figure 5.7: Diagram of a loudspeaker under combined feedback/feedforward control. On the left a schematic representation of the loudspeaker under control with the representative variables and on the right the corresponding block diagram.

impedance control since both the sound pressure and velocity are involved. A general representation of the combined feedback and feedforward control is given in Fig. 5.7.

From the control engineering perspective, combining Eq. (5.11) and Eq. (5.13) can be expressed as

$$e(t) = \Gamma_p p(t) - \Gamma_v v(t) \quad (5.15)$$

Strictly speaking and according to Eq. (5.6), the control law given by Eq. (5.15) could also be written as $e(t) = K_p \varepsilon(t)$, where K_p is a proportional gain such that $K_p = \rho c \Gamma_p = \Gamma_v$. For ease of understanding, however, the control law (5.15) is preferred in the following developments.

Substituting the Laplace transform of Eq. (5.15) in the characteristic equations (3.19) yields the following specific acoustic admittance of the loudspeaker under combined feedback and feedforward control

$$\frac{V(s)}{P(s)} = \frac{SL_e s + SR_e + Bl \Gamma_p}{M_{ms} L_e s^3 + (M_{ms} R_e + R_{ms} L_e) s^2 + \left(R_{ms} R_e + \frac{L_e}{C_{mc}} + (Bl)^2 + Bl \Gamma_v \right) s + \frac{R_e}{C_{mc}}} \quad (5.16)$$

Not surprisingly, the loudspeaker under combined feedback/feedforward control is still a third-order system. When $\Gamma_v/\Gamma_p = \rho c$, a target acoustic resistance value can be achieved on a relatively large bandwidth, as shown in Fig. 5.8. As in motional feedback, the extension of the control bandwidth is made possible by increasing gain Γ_v , theoretically up to infinity.

As shown in Fig. 5.9(a) the Q -factor diminishes when applying positive gains but increases with negative gains. As further discussed, an actual limitation of gains is encountered in

practice, however, mainly due to the variation of L_e and R_e with frequency that are not considered in this model. The setting of the electroacoustic resonator with combined control is quite straightforward. It is first to adjust the ratio of gains to equal a desired acoustic resistance value, and then increasing simultaneously the two gains (while their ratio $\Gamma_v/\Gamma_p = \rho c$ remains constant) up to the aforementioned instability threshold.

5.4 Advanced control system design

5.4.1 Uncompensated control system analysis

Different ways to actively control the acoustic impedance using a loudspeaker have been discussed so far. The primary objective is to force the loudspeaker, considered now as an electroacoustic resonator, to respond in a manner characteristic of a positive real

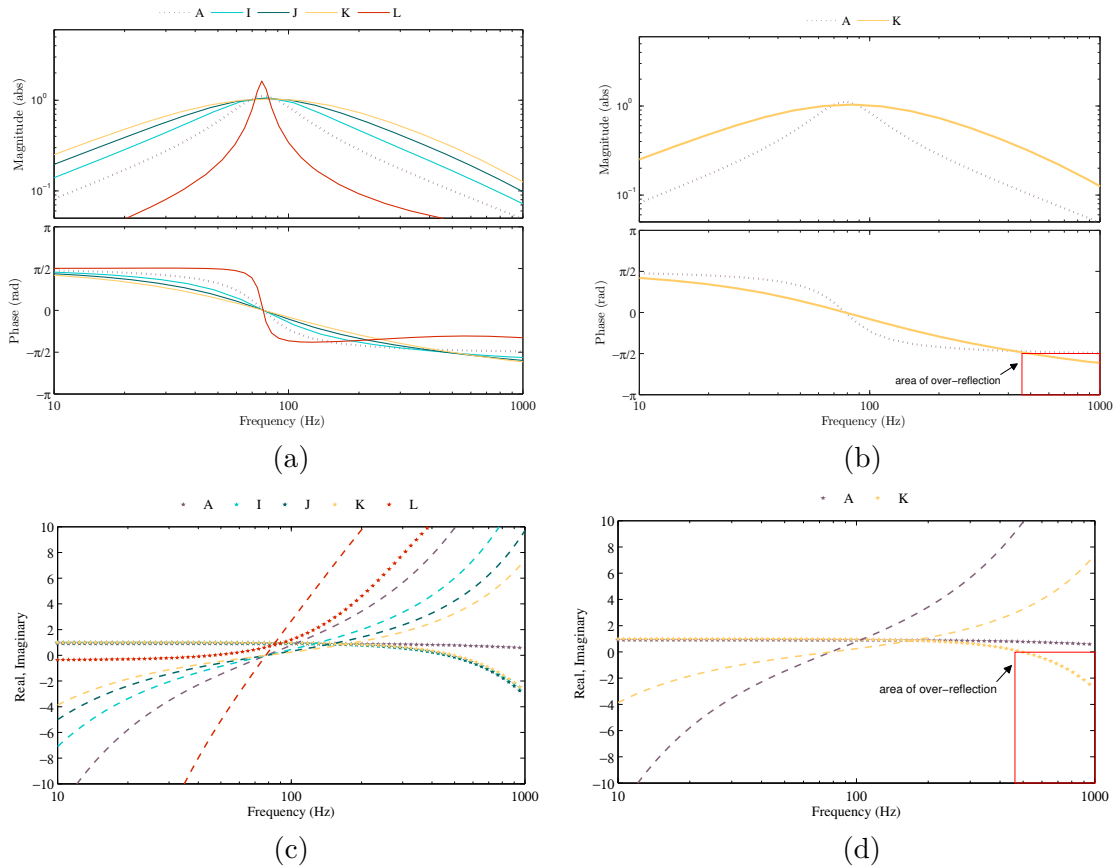


Figure 5.8: Computed frequency response of the loudspeaker under combined feedback/feedforward control. The Bode plot of the specific acoustic admittance ratio is shown at the top and the real (\star) and imaginary part ($---$) of the specific acoustic impedance ratio are shown at the bottom.

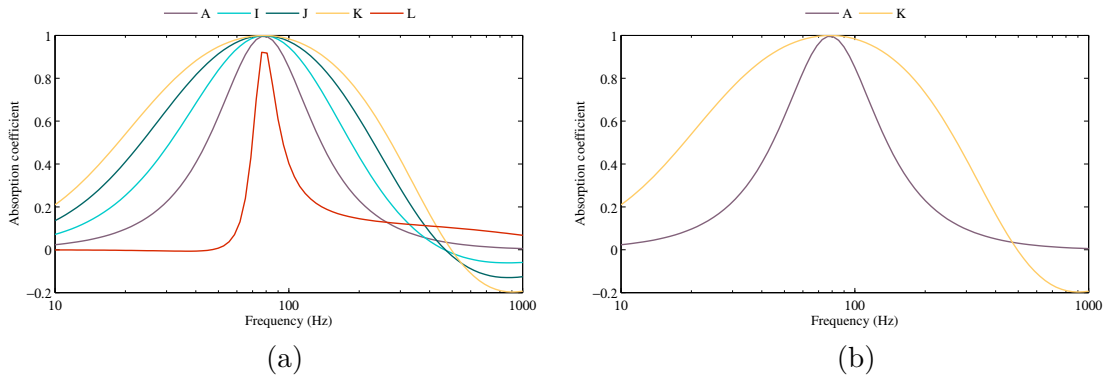


Figure 5.9: Computed absorption coefficient of the loudspeaker under combined feedback/feedforward control.

system, i.e. with ability to dissipate acoustic energy. To summarize the previous section,

1. by feedforward control the system gain can be varied and the real and imaginary part of the specific acoustic impedance can be changed either by a positive or negative gain Γ_p ,
2. by motional feedback control the control bandwidth can be increased; the real part of the specific acoustic impedance can be changed when varying Γ_v without affecting the imaginary part,
3. by combined control, the gains Γ_p and Γ_v can be optimized to make the specific acoustic resistance equal to the characteristic impedance of the medium over a large bandwidth, while decreasing the reactive part.

The underlying question is: can we achieve even better performance?

When it comes to providing acoustic absorption, no reflection is obviously desirable, even outside the desired control bandwidth. From Section 4.4.3, this means that the absorption coefficient α must be between 0 and 1 everywhere in the frequency range of interest. This is equivalent to achieving a target apparent acoustic resistance at the diaphragm, while forcing the normal velocity to be in phase with the pressure acting on it, i.e. canceling the reactive part. Referring to Section 4.4, this condition is met as long as the real part of the specific acoustic impedance ratio $z = Z_s/(\rho c)$ is positive. The electroacoustic resonator may reflect more sound energy than it receive, i.e. $|r| > 1$, for the frequencies where $\Re(z) < 0$. Note that this situation can only occur with a loudspeaker under active control. When reflection is desired instead, as for reinforcing the reverberated sound field in a room for instance, the role of the controller would be to make the real part of the complex quantity z negative.

By applying a proportional control, some unexpected behavior in the diaphragm velocity response may occur in the frequency range of interest. For instance, an over-reflecting behavior can be observed when feedforward gain Γ_p exceeds a certain bound. To be consistent with a real positive system, the phase shift of the electroacoustic resonator must alternate between $\pm \pi/2$, as discussed in Chapter 4. As shown in Fig. 5.8, the phase of frequency response continues to decrease from 550 Hz and deviates from the desired bounds $\pm \pi/2$. This causes the diaphragm to reflect more acoustic energy than it receives. In order to correct such undesired behavior, or to offer a greater versatility and more flexibility, it may be beneficial to consider additional ways of control.

In the following, we shall investigate some classical control techniques for compensating for the transducer response at given crossover frequencies.

5.4.2 PID controller

Proportional-Integral-Derivative (PID) controllers are widely used in industrial control systems to obtain a desired control response. The popularity of the PID controller can be attributed partly to its robustness for a wide range of situations, and partly to its functional simplicity which allows straightforward implementations [79,80]. No reference in the literature does mention the implementation of the PID controller for acoustic impedance control purpose. At first sight such controller seems interesting because it allows to achieve integral and derivative actions on the error signal (5.6). Compared to a purely proportional feedback control, these additional actions make possible to further improve the system performance [79,94,95]. For these reasons it is worth investigating the PID control in order to better satisfy desired specifications. This includes extending the control bandwidth toward low or high frequencies or improving the phase margin.

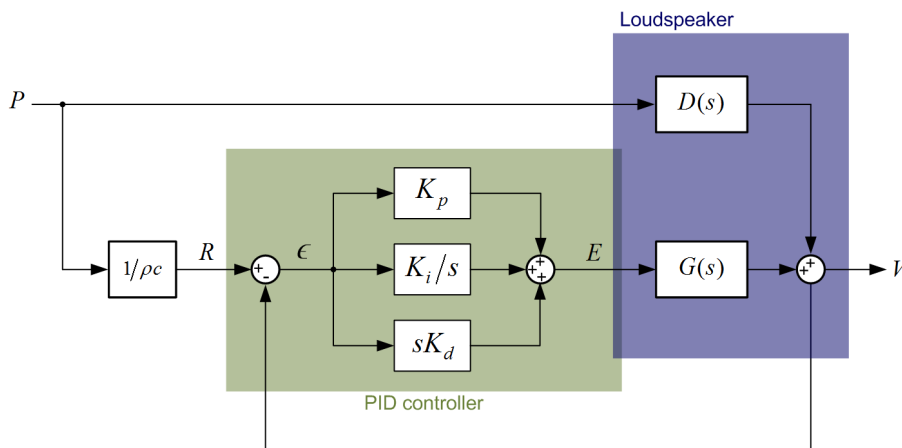


Figure 5.10: Block diagram representation of a PID control architecture where P is the sound pressure acting on the diaphragm, ϵ is the error signal, E is the applied voltage to the loudspeaker, and V the resulting diaphragm velocity.

The basic structure can be explained by the parallel connection of the P, I and D elements shown in Fig. 5.10. When used in this way,

1. P element delivers a signal proportional to the error at the instant t ,
2. I element delivers a signal proportional to the integral of the error up to instant t ,
3. D element delivers a signal proportional to the derivative of the error at instant t .

Mathematically speaking, the time response of the parallel form of the PID controller output is

$$e(t) = K_p \epsilon(t) + K_i \int_0^t \epsilon(\tau) d\tau + K_d \frac{d}{dt} \epsilon(t) \quad (5.17)$$

where K_p is a proportional gain, K_i is an integral gain, and K_d is a derivative gain. At every moment, the controller processes both the integral and the derivative of this error signal. By choosing the control parameters appropriately, the process can be adapted to achieve the desired behavior. Generally speaking, K_p , K_i and K_d have different effects on the closed-loop system. The proportional gain K_p is used to reduce the rise time. The contribution of the integral term K_i is basically to make the response of process toward the set point faster and eliminate the residual steady-state error that occurs with pure proportional controller. The derivative action K_d aims at improving the transient response by lowering the magnitude of overshoot while improving the stability of the whole closed-loop system.

From the block diagram 5.10, the transfer function for the PID controller is

$$C(s) = K_p + \frac{K_i}{s} + sK_d \quad (5.18)$$

Combining Eq. (5.18) with the characteristic equations (3.19) gives the specific acoustic admittance of the loudspeaker under PID control as

$$\frac{V(s)}{P(s)} = \frac{a_2 s^2 + a_1 s + a_0}{b_3 s^3 + b_2 s^2 + b_1 s + b_0} \quad (5.19)$$

where

$$\begin{aligned} a_2 &= SL_e + \frac{Bl}{\rho c} K_d & b_3 &= M_{ms} L_e \\ a_1 &= SR_e + \frac{Bl}{\rho c} K_p & b_2 &= M_{ms} R_e + R_{ms} L_e + Bl K_d \\ a_0 &= \frac{Bl}{\rho c} K_i & b_1 &= R_{ms} R_e + \frac{L_e}{C_{mc}} + (Bl)^2 + Bl K_p \\ & & b_0 &= \frac{R_e}{C_{mc}} + Bl K_i \end{aligned} \quad (5.20)$$

Apart from b_3 , it is obvious that the PID gains (K_p, K_i, K_d) are formally present in each of the other coefficients. Consequently, and they may further modify the specific acoustic admittance.

The control settings considered for running the simulation with PID control can be found in Tab. 5.3. As clearly shown in Figure 5.13(a), the application of a PID control on the error signal (5.17) has a significant effect on the behavior of the loudspeaker. However, it leads to contradictory effects on the system. The action of the PI controller leads to extend the control bandwidth at low frequencies but it also tends to reduce it in the high-frequency range. The opposite occurs in the case of PD controller. As a result, a tradeoff has to be made to favor the bandwidth extension in the low or high frequencies. In the following section we shall see complementary means for improving the desired behavior of a loudspeaker under control by introducing phase compensation techniques.

5.4.3 Lead-lag compensator

A lead-lag compensator is a component that improves an undesirable frequency response in a feedback control system. Such additional component is commonly used to satisfy specifications on steady state accuracy and phase margin. One can also have specifications on gain crossover frequency or closed-loop bandwidth. The phase lead-lag design procedure is basically graphical in nature. All we need is the measured or computed frequency responses of the uncompensated system so as to determine whether the system correction requires a lead or lag compensator, or a combination of the two [79].

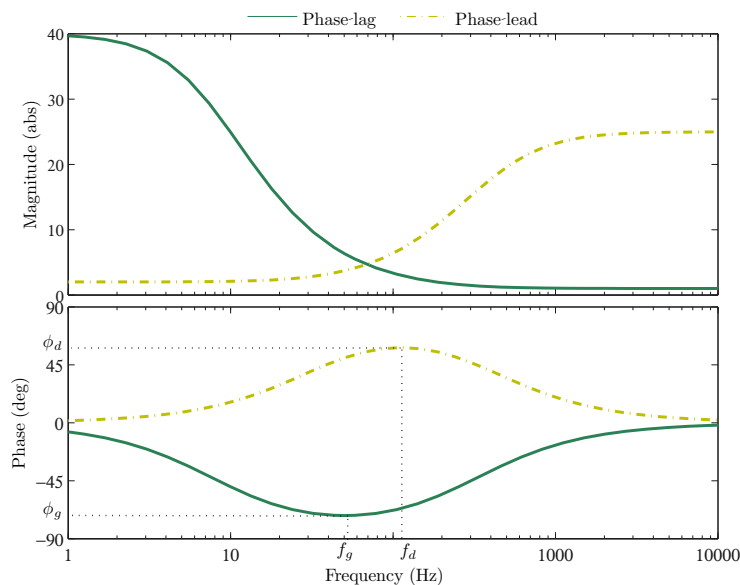


Figure 5.11: Magnitude and phase plots for typical lead and lag compensators.

In [42], the lead-lag compensation technique is introduced in a control system so as to improve the low-frequency dissipation of acoustical energy in a reverberant sound field. In the context of acoustic impedance control, we are first interested in adjusting, if needed, the phase shift between driving pressure and the diaphragm velocity response. The use of a lead or lag compensator provides complementary means to improve the loudspeaker behavior. The main objective is then to investigate whether this technique may prevent the diaphragm from becoming over-reflective in the frequency range of interest, as presented in Section 5.4.1.

Phase-lead compensator

The primary function of the lead compensator is to reshape the frequency-response curve of the uncompensated loudspeaker. This means that a sufficient phase lead must be provided to the system so as to offset the excessive phase lag caused by proportional control, and hence improve the closed-loop system stability. Such compensation is required when the phase shift of the system is less than $-\pi/2$.

The specific structure of the phase-lead compensator is given by

$$C_{\text{lead}}(s) = K_1 \alpha \frac{\tau_1 s + 1}{\alpha \tau_1 s + 1} \quad \text{and} \quad 0 < \alpha < 1 \quad (5.21)$$

where K_1 is a gain, τ_1 is a time constant and α is an adjustment factor for the lead compensator. The major characteristic of the phase-lead compensator is the positive phase shift in the intermediate frequencies, as illustrated in Fig. 5.14. The frequency (in Hz) where the maximum phase-lead occurs and the maximum phase lead in degree are given by

$$f_d = \frac{1}{2\pi} \frac{1}{\tau_1 \sqrt{\alpha}} \quad \text{and} \quad \phi_d = \frac{180}{\pi} \arcsin \left(\frac{1 - \alpha}{1 + \alpha} \right) \quad (5.22)$$

As illustrated in Fig. 5.11, a large positive phase shift is expected at intermediate frequencies which maximum value occurs at the crossover frequency f_d indicated in Eq. (5.22). Changing the gain merely leads to a shift in the magnitude curve of the lead compensator of a factor K_1 . The value for τ_1 and α are chosen to satisfy the phase margin and gain crossover specifications.

Phase-lag compensator

The role of a lag compensator is to provide attenuation in the high-frequency range to allow sufficient phase margin to the system. Compared to the lead compensator, the goal is to adjust the magnitude curve as needed without shifting the phase curve. The frequency that is chosen for the compensated gain crossover frequency should be such

Chapter 5. Changing the acoustic impedance using feedback control

that the phase shift of the system has the correct value to satisfy the phase margin specification.

The specific structure of the phase-lag compensator is given by

$$C_{\text{lag}}(s) = K_2 \frac{\tau_2 s + 1}{\beta \tau_2 s + 1} \quad \text{with } \beta \geq 1 \quad (5.23)$$

where K_2 is a gain, τ_2 is a time constant and β is an adjustment factor for the lag compensator. The major characteristics of the phase-lag are the constant attenuation in magnitude and the zero phase shift at high frequencies. As illustrated in Fig. 5.11, a large negative phase shift is also expected at intermediate frequencies. The maximum phase-lag frequency (in Hz) and maximum phase lag in degree can be derived after

$$f_g = \frac{1}{2\pi} \frac{1}{\tau_2 \sqrt{\beta}} \quad \text{and} \quad \phi_g = \frac{180}{\pi} \arcsin \left(\frac{1 - \beta}{1 + \beta} \right) \quad (5.24)$$

As for the lead compensator, changing the gain moves the magnitude curve by a factor K_2 and the tuning parameters τ_2 and β are chosen to satisfy the phase margin and crossover specifications. More details concerning lead-lag compensation techniques can be found in [79, 80].

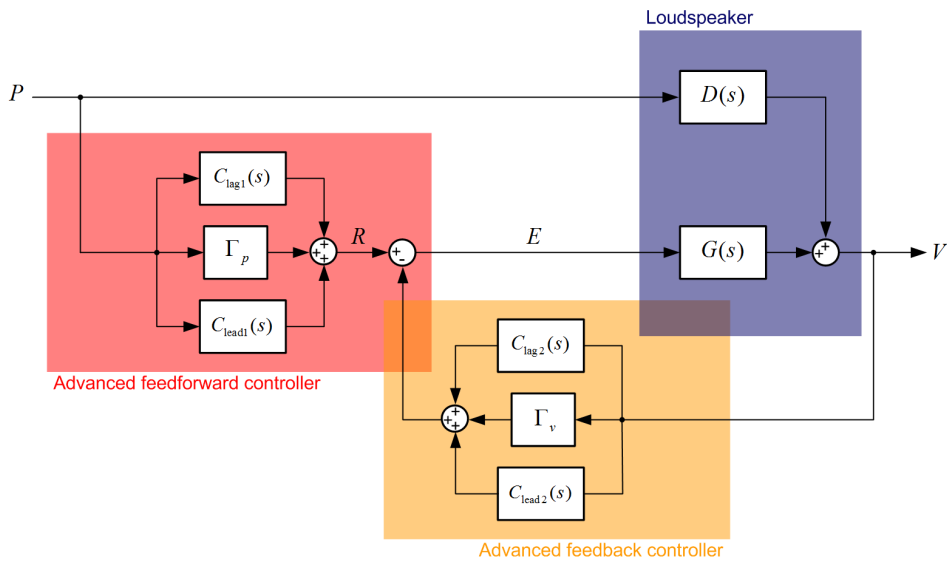


Figure 5.12: Block diagram of a loudspeaker under combined feedback/feedforward control with phase compensators where P is the sound pressure acting on the loudspeaker diaphragm, ε is the error signal, E is the input voltage applied to the electrical terminals, V is the resulting diaphragm velocity. The feedforward controller includes a proportional gain Γ_p , a lead $C_{\text{lead}1}$ and a lag $C_{\text{lag}1}$ compensator, and the feedback controller includes a proportional gain Γ_v , a lead $G_{\text{lead}2}$ and a lag $G_{\text{lag}2}$ compensator.

5.4.4 Advanced design procedure

In order to implement an advanced control system with phase compensation, the design procedure is to determine:

1. the proportional gains for the combined control to achieve the desired bandwidth,
2. the crossover frequencies at which the uncompensated system requires correction,
3. the value of phase shift that the compensator must provide,
4. the value of attenuation that is required to move the magnitude up or down.

The corresponding compensator parameters can then be derived after Eqs. (5.21-5.24).

5.4.5 Closed-loop transfer functions with lead-lag compensation

The transfer function of the closed-loop system can be readily obtained by substituting the controller gains and phase compensators into the characteristic equations of the loudspeaker.

As depicted in Fig. 5.12, the specific acoustic admittance can be written as

$$\frac{V(s)}{P(s)} = \frac{SZ_e(s) + Bl(\Gamma_p + C_{lag1}(s) + C_{lead1}(s))}{Z_m(s)Z_e(s) + (Bl)^2 + Bl(\Gamma_v + C_{lag2}(s) + C_{lead2}(s))} \quad (5.25)$$

In the case of combined control with phase compensation as detailed with settings P (see Tab. 5.4), i.e. $C_{lead1} = C_{lag2} = C_{lead2} = 0$, the closed-loop transfer function with the compensated control system can be expressed as

$$\frac{V(s)}{P(s)} = \frac{a_3 s^3 + a_2 s^2 + a_1 s}{b_4 s^4 + b_3 s^3 + b_2 s^2 + b_1 s + b_0} \quad (5.26)$$

where

$$\begin{aligned} a_3 &= \beta\tau SL_e \\ a_2 &= SL_e + \beta\tau SR_e + Bl(\beta\Gamma_p + K_2) \\ a_1 &= SR_e + \Gamma_p + K_2 \end{aligned} \quad (5.27)$$

and,

$$\begin{aligned}
 b_4 &= \beta\tau M_{ms}L_e \\
 b_3 &= M_{ms}L_e + \beta\tau(M_{ms}R_e + R_{ms}L_e) \\
 b_2 &= M_{ms}R_e + R_{ms}L_e + \beta\tau\left(R_{ms}R_e + \frac{L_e}{C_{mc}} + (Bl)^2 + Bl\Gamma_v\right) \\
 b_1 &= R_{ms}R_e + \frac{L_e}{C_{mc}} + (Bl)^2 + Bl\Gamma_v + \beta\tau\frac{R_e}{C_{mc}} \\
 b_0 &= \frac{R_e}{C_{mc}}
 \end{aligned} \tag{5.28}$$

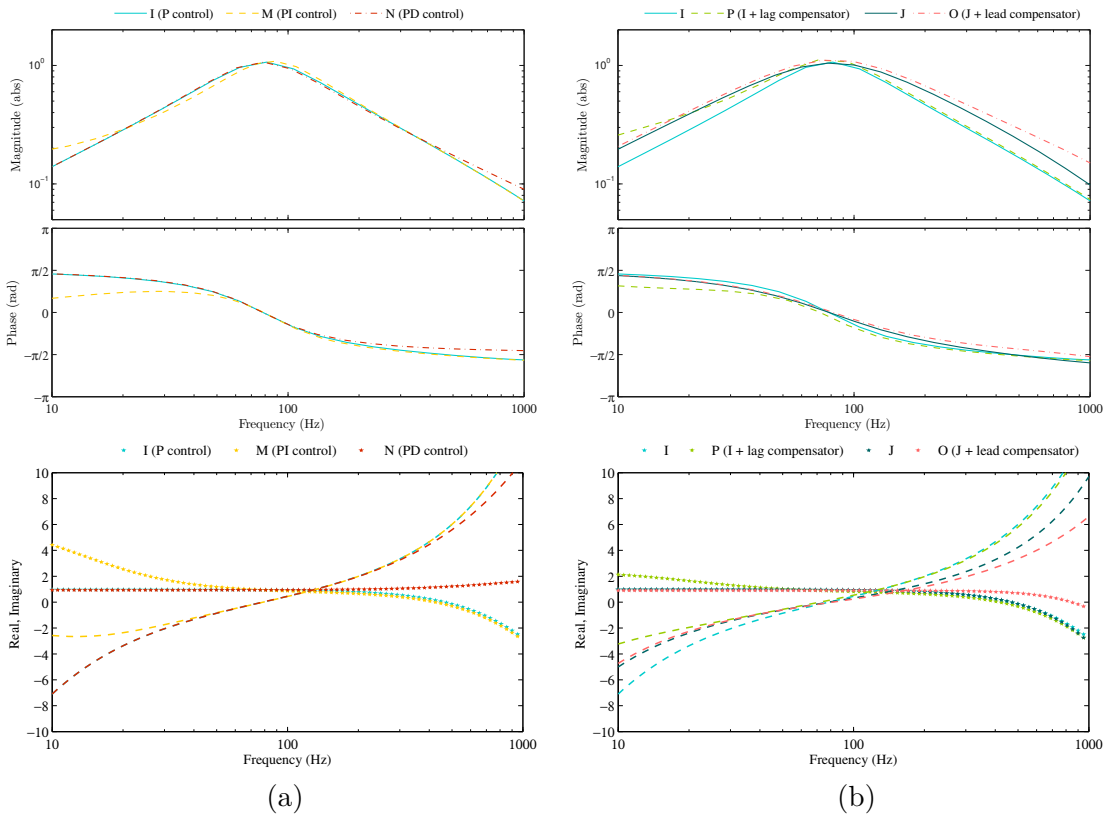


Figure 5.13: Computed frequency response of the loudspeaker under PID control (a) and with combined control and phase compensation (b). The Bode plot of the specific acoustic admittance ratio is shown at the top and the real (\star) and imaginary part (---) of the specific acoustic impedance ratio are shown at the bottom.

Both numerator and denominator the transfer function are affected by the control parameters. As a result, the diaphragm velocity response can be significantly changed, as depicted in Fig. 5.13(b) and 5.14(b). By compensating the phase, a greater bandwidth can be observed while removing the over-reflective behavior. Conventional tools such

5.4. Advanced control system design

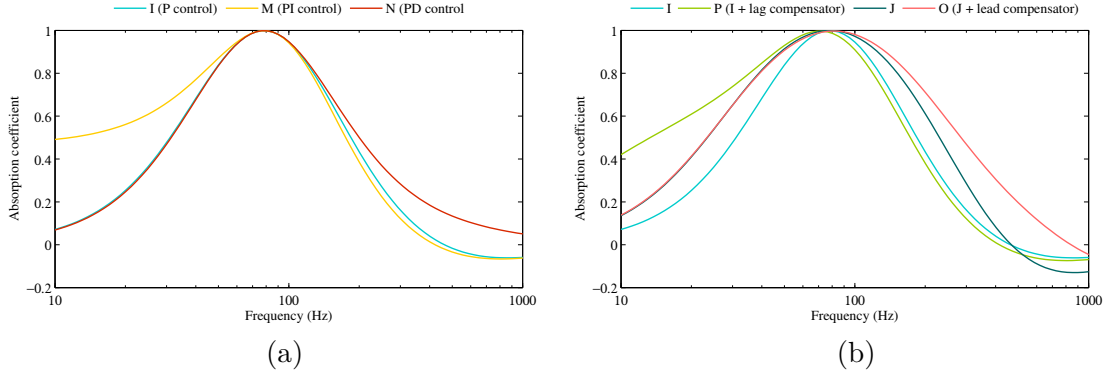


Figure 5.14: Computed absorption coefficient of the loudspeaker under PID control (a) and with combined control and phase compensation (b).

as Matlab Control System toolbox are useful to design and analyze advanced control systems. It becomes easier to visualize system behavior in frequency domain, as well as fine tuning the compensator parameters using Bode plot or pole-zero diagram.

In the case of combined control with phase compensation as detailed with settings O (see Tab. 5.4), i.e. $C_{lag1} = C_{lag2} = C_{lead2} = 0$, the coefficients of the closed-loop transfer function (5.27-5.28) are

$$\begin{aligned}
 a_3 &= \alpha\tau SL_e \\
 a_2 &= SL_e + \alpha\tau SR_e + \alpha Bl(\Gamma_p + K_1) \\
 a_1 &= SR_e + \Gamma_p + \alpha K_1
 \end{aligned} \tag{5.29}$$

and,

$$\begin{aligned}
 b_4 &= \alpha\tau M_{ms}L_e \\
 b_3 &= M_{ms}L_e + \alpha\tau(M_{ms}R_e + R_{ms}L_e) \\
 b_2 &= M_{ms}R_e + R_{ms}L_e + \alpha\tau\left(R_{ms}R_e + \frac{L_e}{C_{mc}} + (Bl)^2 + Bl\Gamma_v\right) \\
 b_1 &= R_{ms}R_e + \frac{L_e}{C_{mc}} + (Bl)^2 + Bl\Gamma_v + \alpha\tau\frac{R_e}{C_{mc}} \\
 b_0 &= \frac{R_e}{C_{mc}}
 \end{aligned} \tag{5.30}$$

As stated in (5.26), introducing phase compensation increases the order of the closed-loop transfer functions, by one degree for each lead or lag compensator. Applying both a phase lead and lag compensator together on p and v such as given in Eq. (5.25) will result in a closed-loop transfer function of order 7. As an illustration, the diagram of poles and zero with lead-lag compensation is depicted in Fig. 5.15(e) and 5.15(f) .

5.5 System performance using feedback control

5.5.1 System stability

In order to anticipate stability issues, the Routh criterion is applied to the denominator of the closed form expression of the specific acoustic admittance, namely the coefficients (b_3, b_2, b_1, b_0) in Eqs. (5.12), (5.14) and (5.16). As stated in Section 4.4.4, the necessary conditions for stability is that all poles have negative real parts. From Eq. (4.36), this implies that the coefficients (b_3, b_2, b_1, b_0) must be positive and such that $b_2b_1 > b_3b_0$. As discussed above, stability with feedforward control is theoretically ensured because (b_3, b_2, b_1, b_0) are all positive real and the control parameter only affects the numerator of the transfer function. In case of motional feedback or combined control, i.e. when the diaphragm velocity is involved, the condition for stability yields

$$\Gamma_v > -\frac{R_{ms}L_e}{Bl C_{mc}} \left(\frac{L_e}{M_{ms}R_e + R_{ms}L_e} + R_e \right) - Bl \quad (5.31)$$

Roughly speaking, transducer stability is guaranteed as $\Gamma_v > -Bl$.

5.5.2 System poles and zeros

The following focuses on the behavior of the system under control in terms of poles and zeros. As discussed in Section 4.2.7, the closed-loop poles of the loudspeaker under control can be derived after Eqs. (4.26-4.27). The pole-zero diagram given in Fig. 5.15 clearly illustrates the effect of applying the aforementioned control settings to an electrodynamic loudspeaker. With a positive feedforward gain $\Gamma_p > 0$, one zero moves away from the imaginary axis without affecting the poles, in accordance to Eq. (5.12). With $\Gamma_p < 0$, the zero moves in the opposite direction but without changing the poles (Fig. 5.15(a)).

Using motional feedback further alters the transducer dynamics. The pole-zero diagram in Fig. 5.15(b) shows the consecutive effect on the loudspeaker dynamics. With a positive gain $\Gamma_v > 0$ one real pole gets closer from the imaginary axis, while complex conjugate poles move toward the real axis. Note that the zeros stay unchanged, in accordance to Eq. (5.14). As discussed in Section 4.2.7, the damping of the system will increase as the complex conjugate poles move away from the imaginary axis. With a negative gain the trend reverses for the poles but the zeros are unchanged, as depicted in Fig. 5.15(b). With such a control setting, the resonance of the system will become more pronounced, and the diaphragm velocity response to an acoustic perturbation will be faster.

In combined control, the feedforward gains Γ_p is in the numerator while the feedback gain Γ_v is in the denominator of the transfer function that formally describes the behavior of the electroacoustic resonator. Compared to a purely feedback or feedforward control, this is a way to change both the system poles and zeros, as depicted in Fig. 5.15(c). By

5.5. System performance using feedback control

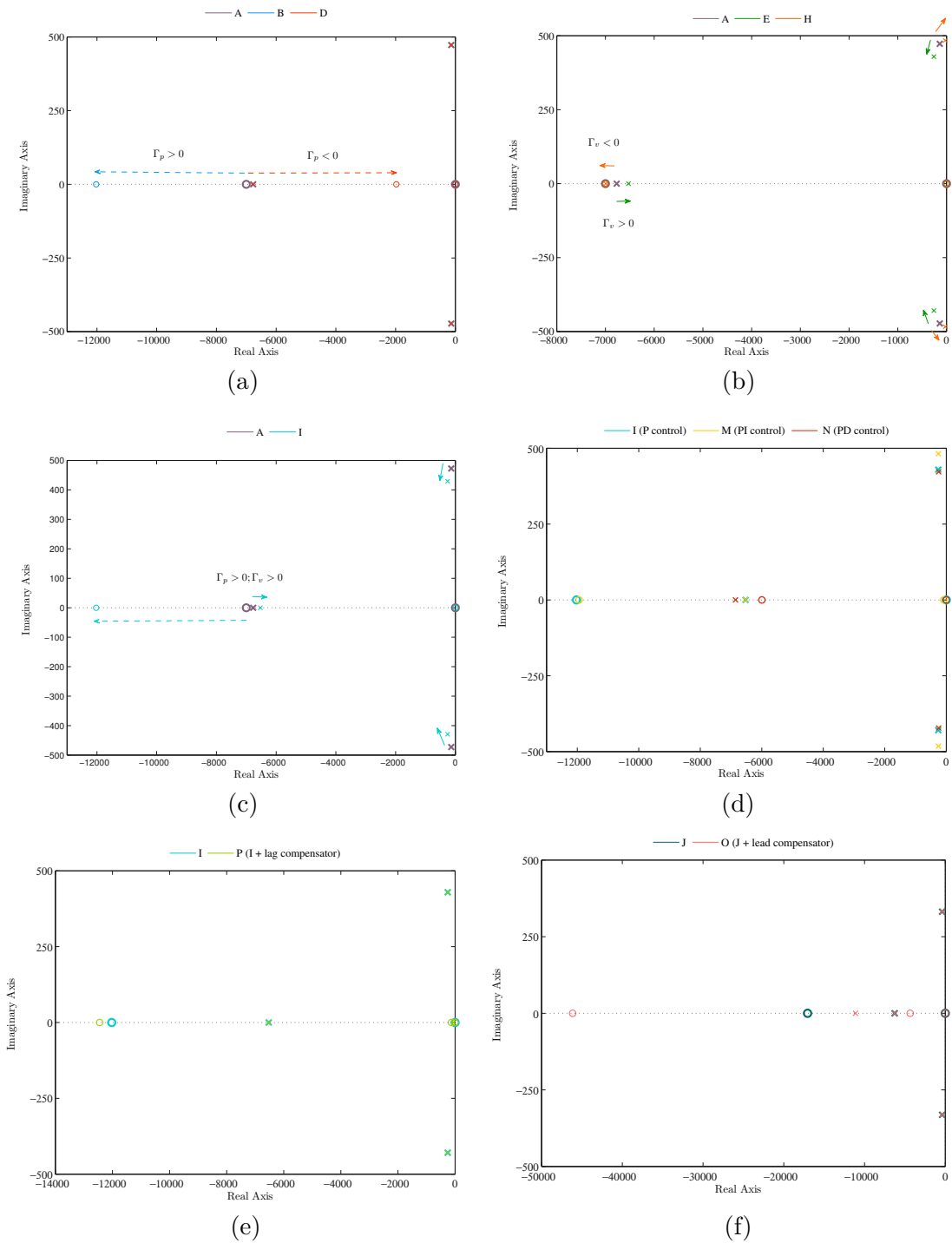


Figure 5.15: Pole-zero diagram of the loudspeaker under control.

applying positive gains Γ_p and Γ_v , one zero moves away from the imaginary axis while the real pole gets closer from the imaginary axis and complex conjugate poles approach

the real axis. With negative gains the trend reverses for the poles and the zero. Applying negative gain may lead some poles in the right-half plane, meaning instability for the system.

In PID control or combined control with lead-lag compensation, we have more degrees of freedom to place the system poles and zeros. The control parameters are indeed associated with most of the coefficients of the transfer function representing the specific acoustic admittance of the loudspeaker diaphragm, as stated in Eqs. (5.19-5.20) and (5.26-5.29). As depicted in Fig. 5.13(e) and 5.13(f), this introduces dominant poles that will help to expand the control bandwidth or to alter the transducer dynamics.

5.5.3 Experimental setup

In order to assess experimentally the acoustic performance when applying feedback control, a Monacor SPH-300TC low-range loudspeaker is employed as an electroacoustic resonator. The small signal parameters of the transducer can be found in Tab. 5.1. The specific acoustic admittance ratio and absorption coefficient are assessed after ISO 10534-2 standard [36], as depicted in Fig. 5.17.



Figure 5.16: Picture of the experimental setup.

For running the simulations, the rear face of the loudspeaker is loaded with a sealed enclosure the volume of which is 23 L. In this setup, an impedance tube is specifically designed (length $L = 3$ m and internal diameter $\varnothing = 310$ mm), one termination of which is closed by an electroacoustic resonator, the other end being open with a source loudspeaker. Three holes located at positions $x_1 = 1.3$ m, $x_2 = 0.9$ m and $x_3 = 0.7$ m from the electroacoustic resonator are the receptacles of 1/2" microphones (Norsonic Type 1225 cartridges mounted on Norsonic Type 1201 amplifier), sensing the sound pressures $p_1 = p(x_1)$, $p_2 = p(x_2)$ and $p_3 = p(x_3)$. The transfer function $H_{12} = p_2/p_1$ and $H_{13} = p_3/p_1$ are processed through a Pulse Bruel and Kjaer multichannel analyzer. This setup is used to measure the performance of electroacoustic resonator under normal incidence plane waves, over a frequency range between 30 Hz and 700 Hz.

5.5. System performance using feedback control

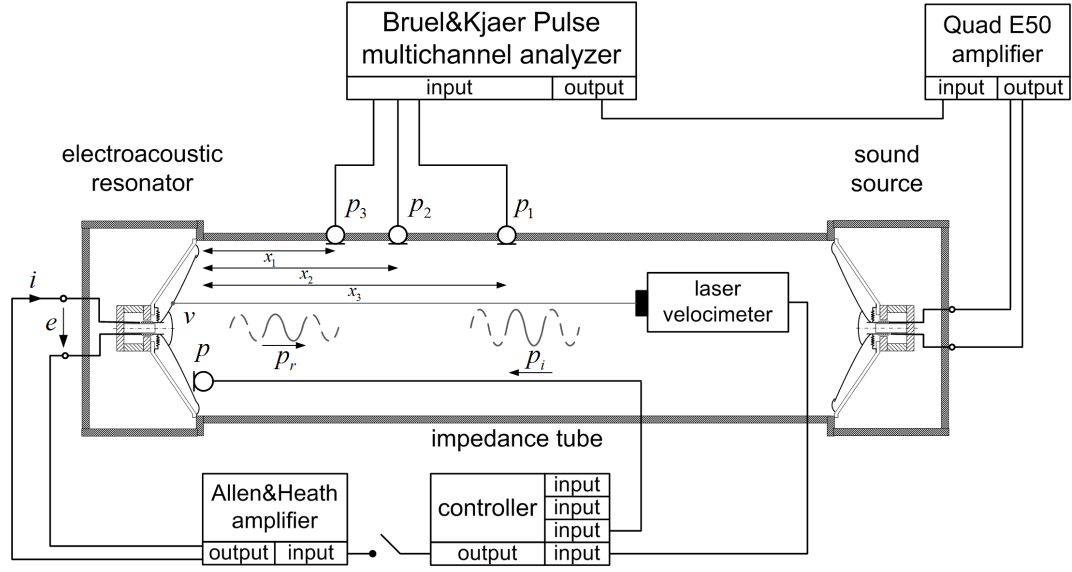


Figure 5.17: Schematics of the experimental setup used for the feedback control techniques.

The motional feedback is processed through a Polytec OFV-505/5000 laser velocimeter (sensitivity of $\sigma_v = 50 \text{ V m}^{-1} \text{ s}$). As depicted in Fig. 5.17, the velocity sensor is positioned within the duct, the laser beam focusing on a single point of the diaphragm at the middle of its radius. The pressure is sensed with an external PCB 130D20 microphone (sensitivity of $\sigma_p = 47.5 \text{ mV Pa}^{-1}$), located at 5 mm of the diaphragm and slightly off-center at a height of 3.2 cm from the duct wall. The digital controller used to apply the control parameters and to mix the input signals has been implemented on a real-time CompactRIO platform (National Instrument). The control signal is amplified with a unit gain before being applied to the transducer terminals, as depicted in Fig. 5.17. Note that an analog controller can be used instead.

Table 5.1: Small signal parameters of the Monacor SPH-300TC low-range loudspeaker considered for the simulations with feedback control.

Parameter	Notation	Value	Unit
dc resistance	R_e	6.3	Ω
Voice coil inductance	L_e	1.0	mH
Force factor	Bl	10.3	N A^{-1}
Moving mass	M_{ms}	68	g
Mechanical resistance	R_{ms}	3.24	$\text{N m}^{-1} \text{ s}$
Mechanical compliance	C_{ms}	0.85	mm N^{-1}
Effective area	S	495	cm^2
Natural frequency	f_0	23	Hz

5.5.4 Sound absorption/reflection capability

Experimental results from the application of feedback control of the acoustic variables p and v are presented in the following. Table 5.2 summarizes the control settings used for running the simulations with proportional control. The control settings used for running the simulations with PID control and with combined control including phase compensation are listed in Tab. 5.3 and Tab. 5.4.

Table 5.2: Control settings for the simulations with proportional control.

Topology	Case	Controller gains	
		Γ_p (V Pa ⁻¹)	Γ_v (V m ⁻¹ s)
Without control	A	0	0
	B	0.024	0
feedforward control	C	0.048	0
	D	-0.024	0
Motional feedback control	E	0	10
	F	0	20
	G	0	50
	H	0	-10
Combined feedback/feedforward	I	0.024	10
	J	0.048	20
	K	0.072	30
	L	-0.024	-10

Table 5.3: Control settings for the simulations with PID control (See Fig. 5.10).

Topology	Case	PID controller gains		
		K_p	K_i	K_d
PI control	M	10	2000	
PD control	N	10		0.002

Table 5.4: Control settings for the simulations with combined control and compensation.

Topology	Case	Controller gain		Lead compensator			Lag compensator		
		Γ_p	Γ_v	K_1	α	τ_1	K_2	β	τ_2
Advanced control	O	0.048	20	2	0.08	0.005			
	P	0.024	10				1	40	0.0005

5.5. System performance using feedback control

The following results show the measured acoustic performance of electroacoustic resonators when subjected to plane waves under normal incidence. Figure 5.18 illustrates the specific acoustic admittance and absorption coefficient obtained by applying the feedforward and feedback control. Generally speaking, the diaphragm velocity response measured in impedance tube is consistent with the behavior expected from the model. The slight discrepancy, however, can be attributed to imperfections in the small signal model.

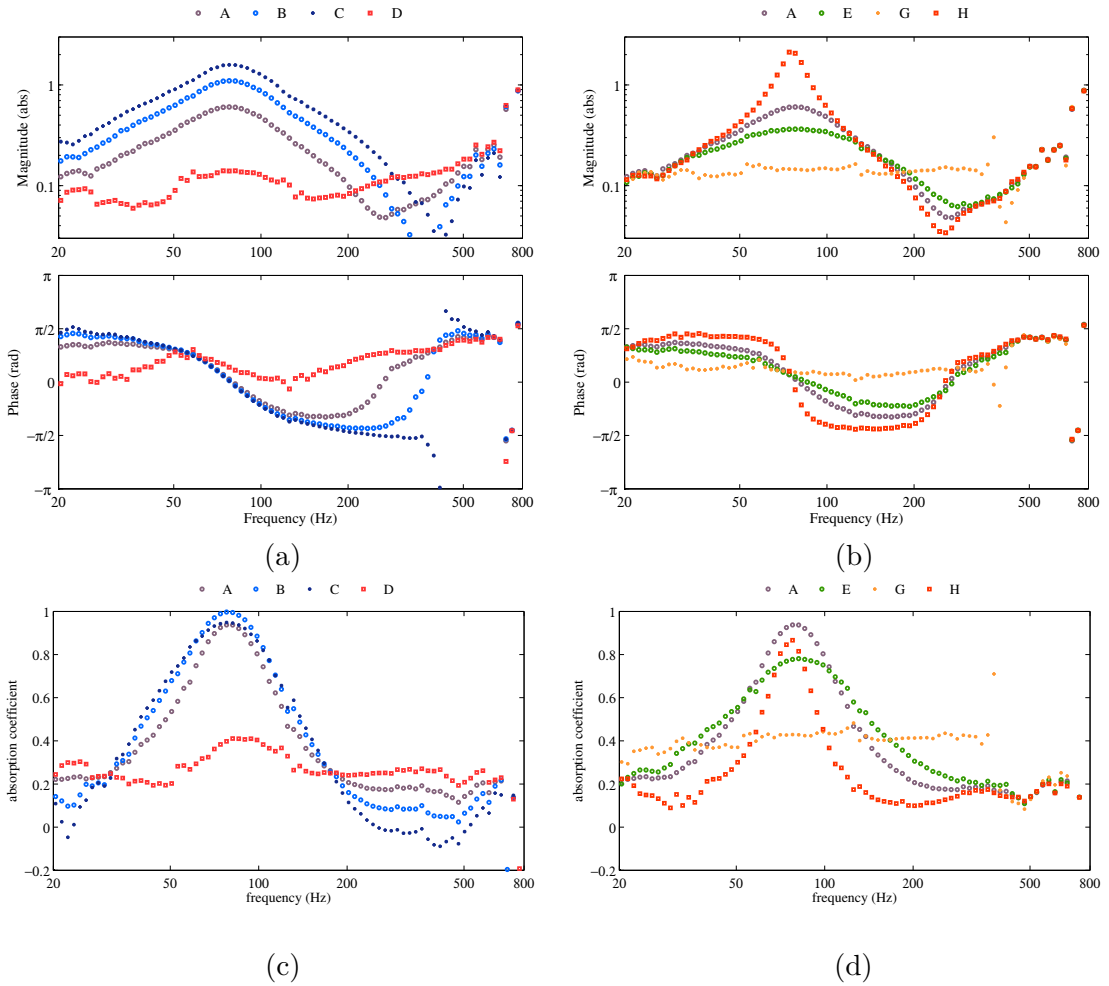


Figure 5.18: Measured acoustic performance with feedforward (a) and feedback (b) control. The specific acoustic admittance ratio is shown in magnitude and phase at the top and the corresponding absorption coefficient is at the bottom.

In case of feedforward control for instance, the velocity gain can be changed by varying Γ_p . It is also possible to figure out an optimal value Γ_p for which a target acoustic admittance can be achieved (see Fig. 5.18(a)). A negative gain (case D) prevents the diaphragm from oscillating. It can also be seen that the phase of the specific acoustic admittance crosses the value $-\pi/2$ when Γ_p exceeds 0.048 V Pa^{-1} (case C). As a result, the absorption coefficient may become negative (see Fig. 5.18(c)).

Chapter 5. Changing the acoustic impedance using feedback control

In motional control (Fig. 5.18(b)), a positive feedback gain Γ_v increases the control bandwidth but a consecutive effect is to move away from the target acoustic admittance. The phase of the specific acoustic admittance alternate between $\pi/2$ and $-\pi/2$ as the stability condition given in Eq. 5.31 is observed. As a result, the absorption coefficient is always positive (see Fig. 5.18(d)).

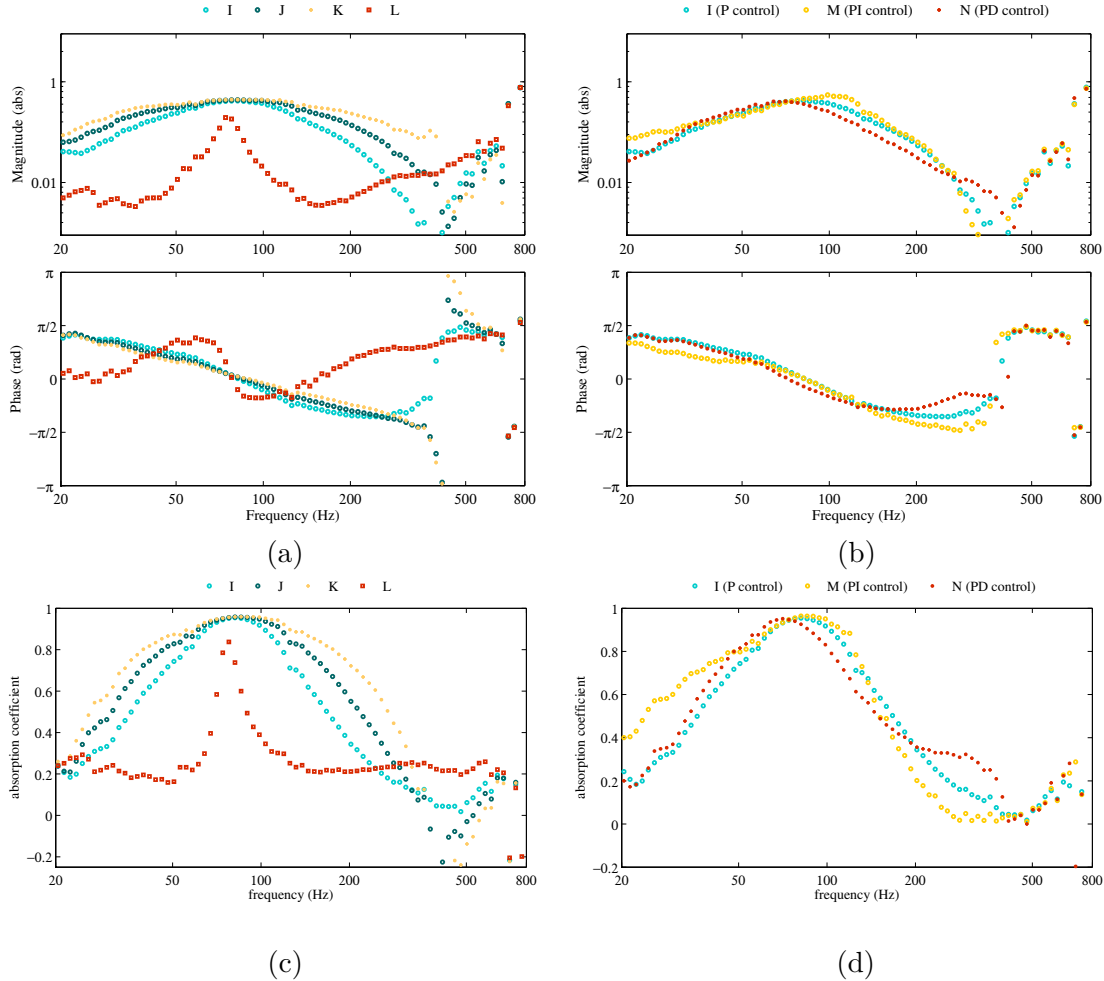


Figure 5.19: Measured acoustic performance with combined feedback/feedforward (a) and PID (b) control. The specific acoustic admittance ratio is shown in magnitude and phase at the top and the corresponding absorption coefficient is at the bottom.

In combined control (Fig. 5.19(a)), the control bandwidth can be extended while satisfying the target specific acoustic admittance. The condition is to observe a constant gain ratio between Γ_v and Γ_p which must equal to the target value, i.e. $\Gamma_v/\Gamma_p = \rho c$. In order to broaden the control bandwidth, gain values must be increased while maintaining the ratio constant. As expected, with a certain feedforward gain the phase of the specific acoustic admittance crosses the value $-\pi/2$ which is a feature of a positive real system. This occurs with case K at a crossover frequency of 450 Hz. With these control settings

5.5. System performance using feedback control

the electroacoustic resonator becomes over-reflecting in the frequency range of interest (see Fig. 5.19(c)). When applying negative gains Γ_p and Γ_v the control bandwidth is significantly reduced, as shown with case L.

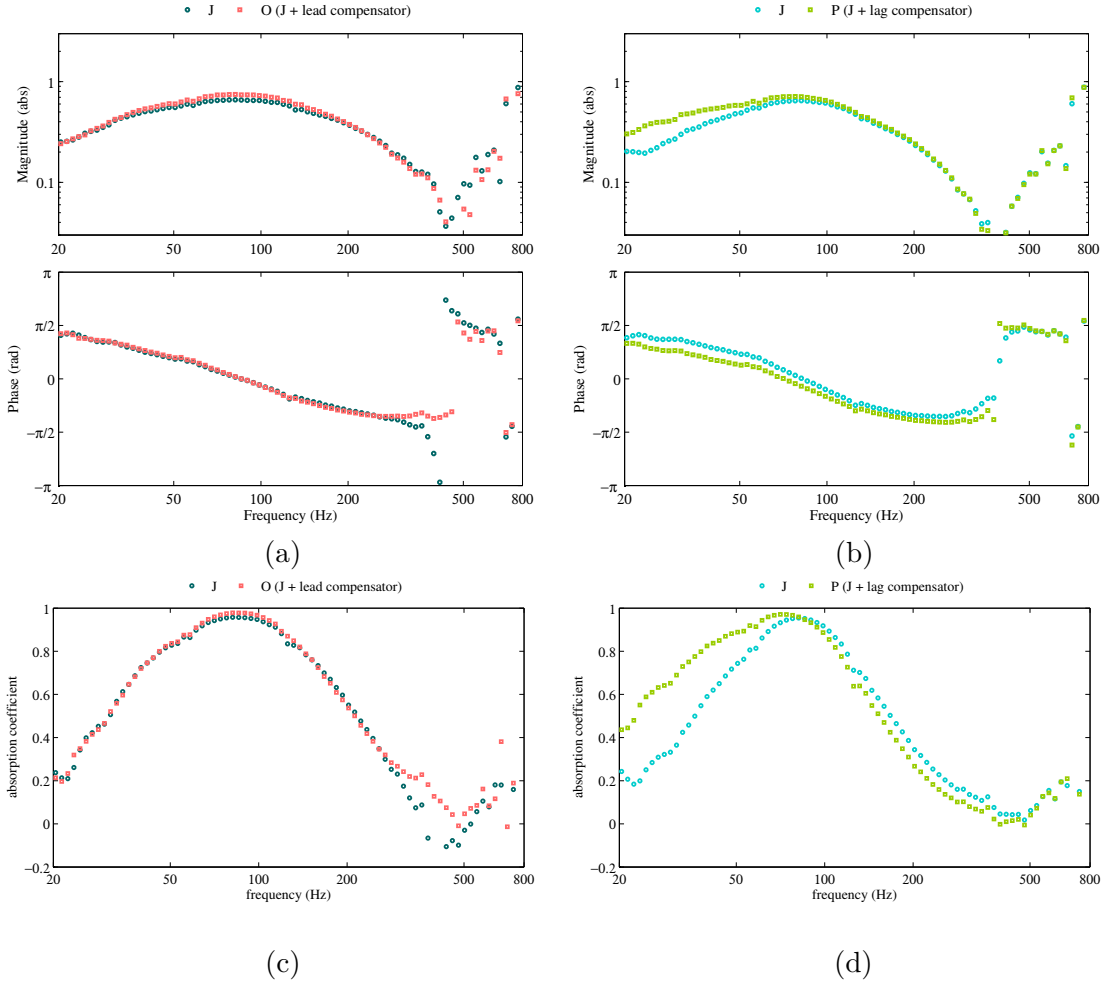


Figure 5.20: Measured acoustic performance with phase lead (a) and phase lag (b) compensation. The specific acoustic admittance ratio is shown in magnitude and phase at the top and the corresponding absorption coefficient is at the bottom.

In PID control (Fig. 5.19(b)), the diaphragm velocity response can be slightly improved, but the benefits are often achieved at the expense of others. The PI control, for example, improves the sound absorption capability of the loudspeaker, but while affecting behavior in the high frequencies. If we seek to further increase the integral gain K_i so as to gain performance in the low-frequency range an adverse effect will result. As discussed earlier, the phase of the specific acoustic admittance will cross the value $-\pi/2$, thus yielding over-reflection at the diaphragm (case M). With a PD control, we improve performance in term of phase margin but the PD action also tends to shift the control bandwidth toward the low frequencies (case N).

With a phase lead-lag compensation, the phase shift between driving sound pressure and diaphragm velocity can be adjusted without reducing the control bandwidth. Figure 5.20(a) clearly shows the benefit on the measured acoustic performances. With a phase lag compensator the control bandwidth can be extended toward to low frequencies while preventing the phase from crossing $\pi/2$ (Fig. 5.20(b)).

5.5.5 Open-loop gain

Stability issues regarding the transducer have been discussed above. In practice, however, instability can still be experienced at higher frequencies due to the reactive components of the loudspeaker such as the voice coil inductance or higher-order resonances of the diaphragm. Within a duct or a room for instance, the electroacoustic resonator and the sound field can interact with each other, and hence cause the acoustic feedback. This may arise when increasing the controller gain, thus representing some limitation relative to the broadband capability of electroacoustic resonators.

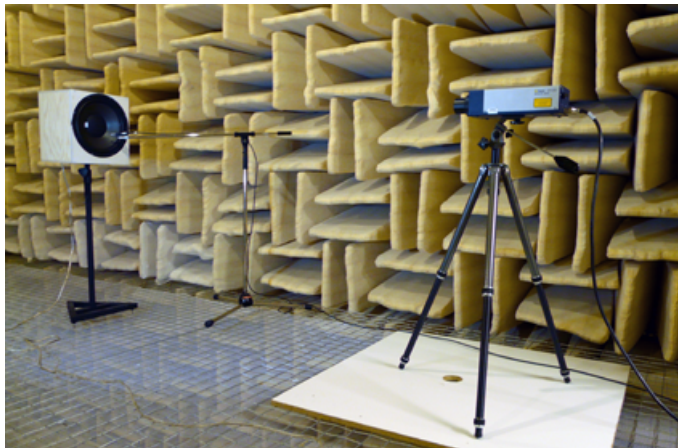


Figure 5.21: Picture of the experimental setup for the measurement of open-loop gains in the anechoic room.

Measuring the open-loop gain in actual situations can be useful in order to anticipate instability issues related to the experimental facilities. It allows easy measurement of phase and gain margins from the Bode diagram, and thus provide information on the stability of the closed-loop system [79]. Figures 5.22 and 5.23 show the measured open-loop gain when the loudspeaker is in the impedance duct and in free field (anechoic chamber). Measured data represent here the transfer function between a random signal applied at the input of the power amplifier feeding the electroacoustic resonator (Allen&Heath amplifier in Fig. 5.17) and the output of the controller. The result is illustrated in Fig. 5.22 when the loudspeaker is controlled with purely proportional gains Γ_p and/or Γ_v , and in Fig. 5.23 with PID control or lead-lag compensators.

5.5. System performance using feedback control

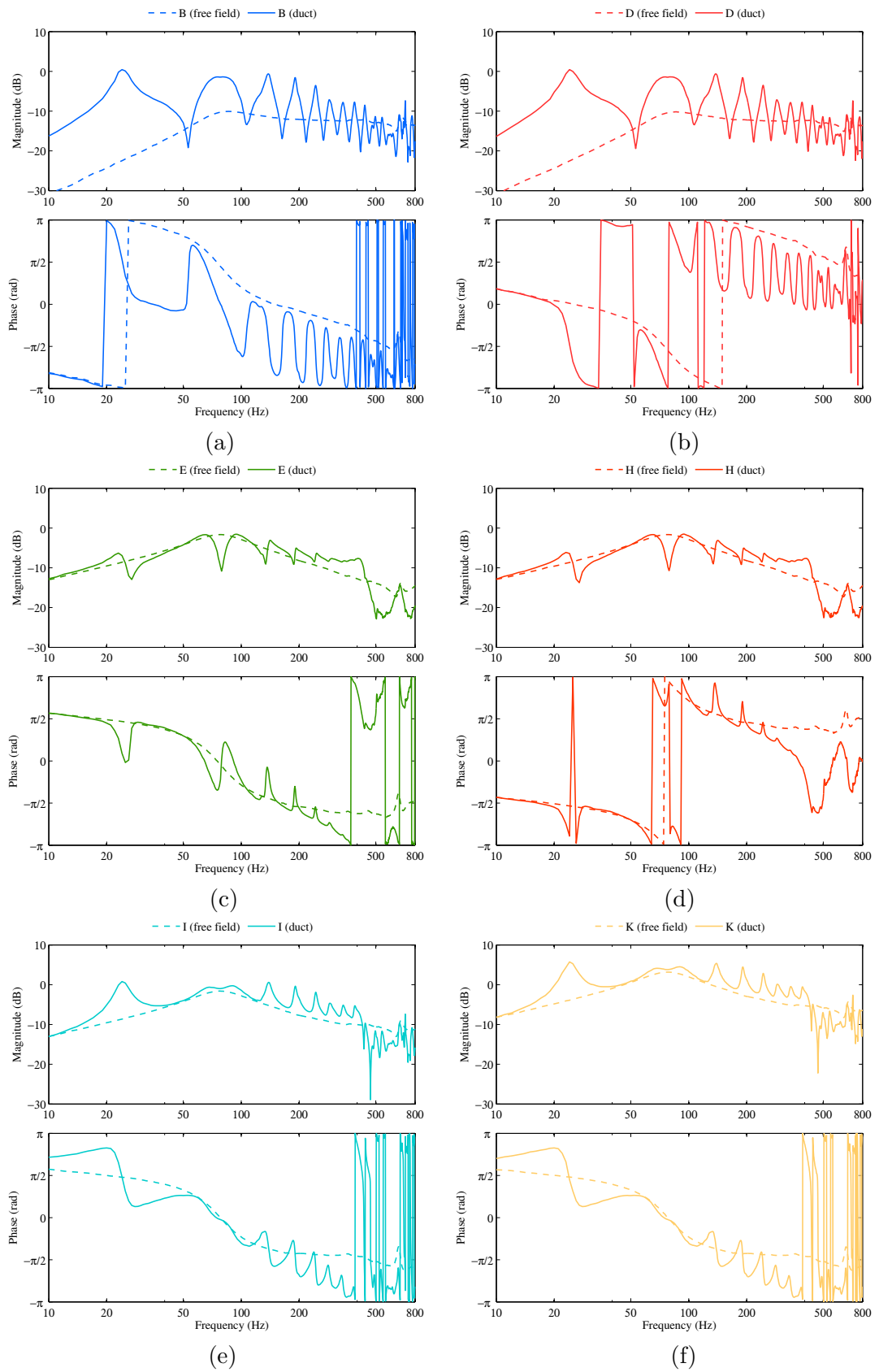


Figure 5.22: Measured open-loop gains for with proportional gains Γ_p and/or Γ_v . 91

Chapter 5. Changing the acoustic impedance using feedback control

Table 5.5 summarizes the phase and gain margins measured in impedance tube and in free field on electroacoustic resonators with various control settings. The gain margin, which is the level in decibel by which the gain can be increased before marginal stability results, are readily obtained from the bode plot of the system in open loop. The phase margin is obtained by adding 180 deg to the phase angle at the gain crossover frequency. The gain crossover frequency is defined to be the frequency at which the magnitude of the open-loop frequency response function is unity (or the level is 0 dB). For a resonant system such as an enclosed sound field, there are multiple gain crossover frequencies; however, the one with the smallest phase margin dictates the stability margin [42].

Table 5.5: Summary of the phase and gain margins measured in impedance tube and in free field.

Case	Phase margin		Gain margin	
	Free field	Impedance tube	Free field	Impedance tube
B	∞	239.6° (25 Hz)	22.0 dB (25 Hz)	5.4 dB (20 Hz)
D	∞	94.6° (24 Hz)	11.8 dB (150 Hz)	1.4 dB (79 Hz)
E	∞	∞	>30 dB	8.0 dB (372 Hz)
H	∞	∞	1.7 dB (74 Hz)	1.7 dB (64 Hz)
I	177° (79 Hz)	94.6° (141 Hz)	>30 dB	5.4 dB (391 Hz)
J	177° (79 Hz)	44.7° (247 Hz)	>30 dB	2.4 dB (391 Hz)
K	177° (79 Hz)	35.6° (251 Hz)	>30 dB	0.6 dB (391 Hz)
M	123° (79 Hz)	47.1° (139 Hz)	>30 dB	1.3 dB (146 Hz)
N	202° (79 Hz)	95.2° (108 Hz)	>30 dB	6.5 dB (349 Hz)
O	177° (79 Hz)	65.4° (246 Hz)	>30 dB	3.3 dB (713 Hz)
P	177° (79 Hz)	89.4° (140 Hz)	>30 dB	14.9 dB (695 Hz)

Generally speaking, the behavior of the electroacoustic resonator is considerably modified by the natural resonances of the impedance tube. When increasing the gain the values of phase and gain margins become smaller, meaning that the system could become unstable to a small perturbation (see case K). Lowering the gain increases the stability margin but this will also result in a slight reduction of the control bandwidth (see case J). Notice that the phase and gain margins are improved by using phase compensation (see case O and P). This leads to improving the robustness and stability of electroacoustic resonators.

One can observe that these margins are significantly increased in the case where the electroacoustic resonator is in a free-field environment. Apart from case H, i.e. when the feedback gain Γ_v approaches the limit of stability (see Eq. (5.31)), phase and gain margins are always large in free field. As shown in Fig. 5.22 and 5.23 the resonances of the impedance tube represent the most important factor of magnitude and phase variation in the open-loop gain. Therefore, the observed instability issues should not be entirely taken for an intrinsic property of the electroacoustic resonator.

5.5. System performance using feedback control

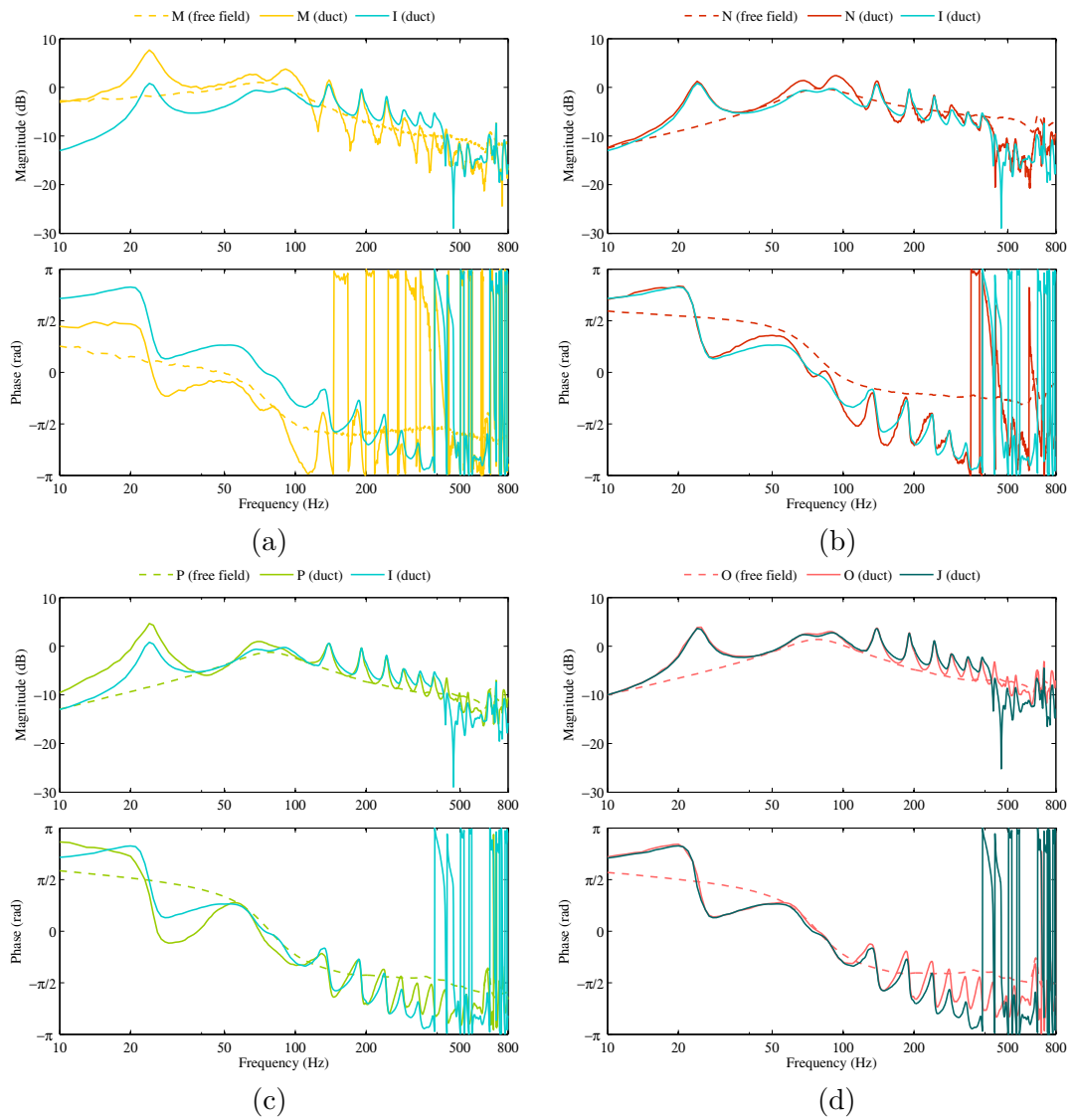


Figure 5.23: Measured open-loop gains with PI control (a), PD control (b), and combined control with phase lag (c) and phase lead (d) compensation.

5.6 Conclusions

In this chapter, the development of electroacoustic resonators has been investigated from the control theory perspective, i.e. by means of sensors and controllers. By sending back an appropriate control voltage to the transducer terminals, the diaphragm acoustic impedance can be varied, specifically in the low-frequency range where the use of passive materials is impractical. A thorough analysis of classical active control techniques applied to a loudspeaker system have been presented. Applying a combined feedback and feedforward control law for instance, is a straightforward way to achieve the desired bandwidth at a target acoustic impedance value. The condition for providing active sound absorption is to achieve a constant ratio $\Gamma_v/\Gamma_p = \rho c$. Computed results are confirmed with experiments in impedance tube. The Routh's criterion and open-loop gain measurements have been applied in order to anticipate stability issues. This work gives insights into the ability of loudspeakers to achieve optimal sound absorption. Therefore, it provides valuable information for the design of dedicated controllers.

If the primary objective is to force electroacoustic resonators to respond as a real system, i.e. the real part of the specific acoustic impedance should be positive, the phase should alternate between $\pm \pi/2$. When the gain Γ_p exceeds a certain bound, however, the diaphragm may become over-reflective in the frequency range of interest. Such an effect can be either compensated or reinforced, depending on whether the objective is to absorb sound energy or not. To that purpose, the lead-lag compensation technique has been introduced to offset the transducer dynamics, and hence achieve the necessary phase adjustments. Through other phase compensator parameters, it is possible to change the transducer dynamics significantly. With a negative gain K_1 or K_2 the phase shift effect is reversed. The phase can cross the bounds $-\pi/2$ or $\pi/2$, thus resulting in significant change in the behavior of the electroacoustic resonator.

Note that the purpose of this chapter is simply to show the potential of feedback control techniques in the context of acoustic impedance control. A wider control bandwidth can be achieved with another type of loudspeaker, as shown in [16]. This also emphasizes that the choice of the transducer is essential in relation to the target acoustic impedance to achieve.

The particularly wide field of control theory and the many techniques and methods involved have, obviously, not all been studied in depth. Optimal control for instance, is a particular control technique in which the control signal optimizes a certain cost function with respect to given constraints. It is commonly used to solve nonlinear problems which, generally, do not have closed form solutions. In the context of acoustic impedance control, and given the relative simplicity of the system to control, it does not seem necessary to turn to this option. In this thesis, we have opted for a simple engineering approach, in the sake of making the developed control strategies easily applicable.

6 Matching the acoustic impedance through electrical network

6.1 Introduction

Turning an electrodynamic loudspeaker into a sound absorber may require to provide additional damping, or to shift the peak resonance apart from the natural frequency. By using "off-the-shelf" loudspeakers with given characteristics, there are only few means to improve the system performance. In [58] for instance, the effect of increasing the moving mass, that of varying the compliance by tailoring the volume of the cabinet for instance, or simply adding damping by filling the enclosure with porous materials are detailed through designed experiments [102,103]. The only way to improve performances without affecting the design of the transducer or enclosure is either to apply some control strategy that could alter the dynamics of the system. But in the following, rather than employing actual sensors for sensing acoustic quantities as discussed in Chapter 5, the strategy will be oriented towards the connection of the transducer terminals to electrical networks.

The technique of impedance matching using passive analog networks was first introduced on piezoelectric materials. In [57], a resistor is connected to a piezoelectric material so as to provide damping to a structure to which it is attached. Such electrical shunt network is very easy to implement, cheap and does not require any power for operation. However, it was shown that damping performance with a purely resistive shunt connected to piezoelectric materials is very poor, and in some applications even not measurable. More efficient are the resonant shunt circuits which are obtained by combining resistive and reactive components so as to achieve a single or multimode damping. As discussed in [57], shunting piezoelectric materials with a resistor and inductor introduces an electrical resonance which can be optimally tuned to structural resonances. Once bonded to a structure, the shunted piezoelectric material works as a mechanical vibration absorber. In the literature, such effect is often compared with a mechanical damper [43,62,104–106]. The technique has been transferred to electrodynamic loudspeakers afterward. By analogy with piezoelectric shunt damping, a basic analog network connected across the terminals of a loudspeaker can be used to damp resonant sound fields [10,43]. However, the idea

of controlling an electroacoustic transducer with a negative resistance had already been discussed in [44]. The objective here is to globally reduce the sound field without the need of collocated pressure or velocity sensors. The key issue is to properly design an electrical matching circuit which, when connected across the transducer terminals, improves the dissipation of acoustic energy. In practice, electrical coupling can be achieved with the help of basic analog networks made up of a combination of positive or negative, reactive or resistive components, in series or in parallel. The resulting shunt electrical impedance is commonly designed to dissipate the electrical energy which has been converted from mechanical energy by the transducer.

This chapter is devoted to studying electrical network topologies that provide some ability to tune an electroacoustic resonator without sensor. The idea is to examine how the parameters of the resonator (damping ratio, gain and resonance) may be affected by electrical means. In the following sections, the interaction between an electrodynamic loudspeaker and various electrical loads is modeled and solved analytically using circuit theory. As a conclusion, general remarks regarding limitations and potential applications in actual situations are discussed.

6.2 Design of matching electrical network

6.2.1 Problem formulation

The key problem of the matching network technique is to find a very simple analog circuit that efficiently allows sound energy dissipation at the loudspeaker diaphragm. The basic idea is to produce a kind of regulation of electrical quantities in the coil circuit. In order to make a current flow, the circuit must be closed in some way. With no electrical load (transducer terminals in open circuit), there is a voltage drop across the output and the loudspeaker behaves as a damped harmonic oscillator with no possibility of adjustment. The general idea is to derive the desired relationship between current and voltage using a two-terminals network, and to combine it with the characteristic equations of the loudspeaker.

As discussed in Section 3.3, the induced voltage generates a current in the coil which, in turn, leads to a feedback force according to Eq. (3.6). The resulting velocity of the loudspeaker diaphragm is thus modified [16]. From the control perspective, the problem is to implement a functional relationship between electrical variables at the loudspeaker's terminals. To that purpose, some types of electrical network can be used to tailor a functional relationship between the current and the induced voltage. The following sections will investigate some network topologies that advantageously combine with an electrodynamic loudspeaker to tune the acoustic impedance to a desired specification.

6.2.2 Electrical network topology

Electrical network topology deals with circuits which contain dipoles, as illustrated in Fig. 6.1. In the context of electrical engineering, a network is a collection of components interconnected in series or parallel. In a series circuit, components are connected along a single electric flow path, so the same current flows through each one [107]. In a parallel circuit, each dipole is connected to the same electrical terminals.

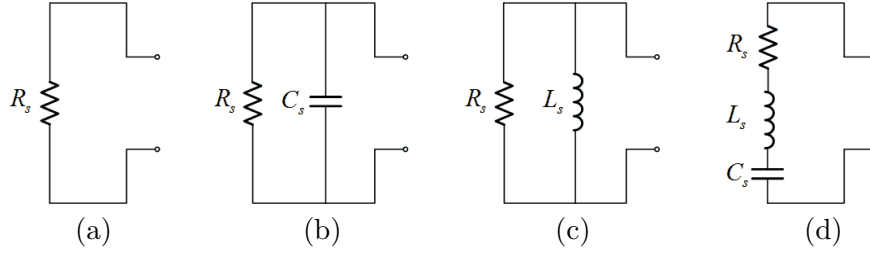


Figure 6.1: Schematics of various topologies of matching networks (a) R shunt, (b) parallel RC shunt, (c) parallel RL shunt, (d) Series RLC. It is assumed that the components are ideal (lossless) and linear.

Passive shunt networks are characterized by the fact that they do not supply energy to the system to which they are connected. When the matching network requires power to operate, it becomes active.

Mathematically speaking, passive shunt electrical impedance can be defined in the frequency domain as

$$\Re[Z_e(j\omega)] \geq 0 \quad \text{or} \quad \Re[E(j\omega)I^*(j\omega)] \geq 0 \quad \forall \omega \quad (6.1)$$

where Z_e is the electrical impedance, ω is the radial frequency, E is the input voltage, I is the electrical current, and $I^*(j\omega)$ denotes the complex conjugate of $I(j\omega)$. According to this definition, the shunt electrical impedance is passive as long as the resistive and reactive values remain positive. With purely resistive shunt networks, stability of the transducer is always ensured because no energy is added to the system.

Conversely, active shunt networks have the ability to add energy to the host system. Mathematically speaking, it can be expressed as

$$\exists \omega, \Re[Z_e(j\omega)] < 0 \quad \text{or} \quad \Re[E(j\omega)I^*(j\omega)] < 0 \quad (6.2)$$

When negative elements are involved in the network, we will see that stability issues should be considered. In the following sections various passive and active electrical networks are discussed.

6.2.3 Model of the unplugged loudspeaker

An electrodynamic loudspeaker mounted in a sealed enclosure behaves as a damped harmonic oscillator when subjected to acoustic disturbances, as discussed in Section 4.2. With no load at its terminals, the specific acoustic admittance, i.e. the ratio of the normal velocity to driving sound pressure, is then defined by

$$\frac{V(s)}{P(s)} = S \frac{s}{s^2 M_{ms} + s R_{ms} + \frac{1}{C_{mc}}} = K \frac{s}{s^2 + 2\zeta\omega_0 s + \omega_0^2} \quad (6.3)$$

where $s = j\omega$ is the Laplace variable. Equation (6.3) underlines the characteristic equation of the resonator where the moving mass M_{ms} , effective compliance C_{mc} (stiffness of the suspension with sealed enclosure) and mechanical resistance R_{ms} determine the resonance frequency, damping ratio and gain, given respectively by

$$\omega_0 = \frac{1}{\sqrt{M_{ms} C_{mc}}} \quad \text{and} \quad \zeta = \frac{R_{ms}}{2M_{ms}\omega_0} \quad \text{and} \quad K = \frac{S}{M_{ms}} \quad (6.4)$$

By simply closing the circuit (shortcut), the functional relationship between the input voltage and current generated is given by

$$i(t) = \frac{1}{Z_e + \frac{(Bl)^2}{Z_m}} e(t) \quad (6.5)$$

where Z_e is the blocked impedance of the voice coil and Z_m is the mechanical impedance of the closed-box loudspeaker. The real part and imaginary part of Z_m in the low-frequency range, typical of a positive real system, are depicted in Fig. 6.2.

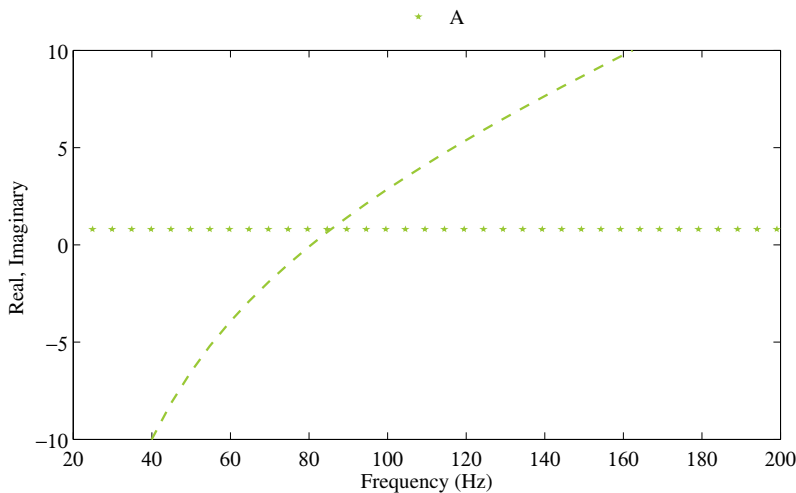


Figure 6.2: Plot of the real (★) and imaginary (---) part of Z_m .

In the following, some electrical network topologies are designed to expand the sound absorption capability at the transducer diaphragm.

6.2.4 Coupling to a resistor

A straightforward manner to consume electrical current is to add a resistive element to the voice coil. Energy dissipation is simply obtained by Joule heating. A basic resistor can be connected across the loudspeaker terminals, as shown in Fig. 6.1(a). The equivalent circuit of the loudspeaker (mechanical side) [11], obtained from the circuit representation given in Fig. 3.6, is depicted in Fig. 6.3.

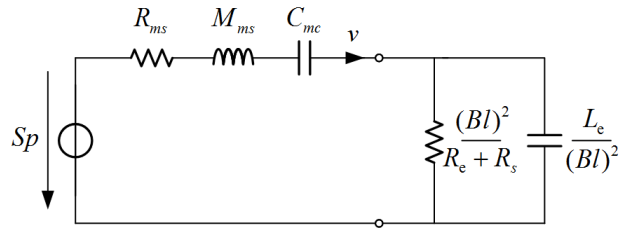


Figure 6.3: Equivalent circuit (mechanical side) of the loudspeaker shunted by a resistor.

From the diagram shown in Fig. 6.3, the mechanical impedance equivalent to connecting a resistor at the transducer terminals can be written in the frequency domain as

$$Z_{me}(j\omega) = \frac{(Bl)^2}{R_e + R_s + j\omega L_e} \quad (6.6)$$

where ω is the radial frequency. The real part and imaginary part of this complex frequency response can be derived after

$$\Re[Z_{me}(j\omega)] = \frac{(Bl)^2(R_e + R_s)}{(R_e + R_s)^2 + (\omega L_e)^2} > 0 \quad (6.7)$$

$$\Im[Z_{me}(j\omega)] = -\frac{\omega(Bl)^2 L_e}{(R_e + R_s)^2 + (\omega L_e)^2} < 0$$

In order to show the effect of R_s on the mechanical impedance Z_m , the real and imaginary parts of Z_{me} can be plotted versus frequency (Fig. 6.4) and compared to $\Re[Z_m(j\omega)]$ and $\Im[Z_m(j\omega)]$ (Fig. 6.2). It can be seen that the mechanical impedance Z_{me} , which is equivalent to connecting a resistor R_s at the transducer terminals, provides additional damping to the system, since the real part is positive. The imaginary part remains close to zero, meaning that the overall reactance of the shunted loudspeaker will not change much, as will the resonance (see Fig. 6.4).

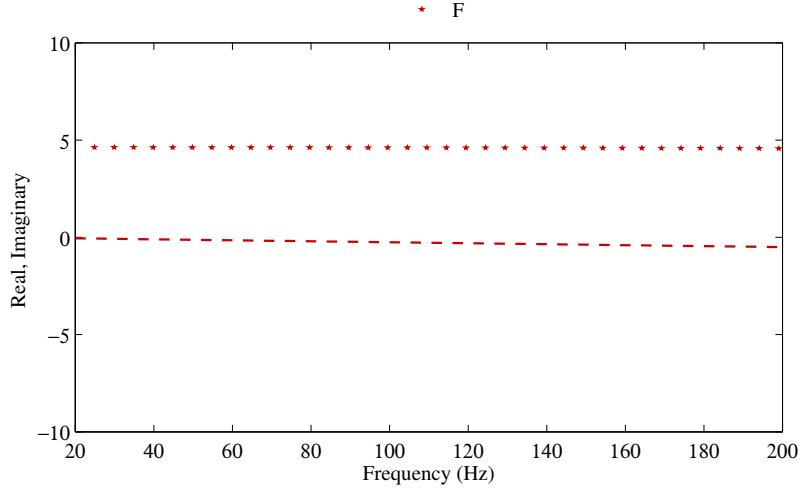


Figure 6.4: Plot of the real (\star) and imaginary (---) part of the mechanical impedance Z_{em} equivalent to connect R_s across the transducer terminals.

Another way to formally demonstrate the effect of connecting a resistor across the transducer terminals is to consider the transducer under a low-frequency assumption. Around the resonance frequency of the electroacoustic resonator, the magnitudes are basically such that $(\omega L_e)^2 \ll (R_e + R_s)^2$ [11]. As a result, the coil inductance L_e can be neglected with respect to the sum of the dc resistance and shunt resistance $R_e + R_s$.

The specific acoustic admittance of the diaphragm can then be written as

$$\frac{V(s)}{P(s)} = S \frac{s}{s^2 M_{ms} + s \left(R_{ms} + \frac{(Bl)^2}{R_e + R_s} \right) + \frac{1}{C_{mc}}} \quad (6.8)$$

Equation (6.8) describes a second-order system with bandpass response. In order to highlight the underlying characteristics of a resonator, the natural frequency in rad s^{-1} , damping ratio and gain can be derived as

$$\omega_0 = \frac{1}{\sqrt{M_{ms} C_{mc}}} \quad \text{and} \quad \zeta = \frac{R_{ms} + \frac{(Bl)^2}{R_e + R_s}}{2M_{ms}\omega_0} \quad \text{and} \quad K = \frac{S(R_e + R_s)}{M_{ms}} \quad (6.9)$$

Compared to the open circuit (case A), additional damping is provided to the system through the term $(Bl)^2/(R_e + R_s)$. The system gain also increases by a factor $R_e + R_s$. From the concept of damped harmonic oscillator discussed in Section 4.2, this results in a decreased of the Q -factor of the loudspeaker [108].

An optimal value for the electrical resistance can be derived in order to attain a desired

Q -value. For a perfect sound absorption, the acoustic resistance at the diaphragm should equal the characteristic impedance of air, i.e. $\Re[Z_s] = \rho c$, where $Z_s = p/v$ is the specific acoustic impedance. As the imaginary part of Z_s is zero at resonance, the optimal electrical resistance can be derived by equating (6.8) to $1/(\rho c)$ as

$$R_{opt} = \frac{(Bl)^2}{\rho c S - R_{ms}} - R_e \quad (6.10)$$

For conventional electrodynamic loudspeakers in the air at $20^\circ C$ ($\rho = 1.18 \text{ kg m}^{-3}$ and $c = 340 \text{ m s}^{-1}$), this optimal resistance is typically of order of a few ohms. For the Visaton AL-170 low-midrange loudspeaker considered in this chapter (see Tab 6.1), the optimal electrical resistance is 4.7Ω and the resonance frequency is 79 Hz.

When the voice coil inductance is not neglected, Eq. (6.8) becomes

$$\frac{V(s)}{P(s)} = \frac{a_2 s^2 + a_1 s}{b_3 s^3 + b_2 s^2 + b_1 s + b_0} \quad (6.11)$$

where

$$\begin{aligned} a_2 &= S L_e & b_3 &= M_{ms} L_e \\ a_1 &= S(R_e + R_s) & b_2 &= M_{ms}(R_e + R_s) + R_{ms} L_e \\ & & b_1 &= R_{ms}(R_e + R_s) + \frac{L_e}{C_{mc}} + (Bl)^2 \\ & & b_0 &= \frac{R_e + R_s}{C_{mc}} \end{aligned} \quad (6.12)$$

As indicated in Eq. (6.11), the loudspeaker when connected to a purely resistive load behaves as a third-order system. Electroacoustic resonators with $R_s > 0$ are always stable since all coefficients in Eq. (6.12) are positive.

Figure 6.5(a) illustrates the computed frequency response (magnitude and phase) of the specific admittance ratio when the loudspeaker (including L_e) is connected with various electrical resistance values. It can be observed that the added resistance allows a significant increase of the absorbing capability of the loudspeaker to the point at which it is perfectly absorbing at resonance. The phase of the specific acoustic admittance alternates between $-\pi/2$ and $\pi/2$, which results in a positive absorption coefficient over the entire frequency range, as shown in Fig. 6.5(c). Connecting a resistive shunt to the loudspeaker is an interesting compared to the state of the art solutions of soundproofing in the low-frequency range in terms of performance and compactness. This results is at the heart of the principle of passive acoustic absorption using shunt networks. With positive shunt resistor, however, no substantial broadening of the control bandwidth can be achieved.

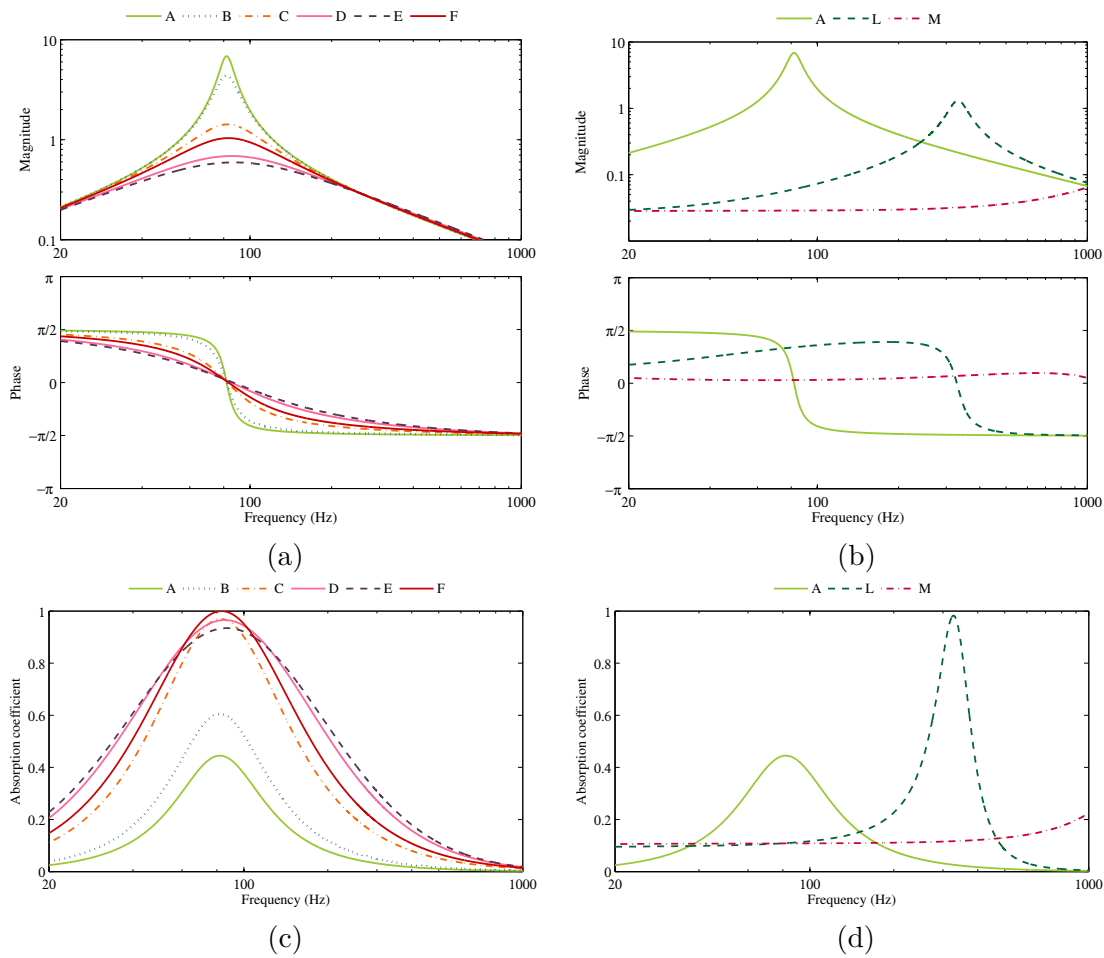


Figure 6.5: Computed acoustic performance with positive and negative electrical shunt impedances. The frequency response of the specific acoustic admittance ratio is shown at the top, and the corresponding absorption coefficient is shown at the bottom.

6.2.5 Coupling to a negative impedance network

Connecting a negative impedance to the terminals is a convenient way to further alter the transducer electrical dynamics. Practically, it can be implemented by a class of circuits referred to as negative impedance converter involving an operational amplifier, as shown in Fig. 6.17(a). Notice that an impedance bridge as discussed in [50, 108] has the same functionality. The basic idea is to generate a negative source impedance so as to cancel the voice coil impedance, and hence control the diaphragm velocity directly from the operational amplifier. Such approach is commonly referred as positive current feedback since a positive current is introduced in the circuit thereby [91, 99, 100].

In the following, the effect of applying a negative shunt impedance across the transducer terminals is quantified using a frequency response approach and the pole-zero diagram.

6.2. Design of matching electrical network

As depicted in Fig. 3.6, the connection of an electrical impedance Z_L is equivalent to adding Z_L in series with Z_e . By substituting Z_L with a pure resistive load such that $R_s \simeq -R_e$, for instance the closed form expression of the specific acoustic admittance can be written as

$$\frac{V(s)}{P(s)} = S \frac{s}{M_{ms} s^2 + R_{ms} s + \left(\frac{(Bl)^2}{L_e} + \frac{1}{C_{mc}} \right)} \quad (6.13)$$

Equation (6.13) describes a second-order system, the natural frequency in rad s^{-1} and damping ratio of which can be derived after

$$\omega_0 = \sqrt{\frac{1}{M_{ms} C_{mc}} + \frac{(Bl)^2}{L_e M_{ms}}} \quad \text{and} \quad \zeta = \frac{R_{ms}}{2M_{ms}\omega_0} \quad \text{and} \quad K \simeq 0 \quad (6.14)$$

By almost canceling the dc resistance of the voice coil, the natural resonance of the loudspeaker is shifted at a slightly higher frequency with a slightly higher quality factor, while decreasing the gain. Instability may arise if the sum $R_e + R_s$ becomes negative. This would result of negative coefficients at the denominator, thus contradicting the Routh's stability criterion (see Section 4.4.4). In practice, the current flowing through the voice coil would increase rapidly until the operational amplifier saturates in either a positive or negative direction [91].

Let us consider now a total compensation of the voice coil electrical impedance, such that

$$Z_L(s) = -R_e - sL_e \quad (6.15)$$

By combining Eq. (6.15) and the characteristic equations (3.19) of the loudspeaker, the specific acoustic admittance will tend to zero since the velocity is zero. Figure 6.5(b) shows the computed frequency response in magnitude and phase of the specific acoustic admittance when connecting a negative impedance at the transducer terminals. Figure 6.6(b) shows the corresponding pole-zero diagram.

In actual situations, obviously, a total compensation of the blocked electrical impedance Z_e is not feasible. Instability of the transducer should arise in case of over-compensation. Furthermore, the inevitable variations in the dc resistance and voice coil inductance due to successive heating and cooling or changes with instantaneous displacement may be detrimental [91]. In practice, this makes it extremely difficult to maintain the load impedance Z_L at the correct instantaneous value. With an actual loudspeaker, only a partial compensation of Z_e can be achieved.

Chapter 6. Matching the acoustic impedance through electrical network

Figure 6.6(a) shows the pole-zero diagram of the loudspeaker when unplugged (case A) and then connected to the optimal shunt electrical resistance (case F) and negative impedance (cases L and M). It can be seen in Fig. 6.6 that the application of a positive or negative electrical load changes the location of poles.

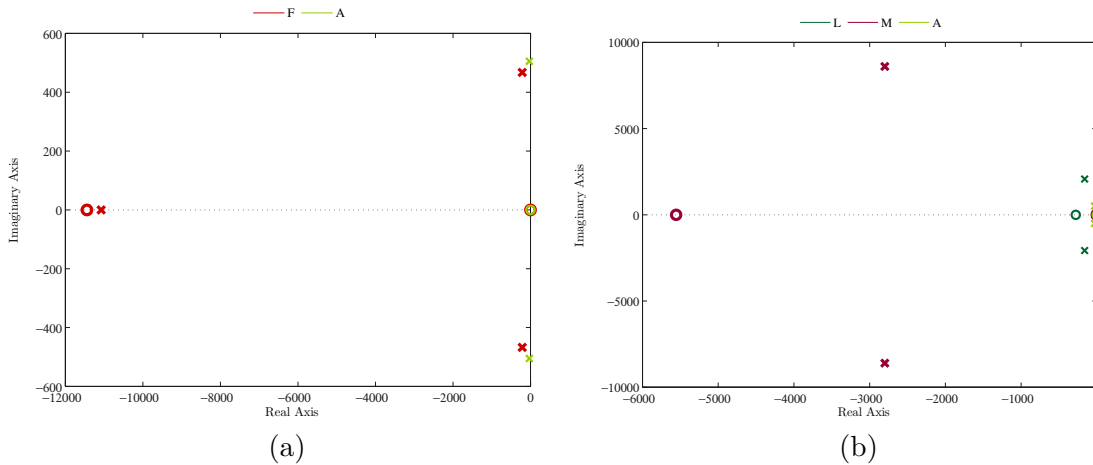


Figure 6.6: Pole-zero diagram of the loudspeaker shunted by a positive (a) and negative (b) electrical load.

6.2.6 Coupling to a parallel RLC network

To further modify the relationship between electrical variables, other matching networks may be considered. A convenient way is to shunt the voice coil of the loudspeaker with a resistor and a capacitor (or inductor) in parallel, thus forming a parallel RC (or parallel RL) network. Such arrangements are commonly used to split or divide the total current flowing in a circuit. The idea here is to use the topology described in Fig. 6.1(b) and 6.1(c) so as to redirect part of the current in the resistor, in a frequency-dependent way.

Parallel RC network

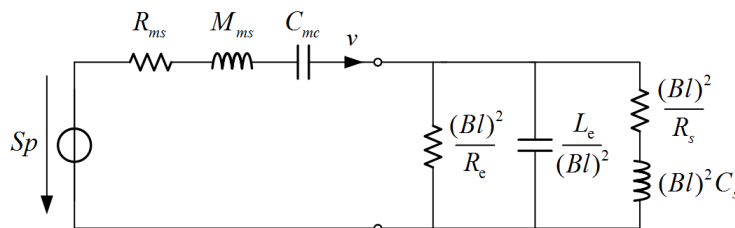


Figure 6.7: Equivalent circuit (mechanical side) of the loudspeaker shunted by a parallel RC network.

Figure 6.7 illustrates the equivalent circuit of the loudspeaker (mechanical side) when connected to a parallel RC network. The shunt electrical impedance of the parallel RC network that is connected to the transducer terminals can be written as

$$Z_L(s) = \frac{R_s}{1 + s R_s C_s} \quad (6.16)$$

Combining Eq. (6.16) with the characteristic equations of the loudspeaker yields the following expression for the specific acoustic admittance

$$\frac{V(s)}{P(s)} = \frac{a_3 s^3 + a_2 s^2 + a_1 s}{b_4 s^4 + b_3 s^3 + b_2 s^2 + b_1 s + b_0} \quad (6.17)$$

where

$$\begin{aligned} a_3 &= S L_e R_s C_s & b_4 &= M_{ms} L_e R_s C_s \\ a_2 &= S(L_e + R_e R_s C_s) & b_3 &= M_{ms} L_e + (M_{ms} R_e + R_{ms} L_e) R_s C_s \\ a_1 &= S(R_e + R_s) & b_2 &= M_{ms} R_e + R_{ms} L_e + \left(R_{ms} R_e + \frac{L_e}{C_{mc}} + (Bl)^2 \right) R_s C_s \\ & & b_1 &= R_{ms} R_e + \frac{L_e}{C_{mc}} + (Bl)^2 + \frac{R_e}{C_{mc}} R_s C_s \\ & & b_0 &= \frac{R_e}{C_{mc}} \end{aligned} \quad (6.18)$$

The coefficients of Eq. (6.18) indicate that connecting a parallel RC network across the transducer terminals affects the mass, compliance and damping of the electroacoustic resonator. In order to show which of these parameters is mainly affected, let us consider the resonator in the low-frequency range.

From the diagram shown in Fig. 6.7, the mechanical impedance Z_{me} which is equivalent to connecting a parallel RC network at the transducer terminals can be written in the frequency domain as

$$Z_{me}(j\omega) = \frac{(Bl)^2}{R_e + j\omega L_e + \frac{R_s}{1 + j\omega R_s C_s}} \quad (6.19)$$

where ω is the radial frequency.

Around the resonance of the electroacoustic resonator, the magnitudes are such that $(\omega L_e)^2 \ll R_e^2$ and $(\omega L_e)^2 \ll |Z_L|^2$ [11]. As a first approximation, the coil inductance L_e can be neglected with respect to the dc resistance R_e and load impedance Z_L . The real

part and imaginary part of Eq. (6.19) can be derived after

$$\Re[Z_{me}(j\omega)] = \frac{(Bl)^2(R_e + R_s + \omega^2 R_e R_s^2 C_s^2)}{(R_e + R_s)^2 + (\omega R_e R_s C_s)^2} > 0$$

$$\Im[Z_{me}(j\omega)] = \frac{\omega(Bl)^2 R_s^2 C_s}{(R_e + R_s)^2 + (\omega R_e R_s C_s)^2} > 0$$
(6.20)

In order to show the effect of connecting a parallel RC network on the transducer mechanical impedance Z_m , the real and imaginary parts of Z_{me} can be plotted versus frequency (Fig. 6.8) and compared to $\Re[Z_m(j\omega)]$ and $\Im[Z_m(j\omega)]$ (Fig. 6.2). It can be seen that the mechanical impedance Z_{me} , which is equivalent here to connect a parallel RC network across the transducer terminals, provides additional damping to the system, since the real part is positive (see case G). The imaginary part remains positive in the frequency range of interest, meaning that the overall mechanical reactance of the shunted loudspeaker will be increased. As a result, the frequency resonance in case G should be decreased (see Fig. 6.4).

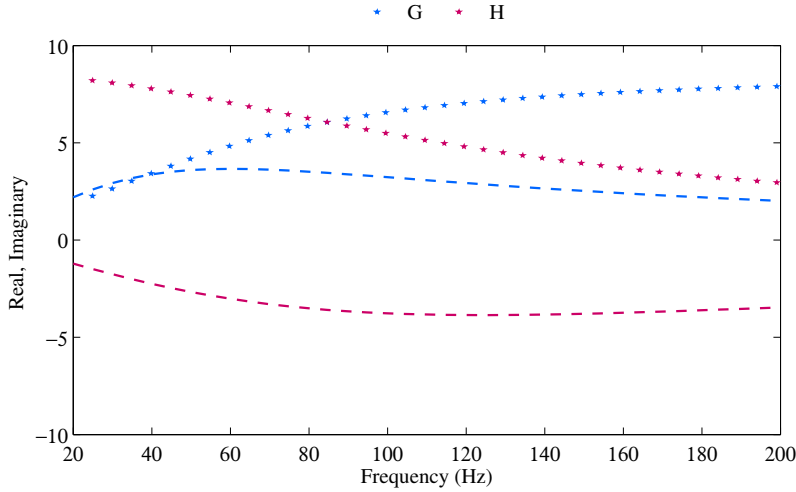


Figure 6.8: Plot of the real (\star) and imaginary (---) part of the mechanical impedance Z_{me} equivalent to connecting a parallel RC (case G) or RL (case H) network across the transducer terminals.

The mass that is virtually added to M_{ms} can be derived after $M_{me}(\omega) = (Bl)^2 R_s^2 C_s / ((R_e + R_s)^2 + (\omega R_e R_s C_s)^2)$. Similarly, the mechanical resistance that is virtually added to R_{ms} can be derived after Eq. (6.20) as $R_{me} = \Re[Z_{me}(j\omega)]$. Note that these parameters are frequency-dependent.

By calculating the values of M_{me} and R_{me} when the reactance is a maximum (here at 55 Hz), one can obtain the characteristics of the electroacoustic resonator in terms of

6.2. Design of matching electrical network

natural frequency in rad s^{-1} and damping ratio as

$$\omega_0 = \frac{1}{\sqrt{(M_{ms} + M_{me})C_{mc}}} \quad \text{and} \quad \zeta = \frac{R_{ms} + R_{me}}{2(M_{ms} + M_{me})\omega_0} \quad (6.21)$$

It is shown that connecting a parallel RC network across the transducer terminals is a simple way to lower the resonance frequency of the electroacoustic resonator. With the Visaton AL-170 low-midrange loudspeaker which is considered for the simulations and with case G (Tab. 6.2), the mass that is virtually added at 55 Hz is $M_{me} = 10.6 \text{ g}$ and the mechanical resistance that is provided is $R_{me} = 4.5 \text{ N m}^{-1} \text{ s}$.

Parallel RL network

From the circuit representation given in Fig. 3.6, the equivalent circuit of the loudspeaker (mechanical side) when connected to a parallel RL network is depicted in Fig. 6.9. The shunt electrical impedance of the parallel RL network that is connected to the transducer terminals can be written as

$$Z_L(s) = \frac{s R_s L_s}{R_s + s L_s} \quad (6.22)$$

Combining Eq. (6.22) with the characteristic equations of the loudspeaker yields the following expression for the specific acoustic admittance

$$\frac{V(s)}{P(s)} = \frac{a_3 s^3 + a_2 s^2 + a_1 s}{b_4 s^4 + b_3 s^3 + b_2 s^2 + b_1 s + b_0} \quad (6.23)$$

where

$$\begin{aligned} a_3 &= S L_e L_s & b_4 &= M_{ms} \frac{a_3}{S} \\ a_2 &= S(L_e R_s + L_s R_e + L_s R_s) & b_3 &= M_{ms} \frac{a_2}{S} + R_{ms} \frac{a_3}{S} \\ a_1 &= S R_e R_s & b_2 &= M_{ms} \frac{a_1}{S} + R_{ms} \frac{a_2}{S} + \frac{1}{C_{mc}} \frac{a_3}{S} + (Bl)^2 L_s \\ & & b_1 &= R_{ms} \frac{a_1}{S} + \frac{1}{C_{mc}} \frac{a_2}{S} + (Bl)^2 R_s \\ & & b_0 &= \frac{1}{C_{mc}} \frac{a_1}{S} \end{aligned} \quad (6.24)$$

When combined to a parallel RL shunt network, Eq. (6.23) indicates that the loudspeaker is a fourth-order system. The coefficients of Eq. (6.24) show that the connection of a parallel RL network across the transducer terminals affects the mass, compliance and damping of the electroacoustic resonator.

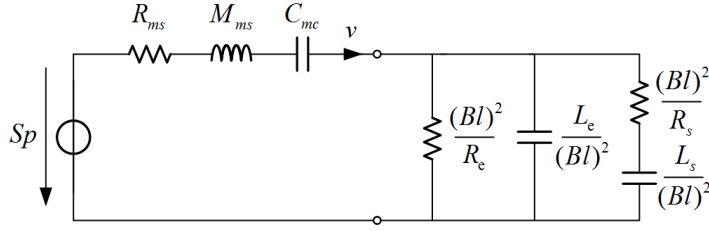


Figure 6.9: Equivalent circuit (mechanical side) of the loudspeaker shunted by a parallel RL network.

As with the parallel RC network, let us consider the resonator behavior in the low-frequency range in order to show which of these parameters is mainly affected. From the diagram shown in Fig. 6.9, the mechanical impedance that is equivalent to connecting a parallel RL network at the transducer terminals can be written as

$$Z_{me}(j\omega) = \frac{(Bl)^2 s}{R_e + j\omega L_e + \frac{j\omega R_s L_s}{R_s + j\omega L_s}} \quad (6.25)$$

Around the resonance of the electroacoustic resonator, the magnitudes are such that $(\omega L_e)^2 \ll R_e^2$ and $(\omega L_e)^2 \ll |Z_L|^2$ [11]. As a first approximation, the inductance L_e can be neglected with respect to the dc resistance R_e and load impedance Z_L . The real and imaginary part of Eq. (6.25) can be derived after

$$\Re[Z_{me}(j\omega)] = \frac{(Bl)^2 (R_e R_s^2 + \omega^2 L_s^2 (R_e + R_s))}{(R_e + R_s)^2 + (\omega (R_e + R_s) L_s)^2} \quad (6.26)$$

$$\Im[Z_{me}(j\omega)] = -\frac{\omega (Bl)^2 R_s^2 L_s}{(R_e + R_s)^2 + (\omega (R_e + R_s) L_s)^2}$$

In order to show the effect of connecting a parallel RL network on the transducer mechanical impedance Z_m , the real and imaginary parts of Z_{me} can be plotted versus frequency (Fig. 6.8) and compared to $\Re[Z_m(j\omega)]$ and $\Im[Z_m(j\omega)]$ (Fig. 6.2). It can be seen that the mechanical impedance Z_{me} provides additional damping to the system, since the real part is positive (see case H). The imaginary part, however, remains negative in the frequency range of interest, meaning that the overall mechanical reactance of the shunted loudspeaker will be decreased. As a result, the frequency resonance in case H should be increased (see Fig. 6.4). The mass that is virtually subtracted to M_{ms} can be derived after $M_{me}(\omega) = (Bl)^2 R_s^2 L_s / ((R_e + R_s)^2 + (\omega (R_e + R_s) L_s)^2)$. Similarly, the mechanical resistance that is virtually added to R_{ms} can be derived after Eq. (6.26) as $R_{me} = \Re[Z_{me}(j\omega)]$. Note that these parameters are frequency-dependent.

6.2. Design of matching electrical network

By calculating the values of M_{me} and R_{me} when the reactance is a minimum (here at 120 Hz), one can obtain the characteristics of the electroacoustic resonator in terms of natural frequency in rad s^{-1} and damping ratio as

$$\omega_0 = \frac{1}{\sqrt{(M_{ms} + M_{me})C_{mc}}} \quad \text{and} \quad \zeta = \frac{R_{ms} + R_{me}}{2(M_{ms} + M_{me})\omega_0} \quad (6.27)$$

It is shown that connecting a parallel RLC network across the transducer terminals is a simple way to increase the resonance frequency of the electroacoustic resonator. With the Visaton AL-170 low-midrange loudspeaker which is considered for the simulations and with case H (Tab. 6.2), the mass that is virtually subtracted at 120 Hz is $M_{me} = 9.2 \text{ g}$ and the mechanical resistance that is provided is $R_{me} = 4.8 \text{ N m}^{-1} \text{ s}$.

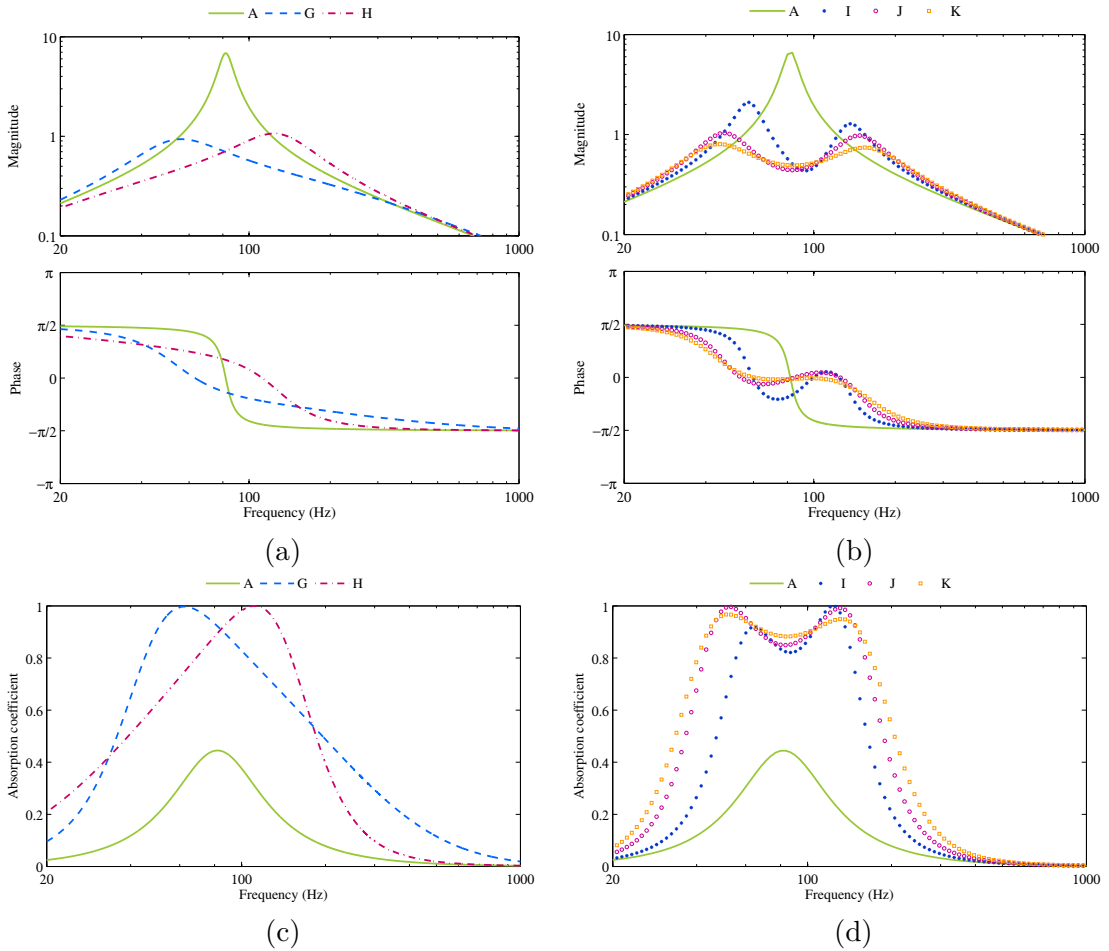


Figure 6.10: Computed acoustic performance in case of a parallel (left) or series (right) RLC network. The frequency response of the specific acoustic admittance ratio is shown at the top, and the corresponding absorption coefficient is shown at the bottom.

Chapter 6. Matching the acoustic impedance through electrical network

Figure 6.10(a) illustrates the computed frequency response (magnitude and phase) of the specific admittance ratio when the loudspeaker is connected to a parallel RC and RL shunt network. Figure 6.10(c) illustrates the corresponding computed absorption coefficient. The control settings that are considered for the simulations can be found in Tab. 6.2. The effects of shunting the transducer with a RC or RL parallel network can be clearly seen. In the low-frequency range, typically when $\omega \ll R_e/L_e$, a parallel RC or RL shunt circuit may take precedence over the natural frequency of the resonator. With a parallel RC the resonance frequency can be decreased from 79 Hz to 55 Hz, while it can be increased to 120 Hz with a parallel RL. The cut-off frequency in a simple RC or RL passive filter can be accurately controlled using just a single resistor in series with a non-polarized capacitor or inductor. From the computed data, the phase of the specific admittance ratio remains between $-\pi/2$ and $\pi/2$, resulting in a positive absorption coefficient over the frequency range of interest. However, actual components are not ideal. As discussed later, both reactive components C_s or L_s have a parasitic electrical resistance that should be canceled (see Fig. 6.17).

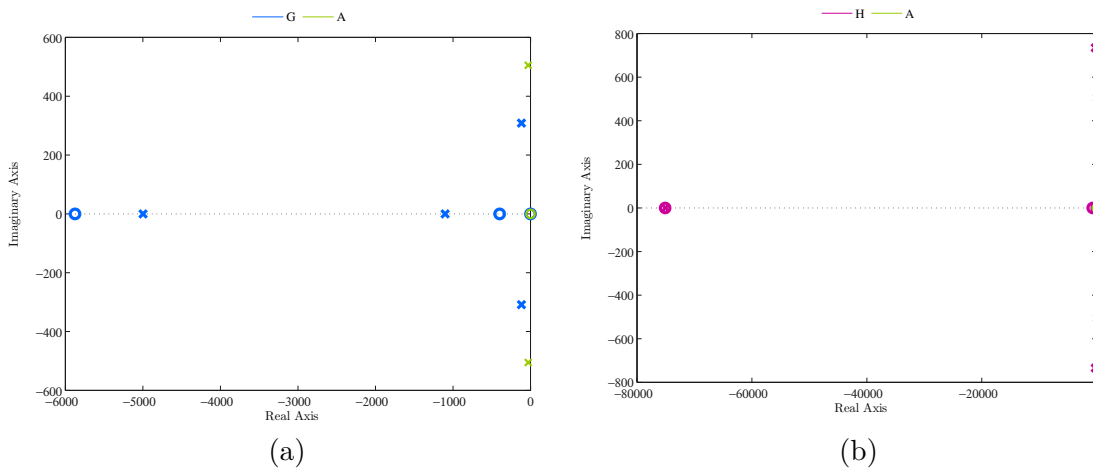


Figure 6.11: Pole-zero diagram of the loudspeaker shunted by a parallel RLC (a) and a series RLC (b) shunt network.

Figure 6.11 shows the pole-zero diagram of the loudspeaker combined with both networks. As shown in Fig. 6.11, a parallel RC network affects the dynamics of the loudspeaker in such a way it decreases the resonance frequency, whereas with a parallel RL the resonance frequency is increased.

6.2.7 Coupling to a series RLC network

An alternative design can be achieved by using a resonant series circuit. The corresponding schematics is shown in Fig. 6.1(d). Compared to a parallel arrangement of resistive and reactive dipoles, a series RLC network splits the voltages in a frequency-dependent way.

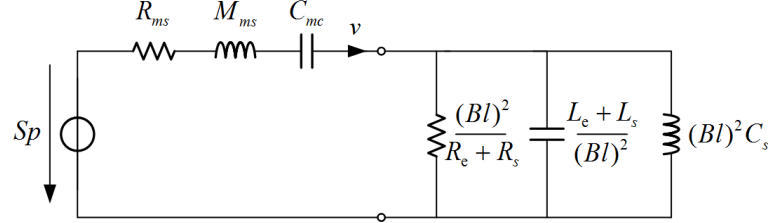


Figure 6.12: Equivalent circuit (acoustic side) of the loudspeaker shunted by a series RLC network.

The shunt electrical impedance of the series RLC network that is connected to the transducer terminals can be written as

$$Z_L(s) = R_s + sL_s + \frac{1}{sC_s} \quad (6.28)$$

Combining Eq. (6.28) with the characteristic equations (3.19) of the loudspeaker yields the closed-form expression for the specific acoustic admittance

$$\frac{V(s)}{P(s)} = \frac{a_3 s^3 + a_2 s^2 + a_1 s}{b_4 s^4 + b_3 s^3 + b_2 s^2 + b_1 s + b_0} \quad (6.29)$$

where

$$\begin{aligned} a_3 &= S(L_e + L_s) & b_4 &= M_{ms} \frac{a_3}{S} \\ a_2 &= S(R_e + R_s) & b_3 &= M_{ms} \frac{a_2}{S} + R_{ms} \frac{a_3}{S} \\ a_1 &= \frac{S}{C_s} & b_2 &= M_{ms} \frac{a_1}{S} + R_{ms} \frac{a_2}{S} + \frac{a_3}{SC_{ms}} + (Bl)^2 \\ & & b_1 &= R_{ms} \frac{a_1}{S} + \frac{a_2}{SC_{ms}} \\ & & b_0 &= \frac{a_1}{SC_{mc}} \end{aligned} \quad (6.30)$$

When combined to a series RLC network, the loudspeaker becomes a fourth-order system. As for the previous cases, it is not obvious to see the effect of the RLC series network on the dynamic behavior of the loudspeaker.

Chapter 6. Matching the acoustic impedance through electrical network

From the diagram shown in Fig. 6.12, the mechanical impedance equivalent to connecting a series RLC network at the transducer terminals can be written

$$Z_{me}(s) = \frac{(Bl)^2 s}{(L_e + L_s) s^2 + (R_e + R_s) s + \frac{1}{C_s}} \quad (6.31)$$

The natural frequency of this resonant circuit is $\omega_0' = 1/\sqrt{(L_e + L_s)C_s} = 95$ Hz.

Now let us have a look to what happens in Eq. (6.31) as a function of the radial frequency ω :

$$\begin{aligned} Z_{me}(j\omega) &\simeq j\omega (Bl)^2 C_s \simeq -\frac{\omega^2 (Bl)^2 C_s}{j\omega} && \text{and } \omega < \omega_0' \\ Z_{me}(j\omega) &\simeq \frac{(Bl)^2}{R_e + R_s} && \text{and } \omega = \omega_0' \\ Z_{me}(j\omega) &\simeq \frac{(Bl)^2}{j\omega (L_e + L_s)} \simeq j\omega \left(-\frac{1}{\omega^2 (L_e + L_s)} \right) && \text{and } \omega > \omega_0' \end{aligned} \quad (6.32)$$

When the radial frequency $\omega < \omega_0'$, it can be shown that the mechanical impedance equivalent to C_s behaves as a negative compliance. Conversely, when $\omega > \omega_0'$ the mechanical impedance equivalent to $L_e + L_s$ behaves as a negative mass. Figure 6.13 illustrates the real part and imaginary part, computed from the control settings listed in Tab. 6.2, of the mechanical impedance that is equivalent to the series RLC network (case I and K).

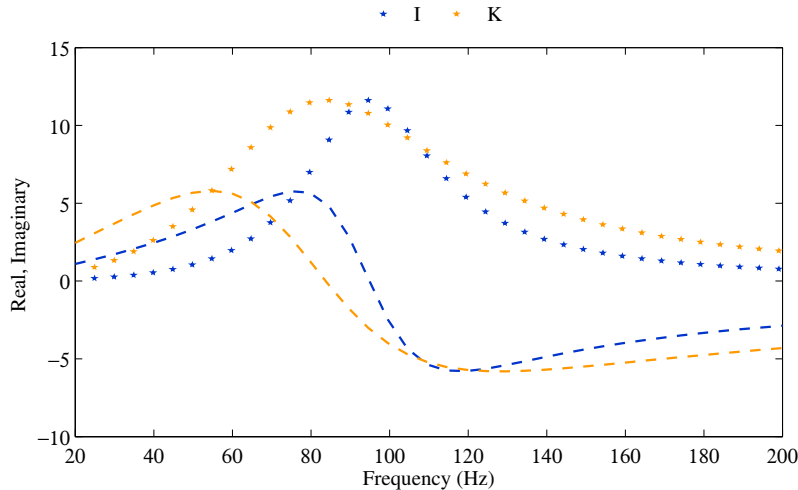


Figure 6.13: Plot of the real (★) and imaginary part (---) of the mechanical impedance. The mechanical impedance Z_m of the loudspeaker when connected to a parallel RC or RL network is shown on the left and the mechanical impedance equivalent to connecting a series RLC network is shown on the right.

6.2. Design of matching electrical network

Figure 6.10(b) illustrates the computed frequency response in magnitude and phase of the specific admittance ratio when the loudspeaker is connected to series RLC shunt networks. Figure 6.14 shows the pole-zero diagram of the loudspeaker combined with a series RLC network (case J). As shown in Fig. 6.14, a series RLC network affects the dynamics of the loudspeaker in such a way it exhibits two resonance frequencies.

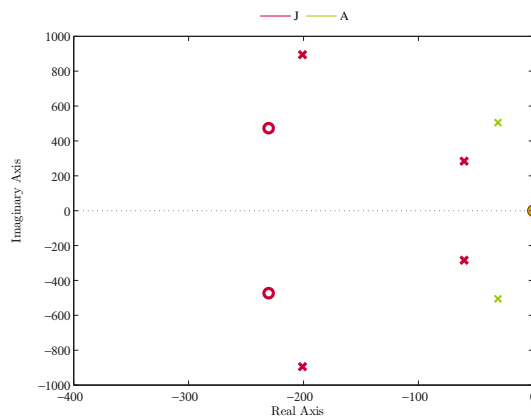


Figure 6.14: Pole-zero diagram of the loudspeaker shunted by a series RLC network.

Other more complex circuits could be discussed. In this section, we chose to present only simple circuits, "canonical", which serve here as examples. The behavior of more complex circuits, however, can not be deduced from these observations.

6.3 System performance using electrical matching networks

6.3.1 Experimental setup

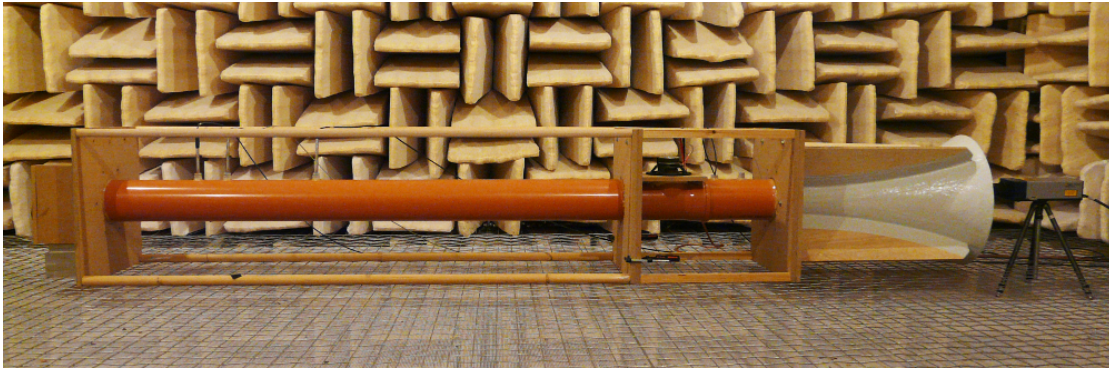


Figure 6.15: Picture of the experimental setup.

In order to assess experimentally the acoustic performance when using electrical matching networks, a closed-box Visaton AL-170 low-midrange loudspeaker is employed as an electroacoustic resonator. The small signal parameters of this transducer can be found in Tab. 6.1. The specific acoustic admittance ratio and absorption coefficient are assessed after ISO 10534-2 standard [36], as depicted in Fig. 6.16.

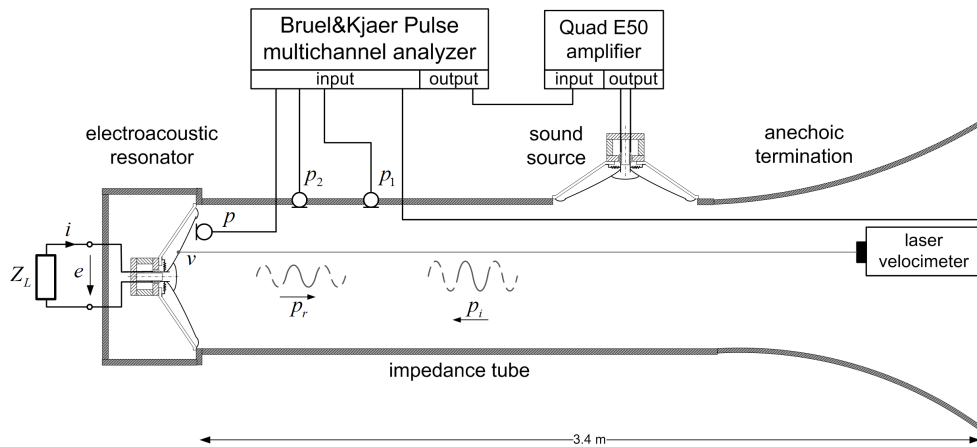


Figure 6.16: Schematics of the experimental setup used with the shunt electrical method.

For running the simulations, the rear face of the loudspeaker is loaded with a sealed enclosure the volume of which is 10 L. In this setup, an impedance tube is specifically designed (length $L = 3.4$ m and internal diameter $\varnothing = 150$ mm), one termination of which is closed by an electroacoustic resonator, the other end being open with a horn-shape termination so as to exhibit anechoic conditions [109]. A source loudspeaker is

6.3. System performance using electrical matching networks

wall-mounted close to this termination. Two holes located at positions $x_1 = 0.46$ m and $x_2 = 0.35$ m from the electroacoustic resonator are the receptacles of 1/2" microphones (Norsonic Type 1225 cartridges mounted on Norsonic Type 1201 amplifier), sensing the sound pressured $p_1 = p(x_1)$ and $p_2 = p(x_2)$. The transfer function $H_{12} = p_2/p_1$ is processed through a Pulse Bruel and Kjaer multichannel analyzer.

Table 6.1: Small signal parameters of the closed-box Visaton AL-170 low-midrange loudspeaker considered for the simulations with the shunt electrical method.

Parameter	Notation	Value	Unit
dc resistance	R_e	5.6	Ω
Voice coil inductance	L_e	0.9	mH
Force factor	Bl	6.9	N A^{-1}
Moving mass	M_{ms}	13	g
Mechanical resistance	R_{ms}	0.8	$\text{N m}^{-1} \text{s}$
Mechanical compliance	C_{ms}	1.2	mm N^{-1}
Effective area	S	133	cm^2
Natural frequency	f_0	38	Hz

The setting parameters of the electrical matching networks considered for the simulations and experiments are listed in Tab. 6.2.

Table 6.2: Parameter settings for the simulations and experiments with electrical matching networks.

Topology	Case	R_s	L_s	C_s
Open circuit	A	∞	-	-
	B	100Ω	-	-
R shunt	C	10Ω	-	-
	D	1Ω	-	-
Closed circuit	E	0Ω	-	-
Optimal R shunt	F	4.7Ω	-	-
Parallel RC	G	34.8Ω	-	$550 \mu\text{F}$
Parallel RL	H	55.0Ω	6.5 mH	-
Series RLC	I	1.5Ω	15 mH	$177 \mu\text{F}$
	J	1.5Ω	8.3 mH	$406 \mu\text{F}$
	K	1.0Ω	5.5 mH	$550 \mu\text{F}$
Negative impedance	L	5.3Ω	-	-
	M	5.3Ω	0.85 mH	-

Chapter 6. Matching the acoustic impedance through electrical network

Figure 6.17 shows the schematics of the practical realization of the electrical matching networks. In practice actually, electrical matching networks depicted in Fig. 6.1 have to be modified by introducing a negative resistance in order to cancel the parasitic resistance of the reactive components C_s and L_s .

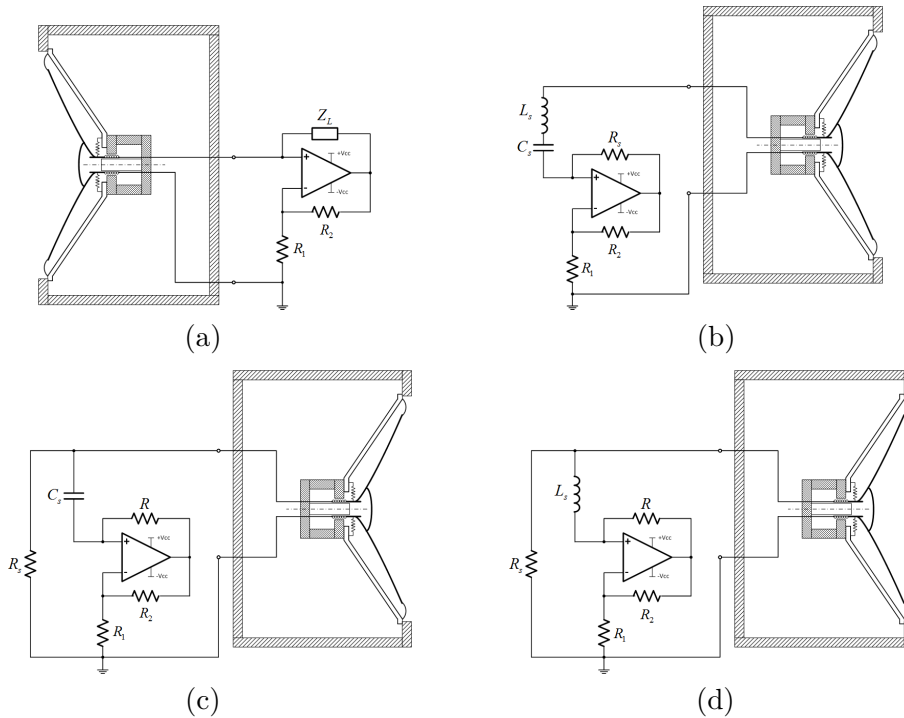


Figure 6.17: Schematics of the practical realization of the electrical matching networks. The negative impedances (a) is carried out according to $e/i = -Z_L R_1/R_2$. For the embodiment of the negative impedance converter, we used $R_1 = R_2 = 1 \text{ k}\Omega$. The series RLC network is depicted in (b) and the parallel RC and RL networks are shown in (c) and (d), respectively.

6.3.2 Sound absorption/reflection capability

In the following, some experimental results from the application of electrical matching networks across the transducer terminals are presented. The corresponding setting parameters can be found in Tab. 6.2. The small signal parameters of the loudspeaker used for the measurement are listed in Tab. 6.1. The curves show the acoustic performances of electroacoustic resonators when subjected to plane waves under normal incidence.

Experimental results from the coupling of positive and negative electrical impedance across the loudspeaker's terminals are shown in Fig. 6.18. As expected with the optimal value of shunt resistance the electroacoustic resonator is perfectly absorbing at resonance. Compared to the system in open circuit ($\alpha \simeq 0.6$ at 79 Hz) the absorption coefficient is

6.3. System performance using electrical matching networks

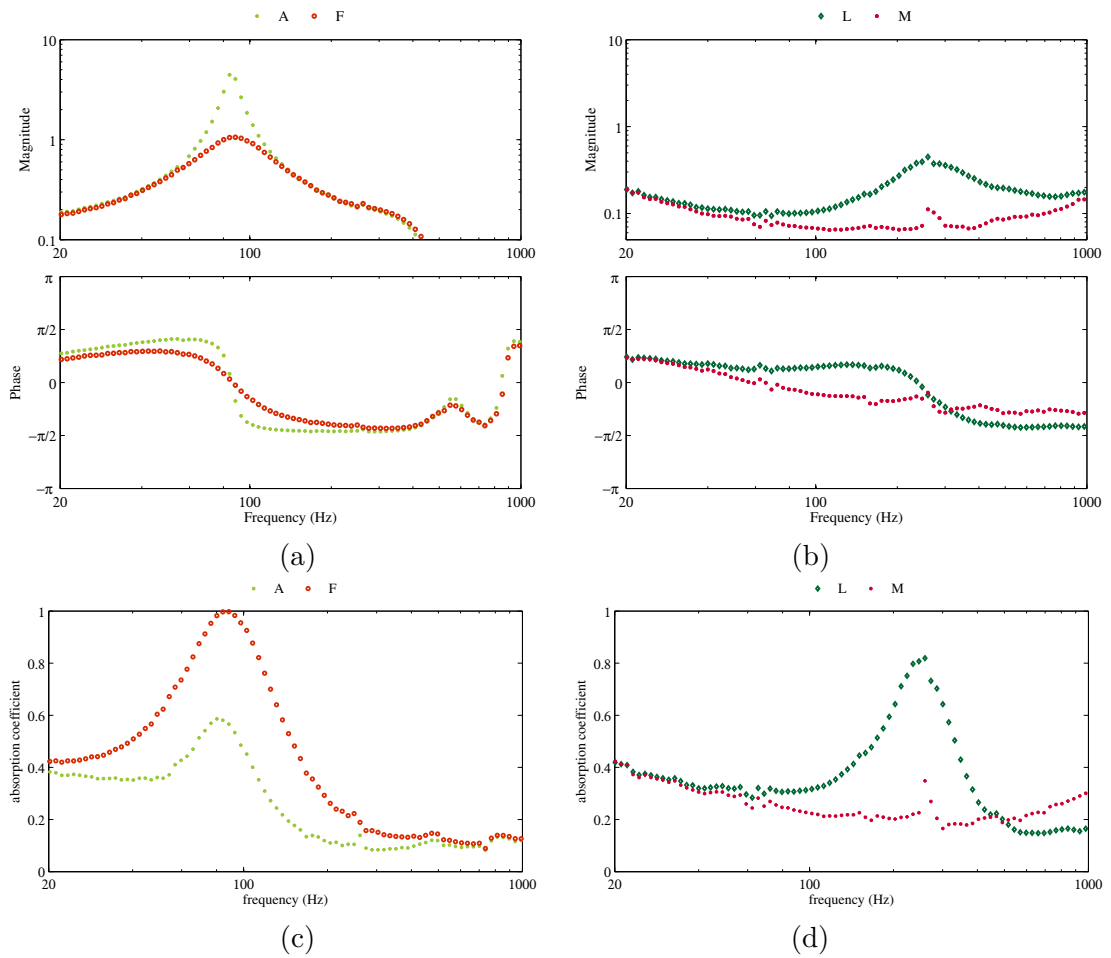


Figure 6.18: Measured acoustic performance when connecting a positive (left) and negative (right) electrical impedance across the transducer terminals. The frequency response of the specific acoustic admittance ratio is shown at the top, and the corresponding absorption coefficient is shown at the bottom.

close to 1. When the dc resistance of the transducer is almost completely cancelled, a shift of frequency of the resonance peak can be observed ($\alpha \simeq 0.8$ at 280 Hz), in accordance with the computed results.

As depicted in Fig. 6.19, the measured acoustic performance of electroacoustic resonators when connecting a parallel or series RLC network is quite similar to the computed results. The measured absorption coefficient with a parallel RC and RL network is $\alpha \simeq 1$ at 55 Hz with case G and $\alpha \simeq 0.99$ at 122 Hz with case H, respectively (see Fig. 6.19(c)). With a series RLC (see Fig. 6.19(d)), the absorption coefficient at the diaphragm is $\alpha \simeq 1$ at 65 Hz and 110 Hz with case I, $\alpha \simeq 0.98$ at 54 Hz and 119 Hz with case J, and $\alpha \simeq 0.94$ at 49 Hz and 131 Hz with case K.

Chapter 6. Matching the acoustic impedance through electrical network

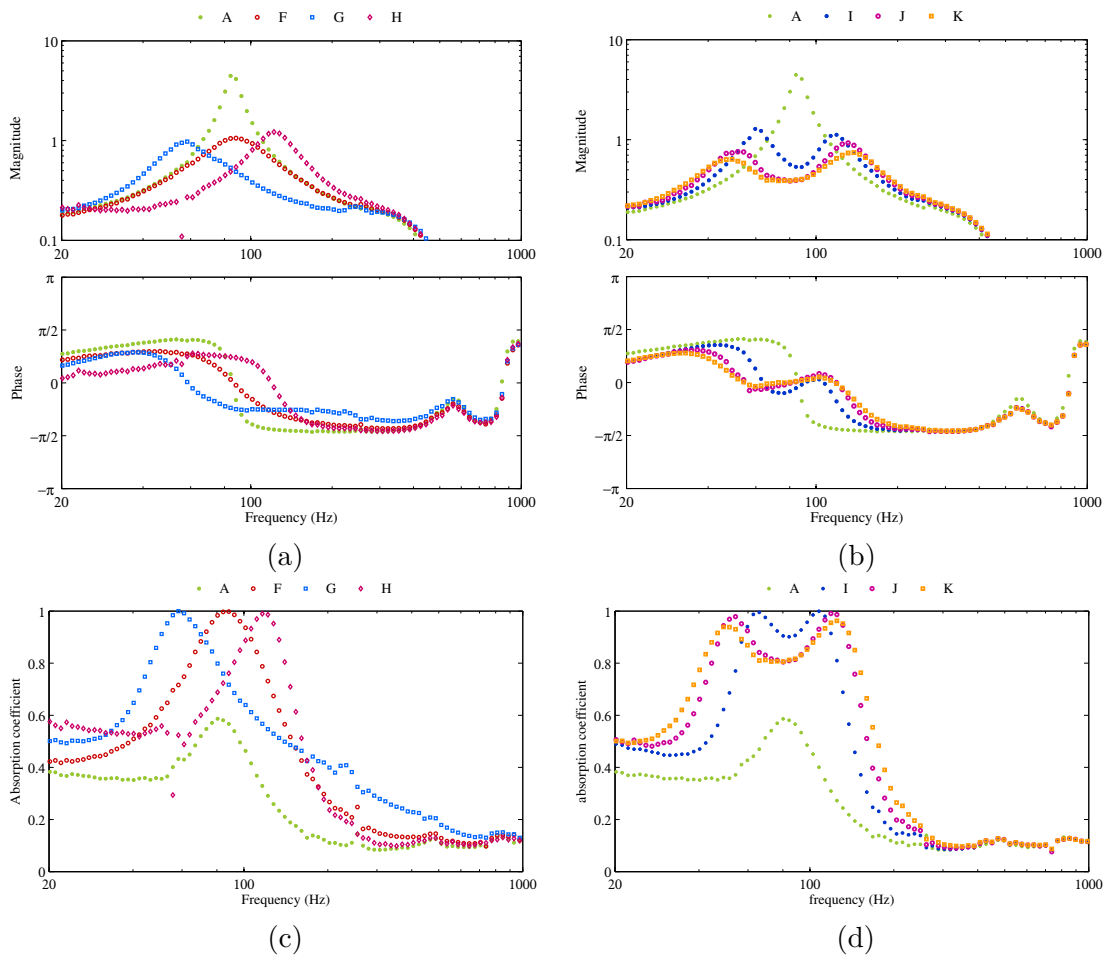


Figure 6.19: Measured acoustic performances when connecting a parallel (a) and series (b) RLC shunt network. The frequency response of the specific acoustic admittance ratio is shown at the top, and the corresponding absorption coefficient is shown at the bottom.

6.4 Conclusions

In this chapter the development of electroacoustic resonators has been discussed from the view point of electrical engineering. Different topologies of electrical network for matching the acoustic impedance of a loudspeaker to the characteristic impedance of the air have been discussed. By using basic dipoles interconnected in series or in parallel, the voltage and current can be tailored in such a way that the loudspeaker dynamics is altered properly. The performance and flexibility, however, are relatively low, especially with purely passive network. A simple resistor connected across the terminals can best achieve an optimum acoustic resistance at resonance, but not substantially change the quality factor. For more flexibility, such as shifting the resonance peak above or below, or significantly changing the damping of the system, some active components must be involved. Parallel or series arrangements which include reactive components can provide some ability to tune the resonance peak apart from the natural resonance of the transducer. With such networks, negative impedance converter involving operational amplifiers can be used so as to compensate the parasitic resistance of the inductor or capacitor. As a result, the electrical network can no longer be seen as passive since it requires power to operate. In such cases, stability issues must be considered since instability arises when the negative impedance Z_L presented by the load is higher than the positive output impedance Z_e presented by the loudspeaker.

This strategy removes the need of sensors and is thus extremely relevant in view of a cost-effective implementation. The major drawback is a limited bandwidth around the resonance of the transducer. In practice, the same loudspeaker can address a certain frequency range which may extend over some octaves. When it comes to achieving a target acoustic impedance, no substantial broadening of the control bandwidth is possible through such a passive approach. However, this approach can be an interesting option with applications requiring high reliability and for high impulsive level, especially when electrical matching networks involve some stable electrical impedances.

7 Synthesis of electrical loads for acoustic impedance matching

7.1 Introduction

Various ways of controlling the acoustic impedance at the diaphragm of an electrodynamic loudspeaker have been discussed so far. In Chapter 5, the problem is addressed through the development of control systems. Sensors are used to provide the necessary information to the controller which, in turn, drives the transducer appropriately. The resulting apparent acoustic impedance of the diaphragm can then be easily matched to the characteristic impedance of the medium over a wide frequency range. In Chapter 6, the problem is solved by the implementing a functional relationship between current and voltage at the transducer terminals. With the help of basic dipoles interconnected in series or parallel, the current flowing in the coil can be tailored from the induced voltage. The resulting feedback force is optimized so as to counteract the incident sound waves appropriately. In this way, the diaphragm acoustic impedance can be matched to the characteristic impedance of air.

These control techniques have their advantages and disadvantages. In terms of control bandwidth, the feedback control yields desired performance over a wider frequency range. In terms of system stability, electrical shunt methods are unlikely to cause acoustic feedback, provided that the electrical load is passive. When the network becomes active, as for further modifying the functional relationship between voltage and current, instability may arise. This is the case when the negative electrical impedance Z_L presented by the load is higher in absolute value than the voice coil impedance Z_e . The shunt loudspeaker method is the most cost-effective solution since no sensor is required. Only basic components such as resistor, inductor and capacitor are needed to implement the electrical matching networks. From the practical view, this method is particularly interesting since it operates independently, and in some cases without power supply. However, it only provides a fixed performance objective. For more flexibility and versatility, feedback control techniques allow to achieve better performance.

The question now: Is there a way to combine or merge the two approaches? The underlying idea is to achieve the performance obtained by a feedback control but with the simplicity of the matching network, i.e. without sensor or controller. To that purpose, we propose to go further into the implementation of the functional relationship between electrical variables at the transducer terminals.

The following focuses on examining the practical implementation of synthetic loads both in the analogue and digital domains. By first identifying the formal analogies between the feedback control and shunt loudspeaker techniques, we shall then discuss how to further extend the control bandwidth of tunable electroacoustic resonators without sensor.

7.2 Merging active sound absorption and shunt methods

This section discusses ways to combine and merge the feedback control techniques with electrical shunt methods and includes some of the results published in [16, 110, 111].

7.2.1 Identifying the formal analogies

As previously discussed, there is some formal analogies between the feedback control and shunt methods. With the former case a control voltage is applied to the transducer terminals, while the other regulates the voltage induced within the coil through an electrical load. From the characteristic equations of the loudspeaker and the corresponding electrical coupling, a closed form expression for the specific acoustic admittance at the diaphragm can be easily derived, as detailed in Chapters 5 and 6. The formal analysis of the transfer functions reveals many similarities. Under feedforward or feedback control, or even when combining both, the loudspeaker exhibits the behavior of a third-order system (under small signal assumption) with bandpass response. The same behavior is obtained when the loudspeaker is connected to an electrical load such as a resistor or a negative impedance.

The frequency response analysis clearly shows that applying a feedforward control allows achieving a target value for the specific acoustic admittance. As illustrated in Fig. 5.4(a), the diaphragm acoustic resistance decreases with a positive gain, while the opposite effect happens with a negative gain. A similar effect can be observed when the value of the resistor across the transducer terminals is varied (see Fig. 6.6(a)). An optimal resistor value can be determined in view of matching the diaphragm acoustic impedance to the characteristic impedance of air, as indicated in Eq. (6.10). The case of motional feedback is to be compared to electrical shunt with a negative impedance. A noticeable effect is to extend the control bandwidth with both approaches. In a motional feedback, this is achieved by applying a gain $\Gamma_v > 0$ on the diaphragm velocity (See Eq. (5.14)). By using a negative impedance, this is achieved by compensating almost completely the electrical

impedance of the voice coil. Simultaneously, the diaphragm acoustic resistance increases gradually as does the bandwidth (see Fig. 5.4(b) and Fig. 6.5(b)). Consequently, the specific acoustic admittance moves away from the target, and the absorption coefficient decreases.

To further show the formal analogies, let us consider the closed form expression for the specific acoustic admittance in the low-frequency range where the voice coil inductance is commonly neglected [11]. With a shunt resistor R_s , the simplified expression for the specific acoustic admittance is given by Eq. (6.8). When applying a combined feedforward/feedback control (see Section 5.3.3, Eq. (5.15)), the corresponding closed form expression can be expressed as

$$\frac{V(s)}{P(s)} = S \frac{s}{s^2 M_{meq} + s R_{meq} + \frac{1}{C_{meq}}} \quad (7.1)$$

where

$$\begin{aligned} M_{meq} &= \frac{M_{ms} R_e}{R_e + \frac{Bl}{S} \Gamma_p} \\ R_{meq} &= \frac{R_{ms} R_e + (Bl)^2 + Bl \Gamma_v}{R_e + \frac{Bl}{S} \Gamma_p} \\ C_{meq} &= C_{mc} \left(1 + \frac{Bl \Gamma_p}{S R_e}\right) \end{aligned} \quad (7.2)$$

denote the mechanical equivalent components, in the low-frequency range, of the loudspeaker under combined control.

Equation (7.2) indicates that, assuming feedback gain $\Gamma_v \gg -Bl$, the target resistance is directly accessible through the ratio Γ_v/Γ_p that should equal the value of the characteristic impedance of air, i.e. 413.3 N s m^{-3} at 20°C , in view of optimal sound absorption. It can be pointed out that any increase of feedforward gain Γ_p in positive value leads to the reduction of the apparent mass M_{meq} together with the increase of the effective compliance C_{meq} . This yields an increase of the control bandwidth. With a shunt resistor (see Eq. (6.8)), however, the effective mass and compliance are not affected.

In order to highlight the underlying characteristics of a resonator, the mechanical equivalent components in Eq. (7.2) can be replaced by the following set of parameters

$$\omega_0 = \frac{1}{\sqrt{M_{ms} C_{mc}}} \quad \text{and} \quad \zeta = \frac{R_{ms} + \frac{(Bl)^2 + Bl \Gamma_v}{R_e}}{2 M_{ms} \omega_0} \quad \text{and} \quad K = \frac{S R_e + Bl \Gamma_p}{M_{ms} R_e} \quad (7.3)$$

where ω_0 is the natural radial frequency, ζ is the damping ratio and K the system gain.

Compared to the closed form expression obtained with a shunt resistor (see Eq. (6.9)), the resonator characteristic parameters are quite similar with a feedback control approach. For instance, the natural radial frequency is not affected much by the active control. Regarding the damping ratio, the influence of the feedback gain Γ_v is the same type as that of the shunt resistor R_s . Thus, the concept of electroacoustic resonator allows easy determination of the control parameters R_s and Γ_v in view of matching the desired resonator parameters ω_0 , ζ and K .

7.2.2 Combining the feedback control techniques and shunt methods

After identifying the formal analogies, the question now is: can both techniques be advantageously combined? Remarking that applying a motional feedback to the loudspeaker is equivalent to partially compensating the voice coil electrical impedance, a dedicated "hybrid" controller can be developed according to the topology of Fig. 7.1.

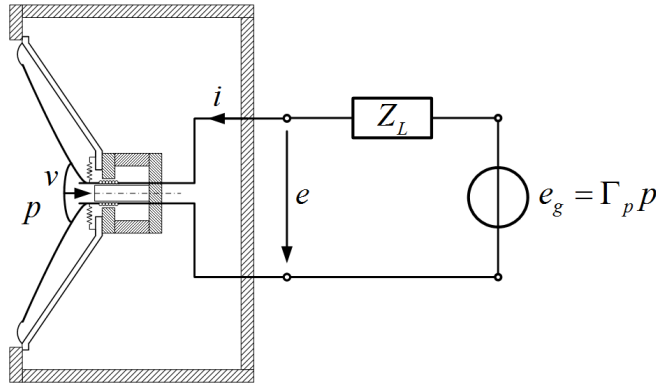


Figure 7.1: Diagram of a loudspeaker under hybrid control combining the feedforward control and a shunt electrical impedance.

In the present case, the controller includes an electrical impedance Z_L in series with a voltage source proportional to p of gain Γ_p . Using the aforementioned formalism, the input voltage applied to the electrical terminals is

$$e(t) = \Gamma_p p(t) - Z_L i(t) \quad (7.4)$$

and the general expression of the specific acoustic admittance in case of "hybrid" control can be expressed as

$$\frac{V(s)}{P(s)} = \frac{S(Z_e(s) + Z_L(s)) + Bl\Gamma_p}{Z_m(s)(Z_e(s) + Z_L(s)) + (Bl)^2} \quad (7.5)$$

Figure 7.2 shows the computed acoustic performance of when combining the feedforward

7.2. Merging active sound absorption and shunt methods

control and electrical shunt methods. The corresponding control settings can be found in Tab. 7.1. Configurations A and B illustrate the combination of the feedforward control with a negative electrical impedance, and with a negative resistance in series with a parallel RLC circuit, respectively. The small signal parameters of the loudspeaker, a Visaton AL-170, considered for this simulation can be found in Tab. 6.1.

Table 7.1: Parameter settings for the simulations with hybrid control.

Topology	Case	R_s	L_s	Γ_p	R	L	C
Hybrid control	A	5.3 Ω	0.66 mH	7 mV Pa ⁻¹			
	B	5.6 Ω	-	6.4 mV Pa ⁻¹	37 Ω	7 mH	90 μ F

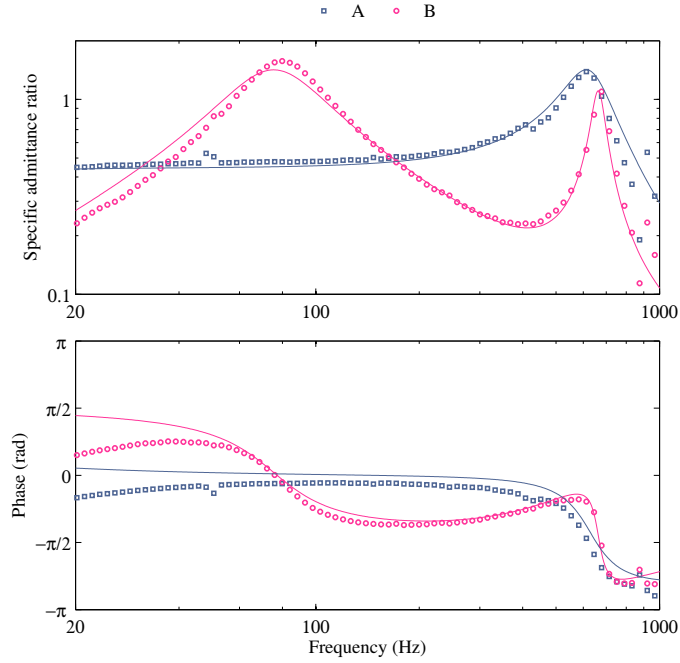


Figure 7.2: Representation of a loudspeaker under combined feedforward and shunt control.

As shown in Fig. 7.2, the effects of each technique are complementary. By compensating almost completely the dc resistance R_e and partially the inductance L_e of the voice coil, the natural resonance of the closed-box loudspeaker can be shifted nearly a decade higher, around 615 Hz (case A). The value of acoustic impedance in this frequency range can be controlled by varying the value of the feedforward gain Γ_p . By compensating almost totally the dc resistance R_e in series with a parallel RLC circuit, and combining with a feedforward control, case B shows that the loudspeaker behaves as a double resonator. Note that the natural resonance at 86 Hz and the resonance peak at 680 Hz, as a result of

the RLC circuit, can be closely matched to the target acoustic admittance. Consequently, feedforward control and electrical shunt methods can be advantageously combined. We shall now investigate whether an analog circuit can be directly designed from the model of equivalent electrical impedance.

Note: From a theoretical view, the formulation of feedback-based acoustic impedance control reveals formal analogies with the shunted loudspeaker method. This observation gave us the idea to synthesize an electrical network that can "mimic" performance obtained through feedback control of acoustic variables. The following discusses how this new paradigm opens the way to a straightforward control strategy for "semi-active" sound absorption.

7.2.3 Expressing the equivalent electrical load

In the previous sections, the closed form expressions of a loudspeaker under control have been derived. The purpose now is to detail how to express the equivalent load across the transducer terminals whatever the control settings.

Let us consider the loudspeaker under combined feedback/feedforward control, as discussed in Section 5.3. It follows from the characteristic equations (3.19), the electrical coupling equation (3.21) and the control law given by Eq. (5.15) that the acoustic variables p and v can be expressed as the functions of the electric current i as

$$e = \Gamma_p p - \Gamma_v v = -Z_{eq} i \quad (7.6)$$

where Γ_p is a feedforward gain, expressed in V Pa^{-1} , Γ_v is a feedback gain, expressed in $\text{V m}^{-1} \text{s}$, and Z_{eq} is the equivalent electrical load impedance in Ω , i.e. the ratio between the total control feedback voltage and the current.

After some further manipulations, Z_{eq} can be rearranged as

$$Z_{eq}(s) = -Z_e(s) + \frac{Z_e(s) + \frac{Bl}{S} \Gamma_p}{1 - \Gamma_p \frac{Z_m(s)}{S Bl} + \frac{\Gamma_v}{Bl}} \quad (7.7)$$

where $s = j\omega$ is the Laplace variable, Z_m is the mechanical impedance and Z_e is the electrical impedance.

Whatever the control settings, Z_{eq} can be viewed as an equivalent electrical load that encapsulates the control settings when the loudspeaker is actively controlled. As clearly seen in Eq. (7.7), Z_{eq} can be split off into a negative series resistance-inductance the role of which is to neutralize the blocked electrical impedance of the voice coil Z_e , and a

complex electrical impedance which depends on the control settings Γ_p and Γ_v .

A closed form expression of this type can be derived for each control cases discussed in Section 5.3. In case of motional feedback control only, Eq. (7.7) reduces to

$$Z_{eq}(s) = -\frac{\Gamma_v}{Bl + \Gamma_v} Z_e(s) \quad (7.8)$$

Equation (7.8) shows that applying a motional feedback produces the same effect as connecting a negative electrical impedance across the loudspeaker's terminals. The higher the gain, the greater the shunt impedance is close to a total compensation of the blocked electrical impedance Z_e . Such control settings help to dampen the diaphragm velocity response up to a point this interface with the air becomes highly reflective to incident sound waves.

In case of feedforward control only, Eq. (7.7) reduces to

$$Z_{eq}(s) = -Z_e(s) + \frac{Z_e(s) + \frac{Bl}{S}\Gamma_p}{1 - \Gamma_p \frac{Z_m(s)}{SBl}} \quad (7.9)$$

This equivalent electrical impedance consists primarily of a neutralization of Z_e and then of a complex electrical impedance which depends on control settings through the gains Γ_p and/or Γ_v . If the transfer functions (7.7-7.9) are realizable, each shall affect the loudspeaker dynamics so that it mimics the corresponding behavior under active control.

Note: This step was a determining milestone in the progress of the thesis. It paved the way, at least conceptually, to a new approach to control the acoustic impedance using an electroacoustic transducer [16]. This section clearly shows the duality between electric and acoustic impedances of both sides of the loudspeaker, which is at the heart of the synthesis process that follows.

7.2.4 Extending the bandwidth by synthesizing an electrical load

The following discusses ways to design a specific load with a view of increasing performance. To that purpose, a model-based approach is suggested. The case of combined feedback/feedforward control discussed in Section 7.2.3 is then equivalent to an electrical network Z_{eq} which is composed of a resistor and inductor in series, the role of which is to neutralize the electrical impedance Z_e of the voice coil, and an additional electrical impedance which depends on the control settings and loudspeaker parameters. This target electrical load can be achieved with the network illustrated in Fig. 7.3, com-

Chapter 7. Synthesis of electrical loads for acoustic impedance matching

posed of resistors R_1 and R_2 , and inductors L_1 and L_2 . The neutralization of the voice coil impedance is achieved using an electrical impedance $-R_e - sL_e$ in series with the electrical circuit of the loudspeaker.

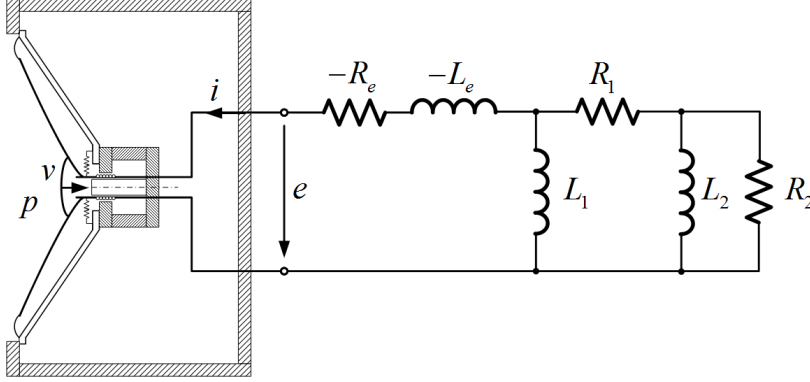


Figure 7.3: Connecting an equivalent electrical impedance to the loudspeaker terminals.

From the arrangement depicted in Fig. 7.3, the synthesized version of the equivalent shunt impedance given by Eq. (7.7) can be expressed as

$$Z_{eq}(s) = -(R_e + sL_e) + \frac{s^2 L_2 \left(1 + \frac{R_1}{R_2}\right) + s R_1}{s^2 \frac{L_2}{R_2} + s \left(1 + \frac{L_2}{L_1} + \frac{L_2 R_1}{L_1 R_2}\right) + \frac{R_1}{L_1}} \quad (7.10)$$

Identifying the parameters of Eq. (7.10) is not straightforward and requires much care, since the number of degrees-of-freedom is lower than the number of coefficients of the target electrical impedance. Nevertheless, to make this identification easier a set of resistors and inductors has been chosen so that the coefficient of s^2 on the numerator of Eq. (7.10) equals 0. In this way, the synthesized impedance fits the target one in the low-medium frequency range.

For illustrative purpose, let us consider a combined control with gains $\Gamma_v = 10 \text{ V m}^{-1} \text{ s}$ and $\Gamma_p = 0.025 \text{ V Pa}^{-1}$. For the Visaton AL-170 low-midrange loudspeaker the parameters of which are given in Tab. 6.1, the equivalent electrical load at the transducer terminals (7.7) becomes

$$Z_{eq}(s) = -5.6 - 0.0009 s + \frac{0.00041 s^2 + 8.5 s}{-0.0019 s^2 + s - 416.44} \quad (7.11)$$

From the simplification discussed above, the components values required for implementing Eq. (7.11) can be identified as

$$R_1 = -R_2 = 8.5 \Omega \quad L_1 = -18.7 \text{ mH} \quad L_2 = 17.4 \text{ mH} \quad (7.12)$$

Replacing now the value of (R_1, R_2, L_1, L_2) in Eq. (7.10) yields the following synthesized electrical impedance

$$Z_{eq}'(s) = -5.6 - 0.0009 s + \frac{8.5 s}{-0.002 s^2 + s - 454.5} \quad (7.13)$$

which is, theoretically, equivalent to applying a combined feedback/feedforward control with gains $\Gamma_v = 10 \text{ V m}^{-1} \text{ s}$ and $\Gamma_p = 0.025 \text{ V Pa}^{-1}$ (Z_{eq}' is referred to as the synthesized version of Z_{eq}).

Figure 7.4(a) clearly shows that the synthesized electrical impedance (7.13) matches the target one (7.11) within the frequency range of interest. As the frequency increases, however, the synthesized impedance curve deviates from the target.

Conversely, this synthesized impedance forms a new electrical shunt network that can be substituted for R_s in Eq. (6.11). Combining Eq. (7.10) with the characteristic equations (3.19) yields the closed form expression of the specific acoustic admittance as

$$\frac{V(s)}{P(s)} = S \frac{s}{s^2 \left(M_{ms} + (Bl)^2 \frac{L_2}{R_1 R_2} \right) + s \left(R_{ms} + \frac{(Bl)^2}{R_1} \right) + \frac{1}{C_{mc}} + \frac{(Bl)^2}{L_1}} \quad (7.14)$$

The resulting specific acoustic admittance with the chosen values of Eq. (7.12) yields a theoretically stable configuration according to Routh's criterion, assuming that the neutralization of the electrical impedance of the voice coil is ideally achieved.

Figure 7.4(b) provides computational results, processed with the aforementioned formulation of the specific acoustic admittance and equivalent electrical load. The "synthesized" electrical impedance Z_{eq}' is processed according to (7.13) and compared to the equivalent electrical load impedance (7.11). Similarly, the "synthesized" version of the specific acoustic admittance is processed according to (7.14) with the chosen value of Eq. (7.12) and then compared to (5.16). Figure 7.4(b) illustrates the computed frequency response in magnitude and phase of Eq. (7.14). Figure 7.4(d) shows the corresponding computed absorption coefficient. Although the curves of equivalent and synthesized electrical impedance agree quite well, some mismatch can be observed when measuring their effect of the acoustic side. Nevertheless, this results illustrates the duality between electric and acoustic impedances of both sides of the loudspeaker. It can be noted that, with the chosen equivalent electrical network, the coefficients of s^2 and s^0 in the denominator of Eq. (7.14) are lower than in the case of a shunt resistor (see Eq. (6.11)). This is in accordance with the objective of lowering the effective mass and increasing the effective compliance of the loudspeaker in order to extend the control bandwidth. Moreover, the equivalent resistance is actually of the same order of that providing the optimal matching, as discussed in Section 6.2. As a result, the equivalent electrical network can be used to adjust the resonator parameters to a desired objective.

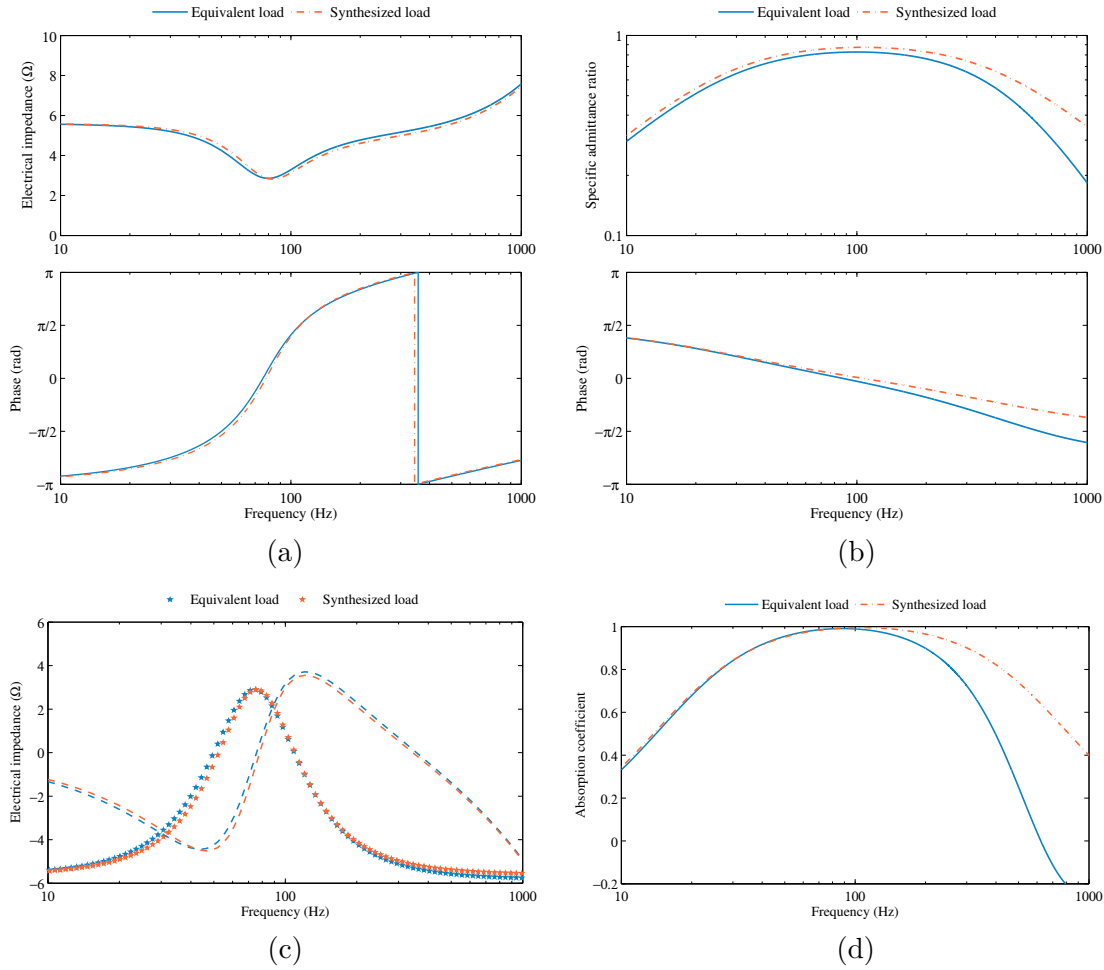


Figure 7.4: Computed frequency response with equivalent and synthesized load for a combined control with gain $\Gamma_v = 10 \text{ V m}^{-1} \text{ s}$ and $\Gamma_p = 0.024 \text{ V Pa}^{-1}$. The Bode plot (a) and the plot of the real (\star) and imaginary ($---$) part (c) of the electrical impedance are shown on the left; the Bode plot (b) of the specific acoustic admittance ratio and the corresponding absorption coefficient (d) are shown on the right.

Note: From a design perspective, a quite simple analog circuitry that mimics performances provided using sensors and a control system can be identified from the transducer model. The practical implementation of this equivalent electrical load is, however, not straightforward and requires a very accurate selection of the electric components. For example, it is necessary to compensate for the parasitic resistance of inductors in the equivalent circuit by using negative impedance converter, which drastically complicates the network. Another major difficulty is to cancel completely the electrical impedance of the coil [91]. Even though the neutralization is possible the components are not ideal, making the equivalent network very difficult to achieve. For these reasons it has

not been possible to implement the equivalent electrical impedances by using analog circuitry. Nevertheless, this theoretical result highlights some interesting properties of electroacoustic resonators and bridges the conceptual gap between active absorption through feedback control and shunted loudspeaker techniques.

7.3 Synthesis of electrical admittance using digital filters

The latter section concludes with practical issues encountered with the synthesis of impedance in the analog domain. To overcome this challenging task and in view to have more accuracy, selectivity and flexibility than with analog networks, we shall now consider the synthesis process in the digital domain.

7.3.1 Problem formulation

The design problem is to synthesize a proper electrical load impedance which, when connected to the loudspeaker terminals, can achieve a desired acoustic impedance at the diaphragm. The core assumption is to consider that each electrical matching network has its counterpart with a feedback control, and vice versa. The idea is to take advantage of the fact that the moving-coil drive unit is a bidirectional device. It results some ability to act as a sensor and an actuator simultaneously. We can therefore consider using the loudspeaker so that it provides information on the surrounding sound field while simultaneously altering it. The following presents a model-based methodology for synthesizing the acoustic impedance using an electroacoustic transducer.

7.3.2 Methodology for acoustic impedance synthesis

Starting from requirements for room correction, the methodology for the synthesis of acoustic impedance through digital filtering can be summarized by the following steps:

1. Requirement Analysis: this preliminary stage takes into account the acoustical specifications and design constraints in order to identify an convenient transducer.
2. Control Strategy Implementation: this modeling stage sets the appropriate control parameters to achieve a desired acoustic impedance using simulation tools.
3. Performance Assessment: this experimental step evaluates the loudspeaker performance when controlled
4. Internal Model Identification: this stage establishes an internal model of the loudspeaker when it meets the desired behavior.
5. Digital Filter Design: this stage is the realization of a digital copy matching the internal model of the loudspeaker through a model-based approach.

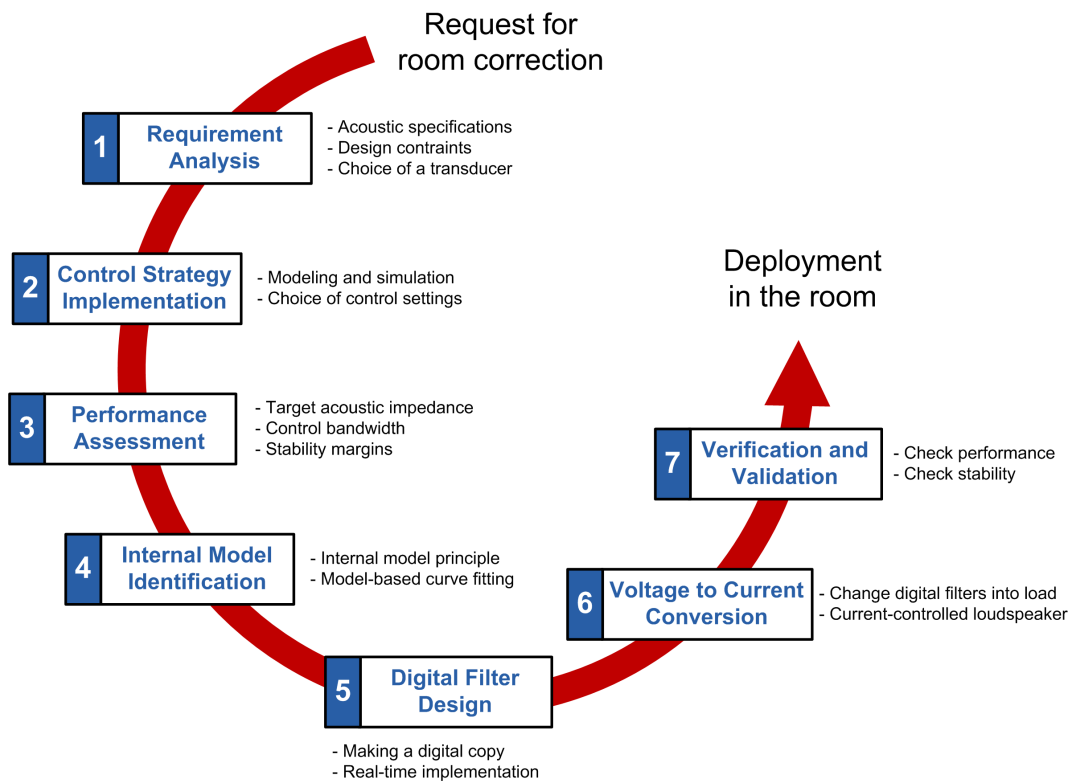


Figure 7.5: Methodology for acoustic impedance synthesis.

6. Voltage to Current Conversion: this stage describes the voltage-to-current conversion required to obtain a current-controlled loudspeaker.
7. Verification and Validation: this last stage verifies and validates performance and closed-loop stability of the loudspeaker once connected to the synthetic load.

The proposed methodology is highly intuitive and quite simple to implement but requires detailed knowledge of the transducer physical properties. The second and third steps can be achieved by referring to Chapters 5 and 6. Identifying the loudspeaker internal model can be carried out by measuring the electrical current and the voltage across the transducer terminals, when the apparent acoustic impedance of the diaphragm meets a desired target.

For the model-based curve fitting step, the closed form expression of the equivalent impedance can be derived after Eq. (7.7). If necessary, an improved model of the voice coil can be used in order to better fit the actual and modeled curves.

7.3. Synthesis of electrical admittance using digital filters

In [112, 113] for instance, an improved model of the voice coil is given by

$$Z_e(s) = R_e + sL_e + \frac{sL_p R_p}{R_p + sL_p} \quad (7.15)$$

where a resistance R_p and inductance L_p , arranged in parallel, are added to R_e and L_e so as to take into account of the lossy inductance.

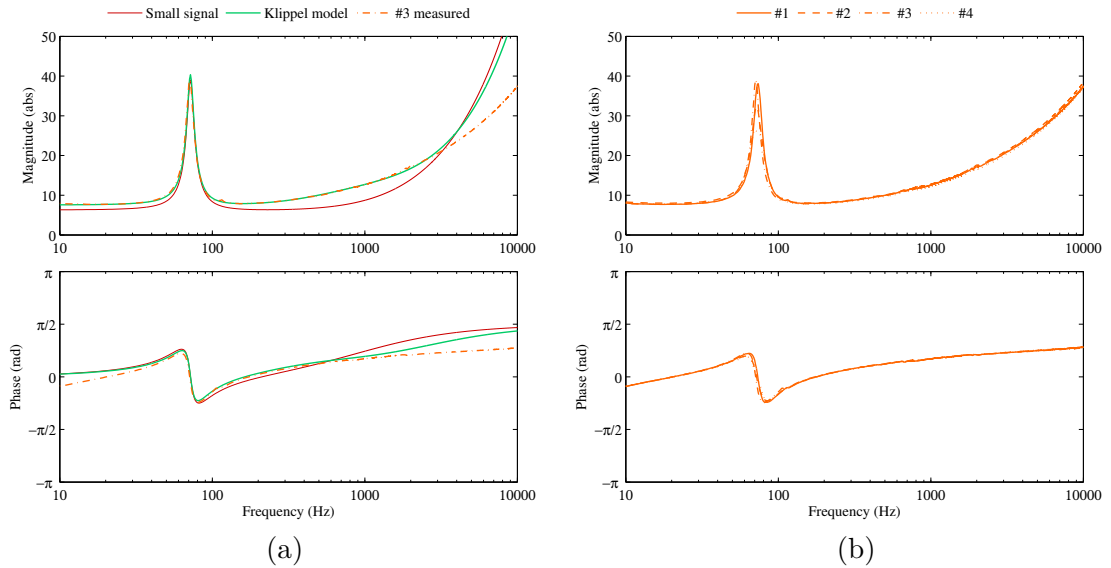


Figure 7.6: Measured and computed electrical impedances of the loudspeaker when placed in free field. Computed results with the small signal and Klippel model are compared to the measured one on the left and the dispersion of the measured electrical impedances for four loudspeakers of the same type is shown on the right.

Figure 7.6(a) illustrates the benefit provided by Klippel model [69, 71, 112, 113]. A noticeable discrepancy on the frequency response can be observed between the computed and measured data, especially with the small signal model. Figure 7.6(a) highlights the vagueness of the simple small signal model which is commonly used for modeling a loudspeaker as a sound transmitter. Figure 7.6(b) shows the measured dispersion on the frequency response of the electrical impedance on four loudspeakers of the same type in free field. It appears that the frequency responses are quite similar but not identical. The remaining steps of the synthesis methodology are discussed in the following.

7.3.3 Filter realization

In this section, the practical implementation of the equivalent electrical admittance through digital filters is presented. To illustrate this, we will perform the simulation for the case of a combined feedback/feedforward control.

Intake of the digital approach

Generally, digital filters can perform many mathematical operations in the discrete-time domain that are impractical or impossible with the use of analog filters. They are programmable and their parameters can be easily adjusted from the software. Digital filters are not subject to components nonlinearities that greatly complicate the design of analog filters. In this way, we can have a high precision over the filter coefficients with regard to the synthetic electrical load to be implemented. In the context of acoustic impedance control, the main constraint of digital processing is to operate in real-time. A certain latency (the difference in time between the input and the response) is caused by the sampling process. In analog filters, latency is often negligible. Strictly speaking, it is the time for an electrical signal to propagate through the filter circuit. In digital filters, latency is a function of the number of delay elements in the system. Compared to analog filters, digital noise may be introduced during the sampling process (analog to digital conversion, digital to analog conversion and quantization). Note also that numerical computation is not exempts of errors.

Hardware specifications

Digital filter systems usually consist of an analog-to-digital converter (ADC) to sample the input signal, followed by a digital processor and some peripheral components such as memory to store data and filter coefficients, and a digital-to-analog (DAC) converter. Program instructions (software) running on the processor implement the digital filter by performing the necessary mathematical operations on the binary numbers received from the ADC. In some high performance applications, an FPGA¹ or ASIC² is used instead of a general purpose microprocessor, or a specialized DSP³ with specific parallel architecture for expediting operations such as filtering [114]. FPGAs are basically reconfigurable Integrated Circuits (ICs) that are used to implement logic functions. They are often employed when prototyping because they can be programmed and inserted into a board in a relative short time.

Note: The questionable choice of FPGA technology was motivated simply by the availability of a CompactRIO system in the drawers of the lab.

Expressing the equivalent electrical admittance in the Laplace domain

Let us consider the general form of the equivalent electrical load impedance given in Eq. (7.7). For reasons of causality, this transfer function cannot be directly implemented

¹Field-Programmable Gate Array

²Application-Specific Integrated Circuit

³Digital Signal Processor

because the order of the numerator is greater than the denominator. The inverse of Eq. (7.7) must be considered in order to handle a proper transfer function. The expression of the load, which is now homogenous to an electrical admittance, can be written as

$$Y_{eq}(s) = -\frac{\Gamma_p \frac{Z_m(s)}{S} - \Gamma_v - Bl}{Z_e(s) \left(\Gamma_p \frac{Z_m(s)}{S} - \Gamma_v \right) + \frac{(Bl)^2}{S} \Gamma_p} \quad (7.16)$$

and after some further manipulations, as

$$Y_{eq}(s) = \frac{a_2 s^2 + a_1 s + a_0}{b_3 s^3 + b_2 s^2 + b_1 s + b_0} \quad (7.17)$$

where

$$\begin{aligned} a_2 &= M_{ms} & b_3 &= M_{ms} L_e \\ a_1 &= R_{ms} - S \frac{\Gamma_v}{\Gamma_p} - \frac{BlS}{\Gamma_p} & b_2 &= M_{ms} R_e + R_{ms} L_e - \frac{S \Gamma_v}{\Gamma_p} L_e \\ a_0 &= \frac{1}{C_{mc}} & b_1 &= R_{ms} R_e + \frac{L_e}{C_{mc}} + (Bl)^2 - \frac{S \Gamma_v}{\Gamma_p} R_e \\ & & b_0 &= \frac{R_e}{C_{mc}} \end{aligned} \quad (7.18)$$

Equation (7.17) is the form for a recursive filter with both the inputs (numerator) and outputs (denominator), which typically leads to an infinite impulse response (IIR) behavior. That is, the filter output will depend on both samples of previous input and output.

Calculation of the z-transform

In discrete-time systems, the digital filter is often implemented by converting the transfer function to a linear constant-coefficient difference equation via the z-transform [114]. The z-transform can be considered as a discrete-time equivalent of the Laplace transform. The general form is given by

$$H(z) = \frac{b_0 + b_1 z^{-1} + \dots + b_N z^{-N}}{1 + a_1 z^{-1} + \dots + a_M z^{-M}} \quad (7.19)$$

where N and M are the number of zeros and poles of the transfer function H . To obtain Eq. (7.19) there are several methods of discretization.

Besides the choice of method, the choice of sampling intervals is also crucial to the proper realization of the digital filter. With electronic controller that emulates continuous-time algorithms this choice is simple: sample as fast as possible. This is due to the

Chapter 7. Synthesis of electrical loads for acoustic impedance matching

approximations that are used to generate the difference equations describing the controller. Smaller sampling intervals mean that the properties of the underlying controller design will be less distorted, hence more predictable and better performances. However, too fast sampling is wasteful of resources and fast sampling intervals will mean that high frequency noise will also be captured in the signal, which is not necessarily beneficial to the performance of the closed-loop control. When the sampling interval is too long, then signal loss will occur. An extreme case is the phenomenon known as frequency aliasing. For this application, the bilinear transform is used for the discretization with sampling intervals of $20 \mu\text{s}$. Note that according to the Nyquist-Shannon theorem, the sampling frequency is greater than twice the maximum frequency component contained in the signals of interest.

Expressing the difference equation

In the discrete-time domain, the difference equation that will be processed on the digital controller can be expressed as

$$y_{eq}[n] = \sum_{k=0}^N b_k x_{eq}[n-k] - \sum_{k=1}^M a_k y_{eq}[n-k] \quad (7.20)$$

where n is an integer, b_k and a_k are the filter coefficients, and N and M are the number of zeros and poles, respectively. As indicated in Eq. (7.20), the filter output $y_{eq}[n]$ depends on both current and previous inputs $x_{eq}[n-k]$ and on the previous output $y_{eq}[n-k]$. More details concerning the implementation of IIR filter can be found in [114, 115].

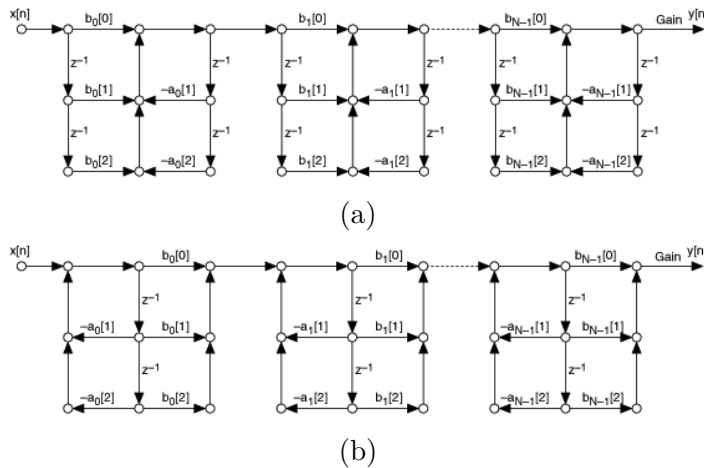


Figure 7.7: Filter structure of direct form I (a) and direct form II (b).

After a filter is designed, a filter structure must be selected to specify how a given set of filter coefficients is used to process mathematically the flow of the input signal. Several

7.3. Synthesis of electrical admittance using digital filters

mathematically equivalent implementation structures are available. These structures have little influence with a floating point digital filter. With a fixed-point filter, however, the choice of structure can lead to different results in the filter output. The software used for the synthesis has two types of filter structure that simultaneously optimize the execution time and are suitable for application in real time. These are the IIR filter structures of direct form I and II, as depicted in Fig. 7.7. For our application we used the direct form II.

Finite precision arithmetics

The way digital filter are realized is of the greatest importance, since an inappropriate implementation can drastically decrease performance. The problem of finite precision arithmetics has to be considered since floating point arithmetics is not supported by the embedded FPGA platform. Each floating-point value must therefore be approximated by a fixed-point value that will be used for the arithmetic functions (sum, multiplication, delay, etc.). Consequently, all possible values cannot be represented. To that purpose, a rounding mode is selected from the software. It ensures that the fixed-point representation is appropriate for a given value, despite a loss of precision. However, since the filters to be implemented are low-order, we can afford to use a large bit size so as to minimize the limitations of fixed point arithmetic. For more details on the quantization, please refer to [114,116].

7.3.4 Real time implementation

The practical implementation of digital IIR filters is performed on a National Instrument embedded real-time FPGA target CompactRIO[®], as depicted in Fig. 7.8.

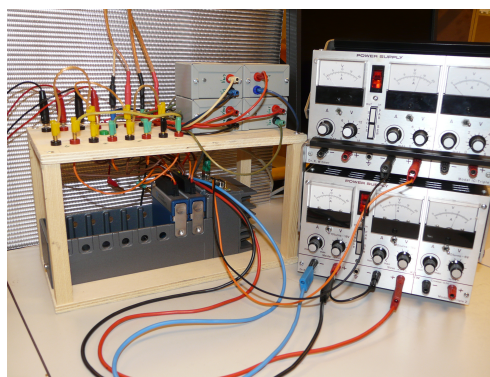


Figure 7.8: Picture of the control system.

This FPGA platform is a processor that allows implantation of logic functions or truth tables via circuits that are reprogrammable. The first step of the digital filter design is to

Chapter 7. Synthesis of electrical loads for acoustic impedance matching

compute a floating-point IIR filter that meets the requirements for the desired synthetic admittance. So as to accommodate the finite-precision constraints of the FPGA platform, a conversion of the filter coefficients to fixed-point representation must be performed while still trying to meet the specifications of the filter. The final step is generating code of the modeled fixed-point filter for the FPGA hardware target using the Xilinx Code Generator. More details concerning the implementation of IIR filter on an embedded real-time FPGA target can be found in [115]. Figures 7.9 and 7.10 illustrate the practical implementation of the digital filters on the real-time FPGA platform with LabVIEW®.

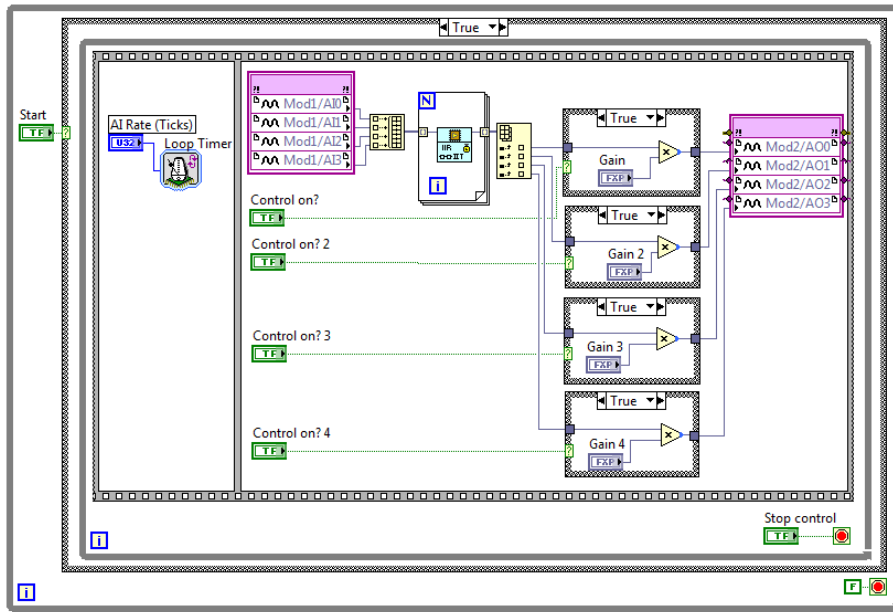


Figure 7.9: Block diagram of the LabVIEW FPGA VI.

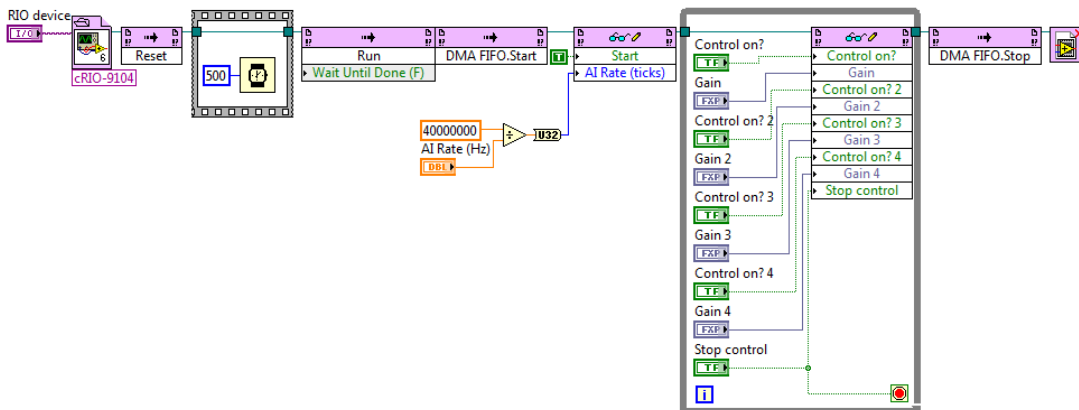


Figure 7.10: Block diagram of the LabVIEW real-time host VI.

7.3.5 Reconfigurable I/O platform

The National Instrument reconfigurable I/O (NI RIO) platform provides a unique architecture that can be used to design and implement various controllers and filters. It combines an embedded real-time processor, a high performance FPGA board, and I/O modules. Each I/O module is directly connected to the FPGA, thus providing low-level customization of timing and I/O signal processing. The required software platform, which includes the LabVIEW graphical programming environment as well as some additional modules and toolkits, makes it easier to create embedded platforms without having in-depth knowledge about hardware (low level) implementation. With the NI RIO architecture, one algorithm can run on the FPGA, which enables loop rates in the order of double-digit kilohertz while maintaining nanosecond determinism, while another algorithm can run on the real-time controller and take advantage of its powerful dual-digit floating point for complex mathematics calculation.

7.3.6 Voltage to current conversion

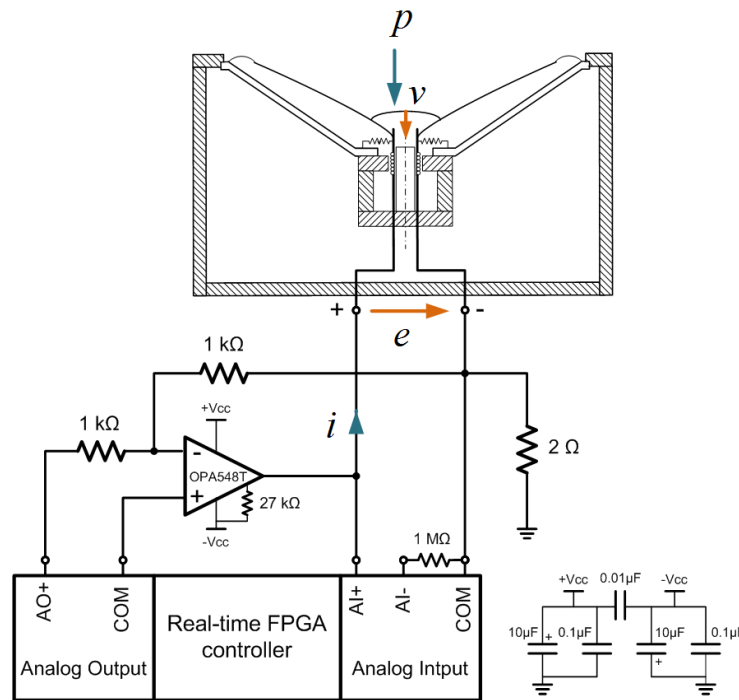


Figure 7.11: Voltage to current conversion circuit. When the loudspeaker diaphragm is subjected to a pressure force Sp , the voice coil will be set into motion with a velocity v . Such movement within the magnetic field will create a voltage $e = -Blv$ at the terminals, as stated in Section 3.3. This induced voltage is used as input for the digital filter. In turn, the filtered output voltage will be converted into an electrical current i which will generate a force $Bl i$ so as to compensate the driving sound pressure.

After a filter is designed, it is downloaded on the embedded FPGA platform to be used by the real-time controller which will process the signal arriving at the analog input module after analog-to-digital conversion. The filtered signal is then delivered by an analog output modules, after digital-to-analog conversion. As the equivalent electric load to be connected across the transducer terminals should be consistent to an electrical admittance, and that the digital filter delivers an output voltage, a voltage-to-current converter must be involved. A schematic representation of the voltage-controlled-current-source is depicted in Fig. 7.11. The choice to produce a voltage-to-current conversion and not the other way is due to impossible to design a causal filter that synthesizes the required electrical impedance. As a result, the loudspeaker becomes controlled by the current.

Note: Due to nonlinearity of the operational amplifier used in the conversion circuit the frequency response is not constant in the frequency range of interest (see Fig. 7.12(b)). In order to minimize the amplitude difference in the frequency response we used a sense resistor $R = 2\Omega$. If a high value of the sense resistor minimizes dc errors, the limiting factor on increasing the sense resistor value are brought on by the fact that load current flows through it [117]. Consequently, voltage drive capability decreases while power dissipation in the resistor increases. This explains the chosen value for the sense resistor. To compensate for it, a gain of 2 has to be included when designing the filter.

7.4 System performance using synthetic electrical loads

This section illustrates the performance of the loudspeakers when connected to a synthetic electrical load. As an illustration, electrical admittances synthesized with two different control settings will be considered so as to show some versatility. The first one, denoted by letter C, corresponds to a combined control with gains $\Gamma_v = 10 \text{ V m}^{-1} \text{ s}$ and $\Gamma_p = 0.025 \text{ V Pa}^{-1}$. The second one, denoted by letter D, corresponds to a case of over-reflection. The small signal parameters of the loudspeaker, a Monacor SPH-300TC, can be found in Tab. 5.1. For running the simulations, the rear face of the loudspeaker is loaded with a sealed enclosure the volume of which is $V_b = 38 \text{ L}$.

7.4.1 Practical implementation

The practical implementation of the synthetic load is not an easy task since many components are involved. The problem is that each component is able to affect the frequency response of the closed loop. This is the case with the power amplifier used for measuring the target electrical admittance and with the conversion circuit which do not exhibit a flat frequency response below 50 Hz, as depicted in Fig. 7.12(a). In order to properly implement the synthetic electric load, we must take into account any phase

7.4. System performance using synthetic electrical loads

shift induced by these components during the digital filter synthesis.

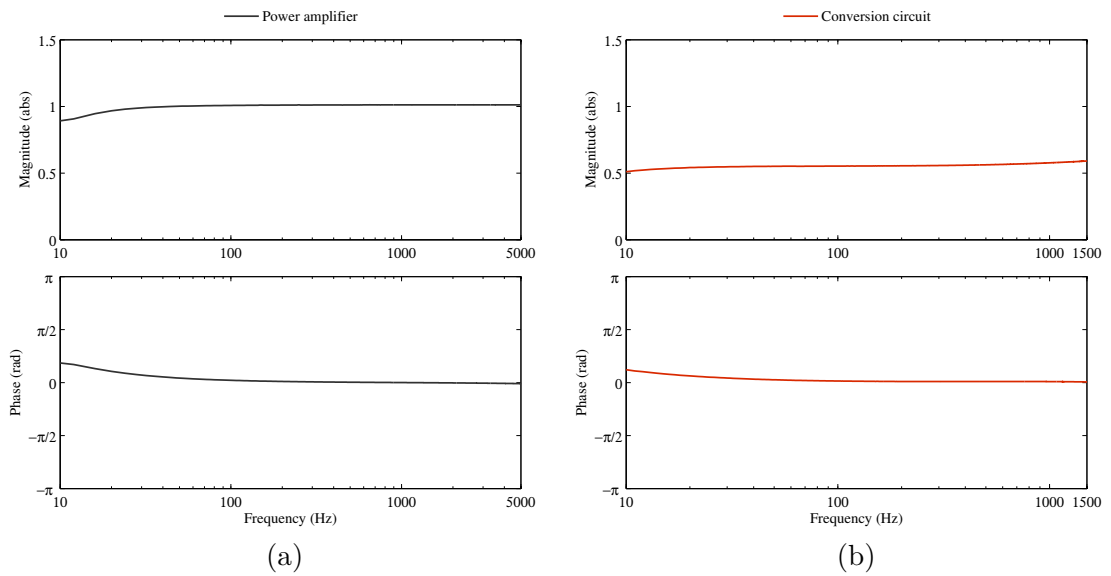


Figure 7.12: Frequency response of the power amplifier (a) and conversion circuit (b).

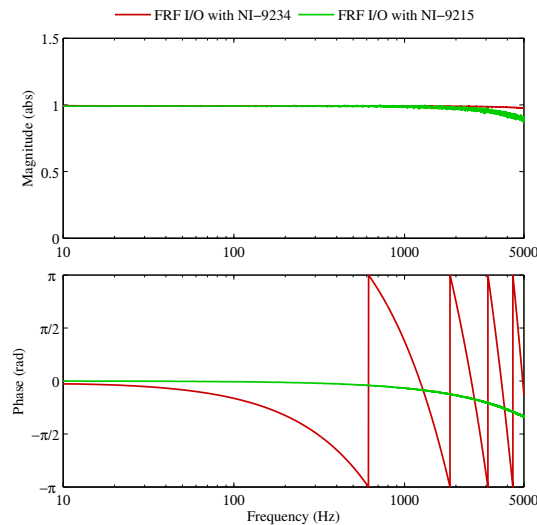


Figure 7.13: Measured frequency response of analog I/O modules NI-9234 and NI-9215.

In NI RIO platforms, two types of conversion are allowed for the modules: delta-sigma converter and direct converter. It turns out that the analog input module dedicated to audio measurements (NI-9234), i.e. including anti-aliasing filter, results in an excessive phase shift, as depicted in Fig. 7.13. This results in instability from a certain crossover frequency, for which the filtered signal is too much delayed to properly affect the system. Finally, we chose the NI-9215 as an analog input module, i.e. direct converter without anti-aliasing filter, for our application.

Chapter 7. Synthesis of electrical loads for acoustic impedance matching

The step of model-based curve fitting is by far the most sensitive of the whole process of synthesis. It appeared that a simple small signal model (see Eq. (3.18)) is not accurate enough to match the curve of the measured electrical admittance correctly. Figures 7.14 and 7.15 illustrate the improvement provided by Klippel model with fine tuning compared to small signal model, the parameters of which can be found in Tab. 5.1.

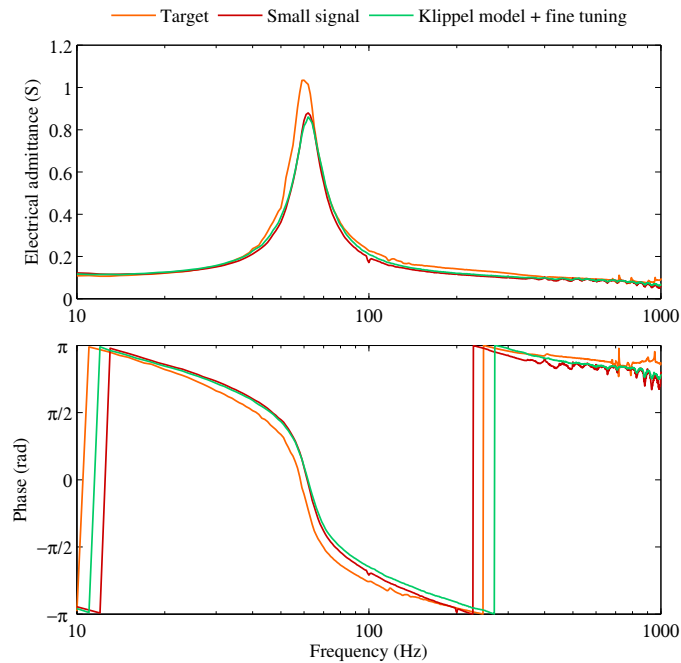


Figure 7.14: Measured frequency response after improving the synthesized electrical admittance.

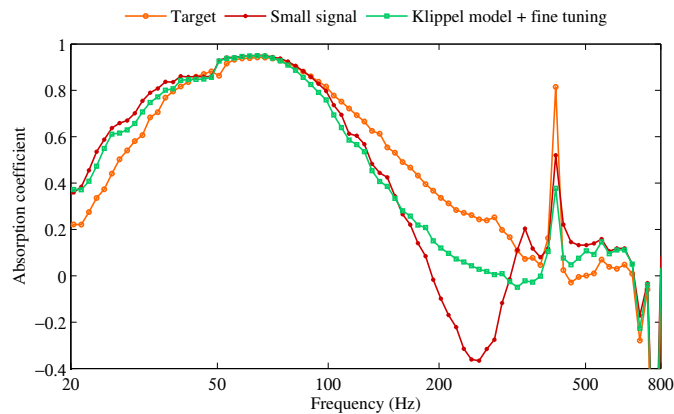


Figure 7.15: Measured absorption coefficient after improving the synthesized electrical admittance.

7.4. System performance using synthetic electrical loads

By fine tuning here, we mean changing the loudspeaker parameters and introducing a phase lead so as to shift the phase up around 250 Hz, and therefore shifting the stability limit. In this way, we take into account the phase shift of the analog-to-digital converter, thus resulting in more degrees of freedom to reach the target admittance without experiencing instability. As in any closed loop system, the system gain must not be greater than unity when the phase crosses $-\pi$. As shown in Fig. 7.14, the phase of the electrical admittance crosses $-\pi$ to a higher frequency. As a result, the measured absorption coefficient becomes positive over the frequency range of interest (Fig. 7.15).

7.4.2 Sound absorption/reflection capability

In the following, some experimental results from the application of synthetic electrical loads are presented. The case depicted by the letter C is designed in view of providing sound absorption at the transducer diaphragm, while the case depicted by the letter D is intended to provide the reverse.

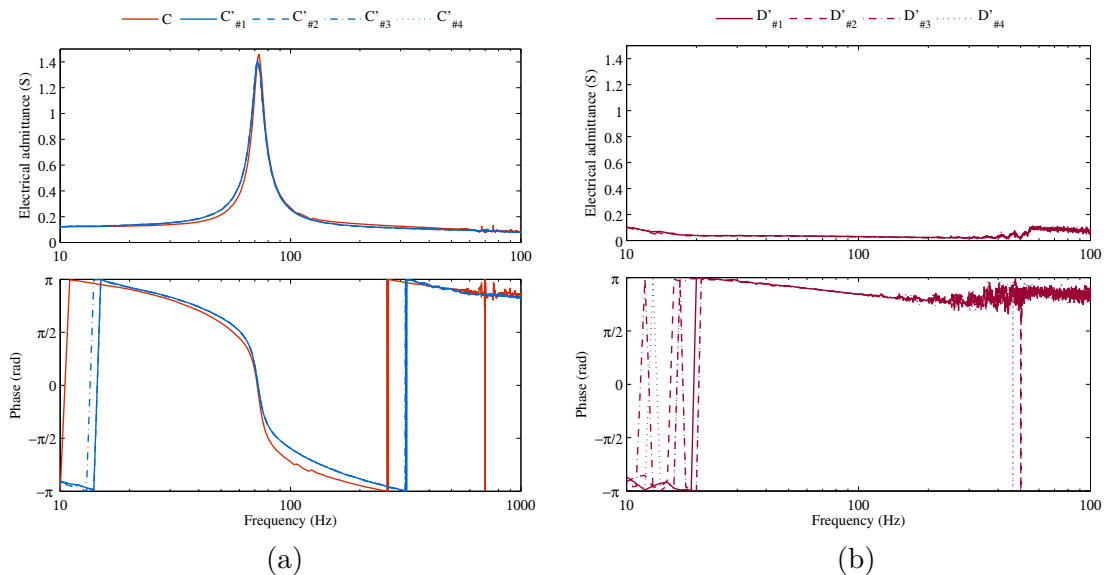


Figure 7.16: Measured frequency response of the synthesized electrical loads.

Figure 7.16 illustrates the small dispersion when applying the same synthetic admittance to four loudspeakers Monacor SPH-300TC, the parameters of which can be found in Tab. 5.1. From a practical point of view, this result is of great interest since it means that the synthesis step should not be repeated for each transducer. A single electrical characterization of the loudspeaker internal model is enough.

Figure 7.17 shows the acoustic performance measured in impedance duct with plane waves under normal incidence [36]. As shown in Fig. 7.17, the measured absorption coefficient is in accordance with the objective. With case C, the electroacoustic resonator

Chapter 7. Synthesis of electrical loads for acoustic impedance matching

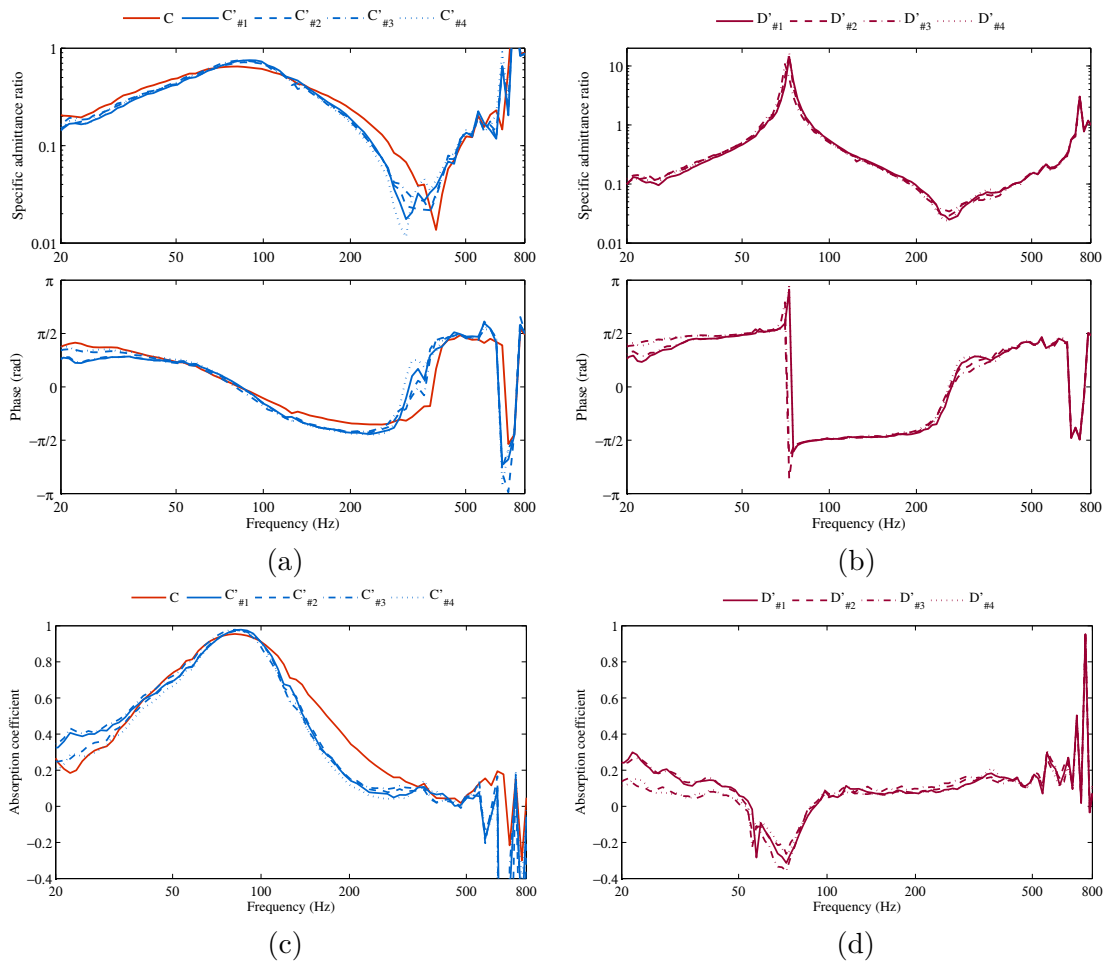


Figure 7.17: Measured acoustic performances using synthesized electrical loads. The Bode plot of the specific acoustic admittance ratio is shown on the top and the absorption coefficient is shown on the bottom.

behaves as an acoustic absorber, whereas in case D it behaves as a sound reflector.

It can be noted that the transducer diaphragm may become reflective in a controlled fashion, as shown in Fig. 7.17(d). This clearly shows that the synthetic load allows significantly altering the dynamics of the transducer so as to achieve a various acoustic impedance. This synthesis methodology allows flexibility for providing various boundary conditions at the transducer diaphragm. As expected, applying the same synthetic electrical admittance to loudspeakers of the same type gives similar results.

7.5 Conclusions

A unifying theory of active acoustic impedance control has been introduced, covering different control strategies from passive shunt to the feedback control of acoustic variables in a single formalism. Applying a feedback or feedforward control to the loudspeaker is shown to be equivalent to connecting an equivalent electrical load at its electrical terminals. Conversely, the closed form expression of the synthetic networks can be derived for any active acoustic impedance control. This theoretical result highlights some interesting properties of electroacoustic resonators and bridges the conceptual gap between active sound absorption and shunted loudspeaker techniques. From a design perspective, it is demonstrated that a quite simple analog network can be derived after the transducer model in order to mimic performance usually obtained using sensor and control system. This chapter has presented an innovative methodology for synthesizing acoustic impedance at the diaphragm of a loudspeaker, without sensor or control system. The question of the feedback control of acoustic quantities is converted into that of a regulation of electrical quantities through a synthetic load connected across the transducer terminals. Duality between electric and acoustic admittances of both sides of the loudspeaker is at the heart of the synthesis process.

This chapter has focused on showing the current performance of loudspeakers when connected to synthetic electrical loads. The methodology is to put the loudspeaker in a situation where it meets the specifications in terms of bandwidth and phase margin, and then to identify the resulting internal model. The synthesis stage is to make a digital copy as accurate as possible from the small-signal model and some fine tuning. Improvements in the design procedure are of course possible, particularly in relation to the process of identifying the internal model. As such, it seems interesting to look in the field of system identification which uses statistical methods to build mathematical models of dynamical systems from measured data.

From the control engineering perspective, the technique can be assimilated to internal model principle, which states that control can be achieved only if the control system encapsulates, either implicitly or explicitly, some representation of the process to be controlled. Since the control scheme has been developed on an exact model of the loudspeaker system, then perfect control is theoretically possible. However, it turns out that a very accurate model of the transducer might be required in some case, which makes it difficult implementing some shunt networks through analog circuitry. Therefore, a digital implementation of a synthetic electrical admittance alleviate this issue. It is also shown that it is not necessary to design a digital filter for each transducer of the same type, which is of great interest when it comes to produce panels of several transducers. The practical implantation using a real-time FPGA platform has been discussed. Note that a digital signal processor (DSP) could also be used. The choice of technology depends on the complexity of the control system, the conditions in which the system is supposed to operate, or any other specification.

Chapter 7. Synthesis of electrical loads for acoustic impedance matching

Although improvements are needed, this sensorless control technique offers a promising direction for practical applications of active sound absorption. In the last chapter, we shall discuss the use of electroacoustic resonator shunted with a synthetic electrical load in actual situations.

8 Modal equalization of a room using electroacoustic resonators

8.1 Introduction

Modal equalization is a method specifically addressing modal resonances issues in enclosed spaces. In general, low-frequency resonances have prejudicial audible effects in the rendering of sound in the room. In this frequency range, the response of a room presents high sound pressure levels at certain frequencies which coincide with the natural frequencies of the room [1, 8–10]. This even leads to an uneven spatial distribution of acoustic energy depending on the nodes and antinodes of sound pressure. When the sound stops the natural resonances of the room may sustain. In case of modulated sound signal diffusion (music), such room effect can be detrimental in terms of sound clarity and definition, or even harmful to intelligibility [11]. Changes resulting from the modulations of the original music can be felt by the audience. Similarly, changes in the frequency characteristics of sound can be heard as a change of timbre. Usual room equalization (filtering the signals of a reproduction system) can only in a limited way mitigate negative acoustic effects and most often is applied once a room has already been treated acoustically.

The problem is that effects caused by the slow decay rate of sound energy due to very pronounced resonances cannot be efficiently controlled with traditional passive means. As discussed in previous chapters, the ability of materials to dissipate sound energy is frequency-dependent. Porous materials generally provide high sound absorption in the medium and high-frequency range, typically above a few hundred Hertz. The resulting energy decay can be controlled to a desired level by involving the necessary amount of absorbing materials on the walls of the room. In the low-frequency range, typically when the sound wavelength is not small relative to the room dimensions, porous materials fail to efficiently control energy decay rate. An alternative for the treatment of low frequencies is to use resonant absorbers or bass traps (see Chapter 4). Unfortunately, this option may require the implementation of heavy enclosures and bulky sound absorbers, which is often not feasible or the cost would be prohibitive for practical use in real rooms.

In [10, 118], an arrangement of shunted loudspeakers is used in order to lower the low-frequency annoyance at a specific natural frequency of a reverberant room. Electrodynamic loudspeakers typically employed in noise control applications have a mechanical resonance somewhere between 20 Hz and 100 Hz, resulting in significant interaction between the enclosed sound field and transducer in the frequency range of interest [9, 42]. Interaction between these dynamical systems can be significant, and some of the acoustic energy of the sound field is dissipated passively through the internal damping in the loudspeaker. Due to the strong coupling of oscillations, the loudspeaker may also appreciably change the natural frequencies of the room that are close to the natural frequency of the loudspeaker. Note that this coupling also happens with Helmholtz resonators and the sound field in an enclosed space [87].

This chapter gives insights into the qualitative and quantitative aspects of the performance of electroacoustic resonator in a real situation. For illustrative purposes, the equalization of the low-frequency resonances of a test room is discussed. This experimental work emphasizes the relevance of the concept of electroacoustic resonators with respect to the usual soundproofing treatments. The problem of the interaction of such electroacoustic resonators with the natural modes of the room is not only of practical, but also of theoretical interest. However, we shall just focus on the practical aspect in the following. More details on wave theory or room acoustics can be found in [1, 119].

8.2 Semi-active modal equalization of a room

8.2.1 Objectives

Generally speaking, the goal of the modal equalization is not to change a listening room into anechoic by eliminating the room resonances entirely. The basic idea is rather to improve overall listening quality without losing the liveliness and a sense of spatial envelopment procured by the room [1, 11]. The main objective is thus to balance the acoustic energy decay rate of the low-frequency modes, and consequently to adapt the "reverberation" of the room in the low-frequency range. To be useful, modal equalization must affect the sound energy decay in the room, at least for the dominant modes, without significant increase in the remaining modes. In order to fulfill both these requirements in the frequency-domain and time-domain, we shall use electroacoustic resonators to control the acoustic impedance in discrete places of the room. In order to meet the objective, each electroacoustic resonator is settled so as to dissipate the acoustic energy of some modes. This experiment does not attempt to solve a real engineering problem, but only to show the potential of the concept of electroacoustic resonator in an actual situation. Apart from this, there is no target objective in terms of sound pressure level or reverberation values to be achieved. The general idea is to demonstrate that few electroacoustic resonators can be used to dampen the dominant modes of a room, and hence improving the sound energy decay rate in a controlled fashion.

8.2.2 Problem statement

The present work considers a room with parallel pairs of walls, the pairs being perpendicular to each other. It will be referred to in the following as rectangular room. The typical listening rooms, however, are more or less irregular in shape, partly due to the furniture that forms part of the room boundary. Although rather distant from the shapes of auditoria or concert halls, this geometry is a good example to understand the low-frequency distribution of acoustic energy in enclosed spaces. Such a typical case is discussed in the following sections to show the benefit of tunable electroacoustic resonators to improve the damping of the low-frequency resonances and the decay time of acoustic energy. We are not aiming a global control of the sound field in the room, but simply to reduce the resonance magnitudes in view of minimizing the audibility of the low-frequency modes.

8.2.3 Room description

The experiment is carried out in a technical room used to store containers of waste sorting, on the ground floor of the building ELE at EPFL. This is a hard-walled rectangular room with a total area of 94.3 m^2 and a volume of 59.3 m^3 (width 3 m by length 5.6 m by height 3.53 m). The geometric description of the room is given in Fig. 8.1. The ground is covered with floor tiles, as illustrated in Fig. 8.5.

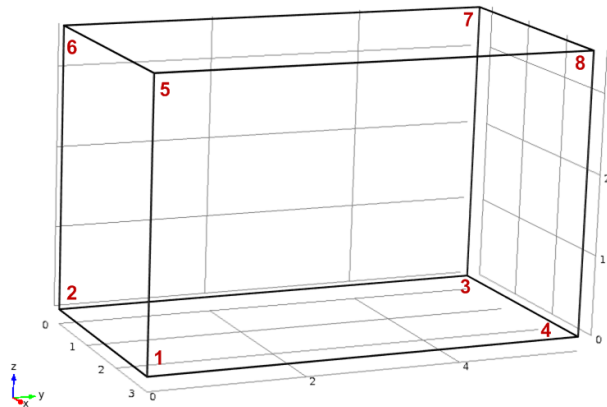


Figure 8.1: Sketch of the rectangular room.

Such a room is characterized by a strong reverberation due to rigid walls and is likely to have isolated modes with long decay times, particularly at low frequencies. The next stage is to find and identify the modes of the room that need to be damped.

8.2.4 Identifying the natural frequencies of the room

The explicit evaluation of the eigenvalues and eigenfunctions of usual rooms is generally quite difficult and requires the application of numerical methods such as the finite element method (FEM) [1]. From the wave theory of room acoustics, the closed form expression of the eigenfunctions can be derived after solving the eigenvalue problem with simple boundary conditions since the shape of the room is particularly simple [119].

In this study, a finite element model of the room has been established using Comsol Multiphysics in order to obtain some insight into the complicated distribution of the sound pressure in the room. By this approach, the solution of the wave equation is sought to satisfy certain boundary conditions which have to be set along the room's boundaries. These boundary conditions describe mathematically the acoustical properties of the wall, the ceiling and the other surfaces. Assuming rigid walls, the natural frequencies of the room the dimensions of which are (l_x, l_y, l_z) can be derived after

$$f_{n_x, n_y, n_z} = \frac{k_n c}{2\pi} = \frac{c}{2} \sqrt{\left(\frac{n_x}{l_x}\right)^2 + \left(\frac{n_y}{l_y}\right)^2 + \left(\frac{n_z}{l_z}\right)^2} \quad (8.1)$$

where f_{n_x, n_y, n_z} is the natural frequency and each triplet (n_x, n_y, n_z) corresponds to the eigenvalues k_x , k_y , k_z , and k_n defining the direction of propagation [1]. The various modes can be distinguished by their structure or vibration pattern. Axial modes are those for which one of the parameters n_x , n_y , or n_z is different from zero. The vibration pattern is along x -, y -, or z -axis. Tangential modes are those for which only one n_x , n_y , or n_z equals zero. Oblique modes are those for which the parameters n_x , n_y , or n_z are all different from zeros. In Tab. 8.1, the lowest fifteen natural frequencies (in Hz) of a rectangular room with dimensions $l_x = 3$ m, $l_y = 5.6$ m and $l_z = 3.53$ m are listed for $c = 343$ m s⁻¹, together with the corresponding combinations of parameters (n_x, n_y, n_z) which indicate the structure of the mode.

The eigenfunctions associated with the eigenvalues are simply obtained by multiplying three cosines [1], each of which describes the dependence of the pressure on one coordinate

$$p_{n_x, n_y, n_z}(x, y, z) = P_{n_x, n_y, n_z} \cos\left(\frac{n_x \pi x}{l_x}\right) \cos\left(\frac{n_y \pi y}{l_y}\right) \cos\left(\frac{n_z \pi z}{l_z}\right) \quad (8.2)$$

where P_{n_x, n_y, n_z} is an arbitrary constant.

Figure 8.2 shows the sound pressure level computed at corner 8 for a point source in the vicinity of corner 1 (see Fig. 8.1) using Comsol Multiphysics without any acoustic treatment, i.e. with hard walls. Figure 8.3 illustrates the isosurface of the total acoustic pressure field for a selection of modes of the room.

8.2. Semi-active modal equalization of a room

Table 8.1: Natural frequencies of the room with dimension $(3 \times 5.6 \times 3.53) \text{ m}^3$. The parameters (n_x, n_y, n_z) indicate the structure of the natural frequency along the length, width and height of the room

n_x	n_y	n_z	Natural frequency		Type of mode
			Computed Hz	Measured Hz	
0	1	0	30.4	31.2	Axial
0	0	1	48.2	48.0	Axial
1	0	0	56.6	54.8	Axial
0	1	1	56.9	58.2	Tangential
0	2	0	60.7	61.5	Axial
1	1	0	64.3	65.3	Tangential
1	0	1	74.4	73.0	Tangential
0	2	1	77.5	76.0	Tangential
1	1	1	80.3	79.7	Oblique
1	2	0	83.0	83.9	Tangential
0	3	0	91.0	91.6	Axial
1	2	1	96.0	95.2	Oblique
0	0	2	96.3	96.8	Axial
0	1	2	100.9	101.3	Tangential
0	3	1	103.0	102.7	Tangential

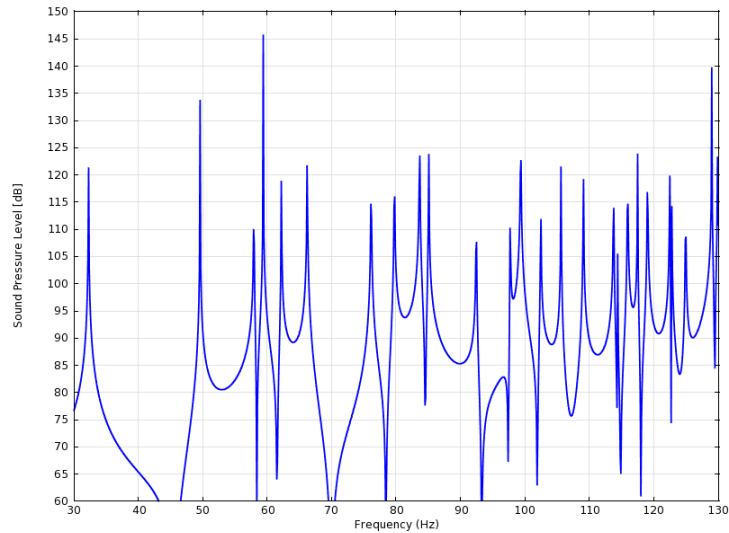
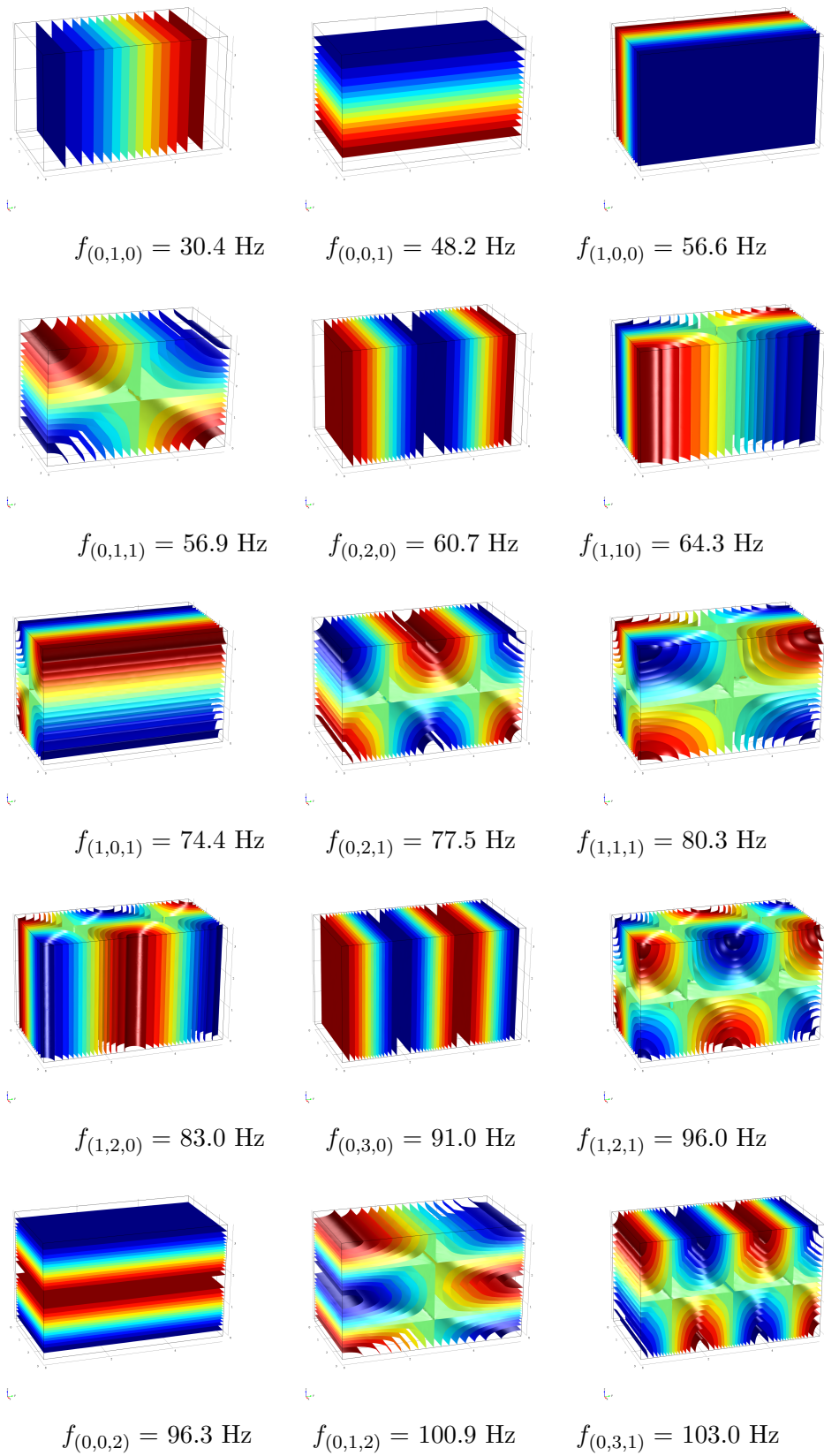


Figure 8.2: Sound pressure level computed in corner 8 of the room using Comsol Multiphysics.



152 Figure 8.3: Acoustic energy distribution of the lowest fifteen modes of the room.

8.2. Semi-active modal equalization of a room

These computed results are very useful to accurately identify the natural frequencies of the room. This will be used later to determine the best locations where control of acoustic impedance should be applied. The graphical representation of the distribution of the acoustical energy in the room clearly illustrates the nodes and antinodes of pressure. A node is a point where the sound pressure is almost zero. Inversely, an antinode is point where the sound pressure is maximum [1]. Nodes can make up nodal lines and nodal planes which can be seen in Fig. 8.3.

Note: This information is of primary interest to determine the convenient locations for the microphones and sound source. For the sake of precise identification of each mode, several microphones have been used to measure the frequency response of the room. Likewise, two locations for the sound source have been tested. This has enabled to identify the mode structure resonances very close to each others from the measured frequency response of the room (see Tab. 8.1).

8.2.5 Defining the location of electroacoustic resonators in the room

The analysis of the distribution of acoustic energy reveals that the electroacoustic resonators must be carefully placed in the room so as to damp each mode effectively. At low frequencies, typically where the size of electroacoustic resonators becomes small relative to the wavelength, there are locations for which they do not couple well into the room. The locations where the coupling with the room is not in favor are (obviously) the nodal lines [9].

To get the best performance, conversely, electroacoustic resonators should be placed on antinodes and their diaphragm should be normally oriented with respect to the mode structure (see Section 8.2.4). This means that, for a given mode, the orientation of the transducer diaphragm must be specified in addition to the location of electroacoustic resonators in the room. Ideally, the loudspeaker systems should be incorporated into the walls so as to be closer to pressure antinodes and also not to hinder the effective volume of the room. For practical reasons, however, they are distributed in the test room near the walls.

The locations and orientations of resonators that have been experienced in this study are described in Fig. 8.4. Some pictures of the configurations tested in the room are presented in Fig. 8.5.

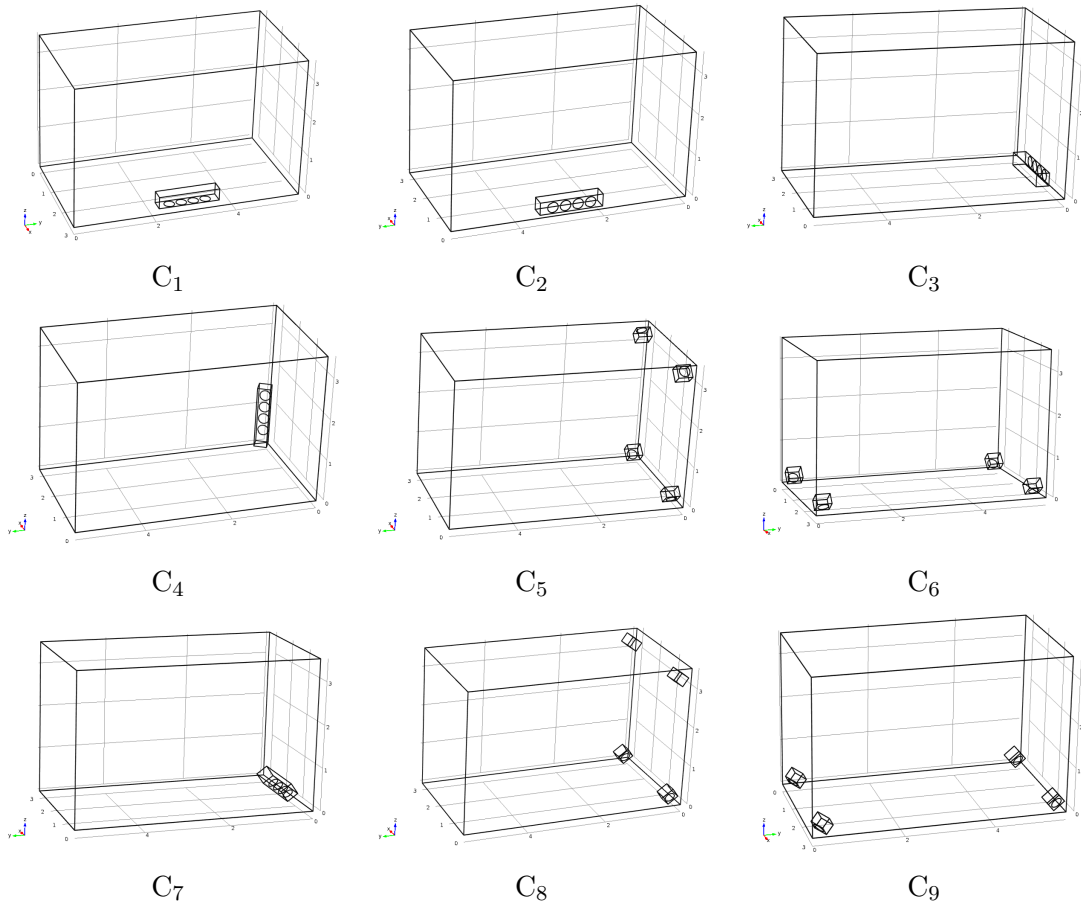


Figure 8.4: Location and orientation of the electroacoustic resonators in the room.

8.3 Results and discussion

8.3.1 Experimental setup

When the location and orientation of electroacoustic resonators have been determined, they must be given a specified acoustic impedance. The small signal parameters of the subwoofer Monacor SPH-300TC used for carrying out this experiment can be found in Tab. 5.1. The sound source used for measuring the frequency response of the room is a low-range loudspeaker in sealed enclosure, designed to provide the necessary acoustic power in the frequency range of interest. It is placed on the floor in the corner 1 of the room (see Fig. 8.1). The excitation is a random pink noise. The resulting acoustic impedance at the loudspeaker diaphragm has been obtained by using a synthetic electrical load, as discussed in Chapter 7.

Figure 8.6 illustrates the measured absorption coefficient under normal incidence (in an



Figure 8.5: Pictures of some configurations experienced in the room. The configuration C_4 is shown in (a), C_6 is shown in (b), C_7 is shown in (c), C_8 is shown in (d) and C_9 is shown in (e) and (f).

impedance tube, under ISO 10534-2 standard) for the Monacor SPH-300TC low-range loudspeaker loaded by an enclosure of volume $V_b = 23$ L (left), and $V_b = 38$ L (right). From this result, we expect effective control between 50 Hz and 100 Hz. The synthetic loads that led to this performance are shown in Fig. 8.7.

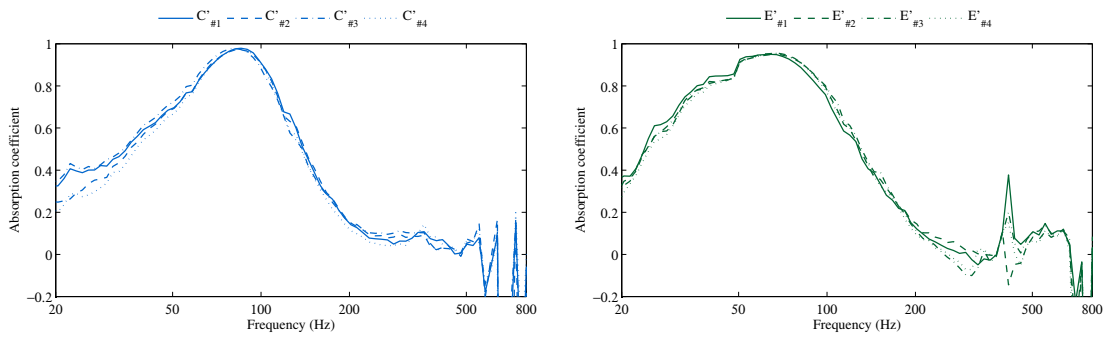


Figure 8.6: Measured absorption coefficient of the loudspeakers when connected to synthetic loads. Results for the "cube" are shown on the left and for the "panel" on the right.

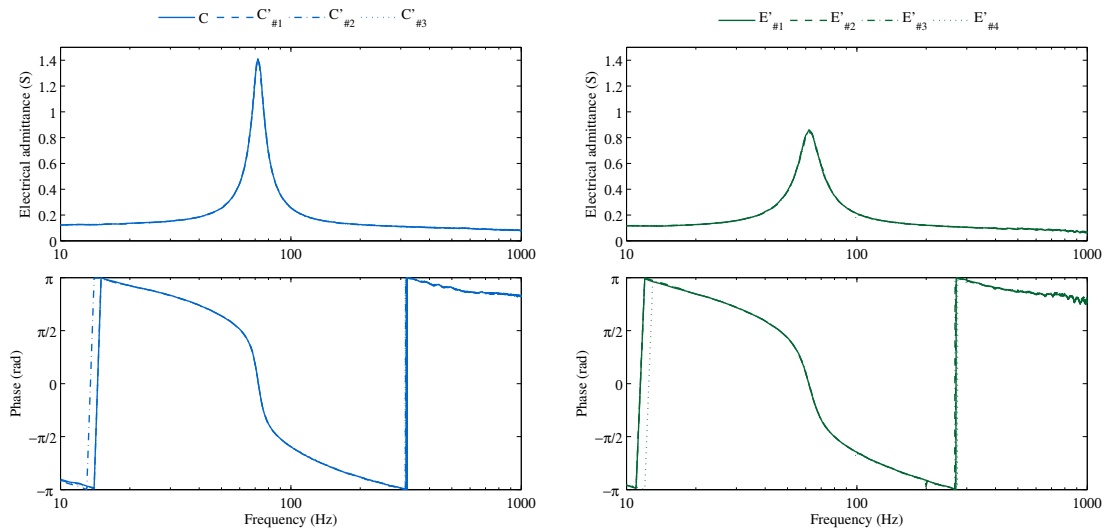


Figure 8.7: Measured electrical admittance of the synthetic loads connected to the loudspeakers. Results for the "cube" are on the left and for the "panel" on the right.

Only the configurations referred by C_1 , C_2 , C_4 , C_5 , C_6 , C_8 , C_9 in Fig. 8.4 will be discussed in the following. For configurations C_1 , C_2 and C_4 , an aligned arrangement of four electroacoustic resonators is used. Because it forms a single element, this arrangement is referred to as "panel" in the following. Acoustic performance for the panel is illustrated in terms of sound absorption coefficient in Fig. 8.6(b). The electrical load that is synthesized to achieve the performance is shown in terms of electrical admittance in Fig. 8.7(b). In C_1 and C_2 , the panel is aligned with the edge (1-4), as depicted in Fig. 8.4. In C_1 each transducer diaphragm is facing the floor and the panel is raised a few inches on wooden battens, whereas in C_2 , the panel is facing the wall. With the C_4 configuration, the panel is arranged in columns along the edge (3-7). The diaphragms of the transducers are facing the opposite corner, i.e. their orientation is along the diagonal (1-3).

With the C_5 , C_6 , C_8 and C_9 configurations, another arrangement of electroacoustic resonators is used. This is a set of four individual electroacoustic resonators that can be distributed in the room. Because of their cubic shape, this arrangement is referred to as "cube" in the following. Each cube is independent and can be distributed anywhere in the room. Acoustic performances for each cube are illustrated in term of sound absorption coefficient in Fig. 8.6(a). The electrical load synthesized to achieve the performance is shown in term of electrical admittance in Fig. 8.7(a). In C_5 and C_8 , the electroacoustic resonators are placed in corners 3, 4, 7 and 8, as depicted in Fig. 8.4. In C_5 , the orientation is such that the diaphragm of each cube is facing edges along the y-axis, whereas in C_8 the orientation is such that the diaphragm of each cube is facing edges along the x-axis. In C_6 and C_9 the cubes are placed on the ground in corners 1, 2, 3 and 4, as depicted in Fig. 8.4. In C_6 the orientation is such that the diaphragm of each cube is facing edges along the y-axis, whereas in C_9 the orientation is such that the diaphragm of each cube is facing edges along the x-axis.

8.3.2 Damping of low-frequency modes

Figures 8.8 to 8.11 show the measured frequency response of the room in terms of sound pressure level for the aforementioned configurations. The maximum gains in decibels provided by controlling the acoustic impedance at different location of the room are summarized in Tab. 8.2 for each configuration.

Table 8.2: Summary of the sound pressure level gains measured for each configuration.

Type of mode		Natural	Configurations						
		Frequency Hz	C_1 dB	C_2 dB	C_4 dB	C_5 dB	C_6 dB	C_8 dB	C_9 dB
Axial	010	30.4	-0.6	-1.7	-4.6	-1.5	-2.2	-1.8	-0.9
Axial	001	48.2	-1.0	-0.8	-0.8	-0.7	-0.7	-0.8	-1.0
Axial	100	56.6	-2.6	-1.5	-2.8	-6.0	-5.5	-3.9	-5.0
Tangentiel	011	56.9	+2.0	+2.0	0	+2.0	-0.8	+0.2	+2.0
Axial	020	60.7	-3.0	-4.0	-0.1	-3.0	-2.9	+2.2	+1.7
Tangentiel	110	64.3	-1.8	-3.0	-8.5	-7.0	-5.3	-5.6	-4.5
Tangentiel	101	74.4	-1.8	-1.7	-10.5	-11.7	-9.1	-12.2	-8.6
Tangentiel	021	77.5	-5.5	-5.5	0	-4.0	-5.7	-4.3	-6.2
Oblique	111	80.3	0	0	-3.3	-6.8	-9.5	-8.6	-9.0
Tangentiel	120	83.0	-4.8	-4.8	-11.4	-7.9	-8.9	-8.5	-9.4
Axial	030	91.0	-2.4	-2.4	-4.1	3.9	-3.2	-5.8	-4.7
Oblique	121	96.0	-5.6	-5.6	-5.6	-7.1	-13.7	-10.0	-13.6
Axial	002	96.3	-11.7	-10.3	-3.8	-7.6	-6.7	-7.6	-6.0
Tangentiel	012	100.9	-1.0	0	-2.6	-7.1	-7.5	-3.8	-8.2
Tangentiel	031	103.0	-3.9	-3.2	-1.8	-5.2	-5.4	-7.2	-6.9

Chapter 8. Modal equalization of a room using electroacoustic resonators

From the analysis of acoustic energy distribution in the room, configuration C_1 is supposed to address mainly the axial modes along the z-axis, i.e. $(0,0,1)$ at 48.2 Hz and $(0,0,2)$ at 96.3 Hz as referred in Tab. 8.1. Using the configuration C_2 instead, the axial mode along the x-axis should be affected, i.e. $(1,0,0)$ at 56.6 Hz, as referred in Tab. 8.1. With configurations C_1 and C_2 , the most substantial gains were seen for the mode $(0,0,2)$ at 96.3 Hz, with -11.7 dB and -10.3 dB, respectively for C_1 and C_2 . This is in accordance with the analysis of acoustic energy distribution in the room, as illustrated in Fig. 8.3. The modes $(0,0,1)$ at 48.2 Hz and $(1,0,0)$ at 56.6 Hz, however, are moderately affected. This can be explained by an equivalent absorption area which is too low for this mode. It should be used more surface area and better distributed in the planes where they are supposed to be effective in damping such modes.

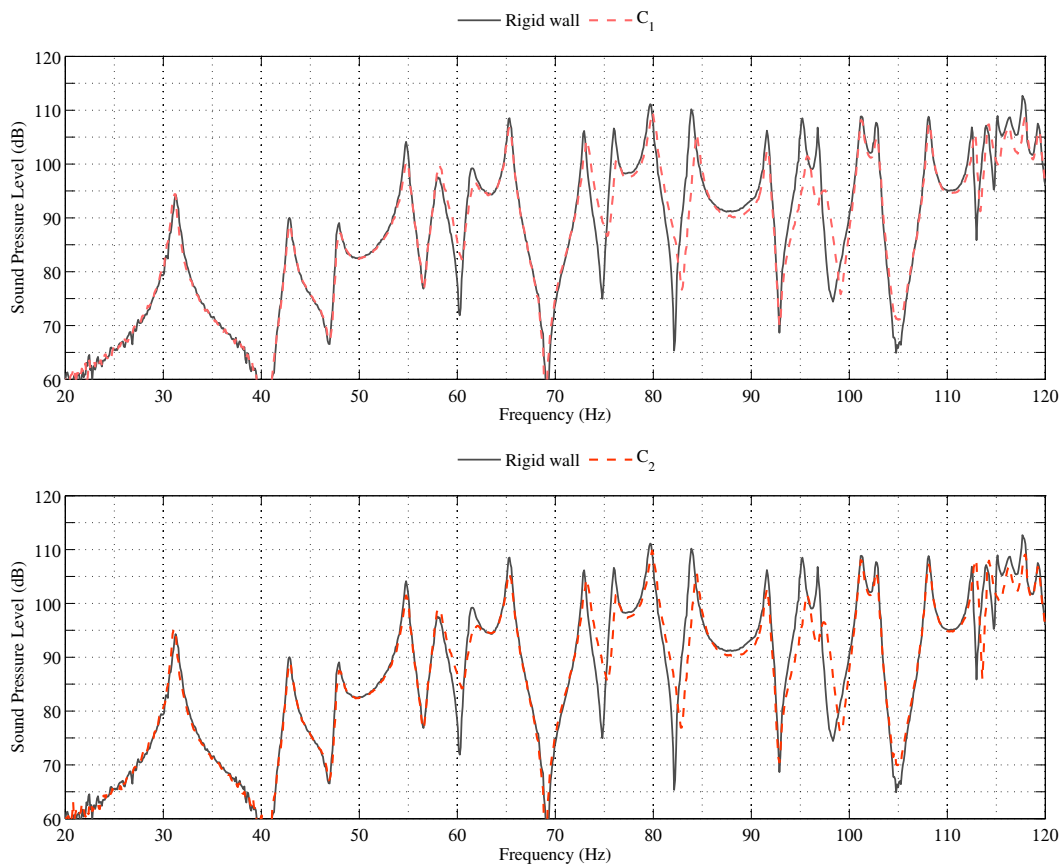


Figure 8.8: Sound pressure level measured in corner 8 with configuration C_1 and C_2 .

Configuration C_4 is supposed to address mainly the tangential modes along the diagonal $(1-3)$, i.e. $(1,1,0)$ at 64.3 Hz and $(1,2,0)$ at 83.0 Hz as referred in Tab. 8.1. As expected, a significant reduction on the measured sound pressure level in corner 8 can be observed at these frequencies. As shown in Fig. 8.9 the gain is -8.5 dB at 60.4 Hz and -11.4 dB at 83.0 Hz. There is also a major gain for the tangential mode $(1,0,1)$ at 74.4 Hz.

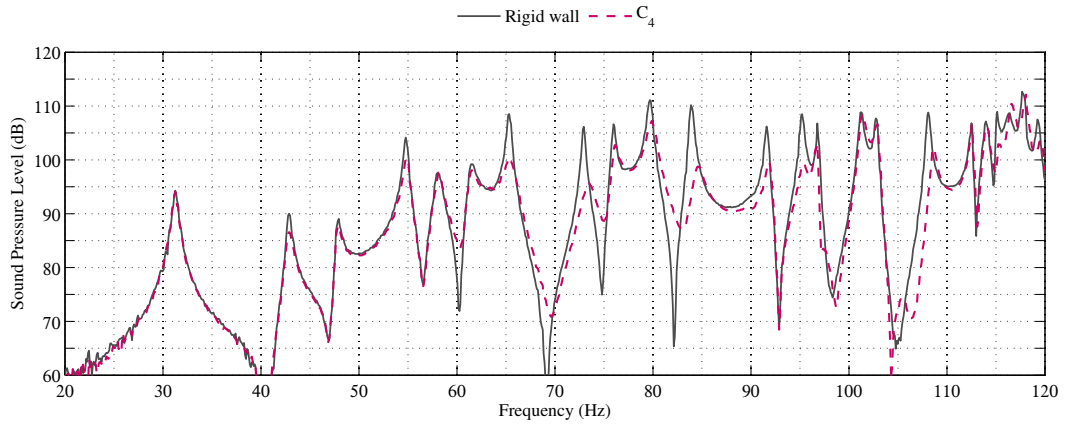


Figure 8.9: Sound pressure level measured in corner 8 with configuration C_4 .

The configurations C_5 and C_8 are primarily intended to damp the tangential and oblique modes.

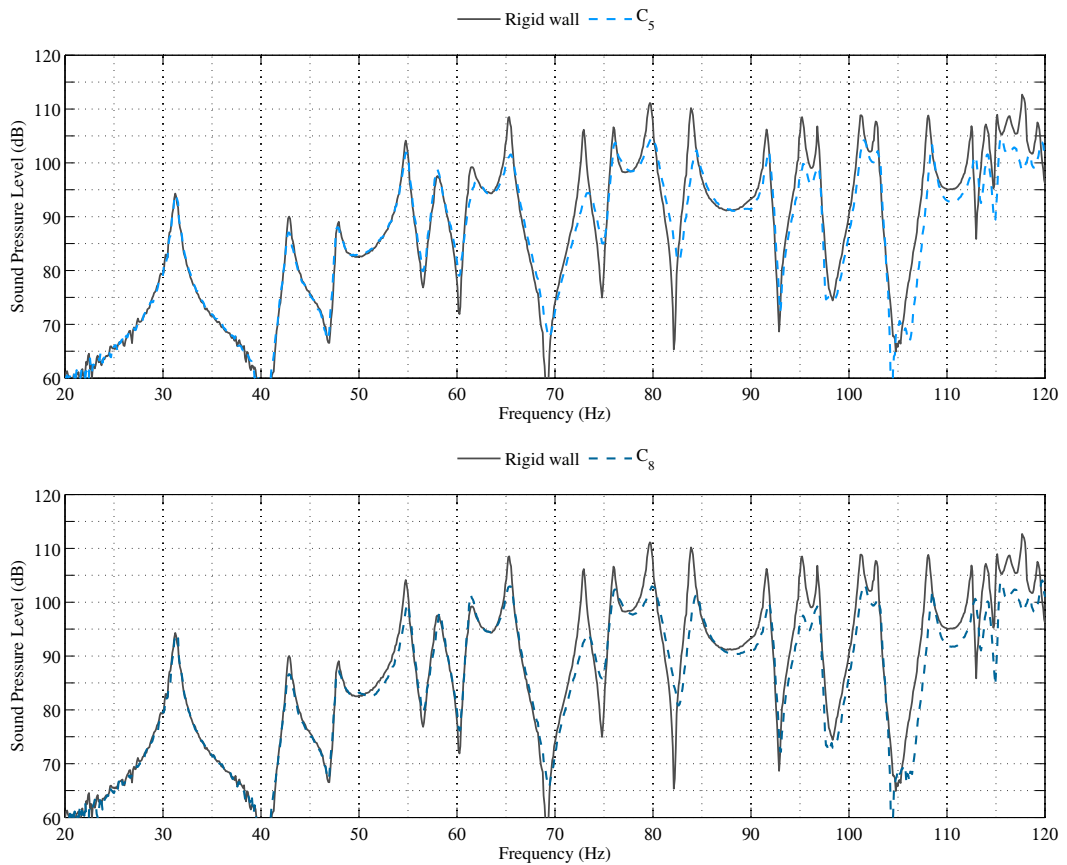


Figure 8.10: Sound pressure level measured in corner 8 with configuration C_5 and C_8 .

Chapter 8. Modal equalization of a room using electroacoustic resonators

Figure 8.10 clearly shows that a noticeable decrease of these modes: -11.7 dB at 74.4 Hz with C_5 , -12.2 dB at 74.4 Hz and -10.0 dB at 96 Hz with C_8 . Note that distributing the absorbers in the corners provide good results for a large number of modes (see Tab. 8.2). This is true in the frequency range where the electroacoustic resonators have an absorption coefficient close to 1.

Configurations C_6 and C_9 have been designed to specifically address tangential and oblique modes. These configurations are particularly effective in damping the oblique modes (1,1,1) at 80.3 Hz and (1,2,1) at 96 Hz. The gains obtained on the different modes are then between 9-13 dB. There are also significant gains for the modes above 100 Hz.

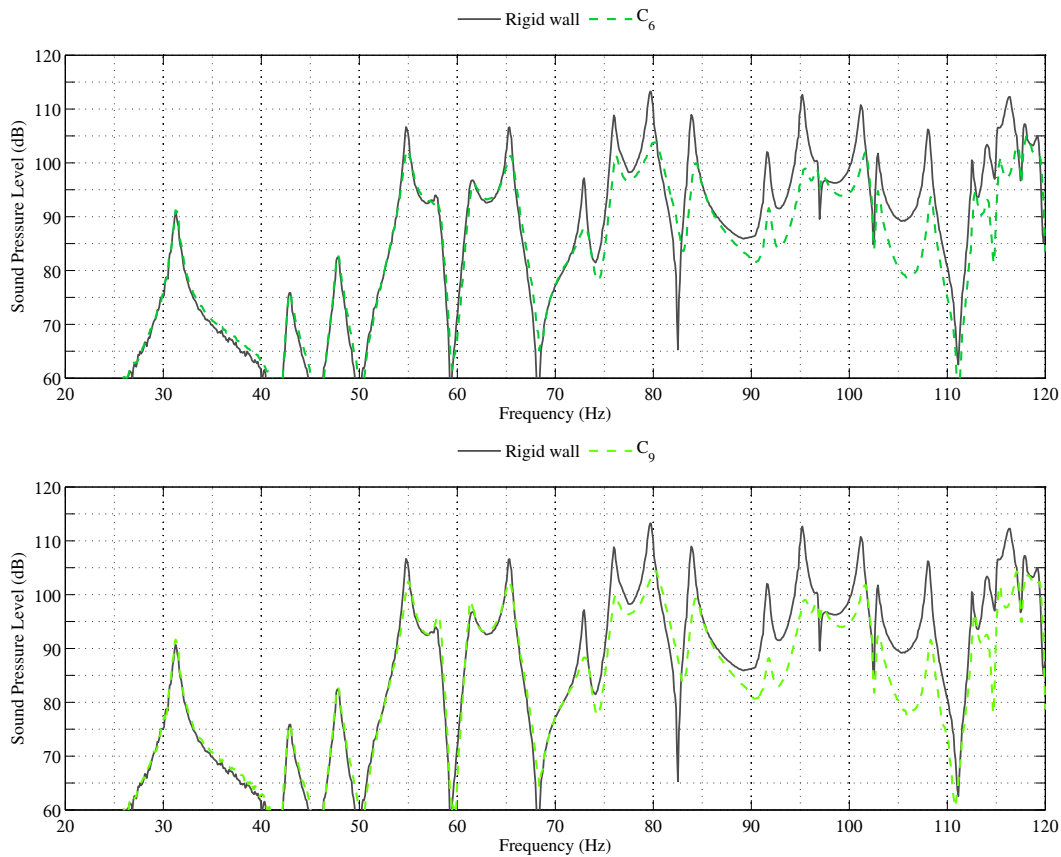


Figure 8.11: Sound pressure level measured in corner 2 with configuration C_6 and C_9 .

These measured data are indicative of the intake of acoustic impedance control in view of damping low-frequency modes of a room. It can be observed that a small treatment area is enough to significantly decrease the sound pressure level of the lowest modes of the room. As given in Tab. 5.1, the effective area of the diaphragm for each electroacoustic resonator equals 0.0495 m^2 only. Even with an absorption area of only 0.2 m^2 (compared to the total surface area 94.3 m^2 of the room), gains of over 10 dB can be measured on some modes. The gains in term of sound pressure level are obviously strongly dependent

on the placement of electroacoustic resonators in the room. The best results are obtained in distributing the electroacoustic resonators in the corners of the room. For the axial modes, however, a distribution on the corresponding edges is more appropriate. Good agreement between the structures of the modes (vibration pattern) to damp on one hand, and the frequencies affected by the corresponding placement of electroacoustic resonators on the other hand has been shown. The shift of frequency that can be observed on some modes due to presence of electroacoustic resonators can be attributed to the aforementioned effects of coupling between the room and the transducers.

8.3.3 Improved acoustic energy decay rate

When sound is generated in the room with reflecting boundaries (rigid wall), repeated reflections result in the rapid establishment of a more or less uniform sound field. The rate at which the sound energy will decay is determined by the absorptive properties of the reflective surfaces and the distance between them. This experiment is devoted to show how the acoustic energy decay can be improved by controlling the acoustic impedance at some places in the room. Table 8.3 summarizes the decay time of acoustic energy measured in the room with the various configurations of electroacoustic resonators.

Table 8.3: Summary of the measured time decay of acoustic energy per one-third octave bands for each configuration.

Configuration	One-third octave bands						Overall
	40 Hz	50 Hz	63 Hz	80 Hz	100 Hz	125 Hz	
	s	s	s	s	s	s	s
Rigid	5.5	6.3	5.3	6.0	7.5	6.5	6.0
C ₁	4.6	4.1	3.7	4.3	5.2	5.5	4.6
C ₂	4.5	4.7	3.6	4.3	5.2	5.6	5.2
C ₄	2.6	4.5	3.2	2.8	6.8	4.9	4.0
C ₅	3.7	4.2	3.4	2.8	4.1	4.1	3.8
C ₆	4.1	3.3	2.6	3.0	4.7	4.7	4.1
C ₈	3.3	4.0	2.9	2.6	3.6	3.7	3.7
C ₉	4.3	3.5	3.0	2.7	4.8	4.4	3.8

The measurement of the acoustic energy time decay is performed by applying a MLS¹ signal to a calibrated source Type 4224 Bruel and Kjaer. This signal is basically a pseudo-random sequence of pulses [120, 121]. The averaged response of the room is picked up by two outdoor microphone unit Type 4198 Bruel and Kjaer (prepolarized free-field 1/2" microphone Type 4189, the sensitivity of which is 50 mV Pa⁻¹). The measured signals are then filtered by one-third octave bands. For each configuration the measured data are averaged (8 averages of 10.2 s for a period of 1 min 22 s). The analysis of the

¹maximum length sequence

Chapter 8. Modal equalization of a room using electroacoustic resonators

decay time was performed using dBbati32 software from 01dB-Mettravib. An illustration of the experimental setup for the assessment of the acoustic energy decay is depicted in Fig. 8.5.

For illustrative purposes, Figure 8.12 describes the phenomenon of acoustic energy decay measured when the source emitting the random signal is interrupted after 20 s and Fig. 8.13 illustrates the measured decay time for the one-third octave band 80 Hz.

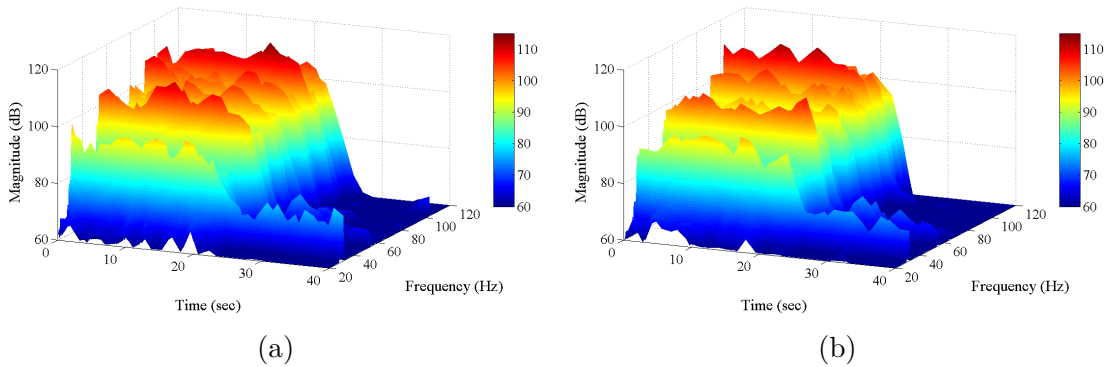


Figure 8.12: Illustration of the decay time of sound energy in the room after switching off the source. Measured data with rigid wall is shown in the top and with configuration C₉ in the bottom.

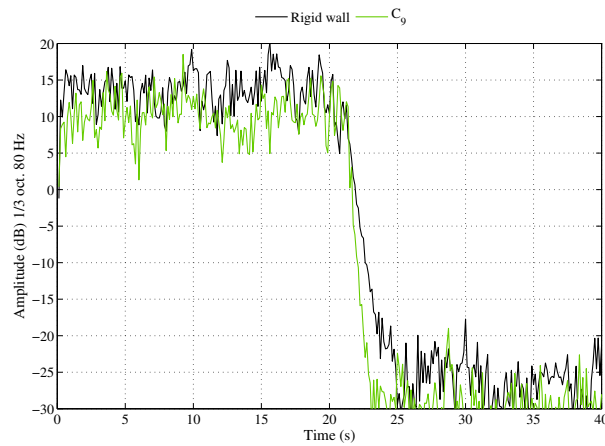


Figure 8.13: Illustration of the measured decay time of sound energy for the one-third octave band 80 Hz.

8.4 Conclusions

In this chapter we discussed a practical realization of the concept of electroacoustic resonator in a real room. It is shown that control of the acoustic impedance at certain locations in a room can change the sound field significantly, even with a small equivalent absorption area. The surface of acoustic treatment provided is 0.2 m^2 , while the total area of the room is 94.3 m^2 . Compared to rigid walls, the measured time decay of acoustic energy with electroacoustic resonators is reduced. The best results are obtained when distributing the resonators in the corners of the room. From this observations, we show that the use of electroacoustic resonators is an attractive option for rooms experiencing an excessive or inadequate decay time of acoustic energy. This experimental work has shown the benefits of the proposed methodology in an area where there is currently no competitive passive solution. The proposed study was mainly restricted to a frequency range between 50 Hz and 100 Hz. In order to address another frequency range, in the case of a larger room or smaller, the transducer should be changed but the expected results would be similar.

When used in this way, the electroacoustic resonators are not distributed so as to cover uniformly the wall or the ceiling of the room. Instead, they are single or separate objects arranged either on a wall or in free space. It should be noted that the behavior of electroacoustic resonators is satisfactory, even when arranged in panel, i.e. close to each other. When controlled by a synthetic load, the interaction of these loudspeakers is not detrimental. The risk of acoustic feedback is alleviated since there is no sensor involved. This experiment confirms the assumptions made previously about the reaction of the transducer diaphragm in the presence of a sound field. Modal equalization of a room by controlling the acoustic impedance can be viewed as a complementary method to improve the listening quality in rooms beyond what is attainable using conventional soundproofing. The question of how much the listening quality is increased through the use of semi-active modal equalization is not addressed in this thesis but could be a relevant subject through psychoacoustic evaluations.

9 Conclusions and perspectives

An interdisciplinary approach for acoustic impedance control

The thesis deals with the use of loudspeakers as sound absorbers in view of noise control applications in rooms. Creating sound absorber out of an electroacoustic transducer is the result of an interdisciplinary effort. Such a challenging task has required to combine conceptual tools, models, and applied solutions, drawing from the fields of audio engineering, control theory, and electrical engineering, both in the analog and digital domains.

An electrodynamic loudspeaker is basically a damped harmonic oscillator the resonance of which occurs in the low-frequency range. The main objective was therefore to seek ways to extend the bandwidth at resonance while targeting a desired acoustic impedance and maintaining satisfactory stability margins. Several control settings have been identified in order to match the apparent acoustic impedance of the diaphragm to the characteristic impedance of air, thus resulting in a passive or active sound absorption. By reviewing earlier works on this topic, some limitations have been noted and corrective actions have been proposed. It has been shown that phase lead/lag compensations should be considered as complementary tools to improve or further change the dynamics of loudspeakers when controlled.

Concept of electroacoustic resonator

In the footsteps of the highlights on the damped harmonic oscillator, the concept of electroacoustic resonator has been presented. Taking into account the electrodynamic coupling suggests two ways for varying the acoustic impedance at the diaphragm of a loudspeaker. The first, via an active control system, is to apply a command voltage related to sensed acoustic quantities. The second, passive or "semi-active", is to connect a well-designed electrical load across the transducer terminals. The adjustment of electrodynamic loudspeakers dynamics is facilitated by the fact they are controlled by resistances around their resonance frequency. To achieve acoustic absorption their remains

to increase the system's ability to dissipate sound energy. Various examples have shown how to modify the resonator parameters (damping, system gain and resonance) through active control or by connecting passive shunt networks. Benefits and drawbacks offered by each control strategy have been discussed and performances have been quantified in impedance tube under plane wave incidence. The shunt loudspeaker approach removes the need of sensors and is thus extremely relevant in view of a cost-effective implementation. The major drawback is a limited bandwidth around the resonance of the transducer.

A unifying concept

A unifying theory of active acoustic impedance control has been introduced, covering different strategies from passive electrical shunt to feedback control out of sensed acoustic quantities, in a single formalism. A joint approach merging the shunt based methods and the feedback control approach is discussed. This research shows that achieving a desired acoustic impedance at the transducer diaphragm is equivalent to the implementation of a functional relationship between the electrical current and voltage across the transducer terminals, and vice versa. This theoretical result highlights some interesting properties of electroacoustic resonators and bridges the conceptual gap between active acoustic absorption through feedback control and shunt loudspeaker techniques. From a design perspective, it is demonstrated that a quite simple analog network can be derived from the transducer model in order to mimic performance usually obtained using sensor and control system. However, it turns out that a very accurate model of the transducer might be required in some case, which makes difficult to implement shunt networks through analog circuitry.

An innovative methodology for the synthesis of acoustic impedance

An innovative methodology based on sensorless control of acoustic impedance has been presented. Duality between electric and acoustic admittances at both inputs of the loudspeaker is at the heart of the synthesis process. Based on the internal model of the transducer, a specific electrical load can be tailored in view of achieving a desired acoustic impedance at the diaphragm. The technological advance resulting from the coupling of a loudspeaker with a synthetic load paves the way to innovative techniques for sound control. The practical realization is proposed by means of digital filters which are processed on a real-time FPGA platform. By operating without sensor the risks of acoustic feedback are alleviated, whereas it is often the weakness of active control strategies. Although some refinement is needed, this sensorless control approach offers a promising direction for future noise control applications. This research work has resulted in the design of a novel electronic circuit allowing to achieve a prototype electroacoustic absorber which is the subject of a patent application.

Workable guidelines

The specifications of electroacoustic resonators are the result of the examination of the anticipated working conditions, technological constraints, and economic considerations. Drawing up such requirements should answer questions relative to the frequency range that the device is supposed to tackle or whether the objective is to provide sound absorption, sound transmission, or a combination of both, taking into account its technological feasibility, and its cost. This is often a difficult problem that requires the definition of performance criteria, which, in turn, depend on the anticipated use of the systems. To that purpose, workable guidelines have been provided for the development of tunable electroacoustic resonators. Not surprisingly, the choice of the transducer is essential in relation to the target acoustic impedance to achieve. In this thesis, however, results have been obtained under assumptions of small displacements (linear hypothesis). Distortion issues in case of more harsh conditions should be considered in a future work.

Applications of electroacoustic resonators

As an example of a practical realization, the control of acoustic impedance at specific boundary surfaces in a real room has been carried out using electroacoustic resonators. It has been shown that the concept of electroacoustic resonators is an efficient means for damping the low-frequency modes in a room, while decreasing the time decay of acoustic energy. Even with a small equivalent absorption area the magnitude of the first modes can be greatly reduced. The behavior of electroacoustic resonators when arranged in a panel, i.e. close to each other, is satisfactory. When controlled by a synthetic load, the interaction of these competing loudspeakers is not detrimental. The risk of acoustic feedback is reduced since there is no sensor involved.

Perspectives

The forthcoming work will mainly be directed towards improving the control bandwidth when using synthetic loads. As a future work it should be also interesting to investigate the diaphragm absorption capability as a function of the angle of incidence, and to further examine the potential of electroacoustic resonators as sound reflectors. The underlying idea is to adapt control strategies for the mid-frequency range, and investigate sound insulation capability. Besides these concluding remarks, it is believed that the technological advances resulting from the coupling of a loudspeaker with a synthetic load should pave the way to innovative techniques in noise control and, hopefully, stimulate research in related areas.

From this work, another perspective of future development should be the practical implementation of acoustic metamaterials [122], which usually require the design of negative mass density and/or bulk modulus within periodical structures, thus achievable with such active electroacoustic resonator concept.

A Solving a cubic equation using hyperbolic functions

This appendix summarizes the method, described in the papers of R.W.D. Nickalls [92] and G.C. Holmes [93], for solving a cubic equation. This technique is especially employed to derive the poles in the expression of the acoustic admittance of the electroacoustic resonator.

Let us consider a cubic polynomial of the form

$$f(x) = ax^3 + bx^2 + cx + d \tag{A.1}$$

A set of compact algebraic formulae based on hyperbolic functions can be derived for evaluating the roots of the cubic equation.

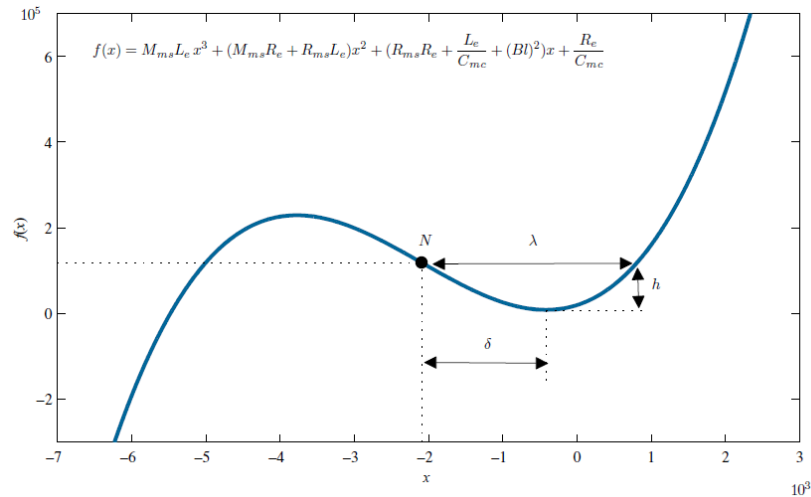


Figure A.1: Characteristic curve describing the loudspeaker as a cubic polynomial.

Appendix A. Solving a cubic equation using hyperbolic functions

Let $N(x_N, y_N)$ be the point of inflection on the curve plotted in Fig. A.1, i.e. the point on the polynomial curve $f(x)$ such that shifting the x -axis by putting $z = x - x_N$ makes the sum of the roots of the new polynomial $f(z)$ equal zero. As it can be seen in Fig. 4.7, N is the point of symmetry of the cubic such that $x_N = -b/(3a)$ and $y_N = f(x_N)$. The sideways S -shape is typical of what should be expected for the shape of a cubic function. The cubic has two turning points; it rises toward positive infinity in one direction and drops toward negative infinity in the other end.

Let the parameters δ , λ , and h be defined as the distances in Fig. A.1. By locating the turning points, it can be shown that λ and h are simple functions of δ , as

$$\delta^2 = \frac{b^2 - 3ac}{9a^2} \quad \lambda^2 = 3\delta^2 \quad h = 2a\delta^3 \quad (\text{A.2})$$

Thus, the shape of the cubic function is completely characterized by the parameter δ . Three cases have to be considered. If $\delta^2 > 0$ the cubic exhibits distinct maxima and minima, if $\delta^2 = 0$ both points are coincident, and if $\delta^2 < 0$ there are no turning points.

As illustrated in Fig. A.1, the characteristic equation of a loudspeaker is such that $\delta^2 > 0$. The curve crosses the x -axis only once, meaning that this particular cubic exhibits one real root. In addition, it reveals that $y_N/h > 1$. In that case, the roots of the original cubic polynomial can be derived using a set of compact algebraic formulae based on hyperbolic functions

$$\begin{aligned} p_1 &= x_N - 2\delta \cosh\left(\frac{1}{3} \cosh^{-1} \frac{y_N}{h}\right) \\ p_2 &= x_N + \delta \cosh\left(\frac{1}{3} \cosh^{-1} \frac{y_N}{h}\right) + i\sqrt{3} \sinh\left(\frac{1}{3} \cosh^{-1} \frac{y_N}{h}\right) \\ p_3 &= x_N + \delta \cosh\left(\frac{1}{3} \cosh^{-1} \frac{y_N}{h}\right) - i\sqrt{3} \sinh\left(\frac{1}{3} \cosh^{-1} \frac{y_N}{h}\right) \end{aligned} \quad (\text{A.3})$$

Finally, the cubic polynomial (A.1) can be rewritten more compactly as

$$f(x) = (x - p_1)(x - p_2)(x - p_3) \quad (\text{A.4})$$

B Optimization of electroacoustic absorbers by means of designed experiments



Optimization of electroacoustic absorbers by means of designed experiments

R. Boulandet*, H. Lissek

Laboratory of Electromagnetics and Acoustics (LEMA), École Polytechnique Fédérale de Lausanne (EPFL), Station 11, CH-1015 Lausanne, Switzerland

ARTICLE INFO

Article history:

Received 10 February 2010
Received in revised form 26 April 2010
Accepted 27 April 2010
Available online 9 June 2010

Keywords:

Electroacoustic absorber
Acoustic impedance matching
Optimization design
Response surface methodology
Design of experiments

ABSTRACT

In multivariate systems, when it comes to identifying actual operating conditions ranges, or optimal settings, the use of constrained optimization is often required. Among the different tools for the engineer to perform such optimization, designed experiments offer accurate performances. In this paper, the optimization process of “electroacoustic absorbers” is investigated by means of response surface methodology. A multivariate linear model is established by a series of designed experiments in order to analyze the modification of electroacoustic absorber performances due to the variation of several constitutive parameters (such as the moving mass of the loudspeaker, the enclosure volume, the filling density of mineral fiber within the enclosure, and the electrical load value to which the loudspeaker is connected), that influence their whole absorbing mechanisms. A simple case study is then provided to illustrate the capabilities of the developed optimization procedure, from which general conclusions on such design methodology, as well as on electroacoustic absorbers sensitivity, are drawn.

© 2010 Elsevier Ltd. All rights reserved.

1. Introduction

Electroacoustic absorbers are semi-active, or eventually active, devices dedicated to noise reduction in the low-frequency range. Basically, such devices consist of a loudspeaker system, including acoustic circuits and enclosures (totally or partially filled with porous material), the whole constituting a resonant system capable of absorbing sound energy within a frequency range in which conventional passive materials are not effective and/or cumbersome. When connecting a resistive load of positive value to the electrical terminals, one can significantly modify the value of the acoustic impedance that the transducer presents to the external environment, in a semi-active manner [2,3]. Thus, by selecting a suitable resistive load the acoustic impedance of the electroacoustic absorber can be tuned so as to match the characteristic impedance of air, and hence the transducer becomes then even more absorbent around its resonance frequency. When it comes to integration however, some design parameters, such as enclosure volume if overall dimensions are limited, are generally specified, which corresponds to a constraint in view of finding out the best compromise in terms of absorption capabilities versus physical embodiment of the device. For instance, in the frame of low-frequency noise control in rooms, the damping of first modal frequencies requires very bulky devices (such as bass-traps or panel absorbers), to which such optimized electroacoustic absorbers with quite low overall dimensions could represent an interesting alternative [4]. Consequently, the overall mechanisms exhibited

by an electroacoustic absorber are a combination of dissipative effects due to the mechanical losses in the loudspeaker's moving body, viscous dissipation of air induced by the penetration of sound waves in a porous medium filling the enclosure, and the dissipation in form of thermal energy induced by the circulation of electrical current within the resistive load connected to the terminals of the loudspeaker.

Although many authors have conducted research on the design of electroacoustic absorbers based on shunt electrodynamic loudspeakers [2] or electromechanical Helmholtz resonators [3], only few of them have reported the optimization study of absorbing/reflecting performances. Regarding the design of acoustic absorbers, some references addressing optimization processes may be found in the literature. In their work, Yu et al. describe an analytical solution of a resonator–enclosure interaction model to optimize the resonator resistance [5]. It is shown that the proposed model serves as an efficient design tool to determine the internal resistance of the Helmholtz resonator in order to achieve optimal sound reduction in the frequency band comprising acoustic resonances. More recently, Ruiz et al. have presented an optimization procedure based on simulated annealing which has been performed to enhance the design of micro-perforated panels, so that the absorptive capabilities of those panels can be fine-tuned to an optimal [6]. In micro-perforated panels, the absorption phenomena do not only rely on dissipative mechanisms (friction losses within micro-perforations), but also on resonant properties (coupling with a back-cavity for example). Through optimization study, an optimal setting has been achieved, and such methodology is demonstrated to allow fine-tuning of the absorbing capabilities with respect to the frequency range of interest.

* Corresponding author.

E-mail address: romain.boulandet@epfl.ch (R. Boulandet).

In general, modifying a factor (or parameter) at a time often leads to select a wrong optimum, due to potential interactions between factors which are not taken into account. To alleviate this situation, the response surface methodology (RSM) has been applied to optimize the acoustic performances of an electroacoustic absorber, since such devices are intrinsically multivariate systems. This method was first introduced by Box and Wilson [7] for developing empirical models of complex processes that could be used to locally represent a process response [7]. A review of the literature of RSM including theoretical aspects and practical applications were carried out by Hill and Hunter [8]. Basically, RSM is used for replacing an overall process by an approximate model based on a series of results collected at various discrete points within the design space. Low-order polynomial functions (second-order is often implemented) are generally employed as they can efficiently model low-order processes, since the processing of the corresponding response surface is fast and cheap. The most extensive applications of RSM can be found in the realm of industrial engineering, particularly in situations where numerous explanatory variables can potentially influence a performance measure, or quality characteristic, of products or processes. The efficiency of the RSM as an advantageous optimization method is documented in many fields and a number of improvements of the method is presented in the literature [7–11].

2. Electroacoustic absorbers

2.1. General presentation

An electroacoustic absorber is an electroacoustic loudspeaker system, including enclosure and acoustic circuit, the acoustic impedance of which can be varied by various electrical means, be it passive or active. In the specific case of the electrodynamic moving-coil loudspeaker given in Fig. 1, the lumped elements model of such devices includes a moving mass M_{ms} , a mechanical compliance C_{ms} , a mechanical resistance R_{ms} , as well as coupling factors (force factor Bl , and radiating surface S). The above-mentioned elements also account for the mechanical counterparts of the acoustic radiation impedances (for instance $C_{ab} = V_b/\rho c^2$ the acoustic compliance of the enclosure of volume V_b , where ρ is the density of air and c the celerity of sound in air, or the acoustic radiation mass and resistance). At last, the electrical conditioning of the loudspeaker electrical terminals is also accounted as equivalent mechanical elements, including the d.c. resistance and self inductance of the coil R_e and L_e , but also any electric load that shunts the loudspeaker electrical terminals [12]. If the electric load is a simple resistor R_s (passive shunt), it has been proven that such device can generally be characterized in terms of equivalent normalized admittance, the expression of which is of the form [1]:

$$Y = Z_{mc} \frac{1}{R_{ms} + \frac{Bl^2}{R_e + R_s} + j\omega M_{ms} + \frac{1}{j\omega C_{ms}}} \quad (1)$$

where $Z_{mc} = SZ_c$ is the equivalent mechanical impedance of characteristic impedance of air, namely $Z_c = \rho c$. For electroacoustic absorbers, the targeted objective functions is usually a global measure of sound energy absorption, namely the acoustic absorption coefficient α :

$$\alpha = 1 - \left| \frac{1 - Y}{1 + Y} \right|^2 \quad (2)$$

To provide a complete absorption, the coefficient must equal 1. If it is not, the performances of the absorber can be increased through optimization design, which is one of the main motivation of this paper.

2.2. Acoustic performance assessment

Measurement of sound absorption coefficient under normal incidence of actual electroacoustic absorbers can be performed in an impedance tube configuration, after ISO 10534-2 standard, using the two-microphone transfer function method [13]. The corresponding one-dimensional experimental setup is described in Fig. 2. Using this setup, the acoustic absorption coefficient is derived from the assessment of sound pressure at two different positions in an impedance tube, one extremity of which is closed with the electroacoustic absorber. The formulation of the absorption coefficient is given below:

$$\alpha = 1 - |r|^2 \quad (3)$$

where r is the reflection coefficient, processed after:

$$r = \frac{H_{12} - H_I}{H_R - H_{12}} \exp(2jkx_1) \quad (4)$$

The term $H_{12} = p_1/p_2$ is the transfer function between the two sound pressure p_1 and p_2 sensed at positions 1 and 2 (see Fig. 2), $H_I = \exp(-jk(x_1 - x_2))$ and $H_R = \exp(jk(x_1 - x_2))$ are the transfer functions corresponding to the incident p_i and reflected p_r sound waves respectively, x_1 being the position of the most distant microphone from the absorber under study and k the wave number. Alternatively, the resulting acoustic performances of electroacoustic absorbers can be assessed in the context of actual rooms, especially in the low-frequency range, and more precisely below the Schroeder frequency. In a recent publication [4] dealing with modal control in rooms, 10 electroacoustic absorbers distributed in a line array configuration and placed at several positions in a reverberant chamber, each single absorber being primarily tuned in an impedance tube, have been assessed and demonstrated to be equally effective for damping several modes at a time in the room, the damping capabilities being more effective within the band (20–40 Hz). In the following, we will then focus on optimizing and assessing single electroacoustic absorbers in a one-dimensional configuration, assuming those performances can be easily extrapolated to practical 3D configurations.

3. Response surface methodology

The methodology of response surface (RSM) is an experimental strategy for exploring the space of a process involving a number of explanatory variables by using empirical statistical models. Using

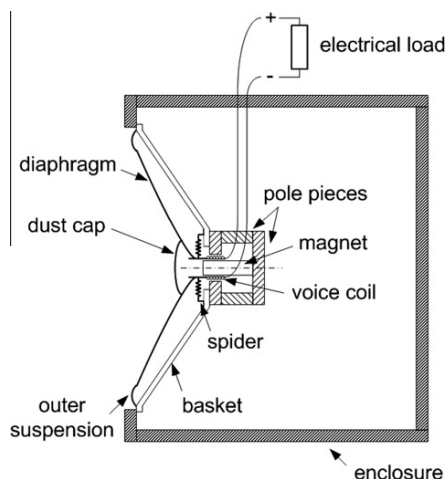


Fig. 1. Schematic of electroacoustic absorber.

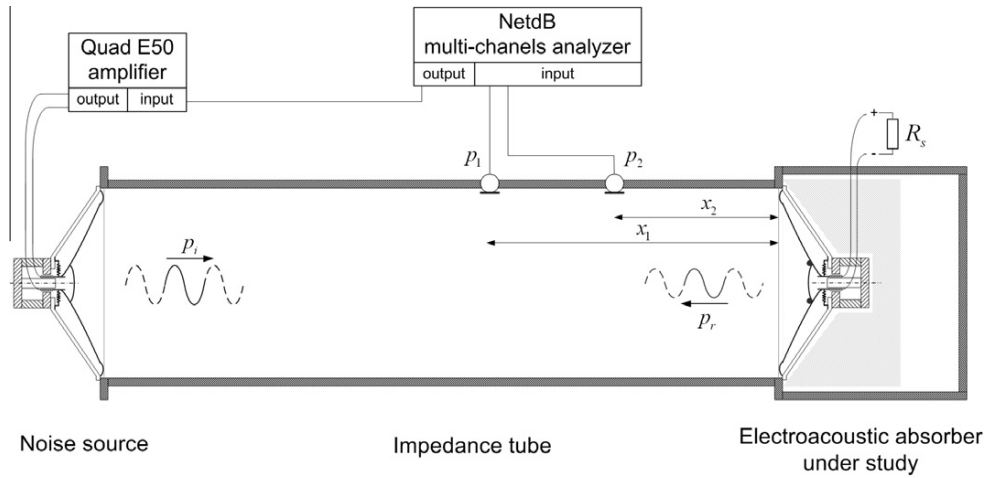


Fig. 2. Experimental setup for the assessment of electroacoustic absorber's absorption coefficient under normal incidence.

this approach, a complex process is replaced by an approximate model based on experimental data evenly collected within the space of the process by varying simultaneously some influential parameters in a structured way. It also includes an optimization method for finding the levels of the controllable input variables that produce desirable values of the response.

3.1. Objective function estimation

The RSM strategy aims at developing an appropriate approximated relationship between obtained responses and explanatory variables. To establish this matching, polynomial functions of second-order are frequently used. The general form of response surface models of second-order with interactions that describes the relationship between the response variable of interest y and m independent explanatory variables may be written as:

$$y = b_0 + \sum_{i=1}^m b_i x_i + \sum_{i=1, j>i}^m b_{ij} x_i x_j + \sum_{i=1}^m b_{ii} x_i^2 + \varepsilon \tag{5}$$

where y approximates the objective function, x_i and x_j are the independent explanatory variables, b_i and b_{ij} represent the polynomial coefficients to identify, and ε the error associated to y , that represents other not accounted sources of variability which are assumed to be normally distributed. Starting from the general form of Eq. (5), the polynomial function restricted to four explanatory variables can be expressed as follows:

$$y = b_0 + b_1 x_1 + b_2 x_2 + b_3 x_3 + b_4 x_4 + b_{12} x_1 x_2 + b_{13} x_1 x_3 + b_{14} x_1 x_4 + b_{23} x_2 x_3 + b_{24} x_2 x_4 + b_{34} x_3 x_4 + b_{11} x_1^2 + b_{22} x_2^2 + b_{33} x_3^2 + b_{44} x_4^2 + \varepsilon \tag{6}$$

For n observations, the model of Eq. (6) may be written in matrix form as:

$$\mathbf{y} = \mathbf{X}\beta + \varepsilon \tag{7}$$

where \mathbf{y} is an $n \times 1$ vector of the observations, \mathbf{X} is an $n \times p$ design matrix, β is a $p \times 1$ vector of the regression coefficients or effects, and ε is a $n \times 1$ vector of random error or noise. The method of least mean squares is commonly used to estimate the unknown regression coefficients in a multiple regression analysis. At last the unknown β terms can be obtained from the formula:

$$\beta = (\mathbf{X}'\mathbf{X})^{-1} \mathbf{X}'\mathbf{y} \tag{8}$$

The β vector is composed with the unknown parameters set which can be estimated by collecting experimental data. The collected data can either be derived from actual physical experiments or from numerical models of the same experiments. When the β terms are substituted into the second-order response surface model given in Eq. (6), the approximating polynomial function can be predicted at any explanatory variable x_i . Once a response surface model is obtained, statistical analysis techniques are usually processed to check the fitness of the mathematical model, and then a canonical analysis can be performed to investigate the shape of the predicted response surface.

3.2. Decomposition of variance

The key to determining the overall utility of the regression equation lies in assessing its ability to account for the variance observed in the response variable. The objective of variance analysis is to estimate to what extent the whole model and its individual parameters contribute to an understanding of the response variable under study. In other words, this test procedure aims at describing if changes in the response are caused by changes in the action between different levels, or by random fluctuations due to the dispersion of responses. The required theory of variance analysis is listed in Table 1.

In this table, the total sum of squares SS_T measures the overall fluctuations of the individual observations of the dependant variables around their average. The regression sum of squares SS_R is the sum of the squared differences between the values of the dependent variable predicted by the regression line \hat{y}_i and those predicted by the mean \bar{y} . The residual sum of squares SS_E represents the sum of the squared differences between the observed values y_i of the response and the ones predicted by the regression \hat{y}_i . To estimate whether certain actions of the model are significant or not, we use the experimental and critical tabulated values of Fisher F -test. Referring to probability statistics, $F = MS_R/MS_E$ is the ratio of the explained variability and the unexplained variability, each divided by the corresponding degrees of freedom [14,15]. The larger the F -test, the more useful the model. When the level of significance σ is specified, the critical value $F_{p,n-p-1,\sigma}$ that satisfies the probability:

$$P\{F > F_{p,n-p-1,\sigma}\} = \sigma \tag{9}$$

can be looked up from F -distribution tables. If $F > F_{p,n-p-1,\sigma}$, then the second-degree polynomial can be considered as a reliable model at

Table 1
Variance analysis table.

	Sum of squares	Degree of freedom	Mean squares	F-test	p-value
Regression	$SS_R = \sum(\hat{y}_i - \bar{y})^2$	p	$MS_R = SS_R/p$	$F = \frac{MS_R}{MS_E}$	$F > F_{p,n-p-1,\sigma}$
Error	$SS_E = \sum(y_i - \hat{y}_i)^2$	$n - p - 1$	$MS_E = SS_E/(n - p - 1)$		
Total	$SS_T = \sum(y_i - \bar{y})^2$	$n - 1$			

Table 2
Loudspeaker Visaton AL-170 technical data.

Nominal impedance	8 Ω
Resonance frequency	38 Hz
Moving mass M_{ms}	13 g
d.c. resistance R_e	5.6 Ω
Inductance of voice coil L_e	0.9 mH
Force factor Bl	6.9 Tm
Effective piston area S	133 cm ²
Equivalent volume V_{as}	34 l
Mechanical Q factor Q_{ms}	3.88
Electrical Q factor Q_{es}	0.43
Total Q factor Q_{ts}	0.39

σ level. This test procedure is therefore a mean to improve the regression equation.

3.3. Canonical analysis

The main reason for performing a canonical analysis is to gain insight into the nature of the response surface, i.e. if the response is a maximum, a minimum, or a saddle point. Moreover, the effects of input variables combinations which have not been carried out in the designed experiments can still be considered [10]. The quadratic fitted model which relates independent explanatory variables $\mathbf{x} = (x_1, x_2, \dots, x_m)$ to a response variable y (see Eq. (6)) can also be expressed in matrix notation as:

$$\hat{y} = b_0 + \mathbf{x}\mathbf{b} + \mathbf{x}'\hat{\mathbf{B}}\mathbf{x} \quad (10)$$

where b_0 , \mathbf{b} , and $\hat{\mathbf{B}}$ are the estimates of the constant, linear, and second-order coefficients, respectively.

$$\hat{\mathbf{B}} = \frac{1}{2} \begin{pmatrix} 2b_{11} & b_{12} & \dots & b_{1m} \\ b_{12} & 2b_{22} & \dots & \dots \\ \dots & \dots & 2b_{33} & \dots \\ b_{1m} & \dots & \dots & 2b_{mm} \end{pmatrix} \quad (11)$$

$$\mathbf{b} = \begin{pmatrix} b_1 \\ b_2 \\ \dots \\ b_m \end{pmatrix} \quad (12)$$

$$\mathbf{x} = (x_1 \ x_2 \ \dots \ x_m) \quad (13)$$

To find the best estimates for the parameters $\hat{\mathbf{B}}$, \mathbf{b} , and b_0 , statistically designed experiments are employed. Once a model has been estimated for a particular space of a process, the direction of maximum gradient is found by normalizing the factors and differentiating on \mathbf{x} .

$$\frac{\partial \hat{y}}{\partial \mathbf{x}} = \mathbf{b} + 2\hat{\mathbf{B}}\mathbf{x} \quad (14)$$

Setting the second term of Eq. (14) to 0 yields the location of the stationary point \mathbf{x}_s and the predicted response \mathbf{y}_s [10]:

$$\mathbf{x}_s = -\frac{1}{2}\hat{\mathbf{B}}^{-1}\mathbf{b} \quad (15)$$

$$\mathbf{y}_s = b_0 + \frac{1}{2}\mathbf{x}'_s\mathbf{b} \quad (16)$$

The nature of the stationary point is determined with the signs of the eigenvalues of matrix $\hat{\mathbf{B}}$, and the relative magnitude of eigenvalues are also helpful in the total interpretation of the response system. At last, the canonical equation for the response surface is expressed as:

$$\hat{y} = \mathbf{y}_s + \sum_{i=1}^f \lambda_i w_i^2 \quad (17)$$

where λ_i is the eigenvalue of matrix $\hat{\mathbf{B}}$ associated to the explanatory variable x_i , and w_i are called the canonical variables.

4. Designed experiments of electroacoustic absorbers

4.1. Design factors and variation ranges

The design factors are the explanatory variables over which the experiments can be actually controlled. In the frame of this study the selected factors are some constitutive parameters of an electroacoustic absorber which reflect some dissipative mechanisms of sound energy, and are also controllable. The corresponding variables are given in Fig. 3. The variation ranges are the physical constraints of each factors, or the limitations imposed by the experimental setup, that define and limit the space of the process.

The selected design factors, whose subscripts from Eq. (1) are removed for ease of writing, are listed hereafter:

- The moving mass M of the moving-coil loudspeaker.
- The enclosure volume V of the closed-box.
- The filling density of mineral fiber τ .
- The electrical load value R to which the loudspeaker is connected.

As presented earlier, the sound absorption coefficient α which is measured in one-third octave bands is used as response variable depending on the frequency.

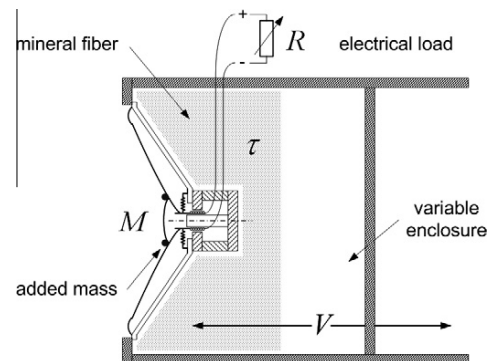


Fig. 3. Schematic of electroacoustic absorber including design factors.

To improve the understanding of the phenomenon by allowing heterogeneous comparison of quantities, it is convenient to transform natural variables into coded variables. Natural variables are expressed in physical units of measurement, whereas coded variables are dimensionless, have zero mean and the same standard deviation. The applied transformations are given hereafter:

$$\begin{aligned} x_1 &= \frac{M - \bar{M}}{\Delta M}; & x_2 &= \frac{V - \bar{V}}{\Delta V} \\ x_3 &= \frac{\tau - \bar{\tau}}{\Delta \tau}; & x_4 &= \frac{\log R - \log \bar{R}}{\log \Delta R} \end{aligned} \quad (18)$$

where for the case of design factor M , $\bar{M} = (M_{min} + M_{max})/2$ and $\Delta M = (M_{max} - M_{min})/4$, the same applying for the other design factors V, τ , and R . As it can be seen in Eq. (18), a logarithmic transformation has been chosen to take account of the large range that relates to the electrical load factor. Using this transformation, physical values of design factors are transformed into coded values $-2, -1, 0, 1, 2$. Table 3 shows the corresponding values between both natural and coded levels.

In order to practically increase the moving mass of the loudspeaker, a certain quantity of sinkers has been stuck to the diaphragm, as illustrated in Fig. 4. Moreover, in order to allow variation of the enclosure volume, a specific cabinet has been designed which was filled with a variable quantity of mineral fiber according the specifications of the designed experiments (see Fig. 4).

Table 3
Coded and natural levels of design factors.

Coded levels	-2	-1	0	1	2
Natural levels					
Moving mass (10^{-3} kg)	13	17	21	25	29
Enclosure volume (10^{-3} m ³)	4	12	20	28	36
Filling density (%)	0	25	50	75	100
Electrical load (Ω)	0.1	1	10	100	1000

4.2. Designed experiments for fitting response surfaces

In statistics, factorial experiments are a class of designed experiments for which the explanatory variables are varied simultaneously, but in a structured way. Such a design consists of two or more factors, each with discrete possible values or levels. The experiments can take all possible combinations of the levels of each factor. However, two-levels factorial designs are insufficient to fit a second-order model. Indeed, with two-levels factorial designs, each factor is only investigated at an upper and a lower level, which bounds the space of the process. Such a design requires the assumption of no curvature within the design space, whereas to describe an extremum, one must estimate quadratic curvature requiring at least three levels for each factor. In order to attain the optimum response, three-levels factorial designs were developed by Box and Behnken [9]. As this study focuses on fitting the second-order model given in Eq. (6) which contains $p = 15$ parameters to be estimated, at least 15 different combinations of design factors must be estimated. However, such designs with m input variables involve a great number of runs $n = 3^m$ compared to the p coefficients to be determined.

To alleviate this situation, central composite designs (CCD) have been developed. This class of experimental designs involves the use of a two-levels factorial, one combined with a $2m$ axial or star points and n_0 center runs [10]. Center runs clearly provide information about the existence of curvature in the system or process under study. As the former are often replicated this can also estimate experimental error. If curvature is found, the addition of axial points allows for estimation of the pure quadratic terms. The value of the axial distance generally varies from 1 to \sqrt{m} which guarantees that the CCD is effective from a variance point of view. The number of runs to be made in both orthogonal or rotatable CCD are thus $n = 2^m + 2m + n_0$, sensibly lower than tree-levels factorial designs. For these reasons, CCD are popular for fitting a second-order surface in experimental optimization processes. In Table 4, the conducted central composite design is illustrated with coded vari-



Fig. 4. Overview of the experimental setup.

Table 4
Central composite design in coded variables.

Run #	Design matrix			
	x_1	x_2	x_3	x_4
<i>Full factorial design</i>				
4	-1	-1	-1	-1
20	-1	-1	-1	1
12	-1	-1	1	-1
6	-1	-1	1	1
8	-1	1	-1	-1
17	-1	1	-1	1
25	-1	1	1	-1
10	-1	1	1	1
13	1	-1	-1	-1
21	1	-1	-1	1
11	1	-1	1	-1
5	1	-1	1	1
18	1	1	-1	-1
19	1	1	-1	1
26	1	1	1	-1
9	1	1	1	1
<i>Axial points</i>				
2	-2	0	0	0
23	2	0	0	0
30	0	-2	0	0
29	0	2	0	0
3	0	0	-2	0
15	0	0	2	0
24	0	0	0	-2
28	0	0	0	2
<i>Center runs</i>				
1	0	0	0	0
7	0	0	0	0
14	0	0	0	0
16	0	0	0	0
22	0	0	0	0
27	0	0	0	0

ables. The description on curve fitting by multiple linear regression, the corresponding analysis of variance and the way for finding the optimum response can be found in Refs. [10,16].

5. Results and discussion

5.1. Measured responses

Figs. 5–8 illustrate the curves of the one-third octave bands absorption coefficients which were measured randomly during the experiment. Coming back to our problem about low-frequency noise control in rooms, some specifications have to be drawn for the electroacoustic absorber in terms of sound absorption performances. In view of damping the first modes in the control room of a recording studio, which dimension are 3.40 m × 2.10 m × 2.15 m the electroacoustic absorber is primarily intended to dissipate sound energy around 50 Hz. Therefore, the following analysis will be focused on the normal 50 Hz one-third octave band. Table 5 summarizes both measured and estimated responses (namely the acoustic absorption coefficient) for the one-third octave band 50 Hz. The physical levels of the natural variables are detailed for each of the $n=30$ experimental runs carried out randomly.

5.2. Analysis of variance

Starting from the experimental results shown in Table 5, an analysis of the variance is performed to investigate the validity of the regression model. Table 6 illustrates the result of the ANOVA which was carried out for a level of significance of 5%, i.e., for a 95% level of confidence. The last column of the table shows the

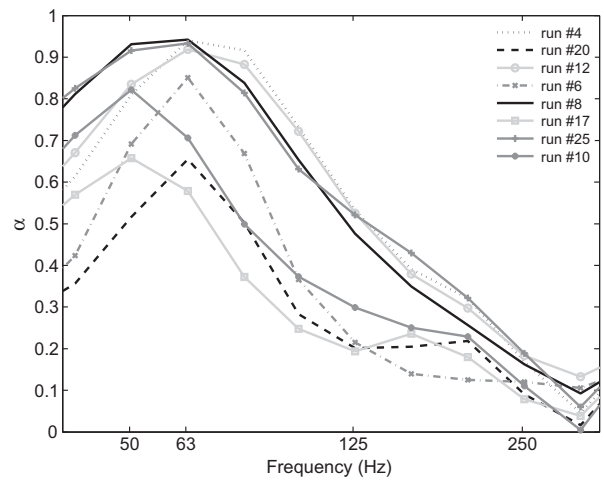


Fig. 5. Measured absorption coefficients of the factorial design.

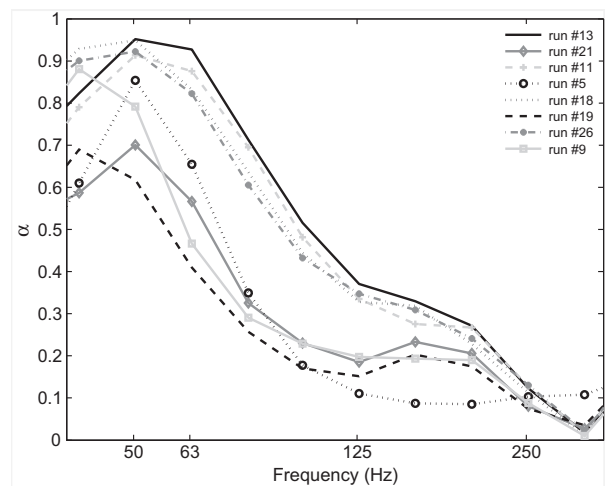


Fig. 6. Measured absorption coefficients of the factorial design.

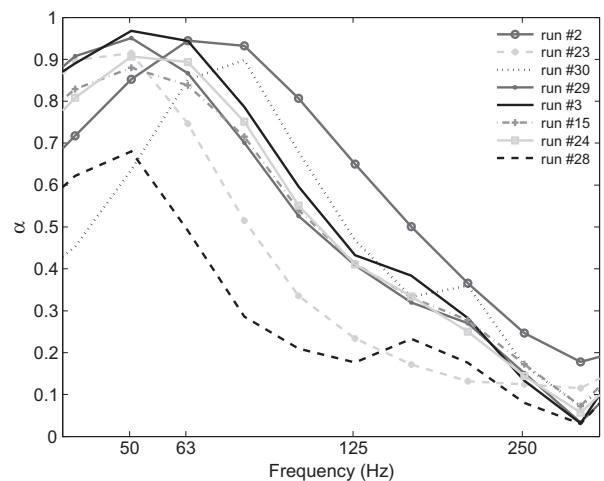


Fig. 7. Measured absorption coefficients at axial points of design space.

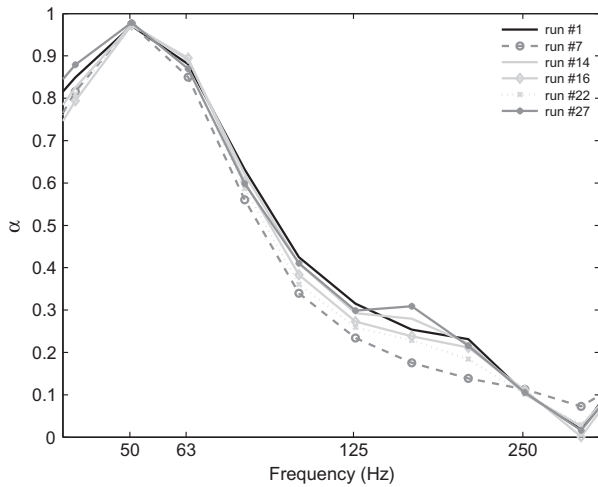


Fig. 8. Measured absorption coefficients at the center of design space.

Table 5
Measured and estimated responses.

Run #	Experimental design			Responses		
	M (10^{-3} kg)	V (10^{-3} m ³)	τ (%)	R (Ω)	y	\hat{y}
4	17	12	25	1	0.81	0.84
20	17	12	25	100	0.52	0.58
12	17	12	75	1	0.83	0.78
6	17	12	75	100	0.69	0.70
8	17	28	25	1	0.93	0.99
17	17	28	25	100	0.66	0.74
25	17	28	75	1	0.92	0.94
10	17	28	75	100	0.82	0.86
13	25	12	25	1	0.95	0.97
21	25	12	25	100	0.70	0.71
11	25	12	75	1	0.91	0.91
5	25	12	75	100	0.85	0.81
18	25	28	25	1	0.95	0.97
19	25	28	25	100	0.62	0.72
26	25	28	75	1	0.92	0.92
9	25	28	75	100	0.79	0.84
2	13	20	50	10	0.85	0.87
23	29	20	50	10	0.92	0.98
30	21	4	50	10	0.64	0.66
29	21	36	50	10	0.95	0.82
3	21	20	0	10	0.97	0.89
15	21	20	100	10	0.88	0.96
24	21	20	50	0.1	0.91	0.91
28	21	20	50	1000	0.68	0.57
1	21	20	50	10	0.97	0.93
7	21	20	50	10	0.97	0.93
14	21	20	50	10	0.97	0.93
16	21	20	50	10	0.97	0.93
22	21	20	50	10	0.98	0.93
27	21	20	50	10	0.98	0.93

Table 6
Variance analysis and evaluation of the regression model.

	SS	df	MS	F-test	p-value
<i>Second-order</i>					
Regression	22.12	15	1.5	370	<0.001
Error	0.06	14	0.004		
Total	22.18	29			

Table 7
ANOVA table for each individual effects.

Source	SS	df	MS	F-test	p-value
<i>Main effects</i>					
M	0.018	1	0.018	4.41	0.053
V	0.039	1	0.039	9.82	0.007
τ	0.007	1	0.070	1.75	0.205
R	0.172	1	0.172	43.02	<0.001
<i>Interaction effects</i>					
$M \times V$	0.023	1	0.023	5.83	0.029
$M \times \tau$	0.001	1	0.001	0.13	0.727
$M \times R$	<0.001	1	<0.001	0.01	0.907
$V \times \tau$	<0.001	1	<0.001	0.01	0.969
$V \times R$	0.001	1	0.001	0.01	0.727
$\tau \times R$	0.032	1	0.032	7.89	0.013
<i>Quadratic effects</i>					
$M \times M$	0.007	1	0.007	1.82	0.197
$V \times V$	0.053	1	0.053	13.30	0.002
$\tau \times \tau$	0.004	1	0.004	1.05	0.322
$R \times R$	0.075	1	0.075	18.71	0.001
Error	0.060	14	0.004		
Total	22.183	29			

contribution (p -value) of the second-order regression model on the total variation.

From the analysis of Table 6, it is obvious that the F -test of ANOVA is greater than the critical value. Indeed, by using F -distribution tables we obtain $F_{(15, 14, 0.05)} = 2.46$, $F = 370 > F_{(15, 14, 0.05)}$ for the second-order regression model. The polynomial representing absorption coefficient is therefore relevant for the corresponding problem. It can be used to analyze the relationship between the objective performance function and the selected constitutive parameters (M , V , τ , and R) of the electroacoustic absorber. The remaining step consists now in investigating the significance of each factorial effect within the global regression model.

Table 7 summarizes the result of the test for significance using ANOVA with a level of significance of 5% for each individual regressor coefficients of the model.

From the analysis of Table 7, the F -test of some effects appears to be lower than $F_{(1, 14, 0.05)} = 4.60$. We conclude that the quadratic terms $M \times M$ and $\tau \times \tau$, and interaction terms $M \times \tau$, $M \times R$, $V \times \tau$, and $V \times R$ have statistically insignificant effect. It can be also noted that, within the frequency range of interest, namely the 50 Hz one-third octave band, the most important effects are influenced by the electrical load value and the enclosure volume. This complementary ANOVA indicates that some terms of Eq. (6) might be removed to get a better model. By removing statistically nonsignificant effects from the second-order model, we obtain a reduced model (Eq. (19)) whose ANOVA is given in Table 8.

$$y = b_0 + b_1x_1 + b_2x_2 + b_3x_3 + b_4x_4 + b_{12}x_1x_2 + b_{34}x_3x_4 + b_{22}x_2^2 + b_{44}x_4^2 \quad (19)$$

From the analysis of Table 8, it is apparent that the F -test of ANOVA $F = 540$ is greater than the critical value $F_{(9, 20, 0.05)} = 2.39$. Therefore, we conclude that the reduced regression model is relevant and can be used in the following.

Table 8
Variance analysis of reduced regression model.

	SS	df	MS	F-test	p-value
<i>Second-order</i>					
Regression	22.12	9	2.46	540	<0.001
Error	0.092	20	0.0046		
Total	22.18	29			

5.3. Fitted second-order response function

The coefficients of the reduced model are estimated by the least mean squares method, as detailed in Section 3. The fitted second-order response function which is obtained after regression is given in coded variables by:

$$\hat{y} = 0.924 + 0.027x_1 + 0.040x_2 + 0.017x_3 - 0.085x_4 - 0.038x_1x_2 + 0.044x_3x_4 - 0.046x_2^2 - 0.046x_4^2 \quad (20)$$

In natural variables Eq. (20) becomes:

$$\hat{\alpha} = -0.011 + 30.5M + 58.7V - 0.11\tau - 0.08 \log(R) - 1187.5MV + 0.18\tau \log(R) - 718.8V^2 - 0.05 \log(R)^2 \quad (21)$$

A similar approach can be envisaged by considering values measured in other range of frequency. The resulting models would be simply different from those obtained in Eqs. (20) and (21).

5.4. Canonical analysis

After the polynomial has been verified, the RSM is processed in *Matlab*[®]. From Eq. (15), the stationary point is observed at $\mathbf{x}_s = (-0.65, 0.71, 1.12, -0.38)$, and the predicted value is $y_s = 0.96$ according to Eq. (16). It can be noted that the distance between \mathbf{x}_s and the center of the design space is lower than the radius of the design space, meaning that the stationary point is included within the experimental domain of investigations. If the point was located outside the region of the experiment, it would not be advisable to use it for defining operating conditions because the fitted model is only reliable inside the design space.

The computed eigenvalues of matrix \mathbf{B} are $\lambda_1 = -0.055$, $\lambda_2 = -0.053$, $\lambda_3 = 0.007$, and $\lambda_4 = 0.009$. The canonical form is therefore given by:

$$\hat{y} = 0.96 - 0.055w_1^2 - 0.053w_2^2 + 0.007w_3^2 + 0.009w_4^2 \quad (22)$$

As the eigenvalues are mixed in sign, the stationary point \mathbf{x}_s is a saddle point. Eq. (22) represents a minimax surface where a decrease in yield is predicted when one moves away from the center of the system in either the positive or negative directions of w_1 and w_2 , and correspondingly an increase in yield is predicted in either the positive or negative directions of w_3 and w_4 . In Eq. (22) it can be observed that all eigenvalues are not of the same order of magnitude. This means that the same displacement in each of the main directions do not cause a comparable variation of the response. Canonical analysis through eigenvalues of matrix \mathbf{B} yields to the main directions which tend to increase (or decrease) the response faster, and to what extent. Response surfaces and the contour plots can then be employed in order to find optimum conditions and to determine more precisely how sensitive the estimated response is for any displacement away from the stationary point.

5.5. Estimation of optimum configurations through response surfaces and contour plots

It is often necessary for practical reason to use constrained optimization to identify potential operating conditions. This is particularly true when the stationary point is a saddle point. The response surface and contour plots provide then one of the most revealing ways of illustrating and interpreting the responses surfaces system. Such graphical displays derived from the polynomial model of process under study, after fixing some factors so as to estimate the response while other factors are free to vary. For ease of graphical representation, only two factors are free to vary while the two other ones are held constant. The following sections illustrate

various configurations obtained from Eq. (21) in order to estimate the levels of factors which yield an optimum.

5.5.1. Moving mass vs. enclosure volume

The response surfaces and contour plots in Figs. 9 and 10 show the effect of the moving mass M and enclosure volume V on the sound absorption coefficient under the condition that the filling density of mineral fiber τ and electrical load value R are held constant. When the enclosure is partially filled with mineral fiber materials ($\tau = 75\%$), and when an electrical load $R = 1 \Omega$ is connected to the electric terminals of the loudspeaker, two areas of optimum conditions can be identified. Indeed, the figures show that a full absorption may be expected for the natural levels ($M \approx 13 \times 10^{-3} \text{ kg}$ and $V \approx 28 \times 10^{-3} \text{ m}^3$), as well as for ($M > 25 \times 10^{-3} \text{ kg}$ and $V \approx 20 \times 10^{-3} \text{ m}^3$). When the volume of the enclosure is left empty ($\tau = 0\%$) and the electroacoustic absorber

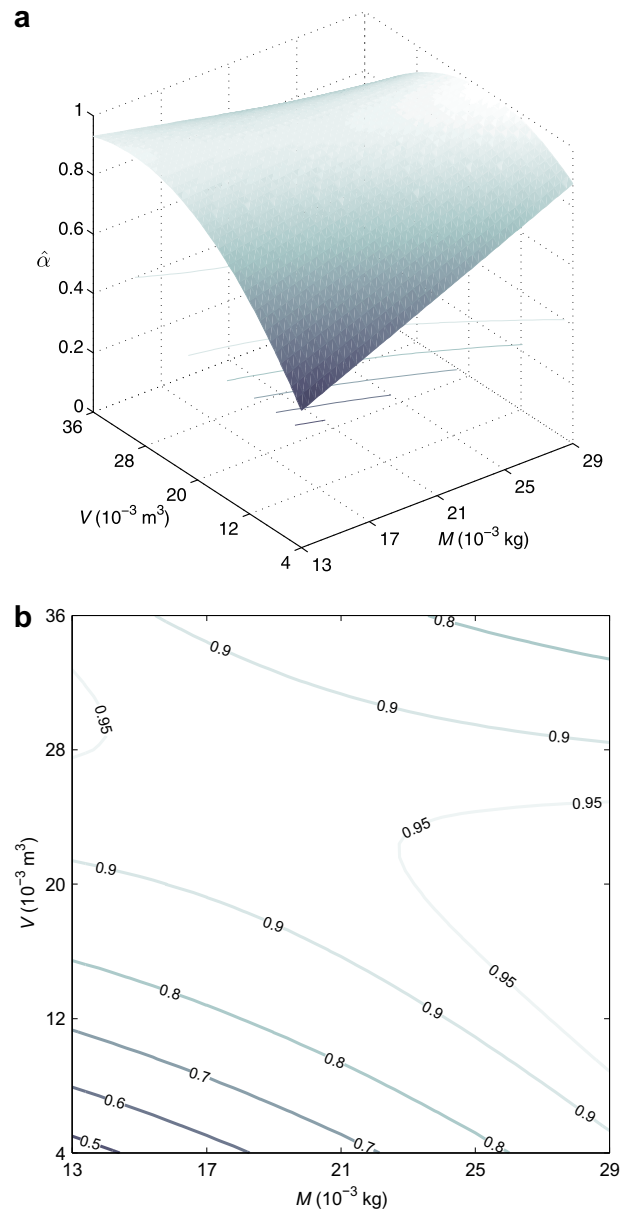


Fig. 9. Moving mass vs. volume, $\tau = 75\%$ and $R = 1 \Omega$.

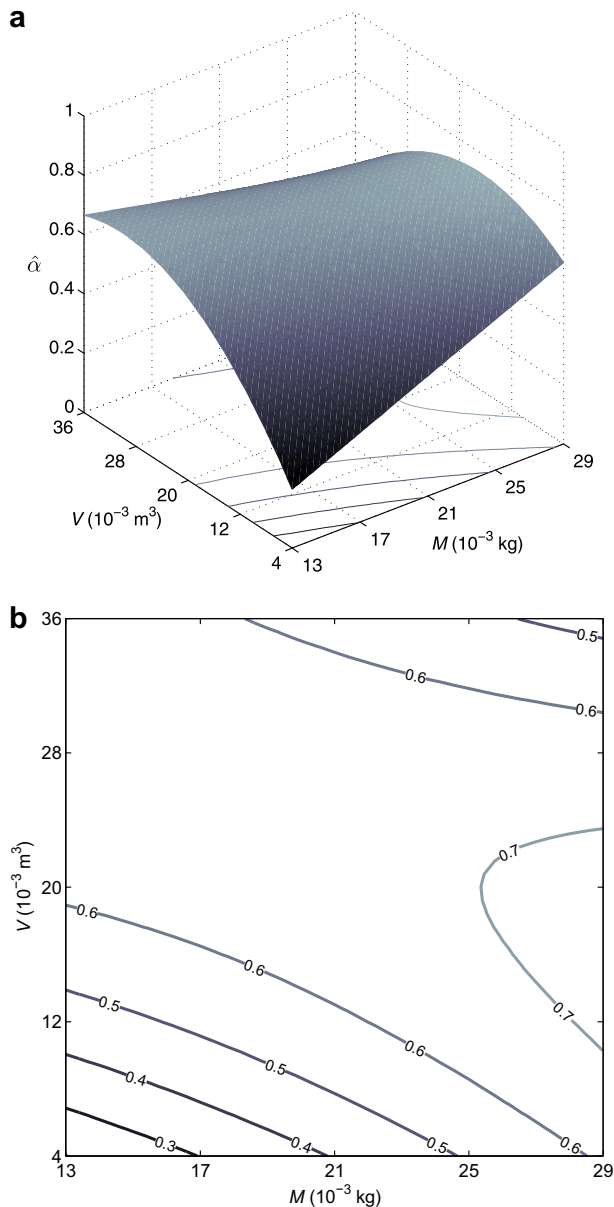


Fig. 10. Moving mass vs. volume, $\tau = 0\%$ and $R = 100 \Omega$.

is shunted with a high electrical load value ($R = 100 \Omega$), one can observe that the optimum conditions are drastically different. With such adjustment, it is not expected to have good absorbent properties, anywhere in the design space (see Fig. 10).

5.5.2. Moving mass vs. electrical load

Figs. 11 and 12 illustrate the effect of M and R over the sound absorption coefficient under the condition that τ and V are held constant. In the case of a volume of $12 \times 10^{-3} \text{ m}^3$ which is partially filled with mineral fiber ($\tau = 25\%$), we can clearly identify the optimum operating conditions around ($M > 25 \times 10^{-3} \text{ kg}$ and $R \approx 1 \Omega$). For other levels of V and τ , the expected response is slightly different. For a larger volume of the enclosure and without any mineral fiber, the expected optimum conditions depend mainly on R , and on M to a worse extent (see Fig. 12).

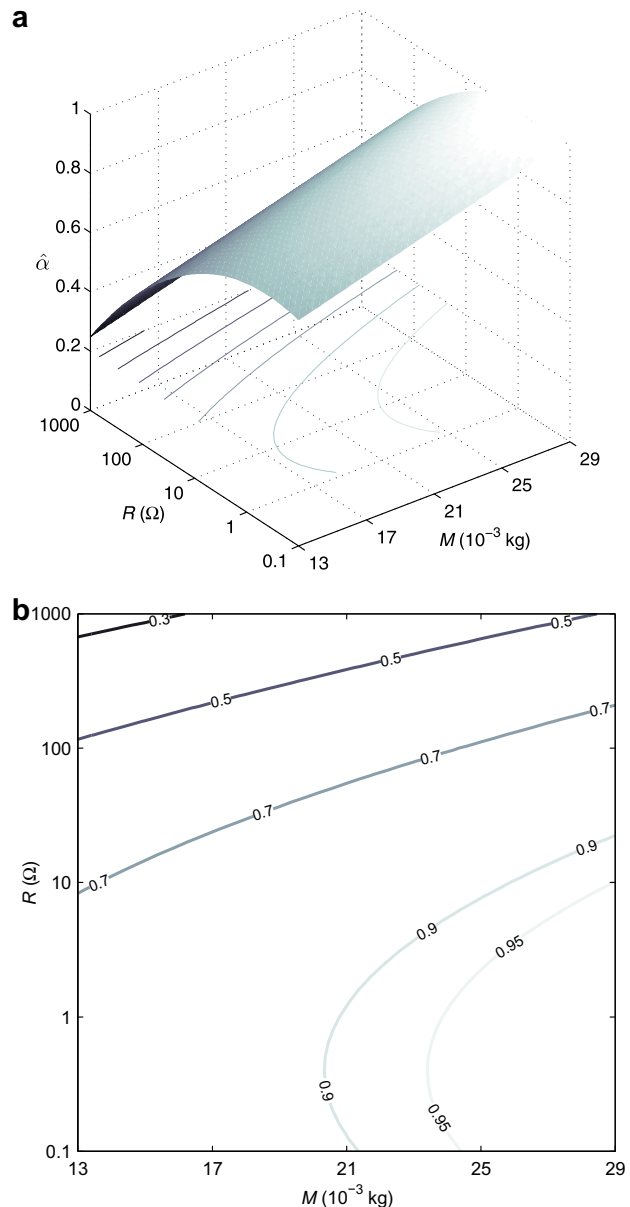


Fig. 11. Moving mass vs. electrical load, $\tau = 25\%$ and $V = 12 \times 10^{-3} \text{ m}^3$.

5.5.3. Enclosure volume vs. electrical load

Figs. 13 and 14 illustrate the effect of V and R over the sound absorption coefficient under the condition that τ and M are held constant. For a moving mass $M = 21 \times 10^{-3} \text{ kg}$ and without any mineral fiber within the enclosure, we identify the optimum conditions when $V \approx 24 \times 10^{-3} \text{ m}^3$ and $R \approx 1 \Omega$. When no mass is added to the loudspeaker's moving mass ($M = 13 \times 10^{-3} \text{ kg}$), and when the enclosure is partially filled with mineral fiber ($\tau = 25\%$), the trend is nearly the same (see Fig. 14).

5.5.4. Enclosure volume vs. filling density

Figs. 15 and 16 illustrate the effect of V and τ on the sound absorption coefficient under the condition that R and M are held constant. For a moving mass $M = 21 \times 10^{-3} \text{ kg}$ and an electrical load of 1Ω , the volume of the enclosure needs to be close to $24 \times 10^{-3} \text{ m}^3$ so as to attain optimum conditions. However, the

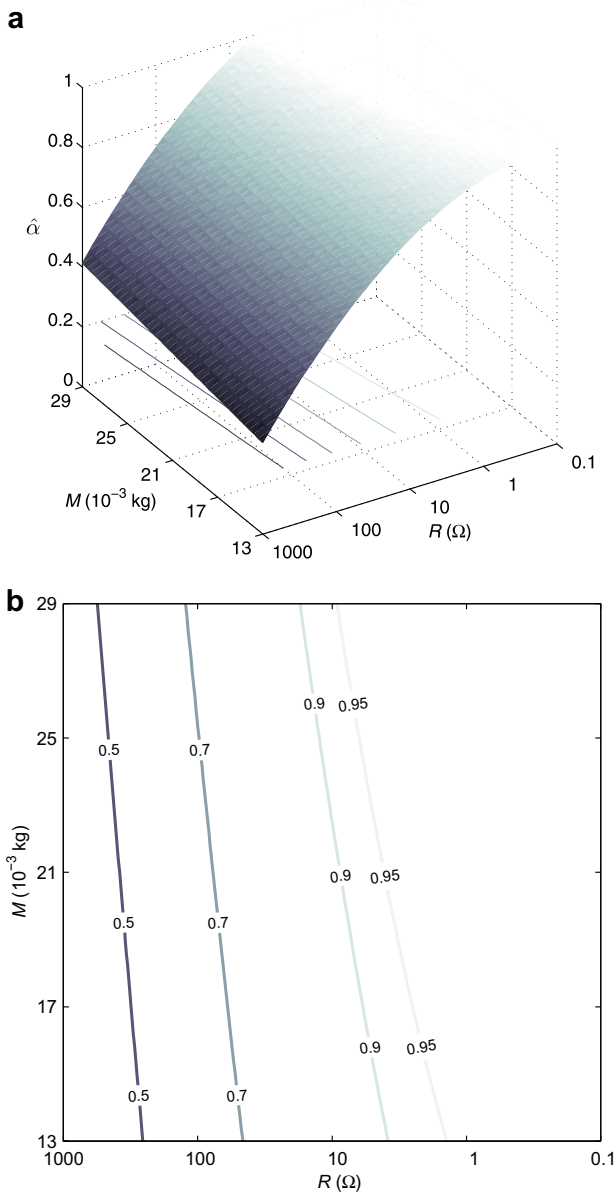


Fig. 12. Moving mass vs. electrical load, $\tau = 0\%$ and $V = 20 \times 10^{-3} \text{ m}^3$.

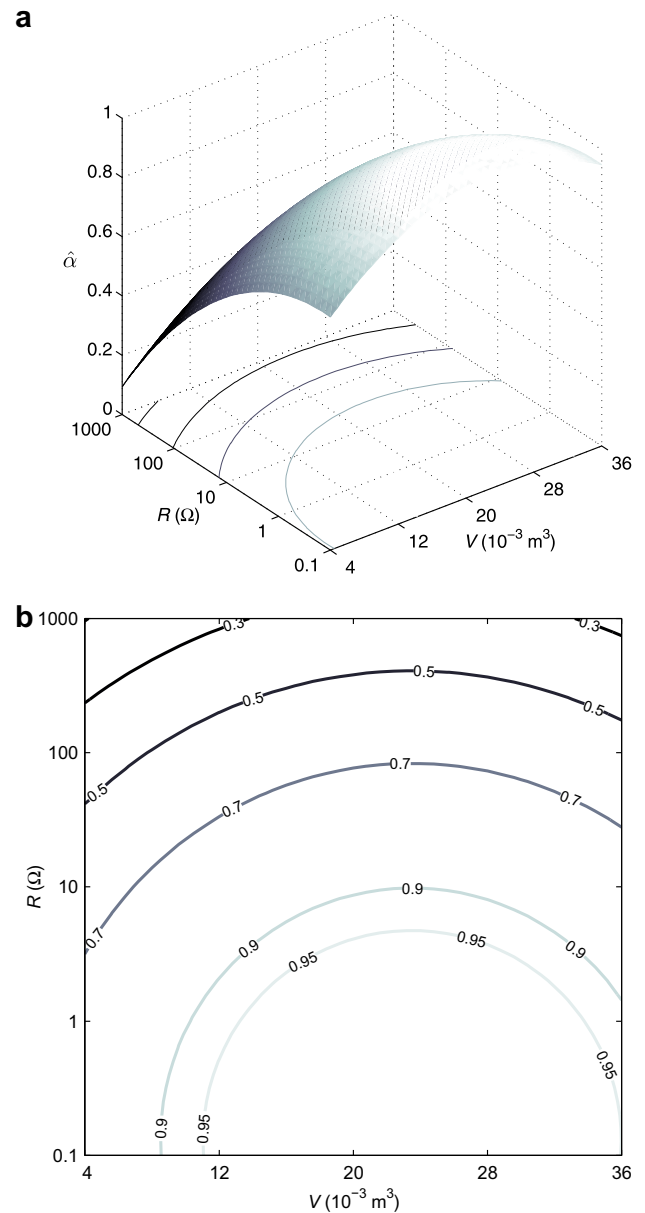


Fig. 13. Volume vs. electrical load, $\tau = 0\%$ and $M = 21 \times 10^{-3} \text{ kg}$.

requirement for τ is less drastic, as illustrated in the Fig. 16. When the moving mass is smaller and the electrical load higher, the volume should be slightly larger ($V \approx 28 \times 10^{-3} \text{ m}^3$) and the filling density upper than 50%. With such an adjustment however, the expected acoustic performance of the absorber should be worse.

5.6. Constraints imposed by the room modal control application

Since the electroacoustic absorber has been designed for a modal control application in rooms, especially the first specific modes around 50 Hz, the main design constraints are relative to the size of the device, and hence the volume of the enclosure to be embedded into walls. The results that follow include two configurations with a fixed volume of 10l initially left empty and then partially filled with mineral fiber. The objective is to find optimum operating conditions associated for both cases. For a volume left empty,

i.e. with $\tau = 0\%$, the expected behavior of the electroacoustic absorber is illustrated in Fig. 17.

For a volume partially filled with mineral fiber, i.e. with $\tau = 80\%$, the predicted absorption coefficient within the bounds of explanatory variables R and M is illustrated in Fig. 18.

These contour plots will help us identify the optimum operating conditions within the imposed constraints. By tuning the electroacoustic absorber at the levels marked by a cross on the contour plots, Eq. (21) estimates the two following absorption coefficients for the 50 Hz one-third octave band:

$$\hat{\alpha}(M = 0.027, V = 0.01, \tau = 0, R = 0.68) \approx 1 \tag{23}$$

$$\hat{\alpha}(M = 0.029, V = 0.01, \tau = 0.8, R = 10) \approx 0.97 \tag{24}$$

In order to validate those computed responses, measurements were performed at these levels after ISO-10534-2 standard using the same setup as depicted in Fig. 2. The two measured curves

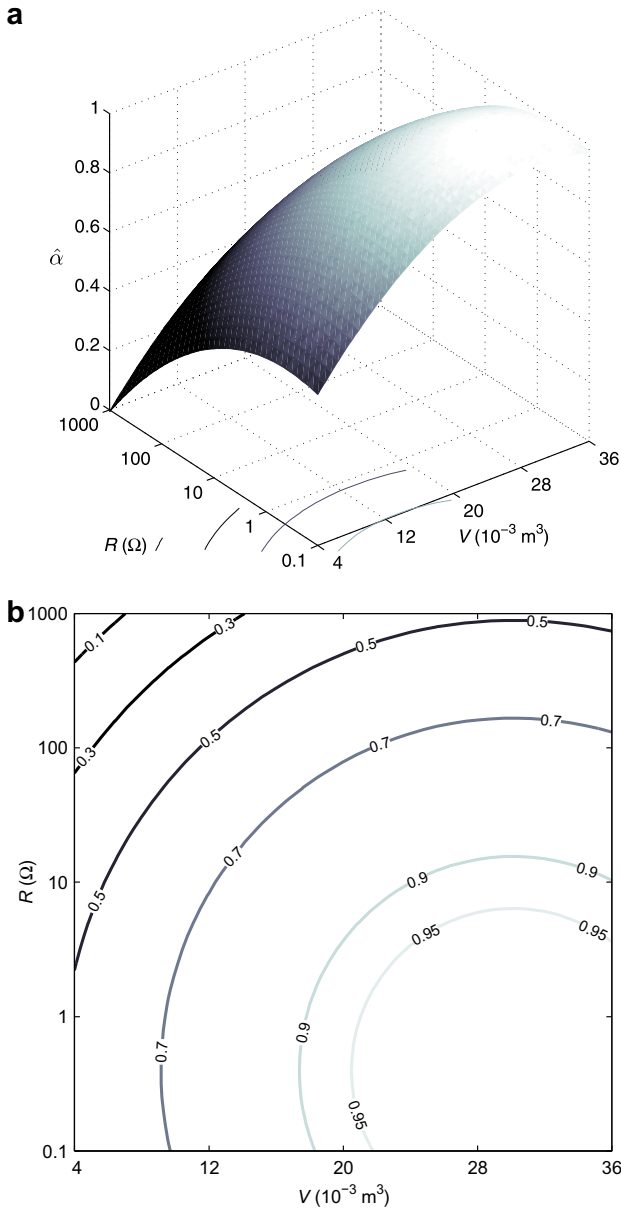


Fig. 14. Volume vs. electrical load, $\tau = 25\%$ and $M = 13 \times 10^{-3}$ kg.

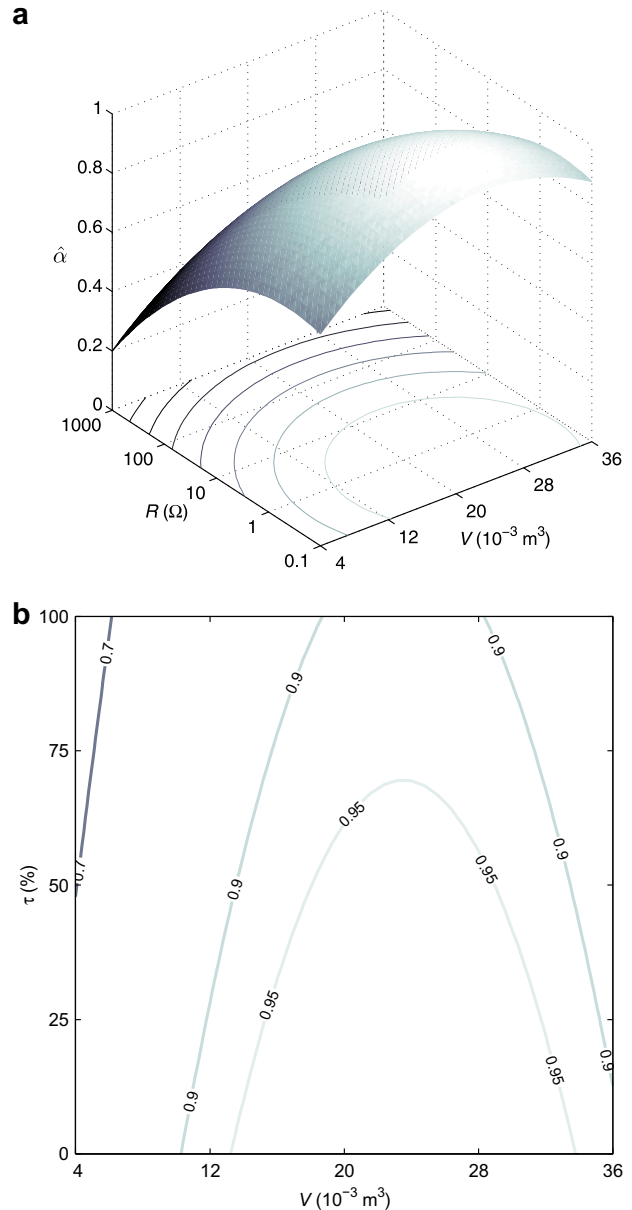


Fig. 15. Filling density vs. volume, $R = 1 \Omega$ and $M = 21 \times 10^{-3}$ kg.

representing the one-third octave bands absorption coefficient for the configurations given by Eqs. (23) and (24) are presented in Fig. 19.

Fig. 19 clearly shows that computed values which are obtained from the fitted second-order response function match the measured absorption coefficient in both cases. Moreover, it can be noted that the required value of electrical load to which the loudspeaker is connected depends on the filling density of mineral fiber. For an enclosure left empty, the optimum operating conditions are expected for a value of electrical load lower than the d.c. resistance of the moving-coil loudspeaker (see Table 2). Conversely, for an enclosure partially filled with mineral fiber, the value of electrical load needs to be upper the d.c. resistance.

In order to assess the capabilities of such devices to damp several modes at a time, the electroacoustic absorber has been installed at one end of a 4 m length duct with the objective to attenuate the first resonant mode around 49 Hz. A main sound

source delivering a swept sine excitation is placed at the opposite end and the resulting sound pressure level is measured with a microphone close to the electroacoustic absorber. Fig. 20 show the measured sound pressure level in case of hard wall and with the electroacoustic absorber in the configurations given by Eqs. (23) and (24).

Fig. 20 clearly shows that the electroacoustic absorber after optimization for the 50 Hz one-third octave band yields a first-mode attenuation of more than 12 dB. Compared to the hard wall configuration, that is to say when the opposite end of the sound source is rigid, it can be observed that the electroacoustic absorber does not affect the response for higher frequencies but tends to slightly attenuate the second resonant mode of more than 4 dB. It is important to note that only a few modes close to the resonant frequency of the loudspeaker can be controlled. Thus, depending on the frequency range of interest, the selection of a suitable loud-

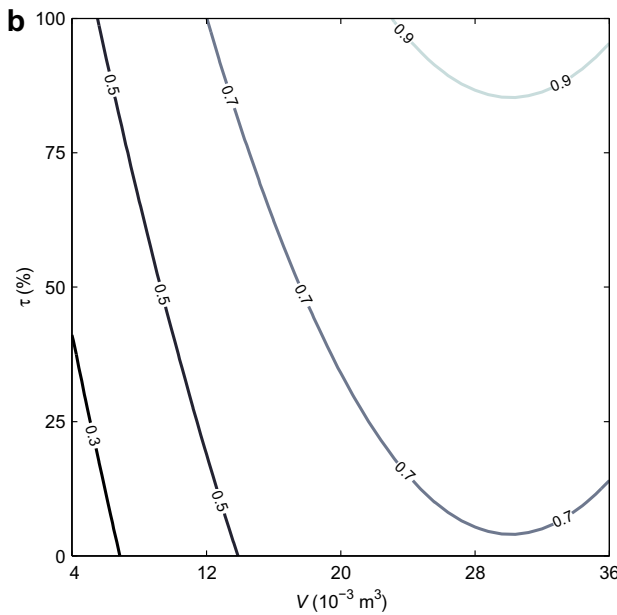
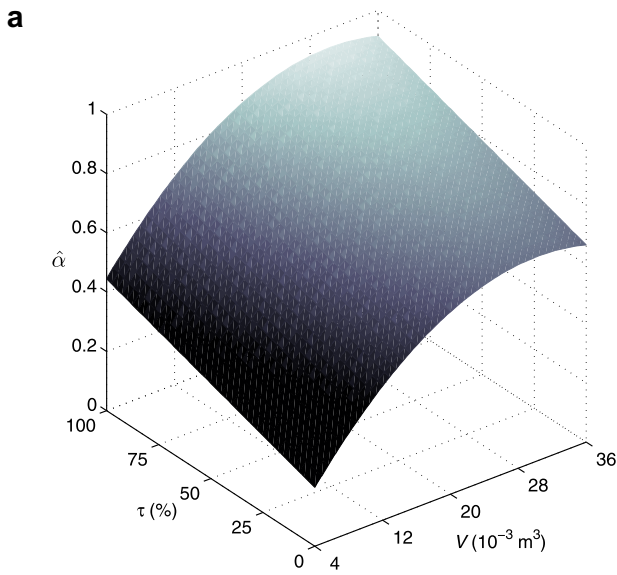


Fig. 16. Filling density vs. volume, $R = 100 \Omega$ and $M = 13 \times 10^{-3} \text{ kg}$.

speaker is critical in order to design an effective sound absorber. Further development phases will now focus on the embodiment of an absorbing panel made of electroacoustic absorbers so as to obtain a large enough surface to significantly damp the first troublesome modes in the control room of the recording studio.

6. Conclusion

In this paper a method for optimizing acoustic performances of an electroacoustic absorber has been proposed. Assuming the change of a factor (or parameter) at a time often leads to select a wrong optimum, due to potential interactions between factors which are not taken into account, the response surface methodology has been applied to alleviate this situation. In this study four influential constitutive parameters have been selected to reflect some dissipative mechanisms of sound energy induced by an elec-

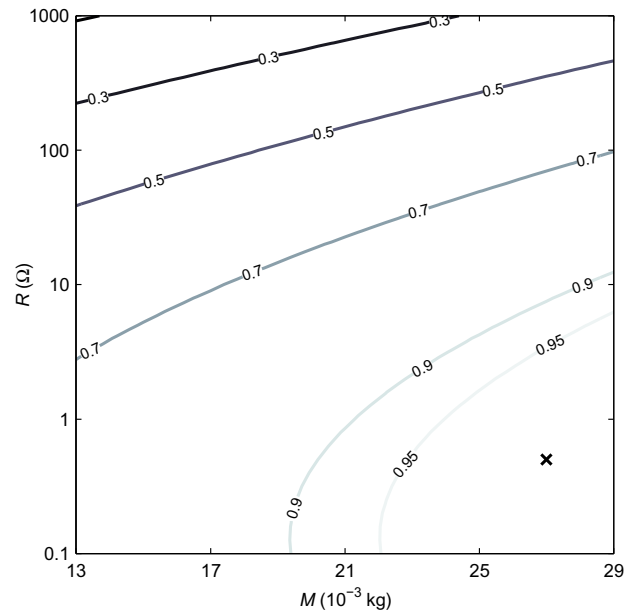


Fig. 17. Expected behavior for $V = 10 \times 10^{-3} \text{ m}^3$ and $\tau = 0\%$.

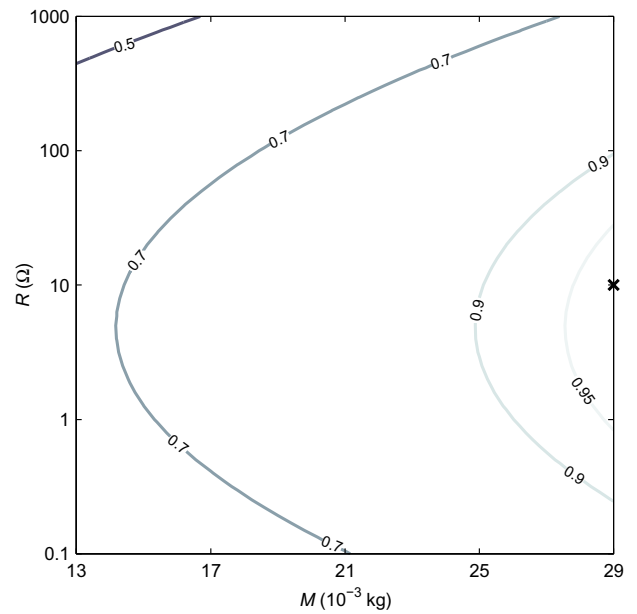


Fig. 18. Expected behavior for $V = 10 \times 10^{-3} \text{ m}^3$ and $\tau = 80\%$.

troacoustic absorber. Without much prohibitive computational efforts to process designed experiments, these methods based on approximation concepts show a real interest for optimizing a multivariate system such as an electroacoustic absorber, introducing statistics from upstream of the experimental process which increases the reliability of the results. From the series of tests carried out, several conclusions can be drawn. First, the information provided by RSM is helpful to give the direction of the design modifications and the fitted surfaces can be used to identify an appropriate direction of potential improvement for absorbing sound energy. Moreover the use of RSM can give a reliable insight into the estimation of the absorption coefficient anywhere within the space of the process. Results relate only to the 50 Hz one-third

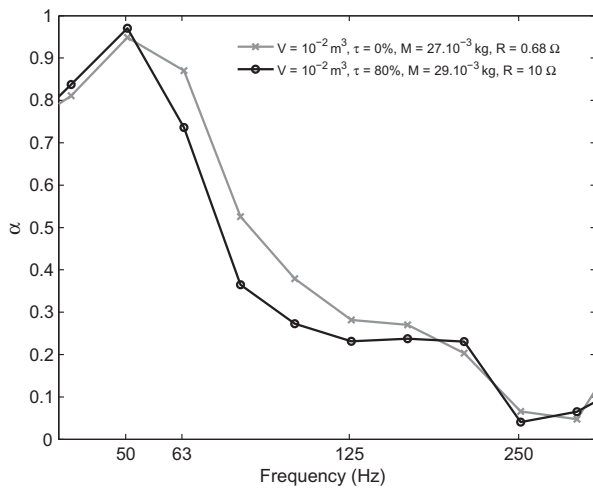


Fig. 19. Measured absorption coefficient after constrained optimization $V = 10 \times 10^{-3} \text{ m}^3$.

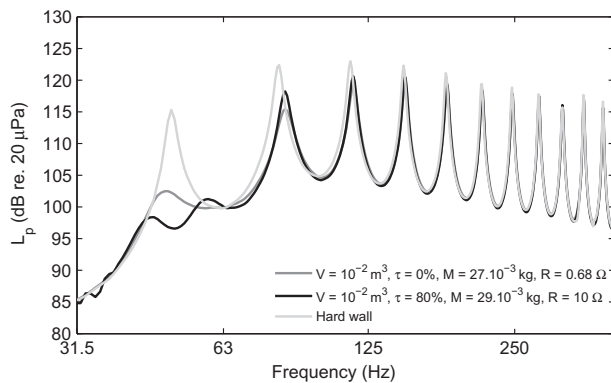


Fig. 20. Measured magnitude of the sound pressure in a duct.

octave band, but by using the same approach it is still possible to identify optimal operating conditions varying with frequency. Moreover, some unexpected effects can be easily highlighted. For instance, it has been shown that the optimal settings of the electroacoustic absorber drastically depends on the quantity of mineral fiber which fill the enclosure. With an empty enclosure the electrical load value needs to be lower than the d.c. resistance of the loudspeaker but nonzero, while conversely it needs to be upper in case of presence of mineral fiber inside the enclosure. Experiments performed after optimization on a closed acoustic duct demonstrate the effectiveness of electroacoustic absorber to attenuate the first

resonant modes without affecting the response elsewhere. At last, it has been proven that, during the process of designing an electroacoustic absorber, the equivalent acoustic impedance of the back-cavity should be taken into account in the models prior to compute the optimal electrical load to connect to the loudspeaker's electric terminals. This experimental technique could be especially useful for designing both electroacoustic transducer and its electrical and acoustical conditioning (enclosure, electric load, etc.) in a single process, without a priori selection of the loudspeaker. It can also alleviate the modeling of the numerous non-linear components of the transducer (suspension, driver) that could have potential prejudicial (or beneficial) effects on the performances on the electroacoustic absorber.

Acknowledgments

The authors wish to thank the Swiss National Science Foundation for supporting this work, under research Grant 200021-116977.

References

- [1] Lissek H. Les Absorbants Electroacoustiques: un Concept Unique pour les différentes Stratégies de Contrôle Actif d'Impédance Acoustique. In: Proceedings of the 10th French congress on acoustics; 2010.
- [2] Fleming AJ, Niederberger D, Moheimani SOR, Morari M. Control of resonant acoustic sound fields by electrical shunting of a loudspeaker. *IEEE Trans Contr Syst Technol* 2007;4.
- [3] Liu F, Horowitz S, Nishida T, Cattafesta L, Sheplak M. A multiple degree of freedom electromechanical Helmholtz resonator. *J Acoust Soc Am, ASA* 2007;122(1).
- [4] Lissek H, Boulandet R, René P-J. Shunt loudspeakers for modal control in rooms. In: Proceedings of ICSV16; 2009.
- [5] Yu G, Li D, Cheng L. Effect of internal resistance of a Helmholtz resonator on acoustic energy reduction in enclosures. *J Acoust Soc Am, ASA* 2008;124(6).
- [6] Ruiz H, Cobo P, Siguero M. Optimization of multiple-layer microperforated panels by simulated annealing. In: Proceedings of inter-noise 2009, INCE; 2009.
- [7] Box GEP, Wilson KB. On the experimental attainment of optimum conditions. *J Roy Statist Soc Ser B (Methodologic)* 1951;13(1).
- [8] Hill WJ, Hunter WG. A review of response surface methodology: a literature survey. *Technometrics* 1966;8(4).
- [9] Box GEP, Hunter WG, Hunter JS. *Statistics for experimenters*. New York: Wiley; 1978.
- [10] Myers RH, Montgomery DC. *Response surface methodology: process and product optimization using designed experiments*. 2nd ed. Wiley-Interscience Publication; 2002.
- [11] Liang X, Lin Z, Zhu P. Acoustic analysis of damping structure with response surface method. *Appl Acoust* 2007;68(9).
- [12] Rossi M. *Audio*, Presses Polytechniques et Universitaires Romandes; 2007.
- [13] ISO 10534-2: Acoustics – determination of sound absorption coefficient and impedance in impedance tubes – part 2: transfer-function method. International Standard Organisation; 1998.
- [14] Box GEP. Non-normality and tests on variances. *Biometrika* 1953;40(3/4).
- [15] Snedecor GW, Cochran W. *Statistical methods*. IOWA State University Press; 1989.
- [16] Archdeacon TJ. *Correlation and regression analysis: an historian's guide*. University of Wisconsin Press; 1994.

Bibliography

- [1] H. Kuttruff, *Room acoustics*. Spon Press, 4th ed., 2000.
- [2] P. M. Morse, R. H. Bolt, and R. L. Brown, “Acoustic impedance and sound absorption,” *J. Acoust. Soc. Am.*, vol. 12, no. 2, 1940.
- [3] P. M. Morse and K. U. Ingard, *Theoretical acoustics*. Princeton University Press, 1968.
- [4] R. Boulandet, X. Falourd, H. Lissek, and M. Rossi, “Localisation des premières réflexions dans une salle par chrono-goniométrie acoustique,” in *Proc. 10ème Congrès Français d’Acoustique*, 2010.
- [5] X. Falourd, L. Rohr, R. Boulandet, H. Lissek, and M. Rossi, “Analyse spatio-temporelle des premières réflexions dans divers lieux d’écoute : de la cabine radiophonique à la cathédrale de lausanne,” *Acoustique et Techniques*, vol. 65, 2011.
- [6] T. J. Cox and P. D’Antonio, *Acoustic absorbers and diffusers: Theory, design and application*. Taylor and Francis, 2nd ed., 2009.
- [7] L. Xiao, T. J. Cox, and M. R. Avis, “Active diffusers: some prototypes and 2D measurements,” *J. Sound and Vibration*, vol. 285, pp. 321–339, 2005.
- [8] R. L. Clark and D. G. Cole, “Active damping of enclosed sound fields through direct rate feedback control,” *J. Acoust. Soc. Am.*, vol. 93, no. 3, 1995.
- [9] P.-J. René, *Contributions aux études sur le couplage électroacoustique dans les espaces clos en vue du contrôle actif*. PhD thesis, Ecole Polytechnique Fédérale de Lausanne, 2006.
- [10] H. Lissek, R. Boulandet, and P.-J. René, “Shunt loudspeakers for modal control in rooms,” in *Proc. 16th International Congress on Sound and Vibration*, 2009.
- [11] M. Rossi, *Audio*. Presses Polytechniques et Universitaires Romandes, 2007.
- [12] M. Melon, P. Herzog, A. Sittel, and M.-A. Galland, “Onde dimensional study of a module for active/passive control of both absorption and transmission,” *Applied Acoustics*, vol. 73, no. 234-242, 2012.

Bibliography

- [13] J.-F. Allard, P. Herzog, D. Lafarge, and M. Tamura, “Recent topics concerning the acoustic of fibrous and porous materials,” *Applied Acoustics*, vol. 39, no. 1-2, pp. 3–21, 1993.
- [14] P. Lueg, “Process of silencing sound oscillations,” *U.S. Patent no US2043416*, 1936.
- [15] H. F. Olson and E. G. May, “Electronic sound absorber,” *J. Acoust. Soc. Am.*, vol. 25, no. 6, 1953.
- [16] H. Lissek, R. Boulandet, and R. Fleury, “Electroacoustic absorbers: bridging the gap between shunt loudspeakers and active sound absorption,” *J. Acoust. Soc. Am.*, vol. 129, no. 5, 2011.
- [17] M. J. M. Jessel and G. A. Mangiante, “Active sound absorber in an air duct,” *J. Sound and Vibration*, vol. 23, no. 3, 1972.
- [18] P. A. Nelson and S. J. Elliott, *Active Control of Sound*. Academic Press Inc, 1993.
- [19] S. M. Kuo and D. R. Morgan, “Active noise control: a tutorial review,” in *Proc. of the IEEE*, vol. 87, pp. 943–973, 1999.
- [20] H. Lissek, *Les matériaux actifs à propriétés acoustiques variables*. PhD thesis, Université du Maine, 2002.
- [21] P. Navi, *Propriétés acoustiques des matériaux*. Presses Polytechniques et Universitaires Romandes, 2006.
- [22] P. Cobo, J. Pfretzschner, M. Cuesta, and D. K. Anthony, “Hybrid passive–active absorption using microperforated panels,” *J. Acoust. Soc. Am.*, vol. 116, no. 4, 2004.
- [23] D.-Y. Maa, “Potentials of micro perforated absorbers,” *J. Acoust. Soc. Am.*, vol. 104, no. 5, 1975.
- [24] D. Guicking, “Active control of sound and vibration: History – fundamentals – state of the art,” tech. rep., Drittes Physikalisches Institut, Georg-August-Universität Göttingen, 2007.
- [25] M. Furstoss, D. Thenail, and M.-A. Galland, “Surface impedance control for sound absorption: direct and hybrid passive/active strategies,” *J. Sound and Vibration*, vol. 203, no. 2, 1997.
- [26] S. J. Elliott, P. Joseph, P. A. Nelson, and M. E. Johnson, “Power output minimization and power absorption in the active control of sound,” *J. Acoust. Soc. Am.*, vol. 90, no. 5, 1991.
- [27] F. Orduña-Bustamente and P. A. Nelson, “An adaptive controller for the active absorption of sound,” *J. Acoust. Soc. Am.*, vol. 91, no. 5, 1992.

-
- [28] B. Naticchia and A. Carbonari, “Feasibility analysis of an active technology to improve acoustic comfort in buildings,” *Building and Environment*, vol. 42, pp. 2785–2796, 2007.
- [29] P. Belanger, A. Berry, Y. Pasco, O. Robin, Y. St-Amant, and S. Rajan, “Multi-harmonic active structural acoustic control of a helicopter main transmission noise using the principal component analysis,” *Applied Acoustics*, vol. 70, pp. 153–164, 2009.
- [30] P. Cobo, A. Fernández, and O. Doutres, “Low-frequency absorption using a two-layer system with active control of input impedance,” *J. Acoust. Soc. Am.*, vol. 114, no. 6, 2003.
- [31] M. Cuesta, P. Cobo, A. Fernández, and J. Pfretzschner, “Using a thin actuator as secondary source for hybrid passive/active absorption in an impedance tube,” *Applied Acoustics*, vol. 67, 2006.
- [32] A. Kundu and A. Berry, “Active control of transmission loss with smart foams,” *J. Acoust. Soc. Am.*, vol. 129, no. 2, 2011.
- [33] A. G. Webster, “Acoustical impedance, and the theory of horns and of the phonograph,” *Proc. Natl. Acad. Sci. USA*, vol. 5, no. 7, pp. 275–282, 1919.
- [34] L. Beranek, *Acoustical measurements*. American Institute of Physics for the Acoustical Society of America, 2nd ed., 1988.
- [35] B. J. Forbes, “Acoustical impedance defined by wave-function solutions of the reduced webster equation,” *Physical Review E*, vol. 72, no. 1, 2005.
- [36] “Iso 10534-2-1998 : Acoustics - determination of sound absorption coefficient and impedance in impedance tubes - part 2 : Transfer-function method,” ISO, Geneva, Switzerland, 1998.
- [37] F. A. Firestone, “A new analogy between mechanical and electrical systems,” *J. Acoust. Soc. Am.*, vol. 4, pp. 249–267, 1933.
- [38] G. J. O’Hara, “Mechanical impedance and mobility concepts,” *J. Acoust. Soc. Am.*, vol. 41, no. 5, 1966.
- [39] J. Yuan and K.-Y. Fung, “A travelling wave approach to active noise control in duct,” *J. Sound and Vibration*, vol. 219, no. 2, 1999.
- [40] C. Guigou and C. R. Fuhler, “Adaptive feedforward and feedback methods for active/passive sound radiation control using smart foam,” *J. Acoust. Soc. Am.*, vol. 104, no. 1, 1998.
- [41] P. Herzog, “Impact des performances de transducteur acoustiques pour le contrôle actif,” in *10ème Congrès Français d’Acoustique*, 2010.

Bibliography

- [42] R. L. Clark, K. D. Frampton, and D. G. Cole, "Phase compensation for feedback control of enclosed sound field," *J. Sound and Vibration*, vol. 195, no. 5, 1996.
- [43] A. J. Fleming and *et al.*, "Control of resonant acoustic sound fields by electrical shunting of a loudspeaker," *IEEE Transaction on Control System Technology*, vol. 15, no. 4, pp. 689–703, 2007.
- [44] R. J. Bobber, "An active transducer as a characteristic impedance of an acoustic transmission line," *J. Acoust. Soc. Am.*, vol. 48, no. 126, 1970.
- [45] L. G. Beatty, "Acoustic impedance in a rigid-walled cylindrical sound channel terminate at both ends with active transducers," *J. Acoust. Soc. Am.*, vol. 36, no. 6, 1964.
- [46] D. Guicking and K. Karcher, "Active impedance control for one-dimensional sound," *J. of Vibration, Acoustics, Stress and Reliability in Desing*, vol. 106, 1984.
- [47] T. J. Cox, M. R. Avis, and L. Xiao, "Maximum length sequence an bessel diffusers using active technologies," *J. Sound and Vibration*, vol. 289, pp. 807–829, 2006.
- [48] J. J. Finneran and M. C. Hastings, "Active impedance control within a cylindrical waveguide for generation of low-frequency, underwater plane traveling waves," *J. Acoust. Soc. Am.*, vol. 105, no. 6, 1999.
- [49] X. Meynial, "Active acoustic impedance control for noise reduction," *Word Patent no. W09959377*, 1999.
- [50] E. D. Boer, "Theory of motional feedback," *IRE Transactions on Audio*, vol. 9, no. 1, 1061.
- [51] S. A. Lane and R. L. Clark, "Improving loudspeaker performance for active control applications," *J. Audio Eng. Soc.*, vol. 46, no. 6, pp. 508–519, 1998.
- [52] S. A. Lane and R. L. Clark, "Dissipative feedback control of a reverberant enclosure using a constant volume velocity source," *ASME J. Vibr. Acous.*, vol. 120, 1998.
- [53] Y. Li and G. T.-C. Chiu, "Control of loudspeakers using disturbance-observer type velocity estimation," *IEEE/ASME Transactions on Mechatronics*, vol. 10, no. 1, 2005.
- [54] P. Darlington, "Loudspeaker circuit for use as combined source-absorber - monitors pressure at speaker and velocity of speaker diaphragm to develop related feedback signal used to modify drive to loudspeaker," *Word Patent no. W09703536*, 1997.
- [55] T. Samejima, "A state feedback electro-acoustic transducer for active control of acoustic impedance," *J. Acoust. Soc. Am.*, vol. 113, no. 3, 2003.

-
- [56] M. Collet, P. David, and M. Berthillier, "Active acoustical impedance using distributed electrodynamic transducers," *J. Acoust. Soc. Am.*, vol. 125, no. 2, 2009.
- [57] N. W. Hagood and A. von Flotow, "Damping of structural vibration with piezoelectric materials and passive electrical networks," *J. Sound and Vibration*, vol. 146, no. 2, 1991.
- [58] R. Boulandet and H. Lissek, "Optimization of electroacoustic absorbers by means of designed experiments," *Applied Acoustics*, vol. 71, 2010.
- [59] P. Albertos and G. C. Goodwin, "Virtual sensors for control application," *Annual Reviews in Control*, vol. 26, no. 101-112, 2002.
- [60] D. J. Leo and D. Limpert, "A self-sensing technique for active acoustic attenuation," *J. Sound and Vibration*, vol. 235, no. 5, 2000.
- [61] B. Hanson and M. Levesley, "Self-sensing applications for electromagnetic actuators," *Sensors and actuators A*, vol. 116, 2004.
- [62] A. J. Fleming, S. O. R. Moheimani, and S. Behrens, "Synthesis and implementation of sensor-less active shunt controllers for electromagnetically actuated systems," *IEEE Transaction on Control System Technology*, vol. 13, no. 2, 2005.
- [63] K. Rajashekara, A. Kawamura, and K. Matsuse, "Sensorless control of ac motors," *IEEE Press Book*, 1996.
- [64] S. Griffin, C. Hansen, and B. Cazzolato, "Feedback control of structurally radiated sound into enclosed spaces using structural sensing," *J. Acoust. Soc. Am.*, vol. 106, no. 5, 1999.
- [65] M. R. Bay and H. Wu, "Robust control of a sensorless bass-enhanced moving-coil loudspeaker system," *J. Acoust. Soc. Am.*, vol. 105, no. 6, 1999.
- [66] F. V. Hunt, *Electroacoustics: the analysis of transduction and its historical background*. American Institute of Physics for the Acoustical Society of America, 2nd ed., 1982.
- [67] R. H. Small, "Direct-radiator loudspeaker system analysis," *J. Audio Eng. Soc.*, vol. 20, pp. 383-395, 1972.
- [68] P. Mills and M. O. Hawksford, "Distorsion reduction in moving-coil loudspeaker systems using current-drive technology," *J. Audio Eng. Soc.*, vol. 37, no. 3, 1989.
- [69] J. Vanderkooy, "A model of loudspeaker driver impedance incorporating eddy current in the pole structure," *J. Audio Eng. Soc.*, vol. 37, no. 3, 1989.
- [70] W. Klippel, "Nonlinear large-signal behavior of electrodynamic loudspeakers at low frequencies," *J. Audio Eng. Soc.*, vol. 40, no. 6, 1992.

Bibliography

- [71] W. M. Leach, “Loudspeaker voice-coil inductance losses: circuit models, parameter estimation, and effect on frequency response,” *J. Audio Eng. Soc.*, vol. 50, no. 6, 2002.
- [72] F. P. Mechel, “Notes on the radiation impedance, especially of piston-like radiators,” *J. Sound and Vibration*, vol. 123, no. 3, 1988.
- [73] L. L. Foldy and H. Primakoff, “A general theory of passive linear electroacoustic transducers and the electroacoustic reciprocity theorem. (I),” *J. Acoust. Soc. Am.*, vol. 17, no. 2, 1945.
- [74] H. Primakoff and L. L. Foldy, “A general theory of passive linear electroacoustic transducers and the electroacoustic reciprocity theorem. II,” *J. Acoust. Soc. Am.*, vol. 19, no. 1, 1947.
- [75] J. C. Maxwell, “On physical lines of force,” *Philosophical Magazine and Journal of Science*, vol. Part II, 1861.
- [76] G. Lehner, *Electromagnetic field and theory for engineers and physicists*. Springer, 2010.
- [77] R. A. Walsh, *Electromechanical design handbook*. Mc Graw-Hill, 3rd ed., 2000.
- [78] R. J. Bobber, *Underwater electroacoustic measurements*. Peninsula Publishing, Los Altos, California, 1988.
- [79] K. Ogata, *Modern control engineering*. Prentice-Hall, Inc, 3rd ed., 1997.
- [80] R. C. Dorf and R. Bishop, *Modern control systems*. Prentice-Hall, Inc, 11th ed., 2008.
- [81] J. Hong, J. C. Akers, R. Venugopal, and M.-N. Lee, “Modeling, identification, and feedback control of noise in an acoustic duct,” *IEEE Transaction on Control System Technology*, vol. 4, no. 3, 1996.
- [82] A. J. Hull, C. J. Radcliffe, M. MiklavČič, and C. R. MacCluer, “State space representation of the non-self adjoint acoustic duct,” *J. of Vibration and Acoustics*, vol. 112, pp. 483–488, 1990.
- [83] A. J. Hull, C. J. Radcliffe, and S. C. Southward, “Global active noise control of a one-dimensional acoustic duct using a feedback controller,” *J. of Vibration and Acoustics*, vol. 115, pp. 488–494, 1993.
- [84] R. Venugopal and D. S. Bernstein, “State space modeling of an acoustic duct with an end-mounted speaker,” *J. of Vibration and Acoustics*, vol. 120, 1998.
- [85] C. R. MacCluer, C. J. Radcliffe, and A. J. Hull, “Diagonalizing acoustic models,” *SIAM Journal on Applied Mathematics*, vol. 51, no. 4, pp. 1006–1010, 1991.

-
- [86] H. F. Olson, *Solutions of engineering problems by dynamical analogies*. Applied Science Library, 2nd ed., 1958.
- [87] G. Yu, D. Li, and L. Cheng, “Effect of internal resistance of a helmholtz resonator on acoustic energy reduction in enclosure,” *J. Acoust. Soc. Am.*, vol. 124, no. 6, 2008.
- [88] R. G. Oldfield and T. J. Cox, “Passive tuned loudspeakers as absorbers for room acoustics,” in *Proc. 19th International Congress on Acoustics*, 2007.
- [89] F. Liu, S. Horowitz, T. Nishida, L. Cattafesta, and M. Sheplak, “A multiple degree of freedom electromechanical helmholtz resonator,” *J. Acoust. Soc. Am.*, vol. 122, no. 1, 2007.
- [90] K. Sakagami, M. Morimoto, and M. Yairi, “A note on the relationship between the sound absorption by microperforated panels and panel/membrane-type absorbers,” *Applied Acoustics*, vol. 70, pp. 1131–1136, 2009.
- [91] M. J. Turner and D. A. Wilson, “The use of negative source impedance with moving coil loudspeaker drive units: an analysis and review,” *J. Audio Eng. Soc.*, vol. 122th Convention, paper 7072, Vienna, Austria, 2007.
- [92] R. W. Nickalls, “A new approach to solving the cubic: Cardan’s solution revealed,” *The Mathematical Gazette*, vol. 77, no. 480, pp. 354–359, 1993.
- [93] G. C. Holmes, “The use of hyperbolic cosines in solving cubic polynomials,” *The Mathematical Gazette*, vol. 86, no. 507, pp. 473–477, 2002.
- [94] H. Seraji and M. Tarokh, “Design of proportional-plus-derivative output feedback for pole assignment,” in *Proc. IEE*, vol. 124, 1977.
- [95] H. Seraji, “Pole placement in multivariable systems using proportional-derivative output feedback,” *Int. J. Control*, vol. 31, 1980.
- [96] T. Rajagopalan, “Pole assignment with output feedback,” *Automatica*, vol. 20, no. 1, 1984.
- [97] V. Martin, *Éléments d’acoustique générale*. Presses Polytechniques et Universitaires Romandes, 2007.
- [98] W. Clements, “A new approach to loudspeaker damping,” *Audio Eng.*, vol. 35, 1951.
- [99] R. E. Werner, “Loudspeaker and negative impedances,” *IRE Transactions on Audio*, vol. 6, no. 4, 1958.
- [100] H. W. Holdaway, “Design of velocity-feedback transducer system for stable low-frequency behavior,” *IEEE Trans. on Audio*, 1963.

Bibliography

- [101] J. A. Klaassen and S. H. de Koning, “Motional feedback with loudspeakers,” *Philips technical review*, vol. 29, no. 5, pp. 148–157, 1968.
- [102] G. E. P. Box and K. B. Wilson, “On the experimental attainment of optimum conditions,” *J. Royal Statistical Soc. Series B (Methodological)*, vol. 13, no. 1, 1951.
- [103] W. J. Hill and W. G. Hunter, “A review of response surface methodology: a litterature survey,” *American Statistical Association and American Society for Quality*, vol. 8, no. 4, 1966.
- [104] A. J. Fleming and S. O. R. Moheimani, “Adaptive piezoelectric shunt damping,” *Journal of Smart Materials and Structures*, vol. 12, 2003.
- [105] D. Niederberger, A. J. Fleming, S. O. R. Moheimani, and M. Morari, “Adaptive multi-mode resonant piezoelectric shunt damping,” *Journal of Smart Marterials and Structures*, vol. 13, no. 4, 2004.
- [106] K. Jaehwan and J. Young-Chae, “Broadband noise reduction of piezoelectric smart panel featuring negative-capacitive-converter shunt circuit,” *J. Acoust. Soc. Am.*, vol. 120, no. 4, 2006.
- [107] O. J. Zobel, “Theory and design of uniform and composite electric wave-filters,” *The Bell System Technical Journal*, vol. 2, no. 1, 1923.
- [108] A. N. Thiele, “Loudspeakers in vented boxes: Part 2,” *J. Audio Eng. Soc.*, vol. 19, no. 6, 1971.
- [109] “Iso 5136-2003: Acoustics - determination of sound power radiated into a duct by fans and other air-moving devices - in-duct method,” ISO, Geneva, Switzerland, 2003.
- [110] H. Lissek, R. Boulandet, and R. Fleury, “Electroacoustic absorbers I: bridging a gap between active acoustic feedback control and shunt loudspeakers,” in *Proc. 18th International Congress on Sound and Vibration*, 2011.
- [111] R. Boulandet, E. Rivet, and H. Lissek, “Electroacoustic absorbers II: implementation of a digital synthetic admittance for controlling the dynamics of electroacoustic absorbers,” in *Proc. 18th International Congress on Sound and Vibration*, 2011.
- [112] W. Klippel, “Tutorial: Loudspeaker nonlinearities - causes, parameters, symptoms,” *J. Audio Eng. Soc.*, vol. 54, 2006.
- [113] K. Thorborg and C. Futtrup, “Electrodynamic transducer model incorporating semi-inductance and means for shorting ac magnetization,” *J. Audio Eng. Soc.*, vol. 59, no. 9, 2011.
- [114] J. O. Smith, *Introduction to digital filters: with audio applications*. W3K Publishing, 2004.

- [115] M. Kehtarnavaz, *Digital signal processing: Labview-based FPGA implementation*. BrownWalker Press, 2010.
- [116] W. T. Padgett and D. V. Anderson, *Fixed-point signal processing - Synthesis lectures on signal processing*. Morgan and Claypool, 2009.
- [117] APEX, “Voltage to current converter,” application note, Cirrus Logic, 2009.
- [118] H. Lissek, R. Boulandet, and A.-S. Moreau, “Stratégie de contrôle semi-actif de l’acoustique des salles aux basses fréquences,” in *10ème Congrès Français d’Acoustique*, 2010.
- [119] M. Bruneau, *Manuel d’acoustique fondamentale*. Hermès, 1998.
- [120] M. R. Schroeder, “Integrated-impulse method measuring sound decay without using impulses,” *J. Acoust. Soc. Am.*, vol. 66, no. 2, 1979.
- [121] J. Borish and J. Angell, “An efficient algorithm for measuring the impulse response using pseudorandom noise,” *J. Audio Eng. Soc.*, vol. 31, no. 7, 1983.
- [122] F. Bongard, H. Lissek, and J. Mosig, “Acoustic transmission line metamaterial with negative/zero/positive refractive index,” *Physical Review B*, vol. 92, no. 9, 2010.

Curriculum Vitae

Romain Boulandet was born on Mars 27, 1977 in Nevers, France. He received the engineering degree (MSc) with honors in Mechanical Engineering, option Applied Acoustics, at the Conservatoire National des Arts et Métiers, Paris, France. His Master thesis on the localization of early sound reflections in a room by acoustic goniometry was carried out at the Laboratory of ElectroMagnetics and Acoustics (LEMA) of the Ecole Polytechnique Fédérale de Lausanne (EPFL), Switzerland. He received the BSc degree with distinction in Vibration, Acoustics, and Signal Processing, at the Université du Maine, Le Mans, France.

From February 2000 to September 2006 he worked as a R&D engineer at Renault S.A.S in the Powertrain Engineering Department, Rueil-Malmaison, France. He was in charge of test campaigns and project management in the field of Noise and Vibration Harshness (NVH) applied to powertrains.

In October 2006 he joined LEMA as a research assistant where he was responsible for several projects with industrial partnerships in the field of sound design (Logitech), noise source characterization (ABB Séchelon SA), and noise reduction (Matisa). As an assistant he was involved in teaching activities in first year of MSc in Audio and Applied Acoustics, at the School of Engineering (STI) of EPFL. He supervised several semester and Master projects.

In May 2008 he enrolled the PhD studies at the doctoral school of Electrical Engineering (EDEE) of the EPFL where he is currently a Research and Teaching Assistant.

List of Publications

Referred Journal Papers

H. Lissek, R. Boulandet and R. Fleury, Electroacoustic absorbers: bridging the gap between shunt loudspeakers and active sound absorption, *J. Acoust. Soc. Am.*, **129**(5), 2011.

R. Boulandet and H. Lissek, Optimization of electroacoustic absorbers by means of designed experiments, *Applied Acoustics*, **71**, 2010.

Referred Conference Papers

R. Boulandet, H. Lissek and E. Rivet, Advanced controller for modifying the acoustic impedance at the diaphragm of a loudspeaker, *Proc. 11ème Congrès Français d'Acoustique*, Nantes, France, 2012.

H. Lissek, R. Boulandet and E. Rivet, Optimization of shunt resonant circuits for electroacoustic absorbers, *Proc. 11ème Congrès Français d'Acoustique*, Nantes, 2012.

Bibliography

E. Rivet, R. Boulandet, H. Lissek and I. Rigas, Study on room modal equalization at low frequencies with electroacoustic absorbers, *Proc. 11ème Congrès Français d'Acoustique*, Nantes, France, 2012.

H. Lissek and R. Boulandet, Design of shunt electric networks in view of sound absorption with loudspeakers, *Forum Acusticum 2011*, Aalborg, 2011.

H. Lissek, R. Boulandet and R. Fleury, Electroacoustic absorbers I: bridging a gap between active acoustic feedback control and shunt loudspeakers, *Proc. 18th International Congress on Sound and Vibration*, Rio de Janeiro, Brazil, 2011.

R. Boulandet, E. Rivet and H. Lissek, Electroacoustic absorbers II: implementation of a digital synthetic admittance for controlling the dynamics of electroacoustic absorbers, *Proc. 18th International Congress on Sound and Vibration*, Rio de Janeiro, Brazil, 2011.

R. Boulandet and H. Lissek, Acoustic impedance synthesis at the diaphragm of moving coil loudspeakers using output feedback control, *Proc. 18th International Congress on Sound and Vibration*, Rio de Janeiro, Brazil, 2011.

R. Boulandet, X. Falourd, H. Lissek and M. Rossi, Localisation des premières réflexions dans une salle par chrono-goniométrie acoustique, *Proc. 10ème Congrès Français d'Acoustique*, Lyon, France, 2010.

H. Lissek, R. Boulandet and A.-S. Moreau, Stratégie de contrôle semi-actif de l'acoustique des salles aux basses fréquences, *10ème Congrès Français d'Acoustique*, Lyon, France, 2010.

R. Boulandet, H. Lissek and A.-S. Moreau, Optimisation d'un absorbeur électroacoustique par plans d'expériences: approche expérimentale et numérique, *10ème Congrès Français d'Acoustique*, Lyon, France, 2010.

H. Lissek, R. Boulandet and P.-J. René, Shunt loudspeakers for modal control in rooms, *Proc. 16th International Congress on Sound and Vibration*, Crakow, Poland, 2009.

H. Lissek, R. Boulandet, M. Černík, J. Václavík and P. Mokřý, Design of switching amplifier used in negative impedance disposal for the active control of transducer's acoustic impedance, *Proc. 16th International Congress on Sound and Vibration*, Crakow, Poland, 2009.

Technical Papers

X. Falourd, L. Rohr, R. Boulandet, H. Lissek, and M. Rossi, Analyse spatio-temporelle des premières réflexions dans divers lieux d'écoute : de la cabine radiophonique à la cathédrale de Lausanne, *Acoustique et Techniques*, vol. 65, 2011.